Technical University of Munich
School of Engineering and Design (ED)
Munich Institute of Integrated Materials, Energy and Process Engineering (MEP)
Center for Combined Smart Energy Systems (CoSES)

**Dissertation**

on

# Technical Implementation and Operation of Prosumer-Based Smart District Heating Networks

by Thomas Licklederer

for the award of the

Doctor of Engineering (Dr. Eng.)

Technical University of Munich
TUM School of Engineering and Design

# Technical Implementation and Operation of Prosumer-Based Smart District Heating Networks

Thomas Licklederer

Complete reprint of the dissertation approved by the TUM School of Engineering and Design of the Technical University of Munich for the award of

Doktor der Ingenieurwissenschaften (Dr.-Ing.).

Chair: Prof. Dr. Klaus Bengler

Examiners:

1. Prof. Dr. Thomas Hamacher
2. Prof. Dr. Christoph Wieland

The dissertation was submitted to the Technical University of Munich on 19.12.2023 and accepted by the TUM School of Engineering and Design on 22.04.2024.

This document is typeset with LaTeX/TeX,
using the services of https://www.overleaf.com.

“For the quest of a doctorate, one must stand on at least two of the following pillars: passion for the topic, joy in the working conditions, enthusiasm for research, hunger for self-challenge, or an unbreakable will for the title. In tough times, one pillar may crumble, while another keeps your journey alive - allowing you to grow professionally and personally.”

*a learning from my doctoral journey*

Thomas Licklederer

Garching bei München, Dezember 2023.

## Acknowledgement / Danksagung

Zuallererst danke ich meinem Doktorvater, Prof. Dr. Thomas Hamacher, der mir die Promotion ermöglichte und auch die Rahmenbedingungen dafür bereitstellte. Seine Überzeugung, dass Forschung zur Lösung realer Probleme eingesetzt werden sollte war prägend für mich. Das frühzeitig entgegengebrachte Vertrauen, hat mir Freiheiten und Verantwortung gegeben, was es mir sowohl ermöglichte mich akademisch zu entfalten, als auch in den Bereich des Wissenschaftsmanagements hineinzuwachsen. Ich danke auch Prof. Dr.-Ing. Christoph Wieland, der mich als wissenschaftlichen Mitarbeiter einstellte und mich während eines Großteils meiner Zeit am Institut begleitete. Meinem Mentor Dr. Michael Kramer gilt mein Dank vor allem für die zahlreichen fachlichen und persönlichen Gespräche. Er hat mich in die Arbeitswelt an der TUM eingeführt und war auch nach seiner Zeit am Institut stets gerne zum Austausch bereit. Ebenso danke ich Prof. Dr. Vedran Peric, einem weiteren Mentor, welcher unsere Forschungsgruppe konstituierte und mit seinem stets kritisches Feedback wissenschaftliche Standards betonte. Darüber hinaus bereicherte er meine Perspektive in unterschiedlichsten Themenfeldern, wie Verwaltung, Gruppenmanagement, wissenschaftliche Community und soziologischen Fragen. Besonders erwähnen möchte ich an dieser Stelle meine engsten Kollegen, Daniel Zinsmeister und Anurag Mohapatra, welche über die Jahre zu Freunden geworden sind. Vielen Dank für die vielen produktiven Diskussionen, die erheiternden Gespräche, sowie die geteilten Herausforderungen und auch Erfolge, insbesondere rund um das CoSES Labor. Ein herzlicher Dank geht auch an alle weiteren Kolleginnen und Kollegen der Forschungsgruppe CoSES, der Lehrstühle ENS & EWK, an Gastforscher, Kooperationspartner und Studierende, mit denen die Zusammenarbeit und der Austausch in freundlicher und produktiver Atmosphäre den Alltag geformt hat. Auch danke ich allen, die meine Publikationen und diese Dissertation korrekturgelesen und verbessert haben. Ich bin außerdem sehr dankbar dafür, dass meine wissenschaftliche Tätigkeit gut vereinbar war mit meinem Lebensunterhalt, ermöglicht über die Forschungsprojektförderung des deutschen Staates.

Diese Dissertation markiert nicht nur einen beruflichen, sondern auch einen privaten Meilenstein in meinem Leben. Schon als Grundschüler antwortete ich auf die Frage nach meinen Zielen halb im Scherz: „Ich möchte einmal Doktor werden.“ Den Ursprung und die Basis für die Umsetzung dieses Erfolgs, stellt meine Familie dar: Meine Eltern Marianne und Erich, sowie mein Bruder Stefan. Ihnen gebührt der größte Dank. Sie haben mir den Rücken freigehalten, mich stets unterstützt, bestärkt, aber auch kritisiert, wenn nötig. Stefans Leidenschaft für Wissenschaft und Forschung war fortwährend inspirierend. Die gesamte Familie bot mir einen Rückzugsort, der mich immer wieder geerdet und mir neue Kraft gegeben hat. Ohne sie wäre ich nicht dort, wo ich heute stehe. Ein besonderer Dank geht an meine Freunde, welche die Hochs und Tiefs einer Doktorandenzeit mit mir gemeinsam durchgestanden haben. Nicht selten mussten sie zurückstecken, was aber mit viel Verständnis hingenommen wurde - Danke dafür. Stellvertretend genannt seien Jakob, Fabi, Niko, Stefan, Matze und Lukas, für ihre langjährige Freundschaft. Mit vielen facettenreichen Momenten habt ihr immer wieder für neue Eindrücke, einen freien Kopf und frische Motivation bei mir gesorgt. Ich möchte auch meinen Partnerinnen Anja, Becci und Conny danken, die mich in verschiedenen Phasen meines Studiums und meiner Promotion begleitet haben und in dieser Zeit wichtige Ankerpunkte in meinem Alltag waren. Abschließend danke ich allen, die meinen Lebensweg gekreuzt und beeinflusst haben, aber hier nicht explizit genannt sind - Freundschaften und Liebschaften, WG-Mitbewohner, flüchtige Bekanntschaften und inspirierende Gesprächspartner.

Durch und mit all diesen Personen, habe ich mich nicht nur akademisch und professionell weiterentwickelt, sondern bin auch in meiner Persönlichkeit gewachsen. In diesem Bewusstsein und mit den wunderbaren Menschen an meiner Seite freue ich mich auf die zukünftigen Abenteuer, die das Leben bereithält.

## Abstract

Smart thermal grids offer the potential to enhance heat supply efficiency and sustainability through distributed renewable generation, as well as synergies among network participants and energy sectors. However, there's a noted gap between theoretical smart management and practical field-level control. Additionally, the effect of distributed actuator operations on the technical network state has not yet been extensively studied. To gain insights into the technical implementation and operation of smart thermal grids, this dissertation investigates a specific sub-type of them: fully distributed, prosumer-based district heating (PBDH) networks, consisting exclusively of peer prosumers, without central plants. A reference network concept is developed, and its component dimensioning is addressed. Based on the reference network concept, the thermohydraulic network behavior in relation to actuator control is modeled and characterized by simulations and experiments. Findings show the sensitivity and nonlinearity of the overall network state to the actuator operating points. These are interdependent, causing systemic effects like pump blocking. A two-layer control framework is developed to address these complexities: A top-layer smart energy management system optimizes the bidirectional network power flows. At the bottom layer, an advanced field-level controller for prosumer substations can process the optimized power setpoints and anticipate systemic effects without direct communication links between participants. In conclusion, this dissertation significantly advances the technical understanding of smart thermal grids and bridges the gap between high-level management and technical execution. Consequently, it contributes to making the potential benefits of smart thermal grids practically usable, thereby paving the way for a more sustainable future energy system.



## Kurzzusammenfassung

Intelligente thermische Netze können die Effizienz und Nachhaltigkeit der Wärmeversorgung verbessern durch die Nutzung verteilter erneuerbarer Energiequellen und von Synergien zwischen den Netzteilnehmern und Energiesektoren. Allerdigs gibt es eine Diskrepanz zwischen dem abstrakten intelligenten Management und der praktischen Regelung auf Feldebene. Darüber hinaus waren die Zusammenhänge zwischen dem Betrieb der verteilten Aktuatoren und dem technischen Zustand des gesamten Netzes bisher nicht ausreichend erforscht. Um Erkenntnisse zur technischen Umsetzung und dem Betrieb intelligenter Wärmenetze zu gewinnen, untersucht diese Dissertation einen speziellen Subtyp dieser Netze: prosumer-basierte Wärmenetze, welche ohne zentrale Anlagen im Netz auskommen und ausschließlich aus Prosumern bestehen. Ein Referenzkonzept für solche Netze wird entwickelt und die Dimensionierung der Komponenten hierfür betrachtet. Auf dieser Grundlage wird das thermohydraulische Netzverhalten in Bezug auf die Steuerung der Aktuatoren modelliert und durch Simulationen und Experimente charakterisiert. Die Ergebnisse zeigen die Sensitivität und Nichtlinearität des Gesamtzustands des Netzes gegenüber Veränderungen in den Betriebspunkten der Aktuatoren. Diese wiederum beeinflussen sich wechselseitig, was systemische Effekte wie das gegenseitige Blockiereng von Pumpen im Netz verursachen kann. Um derartige Komplexitäten zu handhaben, wird eine zweistufige Regelungsstruktur entwickelt: Ein intelligentes Energiemanagementsystem auf der obersten Ebene optimiert die bidirektionalen Energieflüsse im Netz. Auf der unteren Ebene ist ein fortschrittlicher Feldregler für die Wärmeübergabestationen der Prosumer in der Lage, die optimierten Leistungsvorgaben direkt zu verarbeiten und systemische Effekte zu antizipieren, ohne direkte Kommunikationsverbindungen zwischen den Teilnehmern. Zusammenfassend leistet diese Dissertation einen bedeutenden Beitrag zum technischen Verständnis intelligenter Wärmenetze und überbrückt die Lücke zwischen übergeordnetem Management und technischer Umsetzung. Folglich trägt sie dazu bei, die potenziellen Vorteile intelligenter Wärmenetze praktisch nutzbar zu machen und ebnet damit den Weg für ein nachhaltigeres Energiesystem der Zukunft.

# Contents

**Highlight boxes - For those in a hurry**:
In this document, you'll encounter boxes like this one, which concisely summarize the main points to be highlighted. Altogether, these boxes weave a red line throughout the dissertation without delving into details. This enables busy readers to quickly grasp an overview of the narrative and content, delving deeper into specific information only when or where required.

# Part I
# Introduction

# Chapter 1

# Context

“Heating is the world’s largest energy end use, accounting for almost half of global final energy consumption. Industrial processes are responsible for 53% of the final energy consumed for heat, while another 44% is used in buildings for space and water heating and, to a lesser extent, cooking. [...] The heating sector is largely dominated by fossil fuels, with renewable energy sources meeting less than one-quarter of global heat demand in 2021 (and the traditional use of biomass makes up half this amount).” (IEA 2022, [1]) This makes heat supply a significant lever for energy savings and the decarbonization of the energy system.

### Heat supply: local vs. network-based

In the past, two main supply options were distinguished for covering heat demands in buildings - Local supply and network-based supply (compare Figure 1.1a and Figure 1.1b).

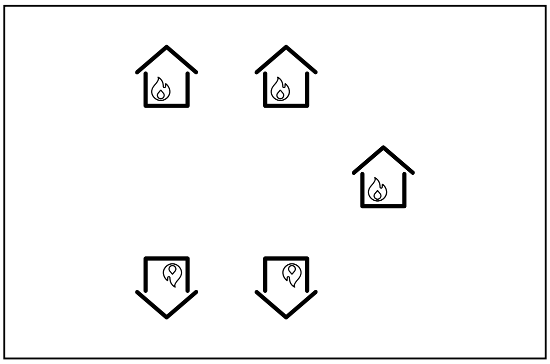

(a) Local heat supply on-site, without network.

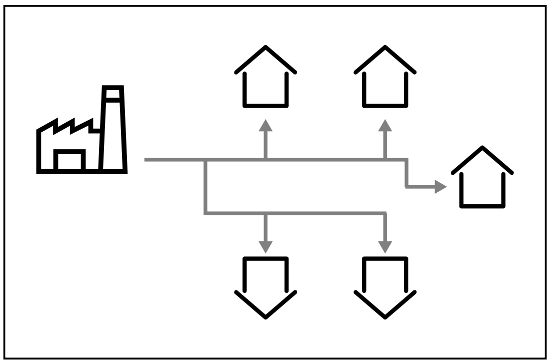

(b) Network-based heat supply by a traditional district heating (TDH) network with a central plant.

Figure 1.1: Local vs. network-based heat supply: network power flows.

Local heat supply is based on systems that perform the final energy conversion on site, such as boilers (gas, oil, biomass, etc.), electric heaters, heat pumps (HPs), or solar thermal panels. The local supply systems can be tailored to individual needs of specific demand types, such as industrial processes.

Network-based heat supply, in turn, relies on a district heating (DH) system. A DH system is a network that efficiently distributes heat from one or several sources to residential, commercial, and industrial buildings within a specific area or district. The network consists of pipelines with several sensors and actuators installed to operate the system according to the consumers’ demands and technical requirements.

### Traditional district heating

The first DH networks were introduced in the early 1880s in the USA [2]. Since then, DH has evolved into a diverse range of network concepts - as will be discussed in more detail in Section 3.3. In order to terminologically capture the current state of the technology, this dissertation uses the term 'traditional district heating (TDH)'. This non-standardized term encapsulates several fundamental aspects of the network architecture and functionality that are widely employed in contemporary DH networks. In this sense, the term 'TDH' is also used in contrast to innovative network concepts from research and development (R&D) that are being investigated or recently implemented in the field.
Traditional district heating (TDH) networks follow a centralized perspective, using only one or a few sources to supply a multitude of consumers. They are usually located in urban areas with high demand density and short transportation distances with low thermal losses. The centrally generated heat is distributed unidirectionally to passive consumers, using circulating water as a carrier medium to transport the heat. The networks commonly exhibit a radial topology. Technical details of TDH networks are discussed in Section 3.2.

The main argument for centralized heat supply by TDH is the economies of scale. Larger plants can be employed by supplying the aggregated demand of the whole area with few central units. They are generally more efficient and can be operated in the optimal range for longer periods. This increases the system efficiency and reduces operational and maintenance costs. Further, the central supply simplifies the installation of redundancies and backups, enhancing system reliability. Circumventing the installation of individual heating systems in every building saves valuable residential space and lowers the upfront investment costs for new buildings.

In 2017, 12% of Europe's space and water heating demand for households, service, and industry sectors were supplied by DH systems [3]. The main technologies for heat production were boilers with approx. 59% of the installed DH capacity, followed by combined heat and power plants (CHPs) with approx. 39% [4]. This is reflected by only 25% of district heat in Europe being produced from renewable sources, with exceptionally high rates in certain northern countries, where more than 50% of DH is fuelled by renewables [5]. In Germany, the share of renewables in DH is about 19% [6], mainly from renewable biomass. So far, the main fuels for DH are gas, oil, and coal.
However, the plans for the development of DH are ambitious: In the 'Net Zero by 2050'[7] scenario of the International Energy Agency (IEA), DH is expected to cover 20% of global space heating needs by 2030, up from 15% in 2020, while more than doubling the share of renewable sources. For Europe, a European Parliament and Council directive formulates clear criteria for shares of renewable sources for sustainable DH in the future decades [8]. For Germany, this is about to be implemented by a law that urges municipalities to make strategic plans for the development of their heating supply and its decarbonization [6], [9]. The draft contains minimum targets for the share of heat from renewable sources and unavoidable waste heat. It sets the framework for Germany's gradual decarbonization and expansion of DH. By 2030, DH networks must be fed to 30 percent and by 2040 to 80 percent with heat from renewable energies or unavoidable waste heat. By 2045, all heat networks in Germany are meant to be climate-neutral. As of 2024, for all new DH networks in Germany, at least 65 percent of the heat fed into the networks must be renewable.

### Distributed generation and synergy exploitation

As the transition towards a more sustainable energy supply gains momentum, features other than economies of scale become driving forces for the development of network-based heat supply [10]–[12]:

a) Distributed generation: The ability to integrate distributed energy resources (DERs) and make them accessible for all network participants. In contrast to local on-site supply, network-based supply makes it possible for all network participants to potentially benefit from any connected source.

b) Synergies: The potential to harness synergies of two kinds. Firstly, synergies can be used between network participants with different load profiles, generation capabilities, and storage capacities. Secondly, synergies between the electricity and heat sectors can be exploited, facilitated through coupling technologies such as CHP units and HPs.

The ability to integrate DERs is of particular interest for the decarbonization by using renewable options, such as geothermal, solar, biomass, and waste heat recovery, e.g., from industrial processes or cooling applications as in data centers [13] or supermarkets [14]. An exemplary benefit of using cross-participant synergies is that efficient and cost-effective distributed heat generators can be optimally utilized by supplying other network participants beyond covering the varying self-consumption, thus replacing less efficient systems. This is especially prominent in mixed-use areas, where various distributed energy sources and sinks are available. Sector coupling additionally allows for more efficient use of the available energy resources and can improve overall energy efficiency by optimizing the energy flows across sectors. The energy conversion between sectors increases the flexibility in the energy system to handle volatile renewable energy sources. For the electricity sector, sector coupling may realize peak shaving, may reduce curtailment and grid congestion and thus improve grid stability and resilience.

### Prosumers and smart grids

The focus on distributed generation and synergy exploitation in the field of DH was induced and inspired by the coupling to the field of electric grids, where these topics have been investigated already for decades [15]–[17]. In this context, the concepts of prosumers and smart grids were also transferred to the field of thermal networks.

The term 'prosumer' is a compound word of 'producer' and 'consumer'. Prosumers are entities that can extract energy from an overarching energy system (consumption) or feed power into it (production) and (can) switch between these two modes over time. That means there are two prosumer modes: production and consumption. Typically, prosumers are sites (like buildings) that combine different units for local generation, local demand, and storage options. Usually, the local generation is used for self-consumption, preferably, while excess energy is fed into the network. In turn, possible deficits, especially in the case of fluctuating renewable generation, can be compensated by extraction from the network. Moreover, controllable generators might benefit the overall network operation by feeding in or extracting energy in a coordinated manner at specific periods and storing it locally at other periods. Figure 1.2 illustrates the concept of prosumers.
From the network perspective, the term 'prosumer' can also be seen as a supercategory of producers and consumers: Prosumers that only feed in energy are producers, while prosumers that only extract energy are consumers.

The concept of smart grids embodies the transition to distributed generation, exploitation of synergies, and integration of the prosumer concept. Adopting the concept of smart grids for thermal networks, an influential paper in the field defines the concept of 'smart thermal grids' as follows: "a network of pipes connecting the buildings in a neighbourhood [...], so that they can be served from centralised plants as well as from a number of distributed heating and cooling producing units including individual contributions from the connected buildings. The concept of smart thermal grids can be regarded as being parallel to smart electric grids. Both concepts focus on the integration and efficient use of

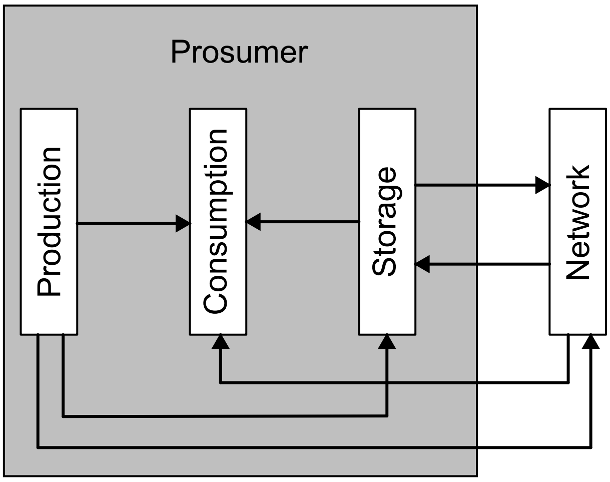


Figure 1.2: Illustration of the prosumer concept: Possible power flows within a prosumer entity and in interaction of the prosumer with an energy network.

potential future [renewable energy sources] RES as well as the operation of a grid structure allowing for distributed generation which may involve interaction with consumers." (Lund et al. 2014, [2])

This definition of smart thermal grids by Lund et al. clarifies that the term 'smart thermal grid' refers more to an abstract construct than specifying a functional network operating principle or distinct hydraulic infrastructure. The concept of smart thermal grids combines the pure forms of local and network-based heat supply (as shown in Figure 1.1) and integrates the prosumer concept. Figure 1.3 illustrates the smart thermal grid concept.
However, the term 'smart grid' originates from power engineering, whereas in DH literature, the term 'network' is traditionally employed. This divergence in terminology leads to a lack of consensus within the scientific community regarding the appropriate usage of 'grid' or 'network' in the context of innovative thermal supply infrastructures. In this dissertation, 'grid' is used to refer to 'smart' infrastructures and electrical grids. Conversely, 'network' is applied to describe thermal systems more generally.

As illustrated by Figure 1.3, in smart thermal grids, the pipelines no longer function as an infrastructure to transport heat from a central power plant to traditional consumers. Instead, it serves as a connecting infrastructure between an expanded set of different network participant types:

- Central power plant(s): feed-in only, significant share in supply
- Traditional consumers: extraction only
- Distributed energy resource (DER): feed-in only, supplementary supply
- Prosumers: can switch between feed-in and extraction

Smart thermal grids aim to facilitate the exploitation of the benefits mentioned above, including the integration of distributed generation and leveraging synergies via network-based supply systems. With this role, smart thermal grids are a puzzle piece of the comprehensive smart energy system concept, complementing electric grids and other supply infrastructure, like gas networks [18], [19]. As a part of smart energy systems, these innovative DH concepts can facilitate an optimized and sustainable energy supply for the future.

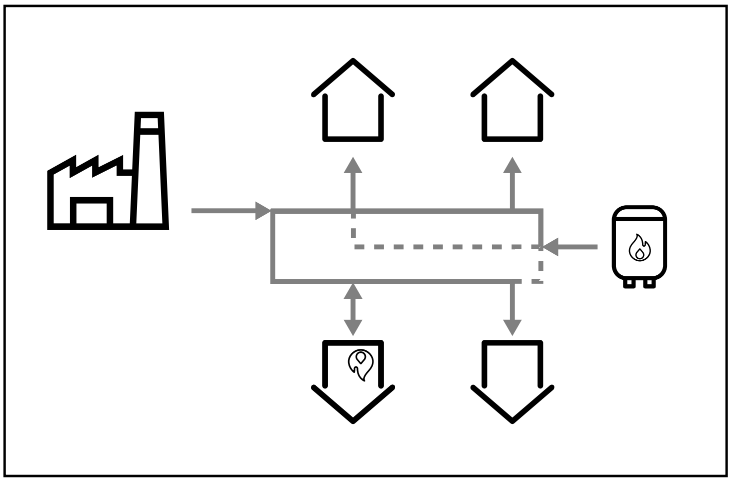

Figure 1.3: Illustration of the smart thermal grid concept, merging local and network-based supply and integrating the prosumer concept: Shown are the possible energy flows in a district heating network with a central power plant (left), three traditional consumers, a DER (on the right), and an active prosumer (bottom left). The network topology can be radial, meshed, or a mixture.

# Chapter 2

# Research Focus

Based on the preceding context, this chapter formulates the research directions (RDs) of this dissertation. To facilitate focused and meaningful investigations, the scope is narrowed and outlined. Within this scope, specific research questions (RQs) are derived and addressed in this dissertation.

Introducing the RDs and RQs in this chapter offers readers an early insight into the dissertation's objectives. Detailed rationales for the RQs introduced in this chapter are given by a later literature review that identifies current research gaps. The literature review is strategically positioned at Chapter 4, following the introduction of technical fundamentals. This intentional placement ensures that, with the technical fundamentals at hand, readers can fully grasp the specificities of the contextual background and the relevance of the RQs within the broader academic discourse.

## 2.1 Research Direction and Scope

This dissertation aims to contribute to implementing the concept of smart thermal grids, thereby facilitating the exploitation of their associated benefits. Given that smart thermal grids embody a broad, abstract construct (see Chapter 1), their practical realization in concrete network concepts through technical implementation and operation is crucial for making the anticipated benefits usable. While smart electric grids have undergone extensive study, smart thermal grids are a relatively new concept. So far, several technical and operational aspects relevant to their practical implementation remain under-explored. Against this backdrop, the primary motivation of this dissertation lies in exploring and advancing the technical feasibility of smart thermal grids.

TDH is characterized by a centralized, hierarchical, and unidirectional nature. This promotes a 'pull'-oriented operation, originating from the demand side: Consumers extract the necessary heat from the network to meet their demands, using unidirectional substations. The central plant compensates for the extracted energy. A network pumping station maintains the unidirectional water circulation to distribute the heat. This means that the central plant and pumping station dominate the overall network state, while the consumers 'take what they need'.

In contrast, in smart thermal grids, distributed feed-in and dynamic modes of prosumers disrupt the traditional hierarchy and change the interaction within the network. The overall thermohydraulic system state emerges from the interference of the operation of all distributed network participants and the characteristics of the pipe network itself. Prosumers exchange heat bidirectionally with the network while multiple distributed generators feed in. This induces bidirectionality also within the network in the form of potentially reversing volume and power flows. The flow trajectories and hydraulic circuits in the network are no longer predetermined and can change dynamically. It is reasonable that, thereby, the technical network operation is significantly more complicated compared to TDH networks.

On the other hand, incorporating DERs and prosumers in the evolution path of DH offers the potential to optimize the usage of sustainable energy sources and to increase the overall system efficiency by exploiting synergies between network participants and energy sectors. However, to leverage these potentials, the diverse network participants must be coordinated to steer the overall network operation. There are potentially multiple sources available for supplying the demand of diverse network participants, introducing new degrees of freedom. Each of the network participants has its own characteristics and features. To make use of potential synergies, the additional degrees of freedom have to be handled by determining a desired optimal network operation that maximizes the system efficiency. Therefore, unlike the 'pull'-oriented operation on a technical level in TDH, smart thermal grids require overarching smart management. This embodies one facet of the 'smart' in 'smart thermal grids'.

To implement coordinative and smart management, enhanced and seamless communication is needed between different layers of automation and between different entities in the network eventually. Establishing this comes along with digitalization on a broad scale. Further, advanced automation and control are required for the conversion of setpoints and the implementation on the field level [20]. These aspects embody another facet of the term 'smart' in 'smart thermal grids'.

Condensing the preceding elaborations, from the altered nature of smart thermal grids compared to TDH networks, two aspects can be derived that are crucial for advancing the practical implementation of smart thermal grids. These two aspects shape the research directions of this dissertation:

**Research Direction (RD): Technical Feasibility of smart thermal grids**

***RD1*** *Technical Implementation: Understanding the intricacies of the interaction between distributed active network participants and the impact of this interaction on the overall network behavior to be able to steer it in a controlled manner.*

***RD2*** *Operation: Designing an operational framework that a) enables the leveraging of synergistic potential within smart thermal grids by strategically identifying the most effective operational trajectories using smart management and b) ensures the practical execution of these trajectories while addressing technical intricacies associated with smart thermal grids.*

Given that smart thermal grids represent an abstract construct, it is reasonable to narrow the scope of investigation to a specific network type. Choosing a type of network in which the RDs above are particularly significant allows to draw conclusions about the investigated aspects that can be generalized for smart thermal grids. Concerning the introduced RDs, networks consisting only of heat prosumers interconnected via the network infrastructure are particularly suitable for this purpose. In the context of this dissertation, such systems are termed 'prosumer-based district heating (PBDH)' networks.

Prosumers represent the most general form of a network participant, as they can be understood as a supercategory of producers and consumers. PBDH networks potentially show the most interaction and mutual influence amongst the network participants and the most distributed network operation. At the same time, they offer maximum degrees of freedom and flexibility, which can be utilized to exploit synergies. We define prosumer-based networks to have no central units, in order to maximize decentralization and to ensure that all prosumers are on an equal hierarchical level (peer prosumers). Consequently, in contrast to traditional networks, there's no central plant, pumping station, or balancing units, as depicted in Figure 2.1.

PBDH networks allow participants to flexibly exchange heat via the network. Meshed, radial, or mixed topologies are allowed [21]. The setup can be perceived as an entirely distributed and network-based heat supply, combining the completely local and completely centralized network-based supply,

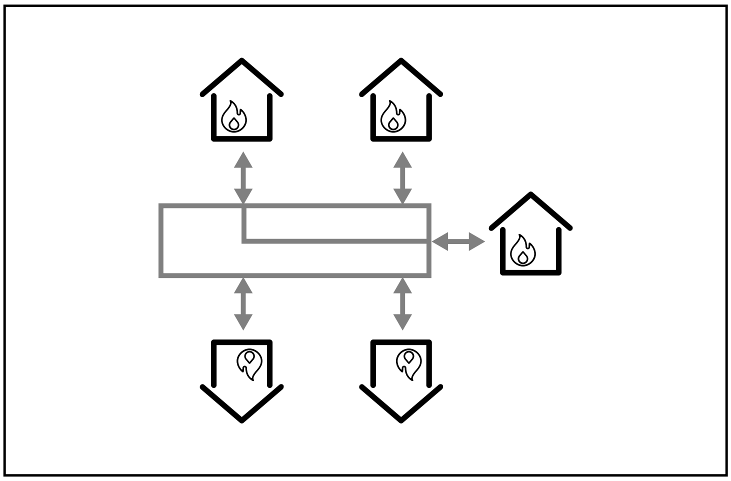

Figure 2.1: Illustration of thermal power flows in prosumer-based networks. Participants can flexibly exchange energy via the network.

as shown in Figure 1.1. While real-world implementations may mix these concepts, PBDH networks epitomize the most distributed smart thermal grids. Addressing challenges in such networks provides insights that are also applicable to less prosumer-centric networks.

The system boundary for investigations in this dissertation are the connection points of the substations to the secondary prosumer side, where idealized prosumer system behavior is assumed. Consequently, the focus is on the primary network side. For investigations on the secondary prosumer side, it is recommended to consult the complementary dissertation of Daniel Zinsmeister and his further work. The scope of this dissertation are prosumer-based district heating networks, but findings can be extrapolated to cooling and combined networks due to analogous physical principles.

> **Scope**
> *This dissertation investigates prosumer-based district heating (PBDH) networks, characterized by the exclusive participation of prosumers without central or dominant entities in the network. PBDH networks are a particular type of smart thermal grids, especially well-suited for studying the impacts and interactions of prosumers on network operations. The system boundary for investigations in this dissertation are the connection points of the substations to the secondary prosumer side, where idealized prosumer systems are assumed. Consequently, the focus is on the primary network side.*

## 2.2 Research Questions

To address the identified RDs within the defined scope, a reference network concept is needed that enables the bidirectional heat exchange in PBDH networks. This opens the first RQ.

> **Research Question 1**
> ***RQ1*** *Design: What is a suitable network concept for prosumer-based district heating (PBDH) networks and how can it be technically implemented?*

Such a network concept includes the hydraulic infrastructure and an underlying functional principle. It provides a blueprint for designing specific network infrastructures. In the context of planning PBDH networks, suitable dimensioning methods for the components in the proposed network concept are a follow-up question.

To ensure a stable and resilient network operation on the technical level, understanding the interplay between prosumer operations and the technical state of the network is crucial. This leads to the second RQ.

> **Research Question 2**
>
> ***RQ2*** *Analysis: How do prosumer-based district heating networks behave on a technical level, i.e., concerning the thermohydraulic system behavior depending on the operation of the distributed actuators?*

The technical network state and behavior cover the thermohydraulic behavior, represented by temperatures, pressures, and volume flows. Further, the characteristic operational behavior is of interest, especially concerning prosumer interactions and transient states.

As introduced, PBDH networks require smart management due to the increased degrees of freedom. Moreover, they shall be operated as an interconnected and integrated part of an overarching energy system. Therefore, setpoints from high-level management must be effectively translated to and implemented at the field level. This raises the third RQ.

> **Research Question 3**
>
> ***RQ3*** *Operation: How can prosumer-based networks be operated and controlled, seamlessly integrated from the management level down to the field level?*

An important aspect here is considering the identified system behavior from RQ2 to preemptively tailor the control design at the field level. Furthermore, the integration and compatibility between the overarching management and the control at the field level is essential so that the synergy potentials anticipated at the management level can effectively be harnessed in the implementation.

## 2.3 Cumulative Structure

After the preceding introduction in Part I, the remainder of this thesis is structured as follows:

Part II provides background information as a basis for the investigations within this dissertation. This covers information on the evolution of DH incl. the current state of technology in the field (Chapter 3). Further, a tailored literature review (Chapter 4) is presented to identify and underline the research gaps, which motivated the RQs, addressed by the dissertation at hand.

Part III is the main part of this document, comprising the conducted investigations of this dissertation. To answer the introduced research questions, seven publications (Pub) form the foundation of the cumulative dissertation at hand.
Figure 2.2 illustrates the structure of Part III, showing the relation between the different chapters, the introduced research questions and the publications, which are listed in detail below. The publications

are numbered according to their integration into the narrative of this dissertation, not according to the order of their creation or publication.

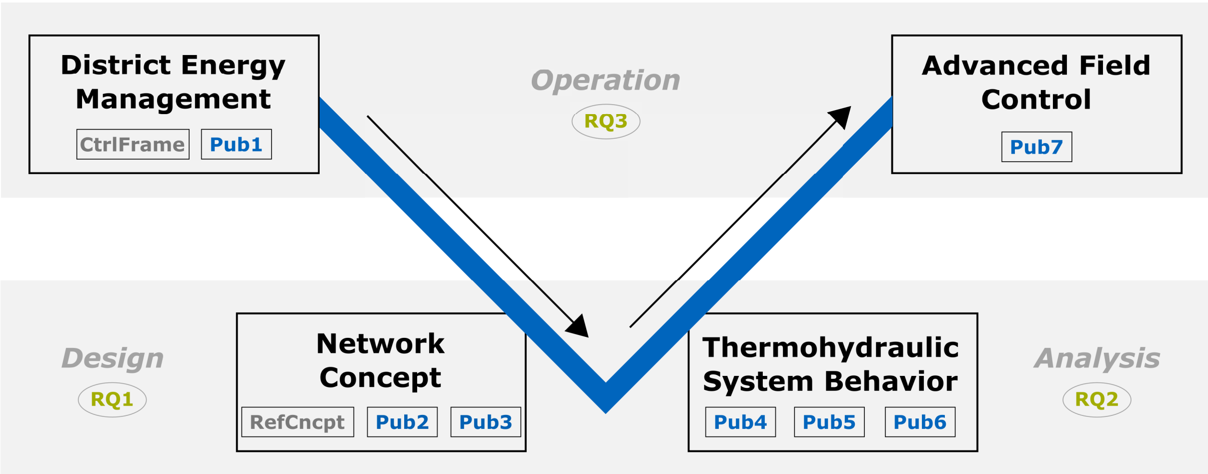


Figure 2.2: Structure of main part of this dissertation.

**Structure of main part of this dissertation**:
Chapter 5 discusses a suitable control framework for smart thermal grids and addresses an according district energy management system (EMS) (Pub1).
Chapter 6 derives a reference network concept for PBDH networks and describes its implementation in a laboratory environment at the Technical University of Munich (TUM) (Pub2). Further, the dimensioning of components for PBDH networks is addressed (Pub3). Chapter 7 investigates the thermohydraulic behavior of PBDH networks. A mathematical model (Pub4) and a simulation library (Pub5) are developed to replicate the technical system behavior. Based on this, characteristics and challenges (Pub6) of PBDH are derived. Chapter 8 focuses on an advanced field level control approach for bidirectional prosumer substations to implementation abstract power setpoints technically at the field level. Alltogether, Chapter 6 is associated with RQ1 (design), Chapter 7 is associated with RQ2 (analysis), while Chapter 5 and Chapter 8 are associated with RQ3 (operation).

All publications that are part of this cumulative dissertation are included directly in the respected chapter. Before each publication, context on the individual paper within the narrative of this dissertation is given. Specific introductions, literature reviews and conclusions can be found in the individual papers. At the end of each chapter, a chapter conclusion is presented, serving to contextualize the insights gained within the broader narrative of this dissertation.

Part IV gives an overall conclusion within the framework of the research questions, and an outlook completes this dissertation.

The appendix presents comprehensive lists of all figures, acronyms, and bibliographic references. Additionally, it contains information about the doctoral candidate's journey, offering context on the development process of this dissertation.

### List of included publications

**Pub1** "A digital platform for real-time multi-energy management in districts using OPC UA: conceptualization, modeling, software implementation, and laboratory validation", T. Licklederer, J. Mayer, D. Bytschkow, et al.; (manuscript submitted to *Energy and Buildings*, revision process ongoing at submission date of this dissertation), preprint is accessible online under http://dx.doi.org/10.2139/ssrn.4861866)

**Pub2** "A prosumer-based sector-coupled district heating and cooling laboratory architecture", *Smart Energy*, D. Zinsmeister, T. Licklederer, S. Adldinger, et al.; https://doi.org/10.1016/j.segy.2023.100095

**Pub3** "Dimensioning radial prosumer-based thermal networks", *Proceedings of the 13. Internationale Energiewirtschaftstagung an der TU Wien*, F. Speer, T. Licklederer, D. Zinsmeister, and V. S. Perić; https://www.researchgate.net/publication/369480633_Dimensioning_radial_prosumer-based_thermal_networks

**Pub4** "Thermohydraulic model of smart thermal grids with bidirectional power flow between prosumers", *Energy*, T. Licklederer, T. Hamacher, M. Kramer, and V. S. Perić; https://doi.org/10.1016/j.segy.2023.100095

**Pub5** "Prosnet – a modelica library for prosumer-based heat networks: Description and validation", *Journal of Physics: Conference Series*, I. Elizarov and T. Licklederer; https://doi.org/10.1088/1742-6596/2042/1/012031

**Pub6** "Characteristics and challenges in prosumer-dominated thermal networks", *Journal of Physics: Conference Series*, T. Licklederer, D. Zinsmeister, I. Elizarov, V. Perić, and P. Tzscheutschler; https://doi.org/10.1088/1742-6596/2042/1/012031

**Pub7** "Control of bidirectional prosumer substations in smart thermal grids: A weighted proportional-integral control approach", *Applied Energy*, T. Licklederer, D. Zinsmeister, L. Lukas, F. Speer, T. Hamacher, V. S. Perić; https://doi.org/10.1016/j.apenergy.2023.122239

# Part II
# Background

# Chapter 3

# Evolution of District Heating

As a basis for the investigations in this dissertations, some background is given on the evolution of district heating. This comprises an introduction to thermohydraulics for understanding the technical aspects of DH. Consecutively, the most relevant technical aspects of TDH networks are presented as a starting point and benchmark for the investigations to be conducted. Finally in this chapter, widely used classifications for DH network concepts incl. innovative approaches are presented, covering also the established vocabulary in this context.

## 3.1 Basic Thermohydraulics

As a knowledge base for the technical understanding of thermal networks in general, a brief introduction to the relevant aspects of thermohydraulics is given in this section.

The underlying physics of thermal networks is principally governed by the interplay between thermodynamics and hydraulics, succinctly termed as thermohydraulics. This is attributed to the intrinsic purpose of thermal networks, which is the controlled and efficient transmission of heat (thermodynamics) using a carrier fluid (hydraulics), namely water. The integration of these two fields for practical application amplifies the complexity of the system's operation in various dimensions. This stands in contrast to electrical supply systems where electrodynamics is the sole governing physical domain.
The fundamental governing laws of thermohydraulics are the Navier-Stokes equations [22] in conjunction with the Laws of Thermodynamics [23]. For practical application within the context of the technical implementation of thermal networks, these can be viewed substantially simplified through the perspective of applied thermodynamics [24] and hydraulic engineering. The central mathematically connecting quantity between the two fields is the volume flow rate.

Technical key components of thermal networks include pipes, pumps, valves, and heat exchangers. As a foundation for understanding the operation of thermal networks and for further investigations, a brief introduction to the relevant fundamental principles will be provided subsequently in the context of these key components.

### 3.1.1 Hydraulics

In thermal networks, pumps are used to set the carrier medium water in controlled motion and induce a volume flow rate $\dot{V}$. Common re-occuring simplifications in the field are:

- the flow (e.g. through pipes) is a 'plug flow', which means the flow is homogeneous in direction and velocity across the entire cross-section. This allows for a simplified one-dimensional representation with variations of flow quantities only along the flow direction.
- the fluid (water) is incompressible, i.e. constant density $\varrho$.

The constant density directly relates volume and mass flow $\dot{m}$ to each other

$$\dot{m} = \varrho \cdot \dot{V} \tag{3.1}$$

Driver for the volume flow is the pressure difference $\Delta p$, caused by a pump (forced convection) - the local pressure downstream after the pump is higher than the pressure before the pump. The water flows in closed hydraulic circuits in the network. When flowing through components (such as pipes, valves, heat exchangers, and others), friction causes a pressure drop along the flow direction. Analogous to the first Kirchhoff circuit law (KCL I) in electrical engineering, the the directed sum of the pressure differences around any closed hydraulic circuit is zero in steady-state. This means pumps as pressure sources compensate for the pressure drop through all other components to maintain the flow. Assuming constant fluid density, the principle of mass conservation can be used to derive an analogy to the second Kirchhoff circuit law (KCL II) from electrical engineering: The algebraic sum of volume flows in a pipe network meeting at a node is zero.
The hydraulic Kirchhoff circuit laws (KCLs) are illustrated in Figure 3.1a.

$$\text{(KCL I)} \quad \sum_{i=1}^{k} \Delta p_i = 0 \tag{3.2}$$

$$\text{(KCL II)} \quad \sum_{j=1}^{n} \dot{m}_j = \sum_j \left(\varrho_j \cdot \dot{V}_j\right) = 0 \tag{3.3}$$

$k$ is the total number of pressure differences in the circuit and $n$ is the total number of pipes with volume flows towards or away from a node.

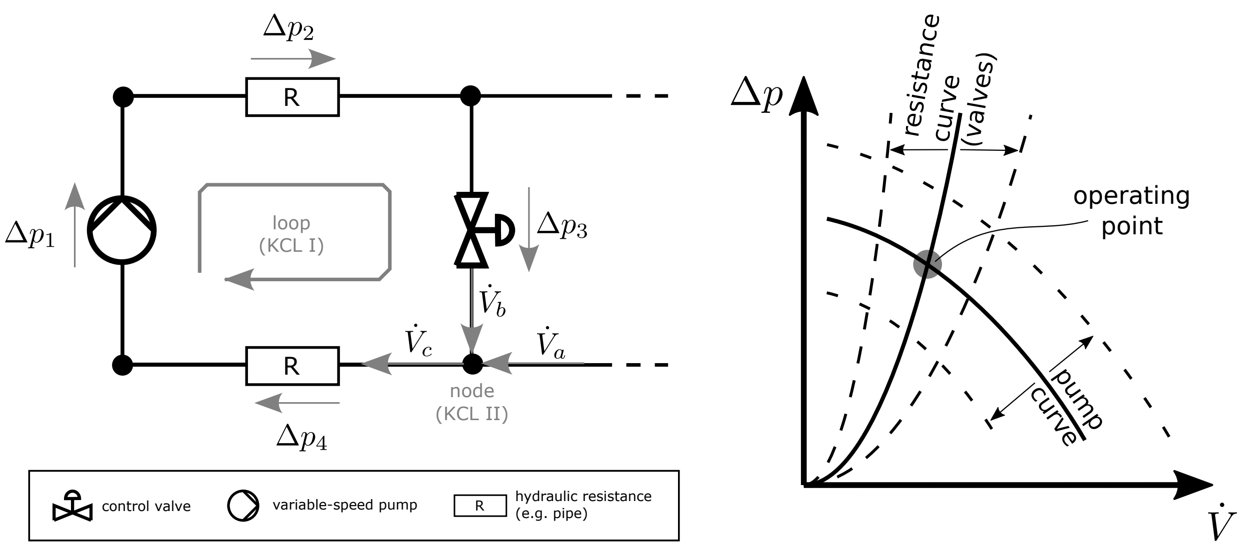


(a) Illustration of Kirchhoff circuit laws in hydraulic circuits.

(b) Hydraulic operating point as intersection of sink and source curves in pressure-flow-diagram [25].

In the context of thermal networks, a hydraulic system state is determined by the combination of a volume flow $\dot{V}$ and a pressure $p$ or pressure difference $\Delta p$ respectively. The pressure difference over an element is coupled to the volume flow through this element by a quadratic relation, usually modelled as follows

$$\Delta p = a_1 \cdot \dot{V}^2 + a_2 \cdot \dot{V} + a_3 \tag{3.4}$$

$a_1$, $a_2$ and $a_3$ are parameters, with $a_2$ often being set to zero. For resistive elements (pressure sinks), like valves and pipes, the paramater $a_3$ is also zero and $a_1$ has a positive value. For pressure sources, like pumps, the parameter $a_1$ has a negative value, while $a_3$ is greater than zero. This is illustrated in the $\Delta p - \dot{V}$-diagram in Figure 3.1b. By opening or closing the valves, the resistance in form of parameter $a_1$ (and $a_2$) can be manipulated, changing the characteristic curve. Variable-speed pumps allow to manipulate the parameter $a_3$ by speeding up or slowing down, thereby also changing the characteristic curve. The hydraulic operating point in a closed hydraulic circuit with pumps and resistances emerges from the intersection of the characteristic curves of the elements in the circuit (see Figure 3.1b). Thus, by operating the control valves and variable speed pumps, the volume flow (and pressure differences) in closed hydraulic circuits can be manipulated.

### 3.1.2 Thermodynamics

The central thermodynamic quantity in the context of heat networks is the temperature $T$. When using warm water for energy transfer, it is important to note that a reference temperature level $T^{ref}$ is always required to calculate a usable energy content.

$$E = \varrho \cdot V \cdot c \cdot \left(T - T^{ref}\right) \dot{Q} \qquad = \varrho \cdot \dot{V} \cdot c_p \cdot \left(T - T^{ref}\right) \tag{3.5}$$

Here $E$ is the energy content of the volume $V$ with specific heat capacity $c$ and temperature $T$, with respect to reference temperature $T^{ref}$. $\dot{Q}$ is a thermal power flow associated with the volume flow $\dot{V}$. A re-occuring simplification on the thermal fluid properties is that the specific heat capacity $c$ is constant at the value of one isobaric specific heat capacity $c_p$, although the specific heat capacity of a fluid in general is a function of the pressure and the temperature.

For understanding the operation of thermal networks, understanding the functionality of heat exchangers is essential. In the context of this dissertation we focus on plate heat exchangers (see Figure 3.2) as the most common option in the context of DH systems. In these devices two fluids stream on two

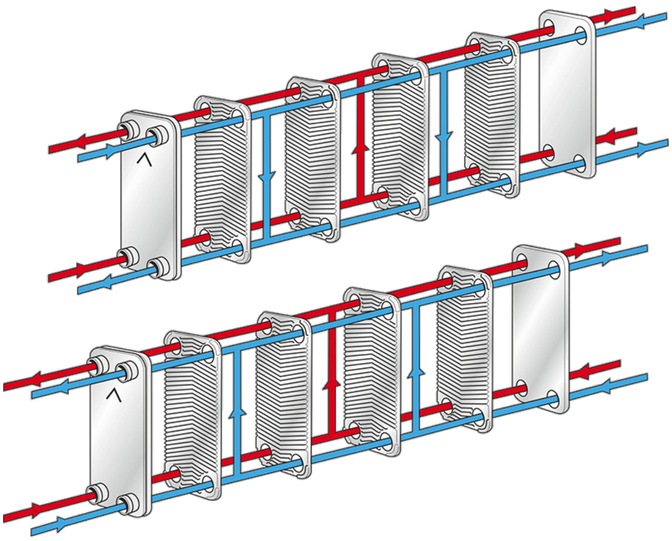

Figure 3.2: Countercurrent flow (top) and co-current flow (bottom) through a plate heat exchanger [26].

sides of thin metal plates through which the heat is transferred by convection and conduction from the warmer to the colder fluid without mixing [24]. Like this, the fluids are hydraulically decoupled, but thermally coupled. The corrugated design of the plates promotes turbulence, enhancing heat transfer, while the compact stacked arrangement allows for a large heat transfer area in a small space. With plate heat exchangers there are two main flow patterns for heat exchange: countercurrent and co-current flow (see Figure 3.3). Countercurrent flow heat exchange is the more efficient one, as the driving temperature difference for heat exchange is higher along the length of heat exchange. Quantitatively this is reflected by a higher logarithmic mean temperature difference (LMTD), as illustrated in Figure 3.3.

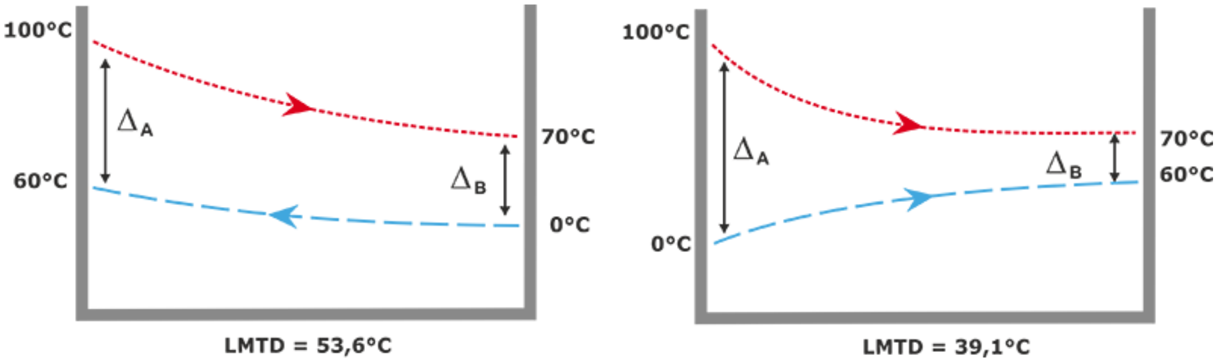


Figure 3.3: Comparison between countercurrent (left) and co-current (right) flow pattern for heat exchange. Resulting logarithmic mean temperature difference (LMTD) for the same inlet temperatures. [26]

Using the equations for ideal countercurrent flows, e.g. from the VDI Heat Atlas [24], the outlet temperatures can be calculated. Let the warmer fluid be denoted with subscript 1 and the colder with subscript 2, while properties of incoming streams are denoted by $'$ and those of outgoing streams are denoted by $''$. Assuming constant density $\varrho$ and constant specific heat capacity $c_p$ for both fluids, as well as the heat transfer surface $A$ and a constant heat transfer coefficient $k$, the equations for the outlet temperatures are:

$$T_1'' = T_1' - (T_1' - T_2') \cdot \frac{1 - e^{\left[\left(\frac{\dot m_1}{\dot m_2} - 1\right) \cdot \frac{k \cdot A}{\dot m_1 \cdot c_p}\right]}}{1 - \frac{\dot m_1}{\dot m_2} \cdot e^{\left[\left(\frac{\dot m_1}{\dot m_2} - 1\right) \cdot \frac{k \cdot A}{\dot m_1 \cdot c_p}\right]}} \text{ for } \dot m_1 \neq \dot m_2 \wedge c_{p1} = c_{p2} = c_p \tag{3.6}$$

$$T_2'' = T_2' + (T_1' - T_2') \cdot \frac{1 - e^{\left[\left(\frac{\dot m_2}{\dot m_1} - 1\right) \cdot \frac{k \cdot A}{\dot m_2 \cdot c_p}\right]}}{1 - \frac{\dot m_2}{\dot m_1} \cdot e^{\left[\left(\frac{\dot m_2}{\dot m_1} - 1\right) \cdot \frac{k \cdot A}{\dot m_2 \cdot c_p}\right]}} \text{ for } \dot m_1 \neq \dot m_2 \wedge c_{p1} = c_{p2} = c_p \tag{3.7}$$

These equations have a definition gap for the special case of same heat capacity flows on both sides, therefore the equations for this special case are:

$$T_1'' = T_1' - (T_1' - T_2') \cdot \frac{k \cdot A}{\dot m_1 \cdot c_{p1} + k \cdot A} \text{ for } \dot m_1 \cdot c_{p1} = \dot m_2 \cdot c_{p2} \tag{3.8}$$

$$T_2'' = T_2' + (T_1' - T_2') \cdot \frac{k \cdot A}{\dot m_2 \cdot c_{p2} + k \cdot A} \text{ for } \dot m_1 \cdot c_{p1} = \dot m_2 \cdot c_{p2} \tag{3.9}$$

The warmer stream gets cooled down, while the colder stream gets heated up, as expected by the first law of thermodynamics. The outlet temperatures are linear in the inlet temperatures and highly nonlinear in the volume flows of both sides. Evaluating the equations for some exemplary boundary conditions, this can be illustrated as in Figure 3.4.
The transferred heat is a function of the volume flows and the difference between inlet and outlet temperature of one side.

$$\dot Q_1 = \varrho \cdot \dot V \cdot c_1 \cdot (T_1'' - T_1') \tag{3.10}$$

This means that by manipulating the volume flows, the outlet temperatures can be controlled according

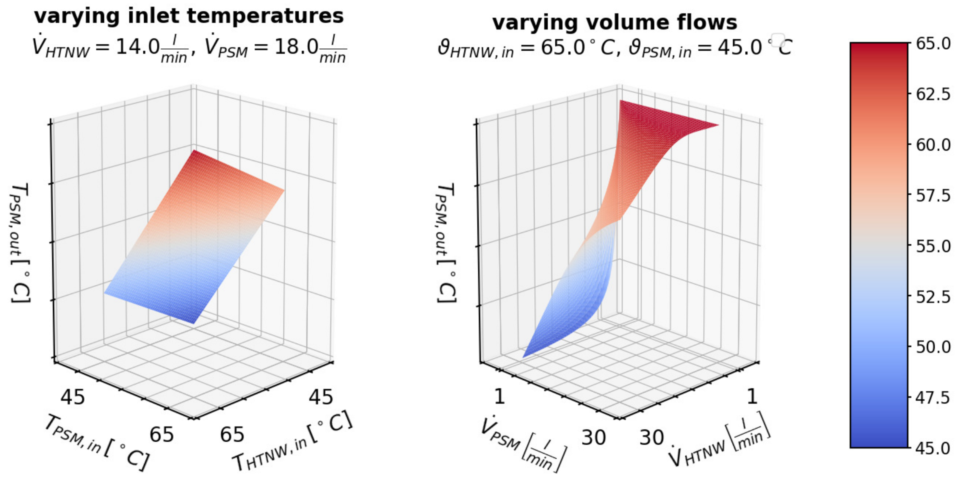


Figure 3.4: Ideal countercurrent flow heat exchanger: Dependency of outlet temperature on the inlet temperatures and the volume flows. 'PSM' stands for prosumer, 'HTNW' stands for heat network.

to Equation 3.6 - Equation 3.9, which then might be inlet temperatures for another heat exchange process in the network. At the same time, by manipulating the volume flows, also the transferred thermal power can be controlled according to Equation 3.10.

Another relevant thermal effect in the networks are heat losses (to the environment). The heat losses are proportional to the temperature difference between the water in the pipes and the ambient temperature. The losses can thus be decreased by decreasing the network temperatures, or by reducing the heat exchange area or increasing the insulation. Hydraulic friction adds thermal energy into the flow. However, this is usually negligible in common models.

## 3.2 Traditional District Heating

In a previous chapter, 'traditional district heating (TDH)' was introduced to encapsulate in one term the state of the technology in the field from the viewpoint of the 2020s. Understanding TDH systems helps to grasp the main principles and nature of current DH systems, therefore builds a benchmark for consecutive research. To enhance this understanding, in this chapter, the technical key aspects of TDH networks are outlined.

In practice, there is not a single network design for TDH systems, but numerous implementation variants exist. For clarity, a basic version is described, which will be used as a common ground for benchmarking. Not all technical details will be delved into; only those relevant for subsequent discussions in this dissertation will be highlighted. The goal is to create an understanding of the basic functioning of TDH networks. The described state of technology is manifested in standard literature on heat networks, such as the *Handbook on Planning of District Heating Networks* by Nussbaumer [27] or *District Heating and Cooling* by Frederiksen and Werner [28]. For more details, readers may consult this established literature, which also serves as the main source for the compiled facts and numbers presented in the following.

TDH networks follow a centralized perspective: A central power plant generates heat and a central pumping station drives the network flow. Substations transfer the heat unidirectionally from the network to the consumers.

### 3.2.1 Infrastructure

The main parts of the infrastructure are illustrated in Figure 3.5.

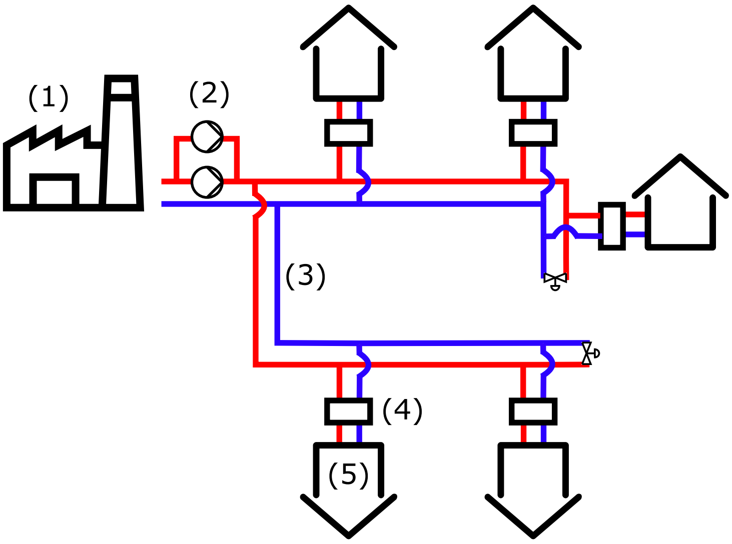


Figure 3.5: Simplified exemplary scheme of typical infrastructure in TDH networks, as a reference in the context of this dissertation: (1) central plant; (2) pumping station; (3) pipe network, warm supply line in red, cold return line in blue; (4) consumer substations; (5) consumer systems.

There are various options for the central plant and in principle any heat supply technology can be used. Most commonly, gas-fired CHP plants are used, as they simultaneously supply heat and electricity, have a high overall efficiency, are well controllable and are able to provide the necessary temperatures also for industrial processes. However, there is a trend towards using deep geothermal plants as a more sustainable alternative.
For the pumping station, speed-controlled circulating pumps driven by an electric motor are used for water circulation in the district heating network. Since pumping is a fundamental functionality for the overall operation, it is common to have two identical pumps in parallel for redundancy.

For the pipe network, pre-insulated steel pipes are most frequently used. The pipe network can have various topologies, with radial networks being the most common, and line networks being a special form of them. In the pipes, warm pressurized water is used as a carrier medium. Modern TDH networks are almost exclusively designed as closed two-pipe systems with a warm supply line and a colder return line. At the end of each network branch, the supply and return line are interconnected via a valve to shortcut them in case of low or no demand. The temperature levels strongly depend on the specific network design, covering $65\ ^{\circ}C$ to $110\ ^{\circ}C$. We consider $80\ ^{\circ}C$ for the supply line as a reference, with a temperature spread to the return line of $30\ K$. The nominal pressure level in the network also depends on the specific network design. In bigger networks with steel pipes it lies between $10\ bar$ and $25\ bar$, in smaller networks and networks with plastic media pipes also pressure levels around $6\ bar$ are usual. We take $12\ bar$ as a reference.

For the consumer side, there are various options of systems that can be connected to the DH network, with several substation architectures being tailored for these systems (see Ref. [29]). The substations transfer the heat unidirectionally from the network (primary side) to the consumer (secondary side). The technical connection requirements and guidelines for the substation design are usually given by the utility that operates the network, e.g. for Munich these can be found in Ref. [30]. This dissertation focuses on the most common and most generalizable application: the indirect connection of a consumer system for (space) heating. Indirect connection in this context means, that network side and consumer side are hydraulically separated by a heat exchanger. Here the conventional solution is a plate heat exchanger operated in counter-current flow mode. Figure 3.6 illustrates a typical substation configuration in TDH networks. Apart from the heat exchanger, the control valve (CV) on the network side and the circulating pump of the consumer's heating circuit are the main installations in the substation.

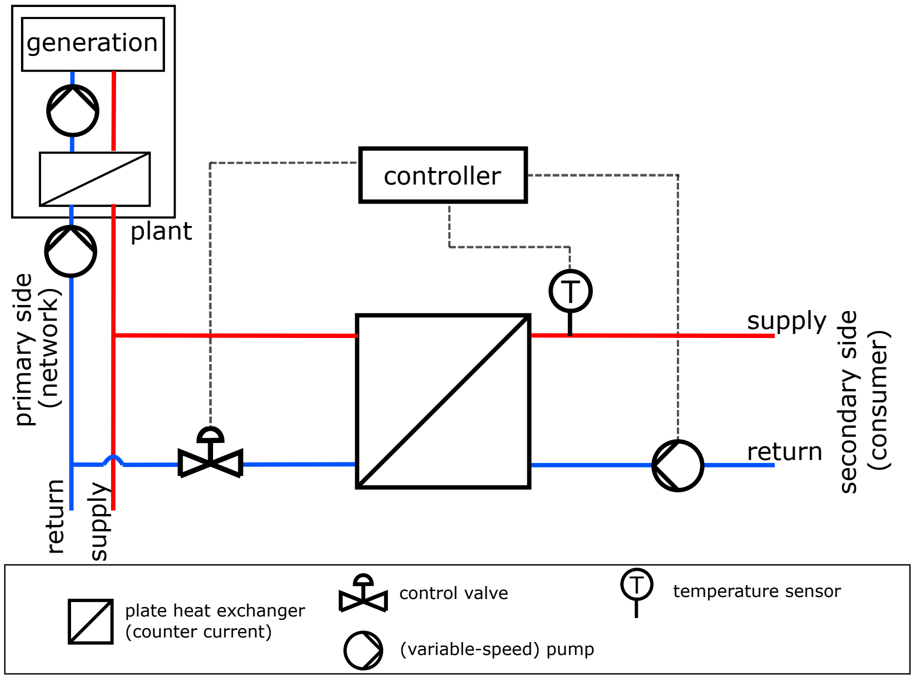


Figure 3.6: Simplified reference configuration of typical substations in TDH networks, as a reference in this dissertation. Indirect connection for space heating application.

Of course, there are several other installations in the network and the substations to guarantee a safe and reliable network operation. For example, due to the thermal expansion of the water in the pipes, expansion vessels are needed. As eleborated before, these elements are not mentioned here for the sake of conciseness.

### 3.2.2 Control

The operation of TDH systems is distributed amongst different actuators, involving many intricacies. In the following we will only address the essential aspects, which serve as a reference for investigations in the context of this dissertation.
The control of TDH networks consists of three main pillars: Temperature control, pressure control, heat demand and flow control [31], [32]. The overall operation is shared between network elements and elements in the substations.

**Network** The central plant feeds in heat to satisfy the heat demand of the whole network, compensating for the thermal power extracted by the consumer substations and for losses. The plant is controlled to provide the necessary primary side supply temperature, which is usually determined by a heating curve depending on the ambient temperature. The central pumping station in the network pressurizes the supply line and is controlled to keep a minimum differential pressure at the critical substation. The targeted minimum differential pressure is usually around $0.7\ bar$. The location in the network, where the differential pressure between supply and return line is minimal, is the so called 'network critical point' (german: 'Schlechtpunkt'). The critical substation lies close to this critical point and is the one, where the pressure drop from the pumping station to the substation is highest. The closed loop between the pumping station and the critical substation forms the critical hydraulic circuit. The critical substation in TDH usually is the one furthest away from the pumping station, as the pressure drop is significantly caused by the hydraulic resistance of the pipes and installations in the pipes. The hydraulic resistances of all closed hydraulic circuits in the networks are further influenced by the opening status of the individual primary side valves in the substations. The network volume flows thus can be manipulated according to the pressure-flow-relation (see Section 3.1) by operating the pumping station in interference with the primary side control valves of the substations. As the plant aims to keep the supply temperature constant, the thermal power fed into the network can be controlled by manipulating the network flows.

**Substation** On the primary side of the substations, the supply line is pressurized by the central pumping station in the network. By opening and closing the CV on the primary substation side, the hydraulic resistance in the according hydraulic circuit is changed and the flow through this specific substation can be regulated. The valve is controlled to reach the setpoint for the secondary side outlet temperature. Mostly a proportional-integral-derivative (PID) controller is used for this purpose [33]. The secondary side supply temperature setpoint is normally given by the consumer heating system and adapted according to a heating curve depending on the ambient temperature.

On the secondary side of the substations, the flow is driven by the circulating pump in the consumer system. In older settings, this consumption pump (CP) is operating at constant speed. In more modern and efficient settings, the speed of the CP is controlled according to the differential pressure of the secondary side hydraulic circuit. When there is higher heat demand - i.e. the thermostat on a radiator is opened - the differential pressure decreases and the pump increases its speed to keep the differential pressure. Thus, the volume flow rate increases. As the supply temperature is kept constant by the primary side valve, the transferred power in this setting is indirectly controlled via the secondary side pump.

### 3.2.3 Component Dimensioning

Planning, constructing and operating DH networks is a demanding endeavor, necessitating extensive expertise, significant intervention in the built environment, and substantial long-term financial investments, spanning 40+ years. Usually, only established, experienced and resilient companies or consortia can handle this.
The planning covers several phases (e.g. according to HOAI [34]), that include amongst others economical, technical, administrative and political aspects. From the technical perspective, the dimensioning of components is a crucial step within the planning process of DH systems, which is closely intertwined with the subsequent network operation. Therefore, as a reference for consecutive investigations, the main steps for dimensioning the key components of TDH networks will be briefly outlined in the following. For more details, it can be referred to Ref. [27].

1. Determine boundary conditions:
   Initial planning steps involve identifying connection points and identifying expected loads, incl. their technical requirements.

2. Network architecture decisions:
   Based on the identified boundary conditions, decisions are made on the network type, topology,

substation design, temperature and pressure levels. For the further dimensioning usually the network temperatures are assumed to be fixed at the design temperature levels.

3. Determine design volume flows:
Knowing the max. thermal power to be transported trough each network segment and the intended temperature levels for supply and return lines, the necessary design volume flows can be determined using Equation 3.10. Due to the unidirectionality of TDH networks, the hydraulic circuits therein remain static over time. That means the network critical point remains at the same location in the network. Each specific network segment belongs to a fixed hydraulic circuit. Each hydraulic circuit comprises the central pumping station and a consumer substation. Due to the static hydraulic circuits in TDH networks, the heat transfer capacity for each network segment can be easily ascertained by summing the peak loads of the consumers.

4. Determine pipe diameters:
Knowing the design volume flows for each network segment, the pipe diameters of each segment can be determined. Therefore, a maximal flow velocity and a maximal pressure gradient along the pipes is assumed. Depending on the specific case, one factor or the other is limiting, the assumed values vary depending on the type of pipe and fluid. It is typical, that in radial networks, pipelines taper as they extend further from the central power plant, reflecting a diminishing need to transport power and, consequently, a reduced volume flow for assumed constant temperatures.

5. Dimension CVs in the substation:
Knowing the pipe diameters, the pressure drops in all hydraulic circuits without installations can be calculated for the design volume flows. Assuming a certain valve authority, the necessary pressure drop across the CVs in the substations can be determined and suitable CVs can be chosen from manufacturers' catalogues. Advanced systems utilize pressure-independent control valves or combination valves, where the concept of valve authority becomes less significant since it consistently remain at a value of 1.

6. Dimension the heat exchangers:
The heat exchangers in the substations can be dimensioned knowing the peak heat transfer of each substation as well as the temperature and pressure levels of the chosen network concept.

7. Dimension the network pump(s):
Knowing the design network flows and the dimensions of all installations (i.e. in the criticial hydraulic circuit), the pump(s) in the central pumping station can be dimensioned. The pump(s) must be able to overcome the pressure difference in the critrical hydraulic circuit, keeping a minimal pressure of $0.7\ bar$ across this substation for all operating points of the network. Further it must be able to provide at minimum the design volume flows in all network branches.

## 3.3 District Heating Classifications and Vocabulary

As mentioned in Chapter 1, DH has undergone an evolution that branched into a wide range of network concepts. In the following, an overview of typical classification approaches for thermal networks and the associated vocabulary is provided. In this context also the terms 'traditional district heating networks', 'smart thermal grids' and 'prosumer-based district heating networks' are allocated within the landscape of thermal network vocabulary.

### 3.3.1 Four Generations of District Heating

Trying to capture the evolution of DH, Lund et al. suggest a classification into generations that is widely recognized and established in the field [2]. Figure 3.7 illustrates the four generations of DH networks, as proposed.

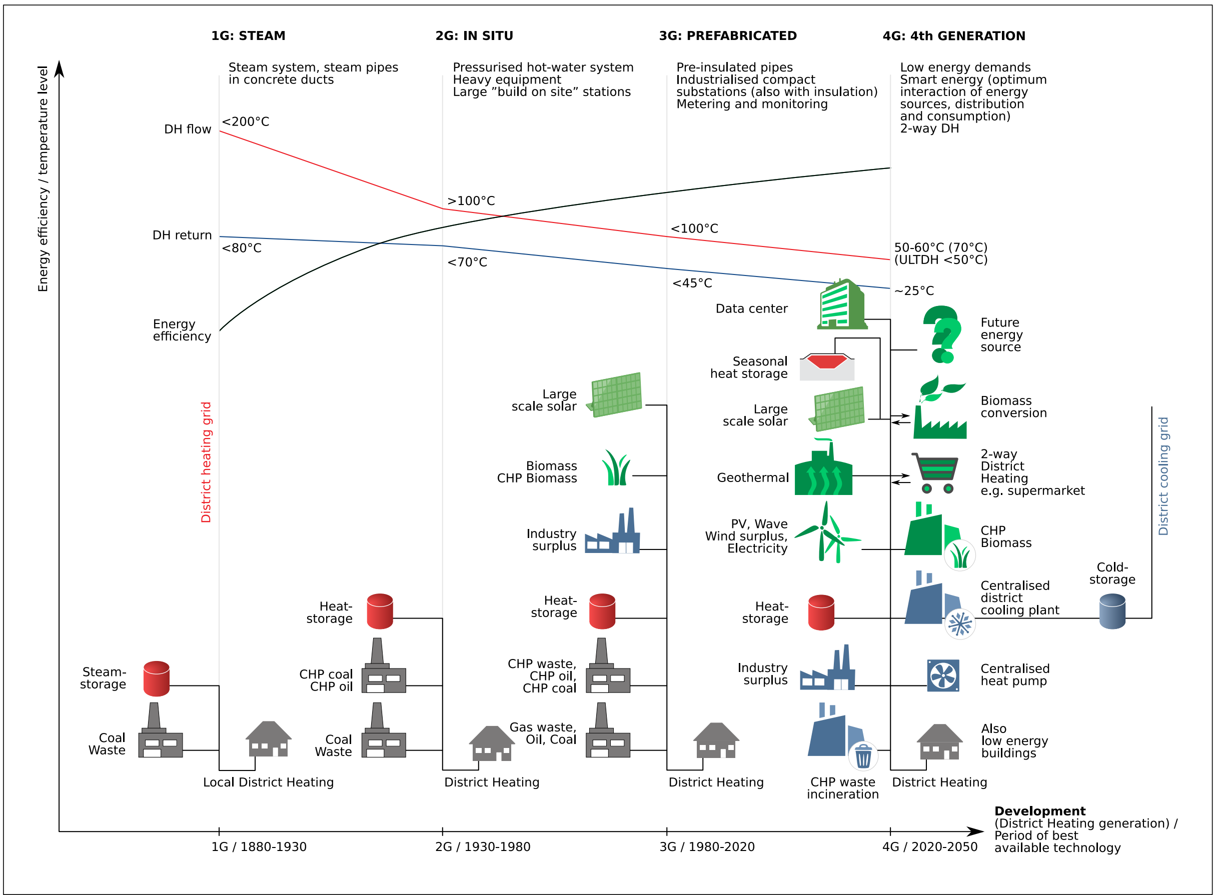


Figure 3.7: Generations of district heating, based on Lund et al. [2]. '5th generation' not included, as term is disputed within the scientific community to be seen in this row of generations.

The development goes from steam-based systems in the first generation district heating (1GDH) transitioning to pressurized water systems above $100\ °C$ in the second generation district heating (2GDH) and to more sophisticated prefabricated systems in the third generation district heating (3GDH), which are the majority of currently operated systems [35], [36]. Traditional district heating (TDH) systems as described in Section 3.2 can also be counted to 3GDH. Networks of the fourth generation district heating (4GDH) are currently being implemented in the field, with a focus on energy efficiency, smart integrated energy systems, and the utilization of locally available renewable energy sources. General trends across the generations are the decrease of system temperatures from above $200°C$ to below $50°C$ and the accompanying increase in energy efficiency of the systems. The driving factors contributing to the reduction in system temperatures include the aim to utilize low-temperature heat sources, minimize heat losses to the environment, and decrease the need for insulation materials, thereby reducing overall costs. Ref [37] gives an overview on the current landscape of existing DH systems in Germany.

### 3.3.2 District Heating and Cooling and the Fifth Generation

Analogous to DH networks, there are also district cooling (DC) networks, although they are significantly less common. The physical principles and functionalities of DH and DC networks are very similar. In line with the categorization of DH, network-based cooling supply is also classified into generations, as proposed by Ostergaard et al. [38]. Cooling constitutes a significant portion of the

final energy consumption. It is expected that this share will increase drastically, driven by increasing personal comfort requirements and not least by climate warming [39], [40].
The development of DH and DC generations proceeded largely independently of each other, despite potential parallels. Only in the most recent generations, there are overlaps in the form of thermal networks that are utilized for both heating and cooling purposes, forming the branch of 'district heating and cooling (DHC)' (or less common 'combined heating and cooling (CHC)').

In this context, building on the categories for DH by Lund et al., the 'fifth generation district heating (5GDH)' or often also 'fifth generation district heating and cooling (5GDHC)' is widely addressed in literature [41]–[50]. The distinctive feature that is named in literature as a defining characteristic of 5GDHC systems is the simultaneous supply of heating and cooling by the same network, using power-to-heat technologies. To enable this, the network temperatures are very low, typically around $-5\ ^{\circ}C$ to $20\ ^{\circ}C$ [45]. So called booster heat pumps (BHPs) that are distributed in the substations are able to use these temperature levels as a source or sink. For heat consumers (= cold producers), the network is warm enough to drive the evaporation process of the BHP operating in heating mode to satisfy the consumer's heat demand. For cold consumers (= heat producers), the network is cold enough to satisfy their cold demand via a direct heat exchanger or the network can be used to re-cool the condenser of a HP in the substation, that operates in cooling mode.
The survey in Ref. [45] covers 53 networks of the latest 5GDHC category in germany and notes that these are primarily planned for small, newly built districts with fewer than 100 buildings. This may be attributed to the fact that older buildings in existing neighborhoods cannot consistently cope with the lower temperature levels, and retrofitting BHPs is cost-intensive. Further, several reviews note that the co-occurrence of heating and cooling demand is crucial for a cost-efficient operation of 5GDHC networks [41], [47], [49].

Lund et al. argue that the term '5GDHC' is "misleading as it renders the intuitive perception that a transition towards 5GDHC systems is a progression. However, improved system energy efficiency is not given for a transition from 4GDH to 5GDHC, which is generally the case for a transition towards 4GDH from a previous generation." (Lund et al., [51]) Also, the authors fear an "inflation of generations". Therefore, the authors promote to see 4GDH and 5GDHC as parallel development paths or "sibling[s] in the larger 4GDH family".

### 3.3.3 Smart Thermal Grids and Prosumer-based Networks

As can be seen, the terminologies in the growing field of heating and cooling networks are not yet firmly established and standardized. For both, 4GDH and 5GDHC, a common overarching aim is the decarbonization through smart energy usage within a thermal network with distributed sources and sinks. Within the context of this dissertation, 4GDH and 5GDHC are seen as manifestations of the abstract construct of smart thermal grids, as introduced in Chapter 1. Allocating the presented PBDH networks in this terminology landscape, they can be categorized as a special case of 4GDH systems, thereby being also a subcategory of smart thermal grids. The network behavior can be assumed to be similar in 4GDH and 5GDH with regard to the feed-in and extraction of bidirectional heat flows. Even without BHPs, heat producers in PBDH networks are at the same time cold consumers, but at a higher temperature level than in 5GDHC. This again demonstrates the closeness of the concepts of 4GDH and 5GDHC.

Just like the term 'prosumer-based district heating networks', there are other terms for specific thermal network types in the literature, which emphasize a certain network feature. Most often, this refers to the temperature levels. This is the case, for example, with 'low temperature district heating (LTDH)', 'ultra low temperature district heating (ULTDH)' or so-called 'ambient networks (AN). All these terms and network types can be summarized under the collective term 'smart thermal grids' and assigned to generations depending on their specific characteristics. Ref. [36] investigates network configurations for implemented low-temperature DH systems and finds that by far the most low-temperature networks still follow the classic network configuration with a central heat source and passive consumer substations.

The absence of a uniform international vocabulary for DHC is not limited to network types but also affects technical terms in this field, as highlighted by Sulzer et al. [52]. One example for this are energy and mass flows whose direction of flow can or cannot reverse over time. For these phenomena, terms such as 'unidirectional' vs. 'bidirectional' as well as 'directed' vs. 'undirected' are used. Some authors include both mass and energy flows when referring to bidirectionality, while others only refer to one or do not provide a precise definition. In the context of this dissertation, 'bidirectional' pertains to both energy and mass flows, encompassing interactions within the network as well as between prosumers and the network.
Similarly, the term 'prosumer' is used in different meanings. In some publications, it refers to network participants which necessarily switch between feeding-in and extracting power over time. In other instances, 'prosumer' is used as a synonym for decentralized producers, while elsewhere, it serves as an umbrella term for any type of network participant. For the purposes of this dissertation and in the context of PBDH, 'prosumer' is understood as a participant capable of switching between production and consumption modes, as this represents the most general perspective.

# Chapter 4

# Related Methods and Research Fields

This dissertation is situated within an ecosystem of interrelated methods and research fields. To delineate the scope and significance of the dissertation, this chapter dives into relevant related methods and areas of research. Thereby, in this chapter specific research gaps in existing literature are underlined that motivated the RQs introduced in Section 2.2 and will be addressed by this dissertation. More context and in-depth literature reviews will be given in the respective publications of this cumulative dissertation.

## 4.1 Coordinated Network Operation for Systemic Synergy Exploitation

As discussed in Section 2.1, some kind of coordinating management of the diverse network participants is necessary in order to leverage the potential systemic synergies in smart thermal grids. Some DERs can be controlled, while the availability of others is subject to fluctuations and uncertainties, being particularly true for renewables and waste heat. Storage allows for the temporal decoupling of demand and supply, thereby enabling more flexible timing in generation. At the same time, each source has unique features, such as production costs, efficiency and $CO_2$ emissions. Therefore, some supply options might be prioritized over others, however this can change dynamically based on changing conditions such as availability or prices. Using these degrees of freedom, an optimal trajectory for the collective operation of the available sources has to be determined to maximize the efficiency of overall network operation with respect to objectives and under the consideration of diverse constraints.

### 4.1.1 Methods from Power Engineering

This problem has a long history in the field of power engineering in the context of plant operation planning [53]. As the idea of smart thermal grids itself, according methods for handling the degrees of freedom are adopted and adapted by the DH community. Mathematical optimization is the prevalent tool to automatically identify the optimal operation trajectory. The economic dispatch is focused on the short-term operational decision of how to allocate power generation among online units to meet the current demand at the lowest cost, given their operational constraints. It assumes that certain power generation units are already running and seeks to optimize their output levels. Unit commitment (UC) problems are a step before economic dispatch, dealing with the longer-term decision of which power generation units to turn on or off over a future time horizon, typically spanning from a few hours to several days. It considers factors such as start-up costs, shut-down costs, and minimum up/down times of units. Once the units to be run are determined, economic dispatch then optimizes their output. Optimal power flow (OPF) goes a step further by optimizing the power flow in the transmission network to meet the demand at the lowest possible generation cost while ensuring network constraints (like voltage limits and line capacities) are not violated. It integrates the decisions made in UC and economic dispatch with the physical realities of the power grid, ensuring that the electricity is not only generated economically but also transmitted efficiently and safely.

A more distributed approach is the concept of local energy markets (LEMs), where each network participant is an agent in the market. Through supply and demand offers combined by a market-clearing algorithm, it is determined how much power each participant exchanges over the network during the planning horizon [54], [55]. This kind of planning replaces the need for solving a centralized, omniscient UC problem or economic dispatch. LEMs often include considerable community involvement, making them closely related to the context of energy communities [56], which are citizen-driven collectives promoting clean energy actions while optimizing community welfare. To steer the market actions of the agents and increase granularity, in the electricity sector the concept of distribution locational marginal prices (DLMPs) emerged (e.g. [57]). Essentially, DLMPs represent the value or cost of electricity at specific locations within a power system, taking into account the operational constraints and conditions of that system.

### 4.1.2 Optimal Operation with Model Predictive Control

Model predictive control (MPC) is the basis for optimal network operation using mathematical optimization [58]. Therefore, an appropriate system model is needed, that predicts the future system outputs, depending on the inputs and boundary conditions (disturbances). Such a model can be based on physical laws, empirical data, or a combination of both. With an appropriate system model, MPC allows to anticipate forecasts for uncertain conditions, such as prices, consumption, or renewable generation, in the calculation of optimal power flows. Concerning the integration of the system model into MPC, two variants can be distinguished: internal and external system models. Figure 4.1 compares the control loops for both variants.

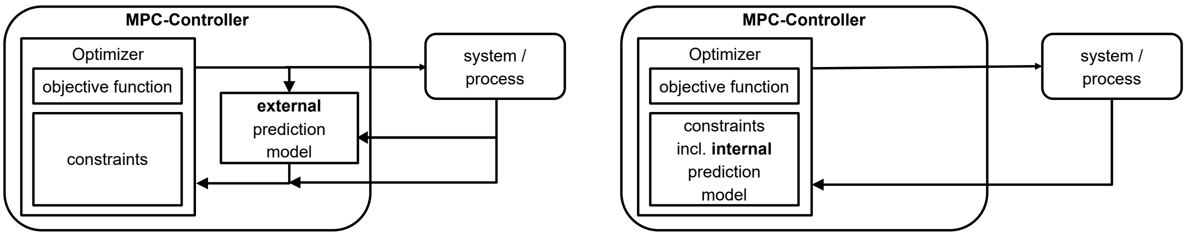


(a) MPC control loop with external system model for prediction.

(b) MPC control loop with internal system model for prediction in the constraints of the optimizer.

Figure 4.1: Comparison of internal and external system models for prediction in the context of an MPC control loop.

Internal prediction models are embedded in the constraints and thereby part of the optimization problem itself. This allows to exploit the known mathematical structure of the model (linear, mixed integer linear, mixed integer quadratic etc.) using dedicated solvers for the specific type of problems. On the other hand, the internal models are mostly simplified by assumptions to a mathematical optimization problem with a structure that can be solved analytically. The analytical solution has the advantage of some guaranteed properties, such as algorithm convergence or global optimality, which cannot be guaranteed with heuristics or without knowing the mathematical structure of the model. External prediction models are treated as blackboxes and iteratively evaluated by the optimizer. Therefore, the external models can by arbitrarily complex, as only the in- and outputs are relevant for the optimizer. Here often co-simulations are used. For optimizing, either assumptions on state space properties of the modelled system (e.g. convexity) or heuristic solvers are needed due to the unknown structure of the external prediction model.

A widespread language to create external system models or 'digital twins' of technical systems is Modelica[1]. Distinguishing features of Modelica are, that it supports multi-domain modeling (electric, mechanical, hydraulic, thermal elements etc.), it is object-oriented, it follows an acasual modeling paradigm (therefore featuring bidirectional relationships), it is able to model dynamic system behavior, relies on an open standard and comes with a free standard library including basic component models. Dymola[2] and SimulationX[3] are common modeling and simulation environments that utilize the Modelica modeling language and provide user-friendly graphical modeling interfaces. Alternative software environments to Modelica are IDA ICE[4], TRNSYS[5] and Simulink[6] with Simscape[7]. Each of them having their distinct advantages and disadvantages, which are not elaborated here for the sake of brevity.

## 4.2 Thermal Network Modeling

In the field of thermal network modeling, four main purposes of modeling can be distinguished:

- investigations on benefits of innovative network concepts, shown with case studies,e.g. [59]–[61],
- network design optimization, e.g. [42], [62]–[64],
- simulation models used as external models for MPC, e.g. [65], [66],
- mathematical models as internal system models for MPC, e.g. [67], [68].

Since PBDH networks are an archetypal form of smart thermal grids, primarily serving research purposes, there are no dedicated models for this type of networks so far. Existing thermohydraulic network models mostly assume traditional networks as context, including central units, such as pumping stations. Decentral feed-in is only seen as support. These networks show a completely different behavior due to the centralized nature. Most available modelling approaches simplify their model by using one or several of the following assumptions:

- no switching between prosumer modes considered: no real prosumer behavior, only distributed generation
- no actuator behavior considered: no direct relation between control inputs and network states, coupling between volume flows $\dot{V}$ and pressure differences $\Delta p$ over pumps and valves ignored
- heat transfer to/from secondary side not considered: product of variable $\dot{V}$ and $\Delta T$ is relaxed
  - constant network temperatures, variable network flows: ignores the behavior of heat exchangers and the influence of the secondary prosumer side on the network state
  - variable network temperatures, constant network flows: unrealistic, as flows are the controlled variables in the networks

[1] https://modelica.org/ (visited on 2023/10/08)
[2] https://www.3ds.com/de/produkte-und-services/catia/produkte/dymola/ (visited on 2023/10/08)
[3] https://www.esi-group.com/products/simulationx (visited on 2023/10/08)
[4] https://www.equa.se/de/ida-ice (visited on 2023/12/13)
[5] https://www.trnsys.com/ (visited on 2023/12/13)
[6] https://de.mathworks.com/products/simulink.html (visited on 2023/12/13)
[7] https://de.mathworks.com/products/simscape.html (visited on 2023/12/13)

- no meshed grid topologies considered: increased complexities due to multiple possible flow paths and resulting hydraulic circuits is ignored

- assuming quasi steady-state: for short discretized time-steps the system is considered to be in steady-state, as the variables change so slowly. This ignores transient system behavior.

This makes the current models not suitable for exploring the RQs outlined in Section 2.2. The main reason is that the use of the aformentioned simplifications in these models does not allow for an in-depth investigation into the relationship between decentralized actuator operation and the overall thermo-hydraulic network behavior, thus failing to address the identified RQs.

## 4.3 Integration of Distributed Sources

Traditional heating networks cater to central generation and unidirectional heat distribution. Bidirectional power flows demand new hydraulic infrastructures. For the integration of distributed generation, substations must be designed to decentrally feed into the network. For prosumers, bidirectional substations are required that allow to reverse the power flow between network and prosumer side depending on the prosumer mode. Decentralized feed-in and bidirectional substations for thermal networks come along with distributed actuators in the substations for network operation. Unlike in centralized TDH, multiple sources and distributed actuators in smart thermal grids are on the same hierarchical level and may mutually influence each other.

Most literature on decentralized feed-in to thermal networks focuses on solar thermal systems [69]–[80]. The investigated solutions are specific to this application context and not universally suitable for prosumers. However, a common feature are distributed actuators, like primary side substation pumps. The scope of this research area is mostly limited to the substations. As a context this research area typically assumes a TDH network, which provides constant boundary conditions for the substation operation in the form of constant primary side inlet temperatures. The effects of decentralized feed-in on the network state and interactions between prosumers through the network remain outside the scope. Nevertheless, several studies point out expected impacts of distributed actuators on the network and expect increased complexities, particularly concerning pressures and temperatures in the context of operation [71], [81]–[83].

In particular, hydraulic challenges are predicted in literature, although the systemic relations have not yet been studied in depth and effects on the thermal behavior have not been focused so far. Ref. [81] states that prosumers influence the pressure state of the whole network and concludes that it is important to investigate the whole DH system not only the local area where prosumers are integrated. Further, Ref. [71] finds that the critical substation changes its location depending on the feed-in point and the demand of other substations, predicting a strong interdependency between the prosumers. Ref. [82] finds that several feed-in points and resulting undirected network flows can lead to locations in the network with zero flow velocity, called supply frontier. Also, Ref. [82] highlights that further investigations on the pressure conditions in the network are necessary for networks with several feed-in points and consumers. Ref. [79] notes that the performance of the system under investigation was significantly lower than expected, because the employed controller for feed-in was not able to handle the variation of the differential pressure between the supply and the return pipe in the DH network under investigation. Ref. [84], [85] suggest that pump interaction via the network together with the fast pressure propagation can lead to unstable pump control.

## 4.4 Research Gaps

There is a substantial amount of research regarding the potential benefits of smartly and comprehensively operating heating networks with DERs and prosumers. Through the use of models, the optimal operation is investigated in particular at the power level. However, when it comes to implementation on the technical level and its practical operation, there are currently no established and universally recognized solutions.

Currently, the operation of smart thermal grids is explored either from the management perspective or from the technical perspective, with minimal intersection between these two fields of study. A smart management calculates abstracted power flows, using methods like UC or OPF. However, due to technical constraints and the system's nonlinear behavior, the underlying models often oversimplify, omitting details that lead to computational challenges incompatible with real-time operation.

Conversely, practical network operation occurs at the field level, utilizing actuators like pumps and valves controlled by local controllers. Traditional local controllers typically target temperatures, flow rates, or pressures, and account for the dynamic behaviors of technical devices. However, they cannot process power setpoints from overarching systems directly. Further, they lack holistic network information, limiting their capacity to anticipate systemic behavior.

The technical integration of distributed sources into thermal networks is mainly tailored to the context of solar thermal plants, without established generalized solutions. The systemic impact of decentralized feed-in and prosumers on the overall technical network state and operation is so far not adressed in literature.

**Research Gaps**

Alltogether, two research gaps can be identified that motivate the RQs introduced in Section 2.2 and drive the investigations of this dissertation.

**Gap1** *In the research on the operation of smart thermal grids, a discrepancy exists between abstract smart management and technical field-level control. While the smart management optimizes power flows by considering systemic synergies, it often omits intricate technical details. Conversely, field-level controls, not designed for derived setpoints like power flows, overlook systemic interplays among participants.*

**Gap2** *Current research lacks a thorough understanding of how distributed actuators in smart thermal grids impact the technical network state. Furthermore, the thermohydraulic interactions among multiple active participants, especially in the context of overall network operation, remain unexplored.*

# Part III
# Prosumer-Based District Heating

# Chapter 5

# District Energy Management

With the goal to automatically exploit network synergies in smart thermal grids between diverse participants and across energy sectors, this chapter discusses in Section 5.1 a suitable control framework for the network operation and addresses an according district EMS in Section 5.2 (Pub1). Thereby, this chapter tackles especially RQ3 from Section 2.2.

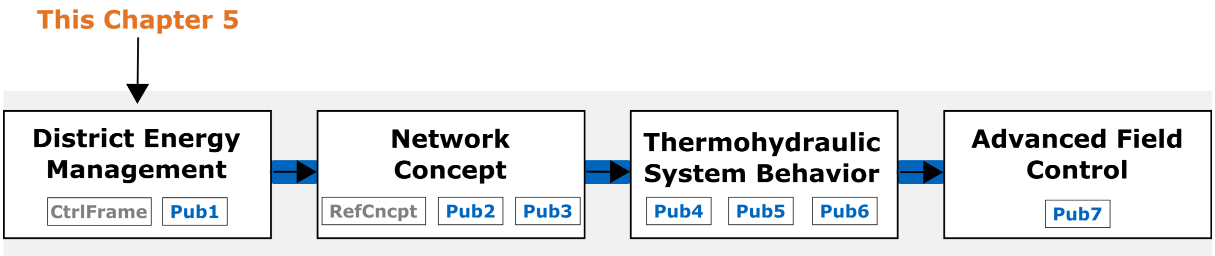


Figure 5.1: Position of this chapter within the overall structure of the main part of this dissertation.

**Chapter 5: District Energy Management**
Two hierarchical control frameworks are proposed for the integrated operation of smart thermal grids: a two-layer approach and a three-layer approach, each featuring a district energy management system (EMS) at the top layer. Therefore, a software tool is developed for optimizing district power flows in interaction with real hardware during live operation. Experimental investigation with the software prototype uncover the limitation of an abstracted view focusing only on power flows. This emphasizes the need for either a more detailed technical model or the consideration of technical details and local dynamics at different control layers. Additionally, the presumption of existing infrastructure for the flexible exchange of thermal energy within districts underscores the need for a hydraulic concept for PBDH networks.

## 5.1 Control Framework

As described in Section 3.2, TDH networks are operated following a 'pull'-oriented philosophy, originating from the demand side. The passive consumers extract heat from the network according to their demand, while the central plant compensates for that. The technical control of the network operation is shared between the consumer substations and centralized units, such as the pumping station and the central plant. The consumers with their substations and the centralized network units are physically coupled via the network, but there is no distinct coordination between them. For smart thermal grids as distributed systems in turn, some kind of overarching management is necessary that coordinates the distributed sources and sinks in order to exploit the network synergies (see Section 2.1).

This raises the question what a suitable control framework for smart thermal grids looks like, that allows to exploit high-level network effects on the one hand, while implementing a technical control on the other hand. Therefore, in the following at first key tasks are identified, which are then merged into a proposed control framework.

Based on the insights from Chapter 1 and Chapter 4 and in light of the RQs, the following key tasks for operating smart thermal grids have been identified:

1. Abstract Network Operation Optimization: High-level, smart coordination of network participants to automatically identify and exploit synergies with the thermal network and in interaction with other sectors.

2. Integration: Ensuring seamless integration into overarching structures, such as billing systems, markets, etc.

3. Prosumer Management: Determination of the demands to be satisfied along with the available capacities and flexibilities of the different prosumers.

4. Technical Constraints: Verification and guarantee of the technical feasibility of abstract network states, considering limitations and anticipating systemic interactions at the technical level (e.g., mutual influences of participants).

5. Dynamic System Behavior: Anticipating the intrinsic and dynamic behaviors of individual components, but also of the overall system for effective control.

6. Implementation: Suitable control of actuators at the field level to technically realize the desired system states.

It shows that the tasks are spread across different levels of abstraction. Therefore, a hierarchical approach is typically used in the operation of technical systems. A common structure is an automation pyramid with the actual hardware at the basis, as illustrated in Figure 5.2.

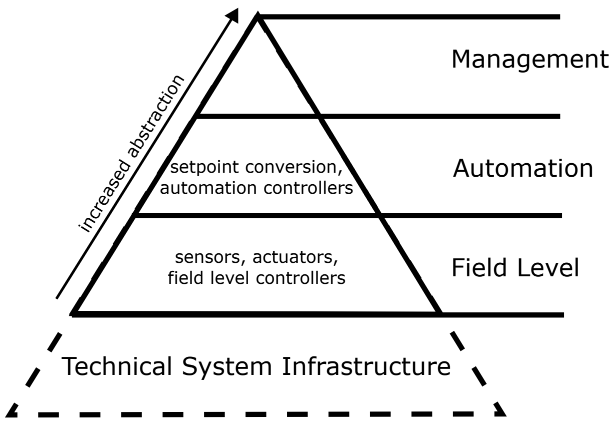


Figure 5.2: Classical automation pyramid, adapted from the field of building automation [86], [87].

Within this automation pyramid, the identified tasks can be allocated to the different layers and organized in task-specific modules. Depending on the chosen framework, each module requires a distinct design and specific interfaces between them. Intuitively, tasks 1 and 2 can be allocated to a smart *district EMS* or a market-based approach. Task 3 necessitates a dedicated prosumer EMS, which is aware of the internal situation of its specific prosumer system and only transmits the information essential for abstract optimization to the district EMS. The prosumer EMS component is excluded in this dissertation, as the focus is on the network side. Intuitively, task 4 can be associated with a more detailed *network model*, which replicates the technical level, thereby permitting the consideration of its restrictions. Task 6 can be assigned to the field level, where controllers interact directly with the hardware. In the context of PBDH networks, the overall system state is exclusively determined by the superposition of the substation operations. Therefore, on the field level the *substation controller* is the mainly relevant component. Task 5 cannot be assigned intuitively and unambiguously: The dynamic behavior can be considered both, at a decentralized field level and within an overall network model. Based on the described modularization of the identified tasks, various operating schemes were considered. Ultimately, two schemes were examined in more detail within the framework of this dissertation (see Figure 5.3).

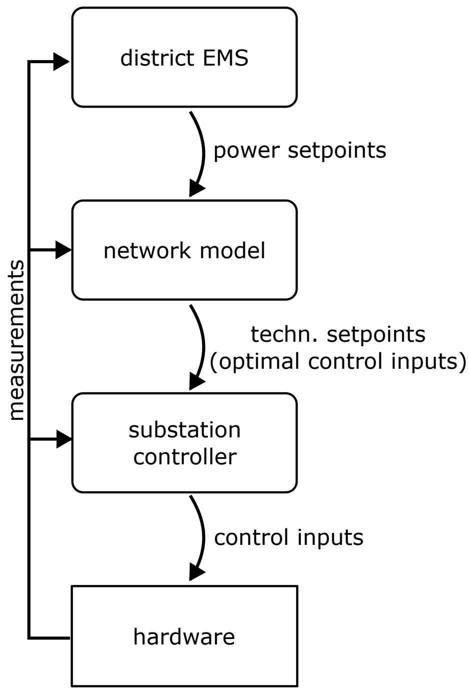


(a) Control framework A with 3 layers: a network model at the middle layer forms the automation layer.

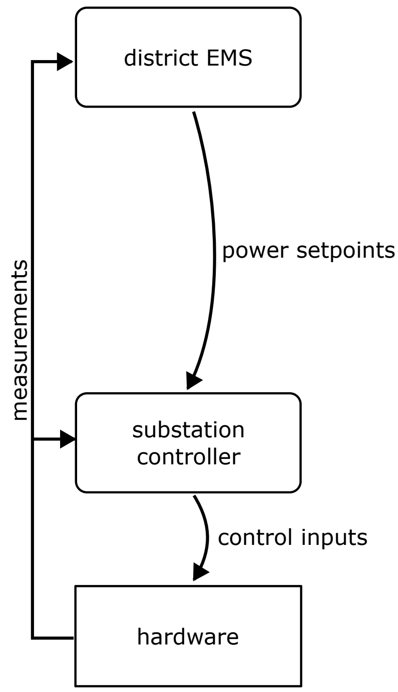


(b) Control framework B with 2 layers and a direct connection between high-level management and field control.

Figure 5.3: Considered control frameworks for smart thermal grids within this dissertation.

In the initial phase of this dissertation, framework A was envisioned, as it follows the three layer structure from the classical automation pyramid (see Figure 5.2). The district EMS, situated at the management layer, is responsible for tasks 1 and 2. A network controller at the automation layer takes over task 4. Meanwhile, the substation controllers at the field layer address tasks 5 and 6.

During the progression of the dissertation, a shift to framework B was made for various reasons, which will be unveiled in the continuation of this dissertation (i.e. in Section 7.4, Section 8.1 and Section 8.2). Framework B is comprised of only two layers: the district EMS remains responsible for tasks 1 and 2. Compared with framework A, framework B is modified, since task 4 is shared between the management and field levels. Tasks 5 and 6 are still managed by the substation controllers at the field level, leaving the automation level unoccupied.

Framework A can be seen as the more centralized version, wherein a central network controller fa-

cilitates the conversion of abstract power setpoints to technical setpoints, while the field level solely implements these setpoints, accounting for local dynamics. In contrast, framework B represents a more distributed version, where the distributed substation controllers on the field level take over also the conversion from abstract to technical setpoints.
The interfaces between the individual levels and modules are highly dependent on the specific characteristics of the modules and how they function internally.

Both structures A and B feature a district EMS, optimizing the overall network operation to leverage synergies amongst participants and across sectors. A digital platform for this purpose is developed in the following Section 5.2.

## 5.2 Pub1: A Digital Platform for Smart Multi-Energy Management in Districts

### 5.2.1 Context

To handle the increased complexity in smart energy systems, higher-level energy management is necessary, as derived in Section 2.1. Traditionally, residential energy management was focused on individual buildings, treating different sectors independently and using rule-based control approaches. Because of this isolated approach, potential synergies are not utilized, plants are often overdimensioned, operate at partial load, resulting in inefficient and uneconomical perfomance.

To leverage synergies across buildings and sectors, both research and industry began to shift towards a more holistic perspective of districts as multi-energy system (MES). There are various specialized tools available for modelling and simulating MES at different levels of detail. These tools can be used to analyse the systems and benchmark the possible benefits. To automatically identify the best operational strategies that leverage systemic synergies, the field of mathematical optimization is dominant, as described in Chapter 4. With the methods and concepts being available, the foundation for optimally operating smart thermal grid is established.

However, for practical application, an interface and compatibility between the theoretical calculations and the real technical system must be guaranteed in order to be able to implement the identified optimal operation strategy. When the work on this dissertation project began, there were only few tools available for this purpose, with no widely-adopted solutions or standards.

Therefore, in the research project 'Multi-Energy Management and Aggregation Platform (MEMAP)'[1], seven partners from industry and research collaborated to develop a digital platform for smart district energy management. The final report of the project consortium can be accessed under https://doi.org/https://doi.org/10.2314/KXP:1839282886 [88].

As application context for the platform to be developed, a neighborhood consisting of diverse buildings with various energy generation devices and different demand profiles is assumed. The neighborhood is assumed to be equipped with the technical infrastructure for flexible electricity and heat exchange between the buildings. Each building is assumed to be equipped with a local EMS and can potentially be a prosumer. The basic idea is to connect the top layers of these local EMS via the digital platform to be developed, in order to smartly manage the energy flows in the district during live operation. Such a

[1] https://www.enargus.de/pub/bscw.cgi/?op=enargus.eps2&q=memap&v=10&id=371648

multi-layer or hybrid approach is proposed or used also in other publications, such as Ref. [32], [89].

Various publications have emerged from the project, which focus on interim stages and individual aspects of the platform development. Ref. [90] focuses on the interconnection of multiple local EMSs to a unified district-level system, employing the Open Platform Communications Unified Architecture Standard (OPC UA)[2], and underscores benefits of the optimization across various buildings and sectors. Further, Ref. [91] augments this framework by including the heat network topology to the problem formulation. A generic hierarchical architecture, pivotal for EMS coordination, is unveiled in Ref. [90], providing a foundational basis for the subsequent software implementation. Along with the district management platform, in the project a user-centric simulation tool was developed to simplify planning neighborhood energy infrastructures, using the same mathematical core. Utilizing this tool, an economic case study for a small village is presented in Ref. [92].
The subsequent Pub1 encapsulates the comprehensive development process of the Digital Platform for Smart District Energy Management. This encompasses the identification of research gaps, conceptualization, modeling, implementation, and validation within a lab environment. The main contribution is that the developed platform prototype is designed for the optimal control of a multi-energy district in real-time operation, while interacting with actual hardware. Thus, the developed platform is suitable as a variant of the district EMS for operating smart thermal grids, as described in Section 5.1.

[2] Standard IEC62541

### 5.2.2 Paper

| | |
|---|---|
| **Title** | **A Digital Platform for Real-Time Multi-Energy Management in Districts using OPC UA: Conceptualization, Modeling, Software Implementation, and Laboratory Validation** |
| **Authors** | Thomas Licklederer, Jan Mayer, Denis Bytschkow, Michael Kramer, Alexandre Capone, Johannes Burger, Markus Duchon |
| **Publication medium** | submitted to *Energy and Buildings*,<br>revision process ongoing at submission date of this dissertation, preprint is accessible online |
| **Copyright** | Included under Elsevier's copyright terms of 2023, which permit the inclusion in a thesis or dissertation provided the thesis is not published commercially. (https://www.elsevier.com/about/policies/copyright, Status: August 2023) |
| **Identifier / URL** | preprint accessible under http://dx.doi.org/10.2139/ssrn.4861866 |
| **Associated repositories** | https://git.fortiss.org/ASCI-public/memap/-/tree/main |
| **Author contributions** | according to the Contributor Roles Taxonomy (CRediT, see [93]) |
| Thomas Licklederer | Conceptualization, Methodology, Software, Validation, Investigation, Writing - Original Draft, Visualization, Project administration. |
| Jan Mayer | Conceptualization, Methodology, Software, Validation, Investigation, Writing – Review & Editing, Visualization, Project administration. |
| Denis Bytschkow | Conceptualization, Methodology, Software, Investigation, Writing - Review & Editing, Funding acquisition. |
| Michael Kramer | Conceptualization, Methodology, Investigation, Project administration, Funding acquisition. |
| Alexandre Capone | Methodology, Investigation, Writing - Review & Editing. |
| Johannes Burger | Software, Investigation, Writing - Review & Editing. |
| Markus Duchon | Writing - Review & Editing, Supervision, Project administration, Funding acquisition. |

# A Digital Platform for Real-Time Multi-Energy Management in Districts using OPC UA: Conceptualization, Modeling, Software Implementation, and Laboratory Validation⋆

Thomas Licklederer[a,∗], Jan Mayer[b], Denis Bytschkow[c], Michael Kramer[d], Alexandre Capone[e], Johannes Burger[f] and Markus Duchon[h]

[a,d,e,f,i] *Technical University of Munich, Center for Combined Smart Energy Systems (CoSES), Lichtenbergstrasse 4a, 85748 Garching, Germany*
[b,c,g,h] *Research Institute for software-intensive systems of the Free State of Bavaria (fortiss), Guerickestrasse 25, 80805 Munich, Germany*

ARTICLE INFO

*Keywords*:
energy management
district
sector coupling
model predictive control
platform
synergies

ABSTRACT

Traditionally, energy management in the building sector takes place at the device or at the building level, different forms of energy are treated separately and rule-based methods are used for automation. However, this isolated approach leaves many synergies between buildings and sectors unexploited. Therefore, in the paper at hand a digital platform solution is developed for smart multi-energy management in districts during live operation. The platform interconnects local building energy management systems (EMS) and performs a sectorcoupled optimization of electrical and thermal power flows with respect to the economical or ecological performance of the overall district. The core is a model predictive controller (MPC) reading the charging states of storages and sending optimized power setpoints to all devices. The MPC approach allows to proactively consider forecasts of time-varying boundary conditions and to exploit storage flexibilities. Generic models allow to represent the most relevant device classes of districts with low parametrization effort. The mixed-integer linear optimization problems (MILP) are automatically formulated and solved in a Java-based actor framework. For communication, the OPC UA standard is combined with a customized information model and specific communication sequence. Experiments with real hardware devices in a realistic laboratory environment validate the functionalities of the open-access platform prototype. The proposed concepts for district energy management systems serve as a reference and foundation for related projects, promoting more sustainable district operation in the future.

## 1. Introduction

For the decarbonization of the energy system, the energy supply of buildings plays an important role, as buildings are responsible for 40% of the energy consumption and 36% of greenhouse gas emissions in the EU [1]. Existing energy management systems mostly operate at the building level, treating different energy sectors separately and often relying on simple rule-based control structures [2, 3]. Due to this isolated approach, possible synergy effects are often unused, plants are oversized, operate at partial load, are inefficient and uneconomical.

In future, buildings are expected to satisfy the local demands for electricity, heating and cooling in an economically and ecologically efficient manner, while being an active part of an integrated and sustainable energy system [4, 5, 6, 7]. Achieving this requires a holistic view of districts as interconnected multi-energy systems (MES) [8]. Such an approach enables the exploitation of two types of synergies. Firstly, synergies can be harnessed among buildings with different load profiles, generation capabilities, and storage potentials [9]. Secondly, synergies can be used between the electricity and heat sectors, facilitated through technologies such as combined heat and power units (CHP) or heat pumps (HP) [10]. Advanced control algorithms can unlock additional efficiency potential by proactively considering forecasts for time-variable boundary conditions and leveraging flexibilities [11]. Therefore, various modeling approaches and tools have been developed to investigate districts as integrated multi-energy systems [12, 13, 14, 15, 8].

However, transferring the advantages of holistic district operation from simulations to practical application necessitates a suitable district energy management solution (EMS). Our research project "Aggregation Platform for Cross-Building Optimization of Energy Efficiency" was one of the first to address this gap with the idea to interconnect and coordinate local building energy management systems by a central software platform (see Fig. 1). The primary objective is to achieve economic and ecological improvements in the overall energetic operation of a district compound compared to the individual operation of its constituent buildings. To fulfill this objective, we have identified several requirements for a suitable district EMS:

- overarching management: optimize power flows across buildings and sectors
- predictive optimization: automatically exploit time-varying boundary conditions, such as variable prices and volatile renewable generation

⋆The paper content was developed within the research project "Aggregation Platform for Cross-Building Optimization of Energy Efficiency", funded by the German Federal Ministry for Economic Affairs and Energy (FKZ:03ET1413)

∗Corresponding author
thomas.licklederer@tum.de (T. Licklederer)
ORCID(s): 0000-0002-9525-418X (T. Licklederer)

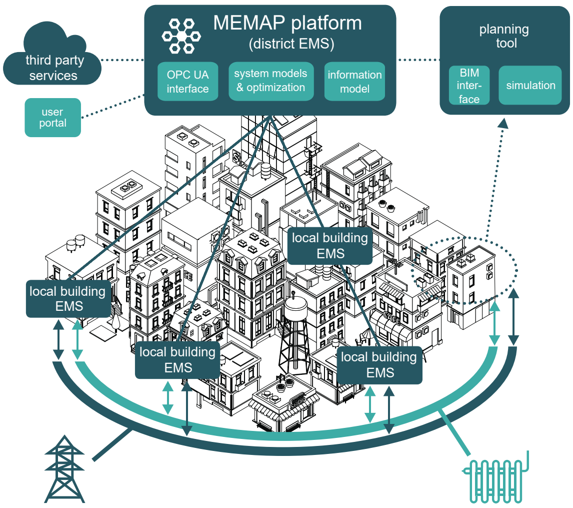


**Figure 1:** Concept of the MEMAP platform as central district energy management system, interconnecting local EMSs. Adapted from [16].

- live operation capability: adaptive and automated optimization process during live operation of the district
- interoperability: communicate with common hardware in the field
- universality, transferability and scalability: ready for diverse settings, from a few connected devices to complex district structures with a variety of device types
- interfaces and usability: connection to third-party services, easy to set up and operate for users

Adressing these requirements, we developed the "Multi-Energy Management and Aggregation Platform" (MEMAP platform). This paper provides a comprehensive description of the platform's complete development path, combining state-of-the-art research from various areas and bringing it into practical application. The insights, concepts, and conclusions derived from this process can serve as a valuable reference for similar or subsequent projects. Additionally, the source code of the MEMAP platform's software framework is openly accessible at `https://git.fortiss.org/ASCI-public/memap`.

The remainder of the paper is structured as follows: Section 2 outlines the state of the art in thematically relevant areas, forming the basis for this work. Section 3 explains underlying assumptions and concepts of the platform development, thereby also defining the scope of this paper. Section 4 details the system modeling as foundation of the platform. Section 5 presents the software implementation of the provided prototype. Section 6 describes the validation of the prototype and its underlying concepts through laboratory experiments with real hardware. Finally, Section 7 summarizes the findings and contributions, providing a conclusion to the paper.

## 2. Background

This section reviews references from literature to provide background information on various aspects that are relevant to the development of the platform solution in this paper.

### Building Management Systems

Traditional control of the energy infrastructure in buildings involved decentralized manufacturer-specific software or integration into a higher-level building automation and control system for larger complexes [17]. Building automation systems vary widely, often being specific to manufacturers and lacking compatibility [3]. These systems typically follow a three-layer architecture: management layer, automation layer, and field layer [18]. This architecture allows in principle to connect at the management layer and send setpointsfrom the central district energy management system that replace the on-site decision-making. In the traditional approach, different aspects such as heating, ventilation, lighting, and alarms are treated separately, resulting in separate management of energy sectors [2]. The control logic at the automation level is usually rule-based and implemented by embedded controllers at the field level, defining setpoints for temperature limits, valve openings, and switch-on/off processes [2, 3]. Reactive logic links setpoints with internal system states and external conditions, like ambient temperature. While schedule-based control is common, proactive behavior is not yet widespread in existing buildings. However, modern systems incorporate proactive measures by utilizing weather forecasts or occupancy predictions to efficiently prepare inert systems such as thermally activated components [19, 2]. Further, there is a shift of operating buildings as an integrated part of neighborhoods [20].

### Multi-Energy Systems

In the transition towards sustainable energy systems, buildings are now seen as part of a smart multi-energy system (MES) instead of standalone entities [4, 11]. MES involve the integration of various energy forms (electricity, heat, cooling, fuels, and transportation) at different levels (neighborhoods, districts, cities, or regions) [6, 7, 21]. The concept of multi-energy prosumers, that can both consume and provide different forms of energy, is gaining attention. Buildings equipped with generation and storage devices can act as prosumers within a district, contributing to the overall energy system when needed. The holistic approach of smart MES enables optimization by considering multiple sectors and buildings simultaneously, leading to synergy effects.

In optimization theory, the optimized performance of a combined system is a best-case benchmark for the total of the optimized performances of its individual parts. Case studies have shown that cooperative optimization and operation of districts as MES can lead to energy cost reductions. Ref. [9] achieved up to a 15% reduction in energy demand costs through district optimization compared to selfish optimization. Ref. [11] reports a 3-6% cost reduction by using a district energy management system based on Model Predictive

Control (MPC) instead of conventional strategies. However, the quantitative benefits of a district-level approach largely depend on specific conditions such as device configuration, demand structure, and pricing.

Therefore, mathematical models are used to explore different scenarios and improve existing settings. The energy hub approach is a commonly used modeling technique for MES, representing energy conversion in devices using linear relationships between power flows [14]. This allows for simulation, optimal power flow calculations, and incorporating device connections. Several software frameworks specialize in modeling and simulating MES at different levels of detail. Examples include commercial tools like TOP-Energy [22, 23] or nPro [24] specialized for district heating systems, as well as open-source tools like MESMO [25, 26], MESCOS [27], and urbs [28] - each with their specific features and focuses.

The assumption that appropriate hardware and infrastructure is installed for bidirectional power flows of heat and electricity, is widespread in the field of MES modeling. However, in particular for the thermal sector, networks enabling flexible and dynamic bidirectional heat exchange between prosumers are not yet widely implemented and still under research [29, 30].

## District Energy Management

Modeling and simulation tools facilitate the exploration and benchmarking of the maximum benefits of a holistic multi-energy system operation. Yet, to leverage these benefits, it's crucial to have suitable district energy management solutions. In general it can be thought of different approaches for a coordinating management in districts: from an omniscient central controller with perfect information on all levels to distributed optimization where only reduced and abstracted information needs to be exchanged [31, 32]. The later covers also market-based approaches, as discussed in Ref. [33]. There are few application-ready district energy management solutions available, most of them commercially sold and operated (e.g. [34]). In parallel to our work, Ref. [35] recently presented the Multi Energy Semantic Platform (MESP) as an open source solution. Another initiative is the openEMS consortium that follows a modular approach, so far focusing on electrical devices and individual buildings mainly. However, to the best of our knowledge, no prevalent district energy management solution (EMS) exists as of now. The lack of established solutions can be attributed to the considerable diversity of energy systems at the district level, which poses a significant challenge in developing a standardized district energy management solution. A major hurdle is the lack of universal communication standards that fit the needs of all local EMS and equipment. This absence hinders the smooth integration and management of different energy assets, limiting the potential gains from a cohesive district energy management strategy.

## Communication and Information models

Communication is essential for the practical application of district energy management, focusing on what, how, and when information is communicated. To ensure that the handled data is unambiguously understood, an information model is the mean of choice. An information models is a conceptual representation that outlines the relationships between data within a specific context, defining its structure, organization, and semantics. The main advantage of such a unified architecture is that stakeholders achieve a common understanding of the data, enhancing consistency, integrity, interoperability, and supporting decision-making processes [36].

Based on that common understanding, communication must occur via a standardized protocol. In the context of Industry 4.0, the IEC62541 standard OPC Unified Architecture (OPC UA) is a robust and secure choice for data exchange [37]. It offers advantages like being open-source, cross-platform compatible, and supporting multiple communication protocols including TCP/IP, UDP/IP, WebSockets, AMQP, and MQTT. It also emphasizes high security and supports object-oriented information models, facilitating domain-specific standardization. Its compatibility with protocols like BACnet extends its use to building automation [38].

## Model Predictive Control

In the scientific community, model predictive control (MPC) and optimization-based methods are gaining traction in building automation [39, 40, 41]. MPC plans the operation of a system (e.g. a building) over a rolling time horizon using mathematical optimization of a cost function. Its popularity arises from its capability to incorporate state and input constraints along with a suitable performance criterion. To meet the different requirements of short- and medium-term control, co-optimization approaches with different horizons can be chosen [42].

Two types of MPC can be distinguished: approaches with external and internal plant models. External plant models involve iterative interaction of the optimizer with detailed simulation models, and solutions often require heuristic algorithms as no structural information can be exploited. In contrast, internal plant models are integrated into the optimization problem as constraints, allowing exploitation of the mathematical structure (e.g. linear formulation) for efficient solutions to linear, mixed-integer linear, or convex problems. This approach offers convergence, optimality, and traceability guarantees, but often requires major simplifications in the models and lacks modularity. A common challenge with MPC is the modeling effort, which can be mitigated using generic, parametrized models.

## Preceding publications

Preceding publications detail interim stages of the research leading to the platform described in this paper. Ref. [43] integrates multiple EMS into a district-level system using OPC UA architecture and showing optimization benefits across buildings and sectors. Ref. [44] extends this by adding a heat network topology with percentage losses. A generic hierarchic architecture for EMS coordination is

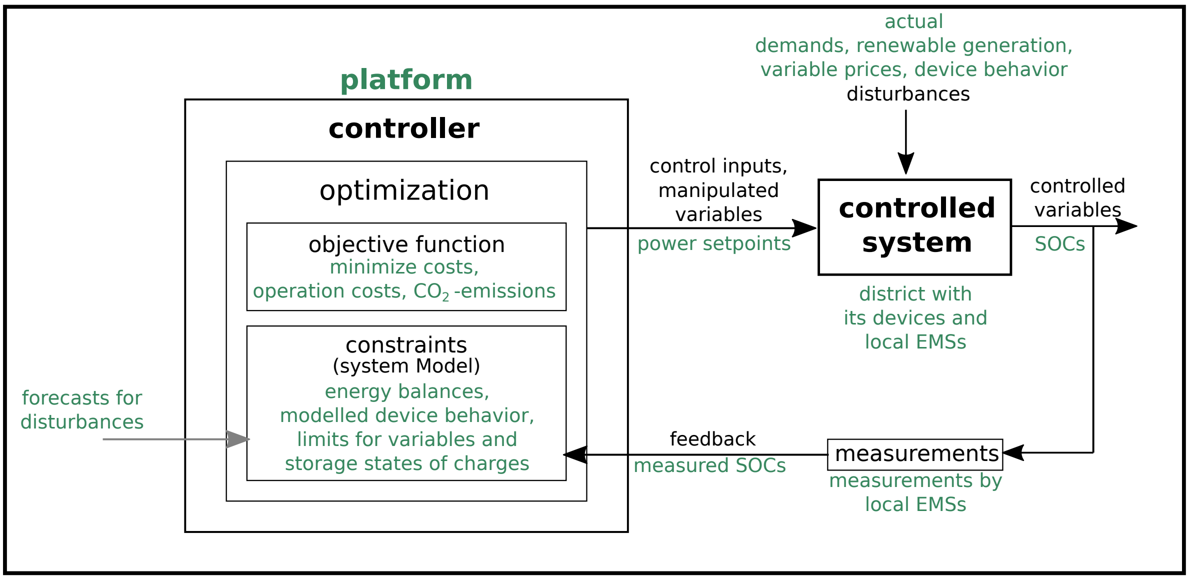


**Figure 2:** The MEMAP platform as model predictive controller (MPC) of a district. In black the general terms of the MPC control loop, in green the respective counterparts in the chosen control approach.

presented in [45], which formed the basis for the software implementation.

As shown in Fig. 1, a user-friendly simulation tool was developed alongside the MEMAP platform, using the same mathematical core to facilitate planning in neighborhood energy infrastructure. An economic case study for a small village using this tool is described in [46]. The platform also allows third-party energy service interactions for forecasting.

This paper provides a comprehensive overview of the full platform development, including underlying concepts, models, software, and validation with real hardware, extending beyond the work in preceding publications.

## 3. Conceptualization

As a basis for the platform development, we define underlying assumptions and our scope of considerations. This defines at the same time limitations of the paper at hand. On this basis, central concepts for the further development are presented: the general control approach and the abstraction to generic device classes.

### 3.1. Assumptions and Scope

As application context of our targeted energy management solution, neighborhoods or districts, organized in energy communities are considered [47]. The buildings in the district have diverse load characteristics and are equipped with different energy generation and storage units. The technical infrastructure facilitating flexible energy exchange between the buildings is assumed to be existing and ready to operate. In particular a suitable thermal network for the bidirectional exchange of heat is required. The thermal network is assumed to be an island grid without a central generation or balancing unit. Further, there is a suitable electric microgrid assumed for the share of electricity between the buildings, including a connection to the public grid. Heat losses in the thermal network are taken into account, while the electrical network is assumed to be lossless. It follows that the topology of the thermal network is relevant in the further considerations, while the topology can be neglected for the electrical grid, where only the cumulative exchange point with the public grid is considered. All participating buildings are assumed to be equipped with local energy management systems (local EMS) that encompass the following functionalities:

- providing a communication interface for district coordination,
- ensuring software compatibility,
- providing information on boundary conditions (i.e. demand and volatile generation) using own algorithms or by acquisition from third parties,
- implementing management setpoints through control of individual devices on the field level,
- measuring technical system states (i.e. in form of storage charging states).

The platform shall be seen as a central district energy management system for the optimization and coordination of the energy flows in a district during live operation. The objective is to optimize the welfare (economic or ecologic) for the district as a whole. Therefore it is assumed that there is no (local) energy market, nor strategic behavior of the participants. Also it is assumed that the legal regulations allow for the flexible exchange of energy between prosumers in the district. For the sake of universality, transferability and scalability, the optimization of the energetic district

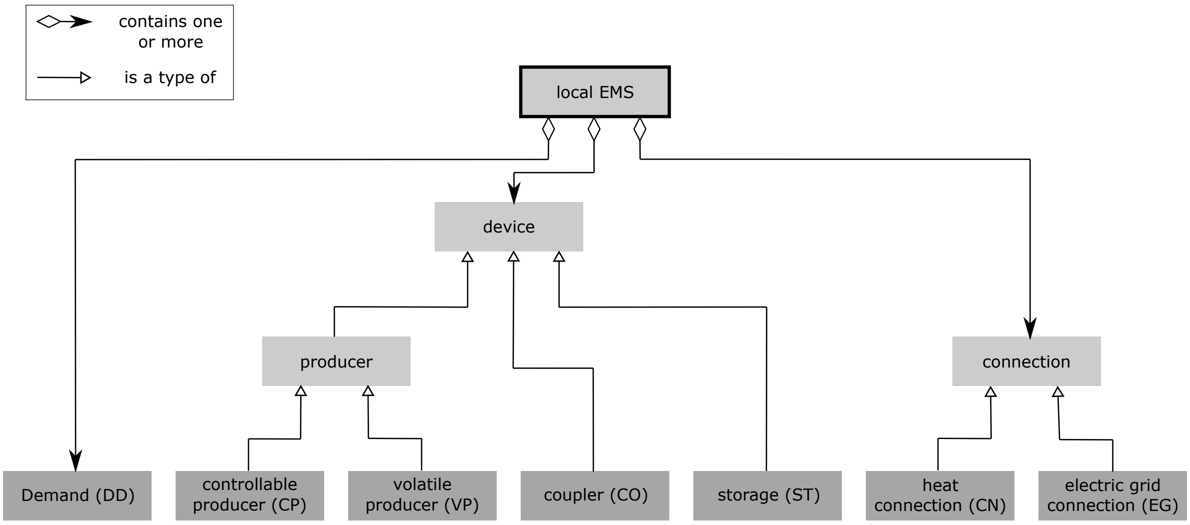


**Figure 3:** Entity-relationship-model of local EMSs and their subclasses.

operation shall be performed at the abstraction level of power quantities and neglect technical quantities, such as voltage or temperatures. Suitable forecasts for boundary conditions (i.e. demand and volatile generation forecasts) are assumed to be available and are not in the scope of this paper.

### 3.2. Control Approach

A model predictive control approach was chosen for the core of the platform, as it intrinsically allows to satisfy the predictive optimization requirement and the live operation capability, as well as the possibility to optimize for economic or ecological objectives. Fig. 2 illustrates the control loop including the platform as controller of the district. The district with its devices and local EMSs forms the controlled system, whose control inputs are power setpoints for the individual devices. The system state is represented by the states of charge (SOCs) of the storages in the district, which are measured in the field and fed back to the platform. From a control perspective, the deviations between the forecasts and the actual values are disturbances to the control system. This refers to demands, volatile generation capacities, time-varying prices, as well as the behavior of the real plants. The platform is an MPC controller with an internal system model (see Section 4.2) embedded in the constraints. The decision variables of the optimization are the power setpoints for the individual devices, as well as their on/off status.

### 3.3. Generic Device Classes

To represent the typical energetic infrastructure of districts and its behavior in a simplified manner, the generic classes are established. They build the lowest level of the tree illustrated in Fig. 3. The two energy sectors heat ($ht$) and electricity ($el$) are considered. Devices and demands (DD) can either be associated with the heat sector or with the electricity sector. The power output of controllable producers (CP) can be set within a certain range using an external input signal. CP can be e.g. gas boilers or electric generators. Volatile producers (VP) can effectively not be controlled, but have production potential that fluctuates over time and may be curtailed. This refers mainly to technologies that use renewable resources, such as photovoltaic panels or solar thermal collector systems. Typical storage systems (ST) on the thermal side are water filled storage tanks as sensible heat storage systems. The equivalent on the electrical side are battery storage systems. Devices of the coupler class (CO) interconnect thermal and electrical power flows. Examples are combined heat and power generation units (CHPs) or heat pumps (HPs). Demands (DD) are forecasts for the expected thermal and electrical demand associated with the respective local EMS. There is a class for the heat connection of the local EMSs. There is one connection instance (CN) per EMS for each connection between two EMSs in the network. The electric grid connection class (EG) represents the connection of the district as a whole to the public grid.

## 4. Modeling

The modeling builds up on the conceptual basis described in the last section. In the following an information model is presented and mathematical models for the relevant technical behavior of the devices as well as their interaction in the multi-energy system of a district are derived. Using them, the optimization problem for the model predictive controller is formulated. In the context of modeling, also the main nomenclature is introduced.

### 4.1. Information Model

An information model as common reference builds the basis for a standardization of the interfaces between the various entities in the district. As the required information for the optimization strongly depends on the used assumptions, models and algorithms, a customized information model was developed for the MEMAP platform. In our definition the information model consists of two parts:

a) entity-relationship-model of local EMSs and their subclasses, see Fig. 3

## Nomenclature

**Abbreviations**

| | |
|---|---|
| $CN$ | heat network connection |
| $CO$ | coupler |
| $CP$ | controllable producer |
| $DD$ | demand |
| $EG$ | electric grid connection |
| $el$ | electricity (sector) |
| $ht$ | heat (sector) |
| $ST$ | storage |
| $VP$ | volatile producer |

**Symbols**

| | |
|---|---|
| $\Delta t$ | discrete time step size |
| $\eta$ | efficiency |
| $d$ | demand |
| $E$ | energy |
| $F$ | forecast |
| $h$ | number of time steps in horizon; last time step of horizon |
| $i$ | discrete time step in horizon |
| $j$ | discrete time step |
| $P$ | power |
| $SOC$ | state of charge of storage |
| $t$ | continuous time |
| $u$ | device setpoint (power) |
| $v$ | losses |
| $x$ | continuous decision variable (power) |
| $y$ | binary decision variable (on[1] / off[0]) |

**Sets**

| | |
|---|---|
| $\mathcal{B}$ | buildings |
| $\mathcal{C}$ | device classes |
| $\mathcal{D}$ | time steps in horizon |
| $\mathcal{M}$ | devices |
| $\mathcal{M}_c^{b,s}$ | devices in district belonging to building $b$, sector $s$ and device class $c$ |
| $\mathcal{S}$ | sectors |

**Matrices and Vectors**

| | |
|---|---|
| $\lambda$ | cost vector |
| $\mathbf{x}$ | vector with decision variables |

**Sub- / Superscripts**

| | |
|---|---|
| $fm$ | from device |
| $to$ | to device |

**Table 1**
Information model - parameters (time-invariant, scalars)

| device | parameter | Symbol | Unit | Range |
|---|---|---|---|---|
| DD | sector | $s_{DD}$ | / | $\{ht; el\}$ |
| CP | sector | $s_{CP}$ | / | $\{ht; el\}$ |
| CP | efficiency | $\eta_{CP}$ | $[-]$ | $\geq 0$ |
| CP | min. power | $P_{CP,min}$ | $[kW]$ | $\geq 0$ |
| CP | max. power | $P_{CP,max}$ | $[kW]$ | $\geq 0$ |
| VP | sector | $s_{VP}$ | $[-]$ | $\{ht; el\}$ |
| VP | max. power | $P_{VP,max}$ | $[kW]$ | $\geq 0$ |
| VP | production costs | $\lambda_{VP}$ | $\left[\frac{€}{kWh}\right], \left[\frac{g_{CO2}}{kWh}\right]$ | $\geq 0$ |
| CO | prim. sector (S1) | $s_{CO,S1}$ | / | $\{ht; el\}$ |
| CO | sec. sector (S2) | $s_{CO,S2}$ | / | $\{ht; el\}$ |
| CO | efficiency for S1 | $\eta_{CO}^{S1}$ | $[-]$ | $]-\infty; \infty[$ |
| CO | efficiency for S2 | $\eta_{CO}^{S2}$ | $[-]$ | $]-\infty; \infty[$ |
| CO | min. power for S1 | $P_{CO,min}^{S1}$ | $[kW]$ | $\geq 0$ |
| CO | max. power for S1 | $P_{CO,max}^{S1}$ | $[kW]$ | $\geq 0$ |
| ST | sector | $s_{ST}$ | / | $\{ht; el\}$ |
| ST | charging efficiency | $\eta_{ST,to}$ | $[-]$ | $[0; 1]$ |
| ST | discharging efficiency | $\eta_{ST,fm}$ | $[-]$ | $[0; 1]$ |
| ST | max. charging power | $P_{ST,max,to}$ | $[kW]$ | $\geq 0$ |
| ST | max. discharging power | $P_{ST,max,fm}$ | $[kW]$ | $\geq 0$ |
| ST | max. capacity | $E_{Cap,ST}$ | $[kWh]$ | $\geq 0$ |
| ST | stand-by losses | $\eta_{ST,sb}$ | $\left[\frac{SOC}{h}\right]$ | $\geq 0$ |
| ST | min. SOC at h | $SOC_{min,h}$ | $[-]$ | $[0; 1]$ |
| CN | losses | $v_{CN}$ | $\left[\frac{1}{100m}\right]$ | $[0; 1]$ |
| CN | pipe length | $l_{CN}$ | $[m]$ | $\geq 0$ |
| CN | max. power | $P_{CN,max}$ | $[kW]$ | $\geq 0$ |

**Table 2**
Information model - forecasts (time-variant, arrays)

| device | input | Symbol | Unit | Range |
|---|---|---|---|---|
| DD | demand forecast | $d(i)$ | $[kW]$ | $\geq 0$ |
| CP | production costs | $\lambda_{CP}(i)$ | $\left[\frac{€}{kWh}\right], \left[\frac{g_{CO2}}{kWh}\right]$ | $\geq 0$ |
| VP | forecast max. production | $F_{VP}(i)$ | $[kW]$ | $\geq 0$ |
| CO | production costs | $\lambda_{CO}(i)$ | $\left[\frac{€}{kWh}\right], \left[\frac{g_{CO2}}{kWh}\right]$ | $\geq 0$ |
| EG | grid sell revenue | $\lambda_{EG,to}(i)$ | $\left[\frac{€}{kWh}\right], \left[\frac{g_{CO2}}{kWh}\right]$ | $\geq 0$ |
| EG | grid buy costs | $\lambda_{EG,fm}(i)$ | $\left[\frac{€}{kWh}\right], \left[\frac{g_{CO2}}{kWh}\right]$ | $\geq 0$ |

b) data model specifying and structuring the relevant data points, see Table 1 to Table 4

The generic classes introduced in Section 3.3 build the lowest level of subclasses of the entity-relationship-model for local EMSs.

The information model additionally comprises different data points associated with these classes. The data model associates a minimum required set of data points with each generic class. Further it groups the data points according to their type (time-dependency and format). The data points can be divided into four categories:

- parameters (Table 1): time-invariant, scalars, often nominal technical specifications of the devices
- forecasts (Table 2): time-variant, arrays, represent the dynamic constraints for the iterative optimization in live operation

**Table 3**
Information model - setpoints (time-variant, scalars)

| device | parameter | Symbol | Unit | Range |
|---|---|---|---|---|
| CP | power setpoint | $u_{CP}$ | $[kW]$ | $\geq 0$ |
| VP | power setpoint | $u_{VP}$ | $[kW]$ | $\geq 0$ |
| CO | power setpoint heat | $u_{CO}^{ht}$ | $[kW]$ | $\geq 0$ |
| CO | power setpoint electricity | $u_{CO}^{el}$ | $[kW]$ | $\geq 0$ |
| ST | charging power | $u_{ST,to}$ | $[kW]$ | $\geq 0$ |
| ST | discharging power | $u_{ST,fm}$ | $[kW]$ | $\geq 0$ |
| CN | heat feed-in | $u_{CN,to}$ | $[kW]$ | $\geq 0$ |
| CN | heat extraction | $u_{CN,fm}$ | $[kW]$ | $\geq 0$ |
| EG | electricity buy community | $u_{EG,to}$ | $[kW]$ | $\geq 0$ |
| EG | electricity sell community | $u_{EG,fm}$ | $[kW]$ | $\geq 0$ |

**Table 4**
Information model - measurements (time-variant, scalars)

| device | input | Symbol | Unit | Range |
|---|---|---|---|---|
| ST | current SOC | $SOC(i=0)$ | $[-]$ | $[0;1]$ |

- setpoints (Table 3): time-variant, scalars, targeted power values for the next time step for each device, result of optimization
- measurements (Table 4): time-variant, scalars, feedback of the real energy system to the platform

By linking the individual data points to the communication infrastructure (see Section 5.1), they can be automatically identified and assigned by machines and programs using the internally stored information model. As a first step towards this automation, a naming convention was derived from the information model and implemented for the different data points.

## 4.2. Internal System Model

In this subsection the mathematical models are derived that are used as internal system models for the MPC (see Section 3.2). Fig. 4 illustrates the system model used for formulating the optimization problem in the platform.

For the modelling, all devices are uniquely identified with the index $m \in \mathcal{M}$. The set $\mathcal{M}$ of all devices in the district can be further segmented by building $b$, sector $s$ and device class $c$. The according sets with the two energy sectors, all device classes and all buildings in the neighborhood are $\mathcal{S}$, $\mathcal{C}$ and $\mathcal{B}$. For the integration with the MPC approach, the continuous time $t$ is discretized using constant time step size $\Delta t$. This results in the general discrete time steps $j$. The rolling horizon of the MPC comprises $h$ of these general time steps, denoted by $i \in \mathcal{H} = \{1, ..., h\}$. It is assumed that all power quantities are constant over the discrete time length $\Delta t$, in particular this is assumed for the electrical and thermal demands $d^{b,el}(i)$ and $d^{b,ht}(i)$. The setpoints $u$ that were introduced in Table 3 with the information model refer to the output power of the respective devices. To consider the behavior of the devices and the thermal network in form of conversion and transport efficiencies, variables $x$ for the power before conversion / transport are introduced. These are the continuous decision variables of the optimization problem to be formulated for the MPC framework. The decision variables are complemented by discrete optimization variables $y$ for devices that can be off or operate between a minimum and a maximum power.

There are three main aspects of the overall system to be modelled: energy balances, power conversion by the devices and the network behavior. In order to obtain a problem formulation that is computationally easy to handle, a mixed-integer linear (MILP) model formulation is used. The device models and in particular the model for the coupler class are inspired by the energy hub approach (see Section 2) and follow a quasi-stationary approach, therefore do not cover dynamics.

### 4.2.1. *Energy balances*

Due to the constant time step size $\Delta t$, the energy balances can be formulated using power quantities. The balances for the heat and the electricity sector are linked by the device model of the coupler class.

As the electrical grid is assumed to be ideal, all generation and demand is aggregated. The buying / selling is performed as one district from / to the public electricity grid. Electricity balances for the overall district for each time step $i \in \mathcal{H}$ in the horizon are formulated:

$$\sum_{b \in B} \left[ \sum_{m \in \mathcal{M}_{CP}^{b,el}} -u_m(i) + \sum_{m \in \mathcal{M}_{VP}^{b,el}} -u_m(i) + \sum_{m \in \mathcal{M}_{CO}^{b}} -u_m^{el}(i) + \sum_{m \in \mathcal{M}_{ST}^{b,el}} \left(u_{m,to}(i) - u_{m,fm}(i)\right) \right] + \left(u_{EG,to}(i) - u_{EG,fm}(i)\right) = -\sum_{b \in \mathcal{B}} d^{b,el}(i) \quad (1)$$

The thermal network connections are modelled as an incomplete graph. Individual thermal energy balances for each building $b \in \mathcal{B}$ and each time step $i \in \mathcal{H}$ in the horizon are formulated:

$$\sum_{m \in \mathcal{M}_{CP}^{b,ht}} -u_m(i) + \sum_{m \in \mathcal{M}_{VP}^{b,ht}} -u_m(i) + \sum_{m \in \mathcal{M}_{CO}^{b}} -u_m^{ht}(i) + \sum_{m \in \mathcal{M}_{ST}^{b,ht}} \left(u_{m,to}(i) - u_{m,fm}(i)\right) + \sum_{m \in \mathcal{M}_{CN}^{b,ht}} \left(u_{m,to}(i) - u_{m,fm}(i)\right) = -d^{b,ht}(i) \quad (2)$$

### 4.2.2. *Device models*

The device models describe the energy conversion processes for the device classes $CP$, $VP$, $CO$ and $ST$. In particular they relate the decision variables $x$ with the setpoints $u$ and thereby represent the lossy conversion from primary energy to secondary energy. Constant conversion

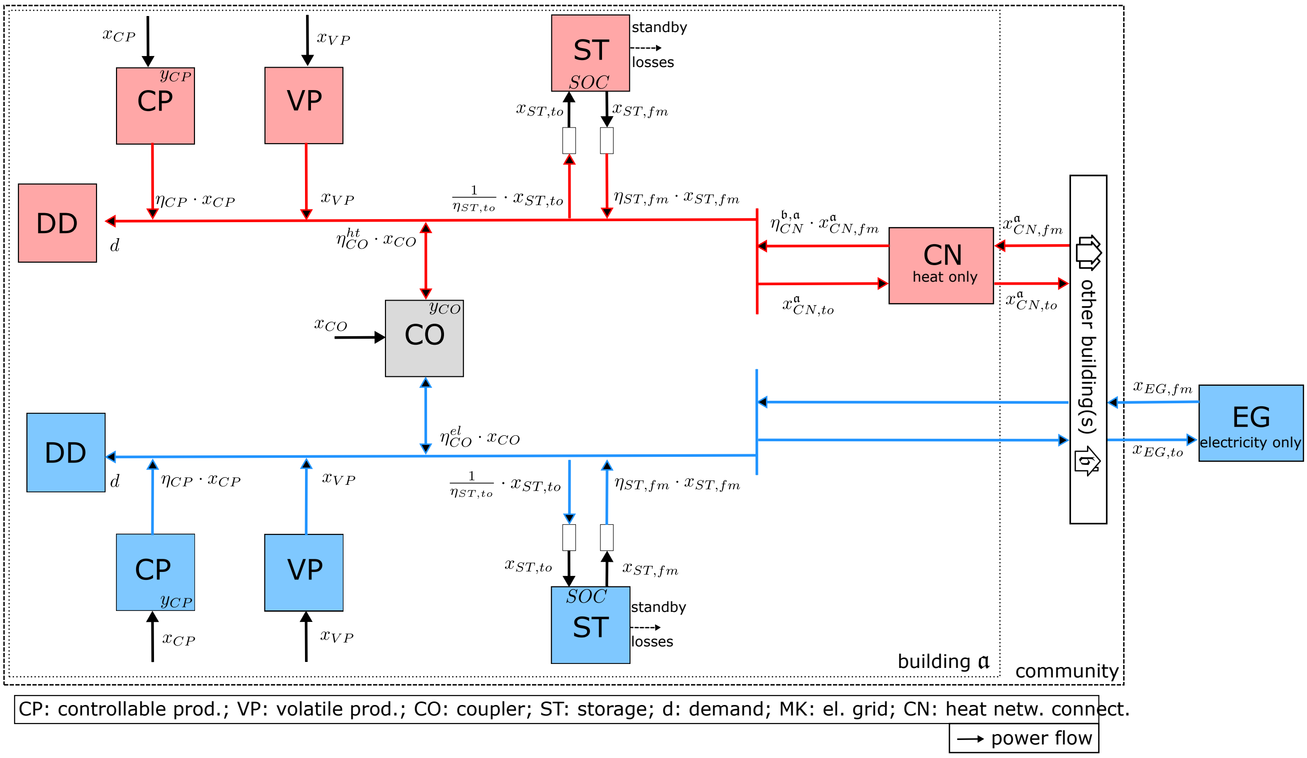


**Figure 4:** Illustration of the considered internal system model in terms of the decision variables $x$, $y$. Heat (top, red) and electricity (bottom, blue) sector are interlinked by the coupler class.

efficiencies are assumed.

### CP, VP and CO

For the classes $CP$, $VP$, $CO$ device specific conversion equations can be formulated for each time step $i \in \mathcal{H}$ in the horizon: For :

$$u_m(i) = x_m(i) \cdot \eta_m \qquad \forall m \in \mathcal{M}_{CP}, \mathcal{M}_{VP} \tag{3}$$

$$\begin{pmatrix} u_m^{ht}(i) \\ u_m^{el}(i) \end{pmatrix} = x_m(i) \cdot \begin{pmatrix} \eta_m^{ht} \\ \eta_m^{el} \end{pmatrix} \qquad \forall m \in \mathcal{M}_{CO} \tag{4}$$

Couplers interlink the electricity and heat sector. For couplers, the continuous decision variable $x$ is the primary energy of one sector (usually $ht$). In the example of a gas-fired CHP unit, the decision variable would be the gas input (primary energy). However, the setpoint for the EMS to control the CHP is usually the thermal or electrical output power, which differs from the gas power decision variable by the respective efficiency. The situation is analogous with heat pumps, where the coefficient of performance (COP) replaces the thermal efficiency $\eta_{CO}^{ht}$, while the electrical efficiency $\eta_{CO}^{el}$ is negative as electricity is consumed.

For more realistic models, the producers' outputs have to be constrained. Volatile producers are constrained by the forecast $F(i)$ for their time-dependent maximum production potential as an upper bound. Zero is set as the lower bound. For each time step $i \in \mathcal{H}$ in the horizon it has to be valid that

$$u_m(i) \leq F_m(i) \qquad \forall m \in \mathcal{M}_{VP} \tag{5a}$$

$$-u_m(i) \leq 0 \qquad \forall m \in \mathcal{M}_{VP} \tag{5b}$$

It is assumed that the forecasts already refer to secondary power, the efficiency of conversion being included. E.g. we assume the maximum thermal power injection from solar collectors to the heating system to be given, not the incident radiant power on the collectors. Due to this assumption the efficiency $\eta_{VP}$ (see Eq. 3) is set to 1. In order to model on/off behavior for production devices in combination with minimum and maximum power bounds, binary variables $y \in 0; 1$ are introduced. For each time step $i \in \mathcal{H}$ in the horizon the following equations must be valid:

$$+u_m(i) - P_{m,max} \cdot y_m(i) \leq 0 \qquad \forall m \in \mathcal{M}_{CP}, \mathcal{M}_{CO} \tag{6a}$$

$$-u_m(i) + P_{m,min} \cdot y_m(i) \leq 0 \qquad \forall m \in \mathcal{M}_{CP}, \mathcal{M}_{CO} \tag{6b}$$

### Storage model

Storage systems are essential for the usage of flexibilities in multi-energy system as they enable the temporal decoupling of energy demand and generation. Therefore, the storage model is a key element. It is the only inter-temporal model that is considered. The energy content of a storage normalized with its maximum storage capacity is called the state of charge (SOC). We use a capacity model for storage units, neglecting further technical details like temperatures or voltages. The energy content is modelled to be influenced by its initial state, the charging and discharging power flows and standby losses. Accordingly the SOC of a storage

$m \in \mathcal{M}_{ST}$ at a certain discrete point in time $j+1$ can be calculated iteratively depending on the quantities of the previous discrete point in time $j$:

$$SOC_m(j+1) = SOC_m(j) + \\ + \left(x_{m,to}(j) - x_{m,fm}(j)\right) \cdot \left(\frac{\Delta t}{E_{Cap,m}}\right) \\ - SOC_m(j) \cdot \eta_{m,sb} \cdot \Delta t \quad (7)$$

The time step length $\Delta t$ is part of the formula for the transition from (constant) power flows to energy content. The efficiency $\eta_{m,sb}$ includes standby losses proportional to the previous SOC. This is especially realistic for thermal storages, where a higher SOC is associated with higher temperatures and therefore higher heat losses to the environment. The relations between the setpoints $u$ and decision variables $x$ comprise charging and discharging losses. For each time step $i \in \mathcal{H}$ in the horizon:

$$u_{ST,to}(i) = x_{ST,to}(i) \cdot \frac{1}{\eta_{ST,to}} \quad (8a)$$

$$u_{ST,fm}(i) = x_{ST,fm}(i) \cdot \eta_{ST,fm} \quad (8b)$$

The charging and discharging power flows of storage systems are bounded for each time step $i \in \mathcal{H}$ in the horizon:

$$u_{m,to}(i) \leq \quad +P_{m,max,to} \quad \forall m \in \mathcal{M}_{ST} \quad (9a)$$

$$-u_{m,to}(i) \leq \quad 0 \quad \forall m \in \mathcal{M}_{ST} \quad (9b)$$

$$u_{m,fm}(i) \leq \quad +P_{m,max,fm} \quad \forall m \in \mathcal{M}_{ST} \quad (9c)$$

$$-u_{m,fm}(i) \leq \quad 0 \quad \forall m \in \mathcal{M}_{ST} \quad (9d)$$

Based on Eq. 7, composite parameters can be defined:

$$\alpha_m := 1 - \eta_{m,sb} \cdot \Delta t \quad (10)$$

$$\beta_{m,to} := \frac{\Delta t}{E_{Cap,m}} \cdot \eta_{m,to} \quad (11)$$

$$\beta_{m,fm} := \frac{\Delta t}{E_{Cap,m}} \cdot \frac{1}{\eta_{m,fm}} \quad (12)$$

This leads to a simpler formulation of Eq. 7:

$$SOC_m(j+1) = SOC_m(j) \cdot \alpha_m + \\ + u_{m,to}(j) \cdot \beta_{m,to} - u_{m,fm}(j) \cdot \beta_{m,fm} \\ \forall m \in \mathcal{M}_{ST} \quad (13)$$

The iterative form (Eq. 13) can be brought into a closed intertemporal form. Based on the optimization variables $x_{m,to}(i)$ and $x_{m,fm}(i)$ for $i \in \{0, ..., h\}$, the values for the resulting storage charging states $SOC_m(i)$ for $i \in \{1, ..., h+1\}$ can be calculated for each storage $m \in \mathcal{M}_{ST}$:

$$SOC_m(i) = SOC_m(0) \cdot \left(\alpha_m\right)^i + \\ + \beta_{m,to} \sum_{k=0}^{i-1} \left[ \left(\alpha_m\right)^{(i-1)-k} \cdot u_{m,to}(k) \right] \quad (14) \\ - \beta_{m,fm} \sum_{k=0}^{i-1} \left[ \left(\alpha_m\right)^{(i-1)-k} \cdot u_{m,fm}(k) \right]$$

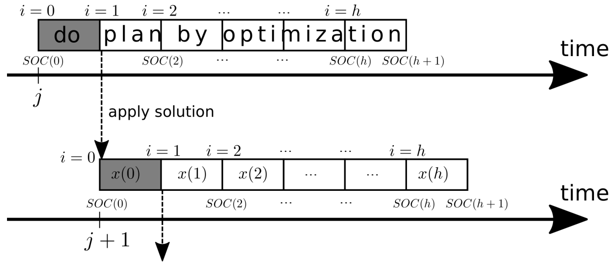


**Figure 5:** Illustration of the rolling horizon optimization in the MPC process. Explanation of which values are optimized and which are executed.

Notice that Eq. 14 contains sums with an iterator $k$ counting up from 0 to $(i-1)$. That means the respective $SOC$ of time step $i$ is calculated based on the initial state $SOC_m(0)$ and power flows of all preceding time steps $k \in= \{0, ..., (i-1)\}$. Like that Eq. 14 is highly correlated to the MPC process and the communication between platform and devices, where values are read and written from / to the real system (see Section 5.2) . Fig. 5 illustrates the connection between optimization variables $x$ and the resulting $SOC$ values within the MPC horizon. $SOC_m(0)$ is read from the real system as initial state. $x_{m,to}(0)$ and $x_{m,fm}(0)$ are known as results of previous optimization iterations, while $x_{m,to}(1)$ - $x_{m,to}(h)$ and $x_{m,fm}(1)$ - $x_{m,fm}(h)$ are variables of the optimization. Within the optimization, $SOC_m(1)$-$SOC_m(h+1)$ are implicitly calculated.

It has to be highlighted that the parameter $\eta_{m,sb}$ describes the proportion of SOC lost per hour and has the unit $\left[{}^{SOC}/_{h}\right]$. Using this proportional loss parameter, the exponential self-discharge behavior of storage systems can be replicated with a linear formulation.

The $SOC$ value should by definition be between 0 and 1. However, the SOC could theoretically reach values below 0 or above 1 under the influence of discharging and charging power flows. To avoid this, the constraints (Eq. 15 and Eq. 16) are added for the storage model. Despite these constraints, the SOC of the real system could theoretically drop below zero. This can happen for inaccurate forecasts or abruptly increasing discharge requirements that were not anticipated by the forecasts and the system model. An SOC drop below 0 is in particular likely when the planned trajectory already discharged the storage to a low SOC. Further, as we use a capacity model, the discharging to low SOC values means for sensible thermal storages that the average temperature is very low. This can lead to problems in real systems, as usually the demand (heating system) has minimum temperature requirements. To avoid the described problems, a minimum SOC can additionally be specified for the end of the observation horizon (Eq. 17). This keeps the flexibility of using the full SOC range from 0 to 1 within the horizon, as long as the system model predicts that it is possible to recharge the storage unit to a minimum SOC until the end of the observation horizon. Like this a deep discharging and negative SOC drops become very unlikely.

$$-SOC_m(i) \leq \quad 0 \quad \forall i \in \mathcal{H} \tag{15}$$
$$SOC_m(i) \leq \quad 1 \quad \forall i \in \mathcal{H} \tag{16}$$
$$-SOC_m(i = h) \leq \quad -SOC_{min,h} \tag{17}$$

### *4.2.3. Network models*

**Thermal network model**

The thermal network model consists of the thermal energy balance per building in Eq. 2 and a model for the transport of heat between the buildings. For a connection of two buildings $\mathfrak{a}, \mathfrak{b} \in \mathcal{B}$ in the network, there are two connection instances $CN$ which each belong to one of the buildings. For each of the connection instances there are two decision variables for the two possible directions of power flow.

$$x^{\mathfrak{a}}_{m,to}(i) = \quad x^{\mathfrak{b}}_{m,fm}(i) \tag{18a}$$
$$x^{\mathfrak{a}}_{m,fm}(i) = \quad x^{\mathfrak{b}}_{m,to}(i) \tag{18b}$$

In the final problem formulation, for each connection between two buildings, one pair of the equivalent decision variables can be chosen. For further explanations it is assumed that $x^{\mathfrak{a}}_{m,to}(i)$ and $x^{\mathfrak{a}}_{m,fm}(i)$ were chosen. Transportation losses due to heat losses to the environment are taken into account by constant transport efficiencies, which are considered at the receiving building. The net power contribution to the thermal energy balance (Eq. 2) can then be expressed as:

$$\begin{pmatrix} u^{\mathfrak{a}}_{CN,to}(i) - u^{\mathfrak{a}}_{CN,fm}(i) \\ u^{\mathfrak{b}}_{CN,to}(i) - u^{\mathfrak{b}}_{CN,fm}(i) \end{pmatrix} = \\ = \begin{pmatrix} -1 & \eta^{\mathfrak{b},\mathfrak{a}}_{CN} \\ \eta^{\mathfrak{a},\mathfrak{b}}_{CN} & 1 \end{pmatrix} \begin{pmatrix} x^{\mathfrak{a}}_{CN,to}(i) \\ x^{\mathfrak{a}}_{CN,fm}(i) \end{pmatrix} \tag{19}$$

The transport efficiencies are calculated with an exponential equation using the length $l_{CN}$ of the network connection between the buildings and the percentage losses $v_{CN}$ per $100m$.

$$\eta^{\mathfrak{a},\mathfrak{b}}_{CN} = \left(1 - v^{\mathfrak{a},\mathfrak{b}}_{CN}\right)^{\frac{l^{\mathfrak{a},\mathfrak{b}}_{CN}}{100m}} \tag{20}$$

The power fed into the thermal network has upper and lower bounds.

$$u_{m,to}(i) \leq \quad +P_{m,max,to} \quad \forall m \in \mathcal{M}_{CN} \tag{21a}$$
$$-u_{m,to}(i) \leq \quad 0 \quad \forall m \in \mathcal{M}_{CN} \tag{21b}$$

$$u_{m,fm}(i) \leq \quad +P_{m,max,fm} \quad \forall m \in \mathcal{M}_{CN} \tag{21c}$$
$$-u_{m,fm}(i) \leq \quad 0 \quad \forall m \in \mathcal{M}_{CN} \tag{21d}$$

As the feed-in to the thermal network is bounded, indirectly the extraction of heat is also limited by the transportation model in the Equations (19) - (20).

**Electric grid model**

A fully connected grid is assumed that allows to share electricity lossless in the district. The energy balance in Eq. 1 accumulates the electricity generation and demands of all buildings and devices for each time step. Central selling or buying of the overall district to/from the public grid balances residual surpluses or deficits. For the whole district, there is only one decision variable for selling ($u_{EG,to}(i)$) and one for buying ($u_{EG,fm}(i)$) of electric energy to / from the public grid, as this is assumed to be done centrally by the district as a whole. The buying and selling variables to/from the electricity grid only have zero as a lower bound and are unbounded apart from that. Thereby, from a modeling perspective the public electricity grid can be seen as a slack bus. For each time step $i \in \mathcal{H}$ in the horizon:

$$u_{EG,to}(i) = \quad x_{EG,to}(i) \tag{22a}$$
$$u_{EG,fm}(i) = \quad x_{EG,fm}(i) \tag{22b}$$

$$-u_{EG,to}(i) \leq \quad 0 \tag{23a}$$
$$-u_{EG,fm}(i) \leq \quad 0 \tag{23b}$$

## 4.3. Optimization Problem

The MEMAP platform is designed as an MPC for the district (see Section 3.2). Based on the system model presented beforehands, mathematical optimization problems are automatically generated at each discrete time step.

The objective is to minimize the overall costs of the district for satisfying their electricity and heat demands in the respective rolling horizon, while considering the behavior and restrictions of the devices and networks. The cost minimization is reflected by a linear objective function that multiplies the power decision variables with the according operation costs. In line with the information model, the costs can be economical or ecological operation costs (€ or $CO_2$-Emissions per $kWh$). To obtain absolute cost values, the objective function must be scaled with the constant time step size $\Delta t$. Adding the proposed system model (see Section 4.2) as constraints, a MILP can be formulated for the core of the platform:

$$\underset{\mathbf{x}}{\text{minimize}} \quad \left(\lambda^T \, \mathbf{x}\right) \cdot \Delta t \tag{24a}$$
$$\text{subject to} \quad \mathbf{A}_{UB}\, \mathbf{x} \leq \mathbf{k}_{UB} \quad , \tag{24b}$$
$$-\mathbf{A}_{LB}\, \mathbf{x} \leq -\mathbf{k}_{LB} \quad , \tag{24c}$$
$$\mathbf{G}\, \mathbf{x} = \mathbf{d} \tag{24d}$$

The vector $\mathbf{x}$ contains all continuous decision variables $x$ together with all discrete decision variables $y$. Using the equations of the system model in Section 4.2, the control inputs $u$ can be determined in a post-processing from the decision variables in $\mathbf{x}$. The equality constraints (Eq. 24d) comprise the thermal energy balances for each house and the electrical energy balance for the whole district. The inequality constraints (Eq. 24c and Eq. 24b) comprise the device models and the thermal network & electric grid model. The number of variables and constraints depends on the involved devices and network configuration in the system under consideration. The obtained MILP can be solved with conventional solving algorithm implementations. In particular we use the MILP solver *lp_solve* (Version *lp_solve_5.5.2.11_java.zip*) [48]. It is freely distributed by the Massachusetts Institute of Technology (MIT) and is based on the revised simplex method and the branch-and-bound method for integers [49].

## 5. Software Implementation

The modeling described in the previous section builds the core for an implemented software prototype. Its source code is freely available via a public git on `https://git.fortiss.org/ASCI-public/memap/-/tree/main`. In the following, different aspects of the software implementation are presented.

### 5.1. Platform with Internal Actor Framework

For the software implementation it was decided to use a platform design, as this enables the easy integration of other important functionalities around the core, e.g. real-time communication to the local EMS, interfaces to a planning tool, user portal, third-party applications, etc. The platform was programmed in Java[1], a widespread general-purpose programming language. An actor system[2] was used to reflect the hierarchical real-life structure of districts and the associated information flow (see also [45, 50]). Our hierarchical actor representation is composed of three layers (bottom up):

i) device level actors: all actors, that have a direct connection to field devices (sensoring and control signals)
ii) building level actors: local EMS and building-like entities without sub-actors, like heat connections (CNs)
iii) district level coordinator

In contrast to composite actors, actors without sub-actor are called ’leafs’. Actors encapsulate state and behavior of an entity and communicate exclusively by exchanging messages which are placed into the recipient’s mailbox. For the internal communication within the actor system, each actor extends an abstract *BehaviorModel* class. It defines an information flow, which is inherited according to Fig. 3. For every actor in the hierarchy, it persists of four stages:

- handle a request from a hierarchically higher level
- send request to a hierarchically lower level and await answer
- make some decision
- return the answer content to the higher hierarchy

[1] `https://www.oracle.com/java/`
[2] `akka.io`

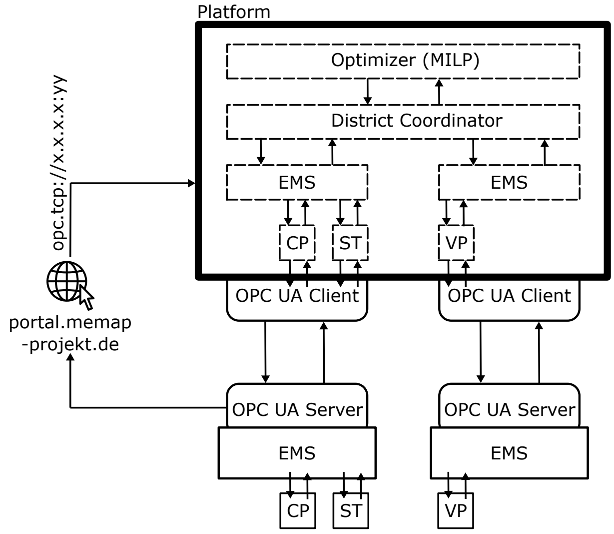


**Figure 6:** Internal and external communication of the MEMAP platform.

However, the internal structure of an actor’s payload is dependent to the device classes and implements the respective data points from the information model or its superclass (Section 4.1). With this platform design approach, every composite can decide either to optimize with the collected information at its level or to forward the information to a higher hierarchy for optimization on a higher level. Multiple district coordinators - or district EMS - can thus be integrated under one inter-district coordinator, by that presenting a self-similar structure according to the composite pattern of [51]. This also enables easy comparison of optimization at EMS level versus optimization at district or inter-district level. The chosen approach provides high extensibility and allows to form arbitrary hierarchies from the same actors, similar to holonic systems. More information on holonic architectures for IoT-enabled energy management can be found in Ref. [52].

### 5.2. Communication

For the external communication, the industrial communication standard *OPC Unified Architecture* (OPC UA) was chosen (see Section 2). By supporting companion specifications, OPC UA allows to easily implement the developed MEMAP information model from Section 4.1. This promotes the extensibility of the concept through standardization. At the same time, ready-to-use security features are provided in OPC UA so that secure communication can be ensured.

To communicate with several local EMSs in the district, each building-level actor instance in the platform that represents a local EMS in the district is associated with an own OPC UA Client (see Fig. 6). On the other side it is assumed that each real local EMS in the district is equipped with an OPC UA server unit providing all information for devices under its control. To establish the connections and configurations of the clients in the platform, a user portal was developed and can be used. At first the OPC UA servers at the local EMSs are set-up, reflecting the real-life device configuration of the respective building. For the onboarding of a local EMS, the .xml-configuration file is uploaded to the portal. Due to the unified naming convention for data points (see Section 4.1), the data points can be automatically detected. In this way, the matching OPC UA Clients for the platform can be automatically generated as counterparts to the servers of the local EMSs.

Following the basic idea of the platform concept, different types of third-party applications can interact flexibly and modularly with the platform via an OPC UA server-client connection.

Along the established client-server connections of platform and EMSs, data is sent / received from / by the platform during the live operation. As potentially a lot of different data sources and sinks are involved in form of the local EMS systems with their individual devices, the communication has to be coordinated. On top of that, the communication has to be synchronized with the iterative MPC procedure (see Section 3.2). To satisfy both requirements, a specific communication sequence between platform and local EMSs was developed and implemented. The iterative loop of the communication sequence can be summarized by *write - read - optimize - wait*:

*1. write* As soon as `TIME == TRIGGERTIME`, the next timestep is reached (horizon shift, see Fig. 5). The platform writes setpoints from last optimization to EMSs. Setpoints are valid for next timestep ($x(0)$). Update the `TRIGGERTIME` by adding the timestep duration: $\texttt{TRIGGERTIME} = \texttt{TRIGGERTIME} + \Delta t$.

*2. read* The platform reads system states ($SOC(0)$) and forecasts from EMSs. The reading is centrally initiated from the platform by sending a `TRIGGER` to all devices. This ensures simultaneous reading.

*3. optimize* The platform optimizes. The optimization horizon is $\mathcal{H} = \{1, .., h\}$ with the foresight being defined by $h$. In each iteration the variables of interest are $[x(1), ..., x(h)]$ and $[y(1), ..., y(h)]$ for the different devices and $[SOC(i = 2), ...SOC(i = h + 1)]$ for all storages. See also Fig. 5 and the storage model in Eq. 4.2.2.

*4. wait* The platform buffers the optimization results. It waits until the fixed time step duration is over. This is reached, when the `TIME` is equal to the updated `TRIGGERTIME`.

The presented communication sequence ensures that all relevant data for a particular iteration step is available at the platform at the same time and refer to the same horizon. Like this, all involved entities are synchronized and the compatibility of the communication with the MPC optimization procedure is facilitated.

# 6. Validation

The functionality of the presented concepts and the developed software platform was validated by simulations and experiments with real hardware in a laboratory environment. The paper at hand will address in particular the validation of the following aspects

- validation of the functionality of the optimization core
- proof of the interoperability of the software with real devices (hardware)
- validation of the
  - generic device models
  - information model
  - communication concept

Explicitly not in the focus of this paper is the verification of the postulated benefits, savings and synergistic effects of the collaborative operation with MEMAP. This was shown already in previous work and literature (see also Section 2).

For the validation, we investigate a case study scenario comprising a certain district setting and given disturbance forecasts (e.g. demand & price profiles). The developed MEMAP platform is used to optimally operate the technical equipment in the district. A simulative case study assumes perfect predictions, models and perfect implementation of the setpoints by the devices. This builds the benchmark for an experimental case study under the same scenario, involving the platform in interaction with real device hardware and imperfect implementation. The experiments are performed in the laboratory environment for Combined Smart Energy Systems (CoSES) at the Technical University of Munich (TUM) [53, 54, 55].

The relevant outcomes of the case studies include simulated and measured time series data on equipment operation in the district, as well as more detailed measurements on the technical device behavior. The developed platform is validated by demonstrating its successful integration into the laboratory environment and interaction with real-time operational systems. Furthermore, the operation of the systems managed by the developed platform is analyzed to assess plausibility in light of the expected optimized behavior. This includes a comparison of simulated and experimental results.

In Section 6.1 we present the case study scenario. In Section 6.2 the integration of the platform into the laboratory environment for the experiments is described. Section 6.3 we present the results of the simulative and experimental case studies. Finally, in Section 6.3 we evaluate the success of the validation.

## 6.1. Case Study Scenario

For the validation of the platform functionalities a case study scenario was designed and investigated. An energy compound is considered and the developed platform is used

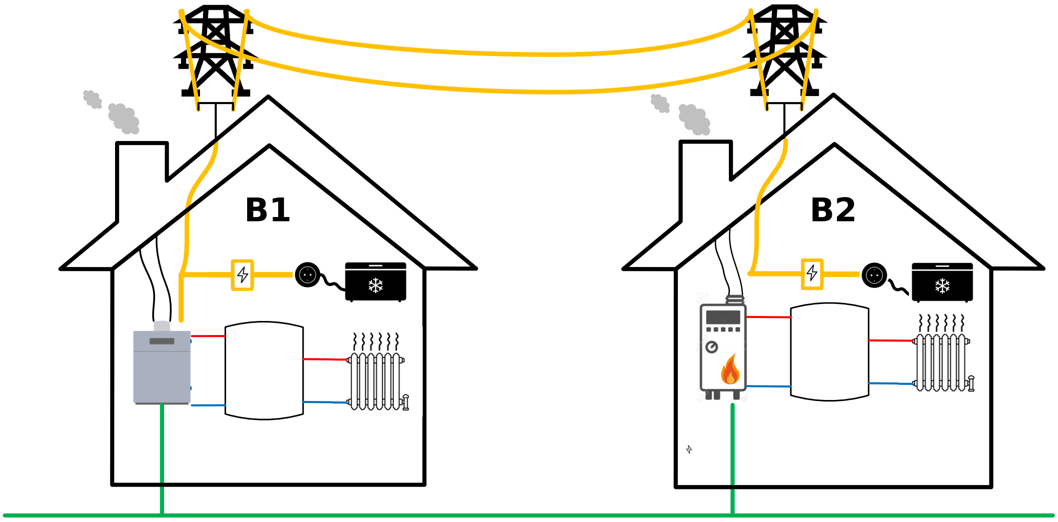


**Figure 7:** Case study scenario for validating the platform functionalities in the CoSES laboratory environment.

**Table 5**
Equipment of buildings in case study scenario.

| | Building 1 (B1) | Building 2 (B2) |
|---|---|---|
| $DD$ $(ht)$ | demand profile $2.9 - 4.0$ $kW$ | demand profile $10.9 - 13.9$ $kW$ |
| $DD$ $(el)$ | demand profile $0.2 - 0.7$ $kW$ | demand profile $0.7 - 2.4$ $kW$ |
| $CP$ | - | condensing boiler 21 $kW$ (nom.) |
| $CO$ | CHP $el$ : 2 $kW$ (nom.) $ht$ : 5 $kW$ (nom.) | - |
| $ST$ $(ht)$ | hot water tank 800 $l$ (nom.) | hot water tank 800 $l$ (nom.) |
| $EG$ | district grid with public grid connection | |

to optimize its operation on the run, considering only economical operation costs. A small scenario is sufficient, as the purpose of the case study was just to validate the functionalities and not to show the benefits of collaborative operation in districts. Therefore we investigate a neighborhood of two buildings without thermal grid connection, but an electrical microgrid that balances residua by buying / selling power from/to the public grid. The selected scenario is illustrated in Fig. 7. The technical equipment of both buildings is summarized in Table 5. More detailed parameters that are passed to the MEMAP platform according to the the information model are listed in Table 6 in the Appendix A.

Perfect forecasts for the demands and prices are assumed in form of predetermined profiles. The effects of imperfect implementation of setpoints on the forecasts are not accounted for. To provide forecasts for the horizon at the end of the experiment, the forecast profiles are looped. Fig. 11a in the Appendix A illustrates the demand profiles over time. These were derived from detailed simulations with the Modelica-based environment Simulation X[3] using the GreenCity library [56]. Fig. 11b in the Appendix A shows the price profiles over time. These are manually specified and chosen to demonstrate various effects in the analysis. As general MPC-parameters, a time step size of $\Delta t = 15$ $min$ is used with a rolling horizon length of $h = 12$ steps (3 hours). The investigation period are 12 $h$ in real time. The measurement results were recorded with a resolution of 10 $s$.

The simulation and the experiment are both conducted with this identical scenario. For the simulations a perfect match between the internal system model and reality, as well as perfect implementation of setpoints by the devices is assumed. Therefore, the SOC values predicted by the platform are used as emulated measurements in the simulative case study. A custom Python server routine facilitates this process. The laboratory experiments use specialized heat sink modules which emulate the desired demand profile. This is achieved by cooling the water in the heating circuit through a controlled heat exchange process [54]. The electrical power flow setpoints are not physically implemented in the lab, as no insights are expected due to the high discrepency in time scales between electrical characteristics and energy management.

## 6.2. Laboratory Integration

The CoSES laboratory replicates the field and automation level of multiple interconnected buildings in a neighborhood, encompassing both hardware and software aspects, including actuators, sensors, and basic component controls [53, 54, 55]. The computation and communication layer is based on National Instruments[4] (NI) products, i.e. LabVIEW (LV) and VeriStand (VS). The interface between

[3] https://www.esi-group.com/products/system-simulation
[4] https://www.ni.com/de-de.html

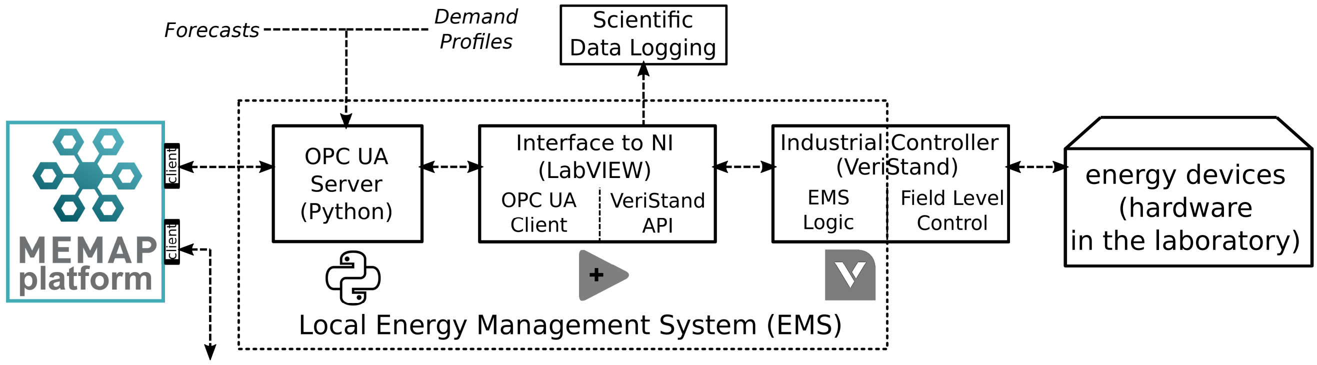


**Figure 8:** Integration of the MEMAP Platform into the laboratory environment - Custom Energy Management System and its software chain.

external software and NI software is established using LabVIEW with the VeriStand Application Programming Interface (VS API). To perform experiments with real devices, the MEMAP platform was integrated into the software and communication framework of the CoSES laboratory. The integration process served as a practical test for the developed platform and communication concept.

The software chain used for the integration is illustrated in Figure 8. Custom local EMSs with identical structures are set up for each building, acting as intermediaries between the platform and the real energy equipment in the laboratory. On one end of the software chain, each custom local EMS has an OPC UA Server implemented in Python, acting as the counterpart to the platform's client. Python routines in the local EMSs handle the loading of profiles and forecasts from .csv files for ongoing experiments. They synchronize with the platform's communication sequence and provide setpoints to consumption emulators for emulating the specified demand profiles. To transition from Python to the NI environment, a LabVIEW virtual instrument with OPC UA clients tunnels data from the Python server through the VeriStand API to models running on the industrial controllers (ICs) in VeriStand. The EMS logic on the ICs performes the actual conversion of power setpoints, which are then passed on to field level controllers, converted again, and checked for safe operation before being transmitted to the real devices via cables. In the opposite direction, sensor data reading and conversion to composite values, such as energy quantities, is carried out. For technical investigations beyond the level of power flows, the local EMSs are connected to detailed scientific data logging.

## 6.3. Results

Overviews of the full results of the simulative and experimental case studies can be found in Appendix A in Fig. 13 and Fig. 14. Detailed figures are used in this subsection to illustrate specific aspects.

### *Simulative Results*

The simulative results, depicted in Figure 13, provide insights into the optimized behavior of the energy compound and serve as a benchmark for the experiment. The observations from the simulation are as follows:

In building 1, intermittent operation of the CHP is observed due to its narrow operating limits. Building 2 initially covers its heat demand with the thermal storage, and when the storage discharges, the gas boiler takes over the heat production, modulating according to the thermal demand. Here, the minimum SOC constraint for the storage at the end of the optimization horizon comes into play.

In contrast, building 1 operates the CHP despite a sufficiently charged storage to supply both buildings with electricity via the microgrid. This CHP serves as a coupling element between the electricity and heat sectors, facilitating synergy utilization across energy sectors and building boundaries. The district energy management platform automatically exploits these synergies. Additionally, the optimization in the platform considers trade-offs, such as the decision to use electricity from the public grid instead of the CHP when it becomes unprofitable due to increased gas prices (at $t = 5\ h$).

The simulative results also demonstrate the advantages of the predictive optimizer. The proactive charging and discharging of the thermal storage allows for leveraging future changes in gas prices. The gas boiler is used between $t = 2.25h$ and $t = 9.25h$ to pre-charge the thermal storage, taking advantage of cheaper gas prices while considering the influence of possible storage losses on economic efficiency.

### *Experimental Results*

Figure 14 presents the measurements from the experimental case study conducted in the CoSES laboratory environment. A comparison between the experimental results and the simulation reveals deviations in the emulated heat demand, particularly in building 2. These deviations can be attributed to technical factors related to the thermal storage system. Unlike the stratified storage in building 1, the thermal storage in building 2 is mixed, resulting in a decreased supply water temperature below the design temperature. To maintain a minimum temperature spread, the heating circuit pump operates at a higher volume flow. However, when the pump reaches its maximum viable volume flow, the required heat demand cannot be met, leading to deviations in the

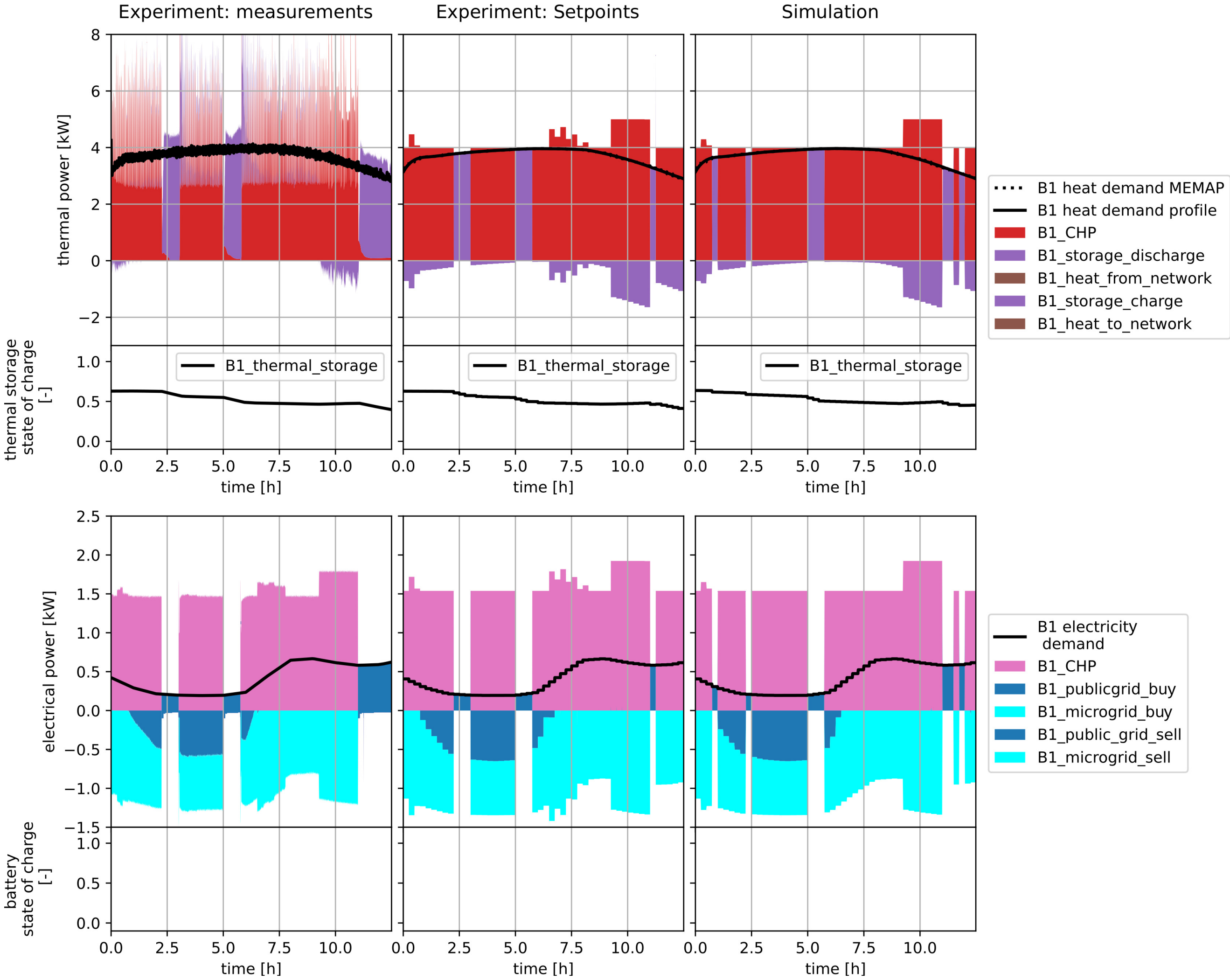


**Figure 9:** Comparison of results for building 1 from the experimental case study (*left*: measurements, *middle*: setpoints) and the simulative case study (*right*). The impact of the interaction with real device hardware can be investigated.

emulated heat demand compared to the given profile. This cascade of mixed storage, minimum supply temperature, and unreachable power output emphasizes the strong coupling between the technical and management levels. Considering the technical details (like temperatures) is essential for explaining such effects.

The comparison between the experimental and simulative results for building 1 is illustrated in Figure 9. A good match is observed between the setpoints in the experiment and the simulation. Minor deviations between can be attributed to implementation differences, resulting in changes in the overall system state. For example, around $t = 6\ h$, the experiment calls for a stronger operation of the CHP compared to the simulation.

Despite these deviations, the devices in the experiment accurately implement the setpoints. The measured thermal output of the CHP exhibits oscillations around the setpoint (see detail in Figure 12), which can be attributed to device-specific control characteristics [57]. However, on average, the energy demand for each time step is met. From $t = 9\ h$ onwards, the CHP is not started despite a request from the platform due to a technical problem in the experiment. The condensing boiler in building 2 closely follows the given power setpoints over the whole experimental time, with short power peaks during start-ups and shut-downs.

Figure 10 provides details on the SOC of the thermal storages in building 1 and 2. Within the timestep length of 15 minutes, the SOC is mainly influenced by charging and discharging. The measured SOC aligns closely with the predicted SOC calculated by the models in the MEMAP platform, demonstrating the accuracy of the model predictive control (MPC) approach and the successful setpoint implementation.

## Evaluation

The simulative case study confirms the effectiveness of the optimization core and abstracted device models in achieving the desired functionalities. The optimization process successfully leverages synergies across energy sectors and building boundaries to optimize district operation. By

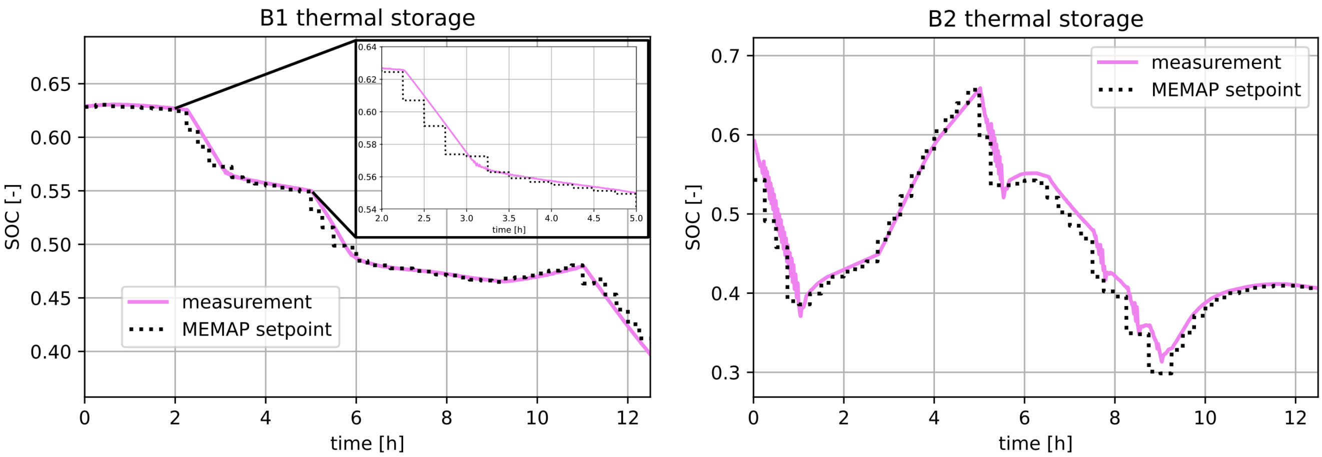


**Figure 10:** Detail of measured SOC vs. the SOC predicted by the MEMAP platform (setpoint) for the thermal storages in building 1 and 2 of the case study.

considering trade-offs and utilizing predictive optimization, the model-based approach effectively exploits forecasted boundary conditions, such as prices, enabling automated proactive charging and discharging of storage units.

The integration of the developed information and communication model into the CoSES laboratory environment validates its compatibility and practicability for realistic settings. The successful 12-hour automated experiment run confirms the interoperability of the MEMAP platform with real devices. The internal storage model of the platform demonstrates excellent predictive capabilities for estimating the state of charge (SOC) of the two storage tanks for future time steps during the experiments.

Some limitations of the optimization on the power flow level were demonstrated in the technical-level experiments. The platform was unable to adequately anticipate insufficient supply temperatures from a fully mixed thermal storage with a high SOC, and the oscillating thermal output behavior of a combined heat and power (CHP) system. These effects fall outside the scope of conventional power flow optimization. Further, it became evident that, in addition to optimal operation, routines for handling technical failures are necessary to ensure the resilience of the district energy management concept. Self-supply fallback options with isolated device operation may be considered in such cases. However, despite the described limitations, the hardware devices implemented the setpoints provided by the platform reasonably well.

In summary, the experiments confirm the suitability of the developed platform for real-time optimization during live operation in the field. Through the simulative and experimental case study conducted in a realistic environment, all key functionalities of the platform were successfully validated.

## 7. Conclusion

This paper presents the development and validation of a smart multi-energy management system for districts, connecting local building energy management systems (EMS) through a digital platform that predictively optimizes district energy flows during live-operation. The paper's contribution builds on four pillars:

***Development process*** Comprehensive description of the platform's development path demonstrates how various aspects from different fields are combined to meet the identified requirements for a suitable district EMS. This provides valuable guidance for similar projects in the future.

- Model predictive control (MPC) for central district EMS
- Generic device classes for fast modeling of diverse settings
- Automatically adaptable MILP multi-energy system model
- Capacity storage model with linear formulation for exponential self-discharge
- Custom information model as data exchange standard
- OPC-UA as communication standard
- Custom communication sequence for synchronizing multiple devices with MPC
- Implementation in actor framework for automated adaptation and optimization in live operation

***Validation and insights*** Through simulative and experimental case studies, the suitability of the system for real-time district optimization is confirmed, while technical limitations of power flow optimization are identified.

- Optimization core automatically exploits synergies
- Interoperability with real hardware proven
- Information model and communication concept validated

- Suitability of generic device models shown
- Temperature behavior can't be anticipated by abstracted models
- Need for fallback routines in case of technical failures

***Software*** An openly accessible software prototype is provided, which can serve as a blueprint for the further developement of products. Prototype available at `https://git.fortiss.org/ASCI-public/memap`.

***Broader findings*** Insights on framework conditions for overarching district energy management are gained as starting points for consecutive studies, paving the way for widespread practical implementation.

- Existing local building EMS don't provide all required functionalities
- Bidirectional heat exchange via district networks is still under research
- Sensitivity analysis on imperfect forecasts and imperfect setpoint implementation necessary
- Requirement for billing concept to distribute savings or additional expenditures fairly among participants
- Central district EMS as benchmark for distributed and market-based approaches
- Challenge of balancing model abstraction vs. representativeness of the models

With these concepts, findings and software artefacts our paper paves the way for the practical implementation of more holistic, efficient, and sustainable energy management systems for districts in the future!

## CRediT authorship contribution statement

**Thomas Licklederer:** Conceptualization, Methodology, Software, Validation, Investigation, Writing - Original Draft, Visualization, Project administration. **Jan Mayer:** Conceptualization, Methodology, Software, Validation, Investigation, Writing - Review & Editing, Visualization, Project administration. **Denis Bytschkow:** Conceptualization, Methodology, Software, Investigation, Writing - Review & Editing, Funding acquisition. **Michael Kramer:** Conceptualization, Methodology, Investigation, Project administration, Funding acquisition. **Alexandre Capone:** Methodology, Investigation. **Johannes Burger:** Software, Investigation, Writing - Review & Editing. **Markus Duchon:** Writing - Review & Editing, Supervision, Project administration, Funding acquisition.

### *Declaration of generative AI and AI-assisted technologies in the writing process*

During the preparation of this work the author(s) used *ChatGPT* by OpenAI and *DeepL Translator* by DeepL SE in order to improve language and readability. After using this tool/service, the author(s) reviewed and edited the content as needed and take(s) full responsibility for the content of the publication.

## A. Appendix

**Table 6**
Device parameters of the case study scenario for the experimental validation according to the information model from Table 1.

CHP - Building 1

| Type | RMB/ENERGIE neoTower 2.0 [57] |
|---|---|
| $s_{CO,S1}$ | $ht$ |
| $s_{CO,S2}$ | $el$ |
| $\eta^{S1}_{CO}$ | 0.65 |
| $\eta^{S2}_{CO}$ | 0.25 |
| $P^{S1}_{CO,min}$ | $4\ kW$ |
| $P^{S1}_{CO,max}$ | $5\ kW$ |

Condensing Boiler - Building 2

| Type | Wolf CGB-2-20 |
|---|---|
| $s_{CP}$ | $ht$ |
| $\eta_{CP}$ | 0.88 |
| $P_{CP,min}$ | $8\ kW$ |
| $P_{CP,max}$ | $19\ kW$ |

Thermal Storage - Building 1 & 2

| Type | Wolf SPU-2-800 [58] |
|---|---|
| $s_{ST}$ | $ht$ |
| $\eta_{ST,to}$, $\eta_{ST,fm}$ | 0.97 |
| $P_{ST,max,to}$, $P_{ST,max,fm}$ | $22\ kW$ |
| $E_{Cap,ST}$ | $62.94\ kWh$ $(773.6\ l,\ 20-90°C)$ |
| $\eta_{ST,sb}$ | $0.021\ ^{SOC}/_{h}$ $(\approx 0.66\ kW)$ |
| $SOC_{min,h}$ | 0.5 |
| $SOC(t=0)$ | 0.641 (B1), 0.592 (B2) |

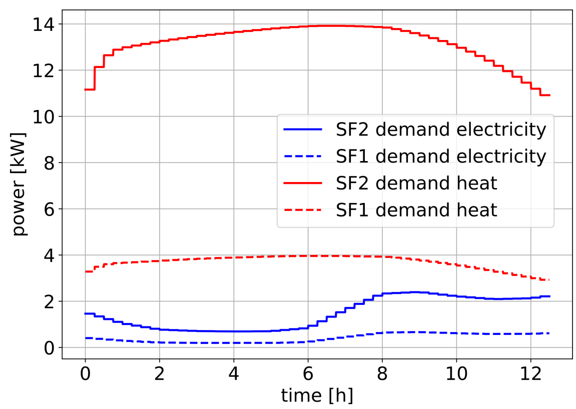


(a) Demand profiles for the case study scenario, resulting from a detailed building simulation.

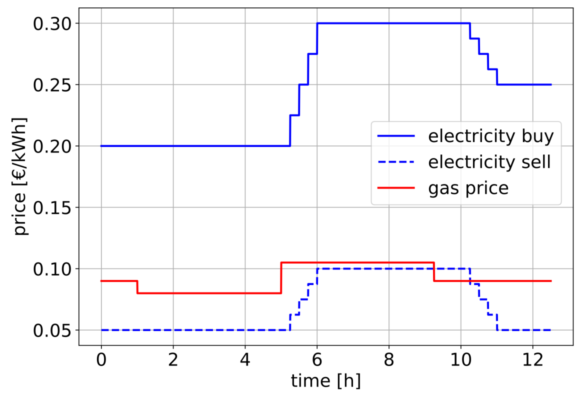


(b) Time series of prices for the case study scenario.

**Figure 11:** Forecast time series for the case study.

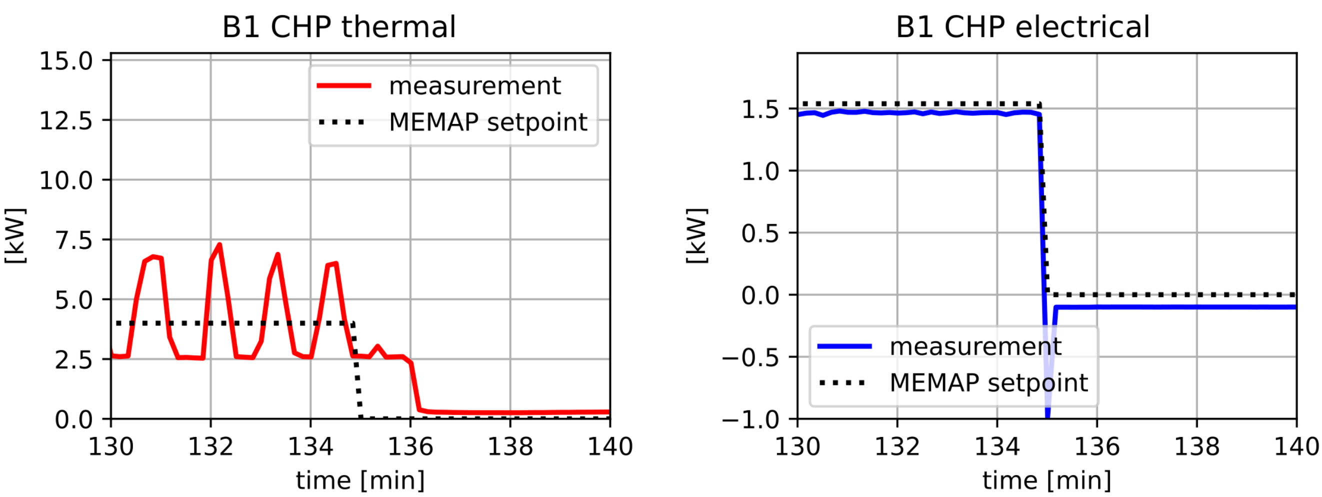


**Figure 12:** Detail of setpoints vs. measurements of thermal *left* and electrical *right* power for the CHP in building 1 of the case study.

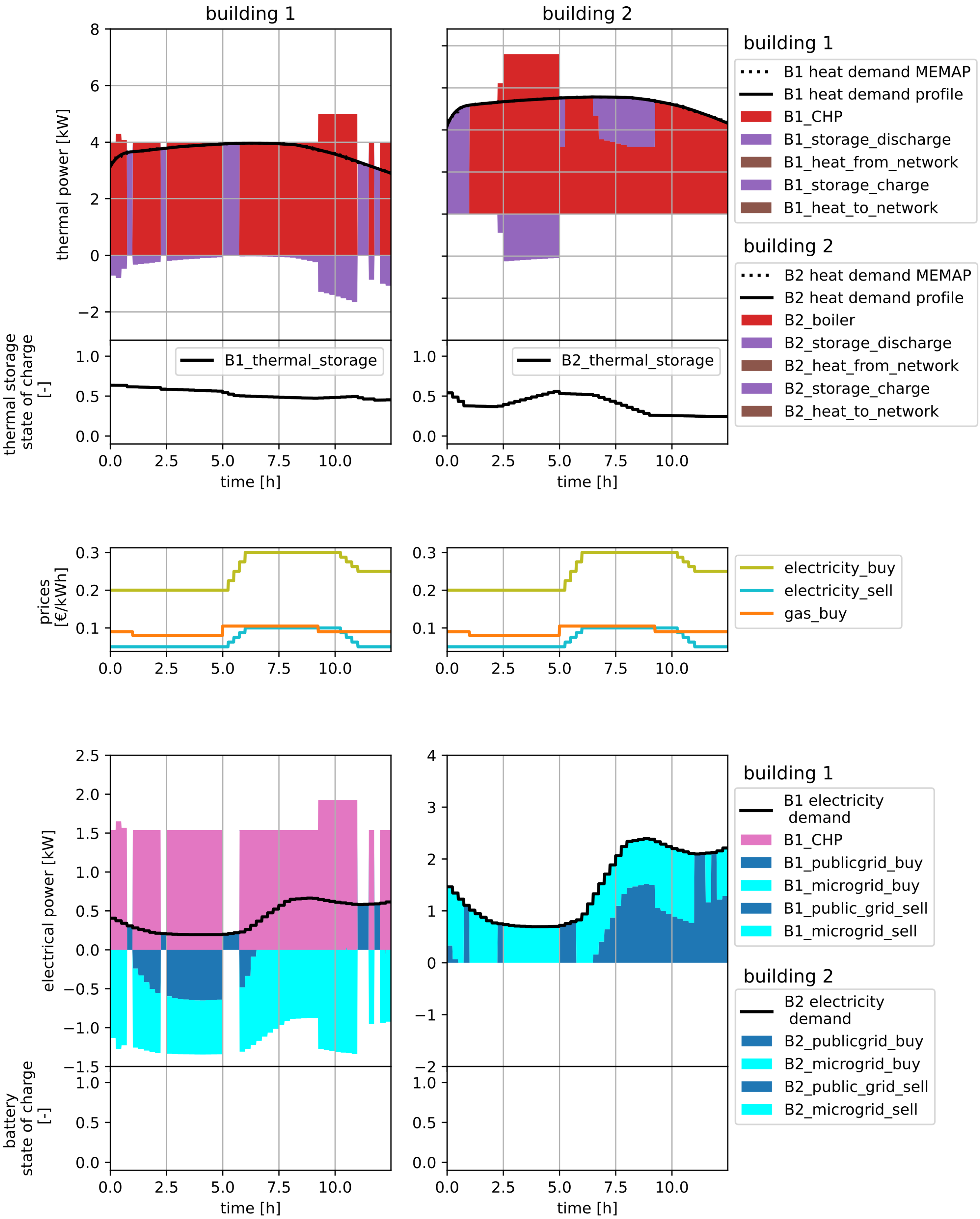


**Figure 13:** Simulation results of case study scenario; assuming perfect predictions, models and perfect implementation of the setpoints by the devices.

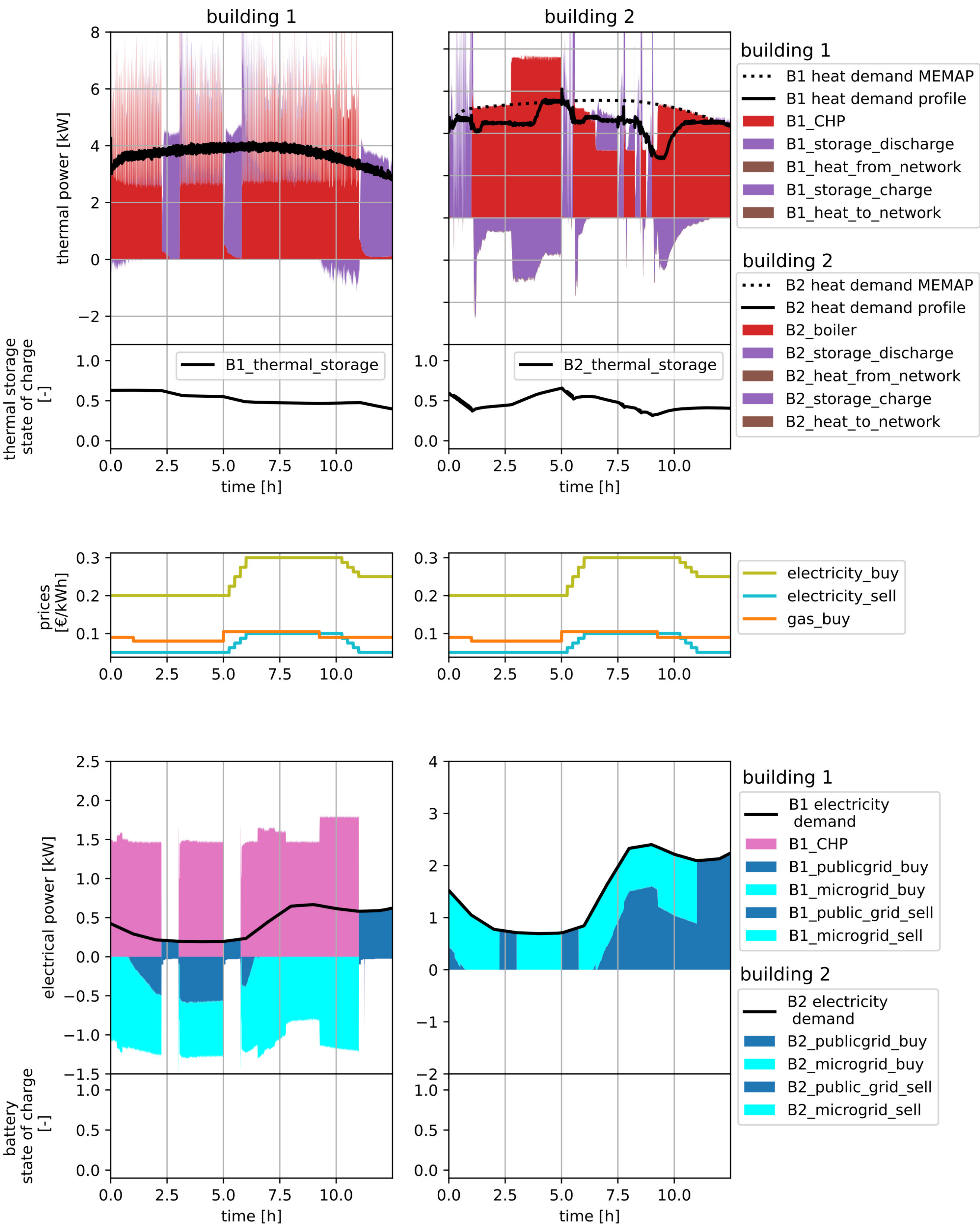


**Figure 14:** Measurements from the experimental case study in the CoSES laboratory environment.

## References


[1] European Commission - Energy Department, In focus: Energy efficiency in buildings | European Commission, 2020. URL: https://ec.europa.eu/info/news/focus-energy-efficiency-buildings-2020-lut-17_enhttps://ec.europa.eu/info/news/focus-energy-efficiency-buildings-2020-feb-17_en.

[2] T. O'Grady, H.-Y. Chong, G. M. Morrison, A systematic review and meta-analysis of building automation systems, Building and Environment 195 (2021) 107770.

[3] P. Domingues, P. Carreira, R. Vieira, W. Kastner, Building automation systems: Concepts and technology review, Computer Standards & Interfaces 45 (2016) 1–12.

[4] J. Ramsebner, R. Haas, H. Auer, A. Ajanovic, W. Gawlik, C. Maier, S. Nemec-Begluk, T. Nacht, M. Puchegger, From single to multi-energy and hybrid grids: Historic growth and future vision, Renewable and Sustainable Energy Reviews 151 (2021) 111520.

[5] G. Schweiger, L. V. Eckerstorfer, I. Hafner, A. Fleischhacker, J. Radl, B. Glock, M. Wastian, M. Rößler, G. Lettner, N. Popper, K. Corcoran, Active consumer participation in smart energy systems, Energy and Buildings 227 (2020) 110359.

[6] E. Guelpa, A. Bischi, V. Verda, M. Chertkov, H. Lund, Towards future infrastructures for sustainable multi-energy systems: A review, Energy 184 (2019) 2–21.

[7] B. Mathiesen, H. Lund, D. Connolly, H. Wenzel, P. Østergaard, B. Möller, S. Nielsen, I. Ridjan, P. Karnøe, K. Sperling, F. Hvelplund, Smart Energy Systems for coherent 100energy and transport solutions, Applied Energy 145 (2015) 139–154.

[8] P. Mancarella, MES (multi-energy systems): An overview of concepts and evaluation models, Energy 65 (2014) 1–17.

[9] A. Staino, H. Nagpal, B. Basu, Cooperative optimization of building energy systems in an economic model predictive control framework, Energy and Buildings 128 (2016) 713–722.

[10] S. Bracco, G. Dentici, S. Siri, Economic and environmental optimization model for the design and the operation of a combined heat and power distributed generation system in an urban area, Energy 55 (2013) 1014–1024.

[11] A. Moser, D. Muschick, M. Gölles, P. Nageler, H. Schranzhofer, T. Mach, C. Ribas Tugores, I. Leusbrock, S. Stark, F. Lackner, A. Hofer, A MILP-based modular energy management system for urban multi-energy systems: Performance and sensitivity analysis, Applied Energy 261 (2020) 114342.

[12] C. Klemm, P. Vennemann, Modeling and optimization of multi-energy systems in mixed-use districts: A review of existing methods and approaches, Renewable and Sustainable Energy Reviews 135 (2021) 110206.

[13] H.-K. Ringkjøb, P. M. Haugan, I. M. Solbrekke, A review of modelling tools for energy and electricity systems with large shares of variable renewables, Renewable and Sustainable Energy Reviews 96 (2018) 440–459.

[14] M. Mohammadi, Y. Noorollahi, B. Mohammadi-ivatloo, H. Yousefi, Energy hub: From a model to a concept – A review, Renewable and Sustainable Energy Reviews 80 (2017) 1512–1527.

[15] J. Allegrini, K. Orehounig, G. Mavromatidis, F. Ruesch, V. Dorer, R. Evins, A review of modelling approaches and tools for the simulation of district-scale energy systems, Renewable and Sustainable Energy Reviews 52 (2015) 1391–1404.

[16] SAUTER Deutschland, Presentation material of the research project MEMAP, 2020.

[17] DIN Deutsches Institut für Normung e.V., Building automation and control systems (BACS) - Part 3: Functions (ISO 16484-3:2005), 2005. URL: https://dx.doi.org/10.31030/9660475.

[18] A. Fernbach, W. Granzer, W. Kastner, Interoperability at the management level of building automation systems: A case study for BACnet and OPC UA, in: ETFA2011, IEEE, 2011, pp. 1–8. URL: http://ieeexplore.ieee.org/document/6059106/. doi:10.1109/ETFA.2011.6059106.

[19] Sauter-Cumulus GmbH, Anwendung «Wetterfrosch» - Sauter-Cumulus GmbH, 2013. URL: https://www.sauter-cumulus.de/unternehmen/news/newsletter/newsletter-februar-2013/anwendung-wetterfrosch/.

[20] J. Fonseca, T.-A. Nguyen, A. Schlueter, F. Marechal, City energy analyst (cea): Integrated framework for analysis and optimization of building energy systems in neighborhoods and city districts, Energy and Buildings 113 (2016) 202–226. Cited By 210.

[21] P. Favre-Perrod, A vision of future energy networks, in: Proceedings of the Inaugural IEEE PES 2005 Conference and Exposition in Africa, volume July 2005, IEEE, 2005, pp. 13–17. URL: http://ieeexplore.ieee.org/document/1611778/. doi:10.1109/PESAFR.2005.1611778.

[22] E. Augenstein, G. Wrobel, I. Kuperjans, M. Plessow, Top-Energy – Computational Support for Energy, in: Proceedings of 1st International Conference from Scientific Computing to Computational Engineering / IC-SCCE, 2004, pp. 8–10.

[23] GFaI Gesellschaft zur Förderung angewandter Informatik e. V., TOP ENERGY, 2022. URL: https://www.top-energy.de/.

[24] M. Wirtz, npro: A web-based planning tool for designing district energy systems and thermal networks, Energy 268 (2023). Cited By 11.

[25] S. Troitzsch, KaiATtum, T. Schelo, Arifa7med, MESMO - Multi-Energy System Modeling and Optimization, 2021. URL: https://github.com/mesmo-dev/mesmo. doi:10.5281/zenodo.5674243.

[26] S. Troitzsch, Multi-Energy System Modeling and Optimization (MESMO), Ph.D. thesis, Technische Universität München, 2022.

[27] C. Molitor, S. Gross, J. Zeitz, A. Monti, MESCOS—A Multienergy System Cosimulator for City District Energy Systems, IEEE Transactions on Industrial Informatics 10 (2014) 2247–2256.

[28] J. Dorfner, K. Schönleber, M. Dorfner, S. Candas, L. Odersky, urbs, 2019. URL: https://zenodo.org/record/3265960#.YhNovejMKF4. doi:10.5281/zenodo.594200.

[29] T. Licklederer, T. Hamacher, M. Kramer, V. S. Perić, Thermohydraulic model of smart thermal grids with bidirectional power flow between prosumers, Energy 230 (2021) 120825.

[30] T. Licklederer, D. Zinsmeister, I. Elizarov, V. Perić, P. Tzscheutschler, Characteristics and challenges in prosumer-dominated thermal networks, Journal of Physics: Conference Series 2042 (2021) 012039.

[31] P. Braun, T. Faulwasser, L. Grüne, C. M. Kellett, S. R. Weller, K. Worthmann, Hierarchical distributed admm for predictive control with applications in power networks, IFAC Journal of Systems and Control 3 (2018) 10–22.

[32] M. Kramer, A. Jambagi, V. Cheng, Distributed model predictive control for building energy systems in distribution grids, in: 2017 IEEE PES Innovative Smart Grid Technologies Conference Europe, ISGT-Europe 2017 - Proceedings, volume 2018-Janua, IEEE, 2018, pp. 1–6. URL: http://ieeexplore.ieee.org/document/8260293/. doi:10.1109/ISGTEurope.2017.8260293.

[33] N. P. R. E. Vespermann, Market Design for Energy Communities, Ph.D. thesis, Technische Universität München, 2022.

[34] AMPEERS ENERGY GmbH, AE DISTRICT MANAGEMENT, 2023. URL: https://www.ampeersenergy.de/operate/ae-district-management.

[35] G. Paludetto, E. Bionda, F. Soldan, MESP - An Interoperable Platform for Multi-Energy Systems, in: 2022 AEIT International Annual Conference (AEIT), IEEE, 2022, pp. 1–6. URL: https://ieeexplore.ieee.org/document/9951779/. doi:10.23919/AEIT56783.2022.9951779.

[36] J. Sauerbrey, T. Bender, S. Flemming, A. Martin, S. Naumann, O. Warweg, Towards intelligent energy management in energy communities: Introducing the district energy manager and an it reference architecture for district energy management systems, Energy Reports 11 (2024) 2255–2265. Cited By 1.

[37] OPC Foundation, OPC Foundation - The Industrial Interoperability Standard, 2022. URL: https://opcfoundation.org/.

[38] A. Fernbach, W. Granzer, W. Kastner, Interoperability at the management level of building automation systems: A case study for BACnet and OPC UA, in: ETFA2011, IEEE, 2011, pp. 1–8. URL: http://ieeexplore.ieee.org/document/6059106/. doi:10.1109/

ETFA.2011.6059106.

[39] D. Sturzenegger, D. Gyalistras, M. Morari, R. S. Smith, Model Predictive Climate Control of a Swiss Office Building: Implementation, Results, and Cost–Benefit Analysis, IEEE Transactions on Control Systems Technology 24 (2016) 1–12.

[40] R. Carli, G. Cavone, M. Dotoli, N. Epicoco, P. Scarabaggio, Model predictive control for thermal comfort optimization in building energy management systems, in: 2019 IEEE International Conference on Systems, Man and Cybernetics (SMC), volume 2019-Octob, IEEE, 2019, pp. 2608–2613. URL: https://ieeexplore.ieee.org/document/8914489/. doi:10.1109/SMC.2019.8914489.

[41] D. Mariano-Hernández, L. Hernández-Callejo, A. Zorita-Lamadrid, O. Duque-Pérez, F. Santos García, A review of strategies for building energy management system: Model predictive control, demand side management, optimization, and fault detect & diagnosis, Journal of Building Engineering 33 (2021) 101692.

[42] C. Saletti, M. Morini, A. Gambarotta, Smart management of integrated energy systems through co-optimization with long and short horizons, Energy 250 (2022). Cited By 15.

[43] D. Bytschkow, A. Capone, J. Mayer, M. Kramer, T. Licklederer, An OPC UA-based Energy Management Platform for Multi-Energy Prosumers in Districts, in: 2019 IEEE PES Innovative Smart Grid Technologies Europe (ISGT-Europe), IEEE, 2019, pp. 1–5. URL: https://ieeexplore.ieee.org/document/8905725/. doi:10.1109/ISGTEurope.2019.8905725.

[44] L. Heidemann, D. Bytschkow, A. Capone, T. Licklederer, M. Kramer, Sector Coupling with Optimization: A comparison between single buildings and combined quarters., Energy Informatics 2 (2019) 31.

[45] D. Bytschkow, A generic hierarchic architecture for the coordination of energy management systems., Dissertation, Technical University of Munich, 2020. URL: http://nbn-resolving.de/urn/resolver.pl?urn:nbn:de:bvb:91-diss-20201013-1542268-1-8.

[46] MEMAP Research Group, Quartiere nachhaltig betreiben, IKZ Haustechnik (2021).

[47] European Comission - Directorate-General for Energy, Energy communities, 2022. URL: https://energy.ec.europa.eu/topics/markets-and-consumers/energy-communities_en.

[48] Massachusetts Institute of Technology, Using lp_solve 5.5 in Java programs, 2022. URL: http://web.mit.edu/lpsolve/doc/.

[49] K. Eikland, P. Notebaert, Sourceforge - lpsolve Files, 2020. URL: https://sourceforge.net/projects/lpsolve/files/lpsolve/5.5.2.11/.

[50] D. Bytschkow, M. Zellner, M. Duchon, Combining scada, cim, gridlab-d and akka for smart grid co-simulation, in: 2015 IEEE Power & Energy Society Innovative Smart Grid Technologies Conference (ISGT), 2015, pp. 1–5. doi:10.1109/ISGT.2015.7131872.

[51] E. Gamma, H. Richard, R. Johnson, J. M. Vlissides, Design Patterns: Elements of Reusable Object-Oriented Software, Pearson Deutschland GmbH, 1995.

[52] J. Mayer, V. Pampana, M. Bernard, D. Bytschkow, T. Stohl, P. Gupta, M. Duchon, Holonic architectures for IoT-empowered energy management in districts, in: 2021 IEEE 7th World Forum on Internet of Things (WF-IoT), IEEE, 2021, pp. 189–194. URL: https://ieeexplore.ieee.org/document/9595252/. doi:10.1109/WF-IoT51360.2021.9595252.

[53] V. S. Peric, T. Hamacher, A. Mohapatra, F. Christiange, D. Zinsmeister, P. Tzscheutschler, U. Wagner, C. Aigner, R. Witzmann, CoSES Laboratory for Combined Energy Systems At TU Munich, in: 2020 IEEE Power & Energy Society General Meeting (PESGM), volume 2020-Augus, IEEE, 2020, pp. 1–5. URL: https://ieeexplore.ieee.org/document/9281442/. doi:10.1109/PESGM41954.2020.9281442.

[54] D. Zinsmeister, T. Licklederer, S. Adldinger, F. Christange, P. Tzscheutschler, T. Hamacher, V. S. Perić, A prosumer-based sector-coupled district heating and cooling laboratory architecture, Smart Energy 9 (2023) 100095.

[55] M. Mayer, A. Mohapatra, V. S. Peric, IoT Integration for Combined Energy Systems at the CoSES Laboratory, in: Proceedings of 2021 IEEE 7th World Forum on Internet of Things (WF-IoT), IEEE, 2021, pp. 195–200. URL: https://ieeexplore.ieee.org/document/9596000/. doi:10.1109/WF-IoT51360.2021.9596000.

[56] R. Unger, T. Schwan, B. Mikoleit, B. Bäker, C. Kehrer, T. Rodemann, "Green Building" - Modelling renewable building energy systems and electric mobility concepts using Modelica, in: Proceedings of the 9th International MODELICA Conference, September 3-5, 2012, Munich, Germany, volume 76, 2012, pp. 897–906. URL: https://ep.liu.se/en/conference-article.aspx?series=ecp&issue=76&Article_No=93. doi:10.3384/ecp12076897.

[57] D. Zinsmeister, T. Licklederer, Characterization of a Combined Heat and Power Unit at the CoSES laboratory, Technical Report, Technical University of Munich, 2021. doi:10.13140/RG.2.2.31035.34089/1.

[58] D. Zinsmeister, T. Licklederer, Characterization of a Thermal Storage at the CoSES laboratory, Technical Report, Technical Univeristy of Munich, 2021. doi:10.13140/RG.2.2.13461.19687.

## 5.3 Chapter Conclusion

For the narrative of this dissertation, several conclusions from this chapter shall be highlighted:

The main tasks to be covered by an control framework for smart thermal grids were identified. Two different control frameworks were proposed and are considered in the context of this dissertation. As a common element of both, a tool for sector-coupled smart district energy management was developed and validated. One unique feature is the live operation capability, faciliated by an OPC UA communication infrastructure in combination with a customized information model and tailored synchronization for the usage within an MPC context. In this approach, from the district management level, optimized power flow setpoints are send to local EMSs.

Thereby, for harnessing networking synergies, it was assumed that the necessary technical infrastructure is in place to facilitate a flexible energy exchange within the district. Regarding the thermal sector, PBDH as outlined in Section 2.1 are the type of network infrastructure that enables this flexible heat exchange. Therefore, the logical next step is a concrete concept for technically realizing PBDH networks - as stated in RQ1 (see Section 2.2). This will be addressed in the subsequent Chapter 6.

Further, the investigations in Pub1 revealed that an abstracted view focusing solely on power flows cannot sufficiently represent and anticipate technical details. Thus, there is a need for either integrating a more detailed technical model at the automation level (control framework A from Figure 5.3), or the consideration of technical details and local dynamics at the field level (control framework B from Figure 5.3). This will be addressed in Chapter 7 and Chapter 8.

# Chapter 6

# Network Concept

For being able to investigate the intricacies of PBDH networks as a representative type of smart thermal grids, this chapter discusses in Section 6.1 their technical implementation in the form of a reference network concept for the infrastructure. The implementation of the proposed reference network concept into the laboratory environment at TUM is discussed in Section 6.2 (Pub2). In Section 6.3 (Pub3), the dimensioning of components tailored for PBDH networks is addressed. Thereby, this chapter tackles especially RQ1 from Section 2.2.

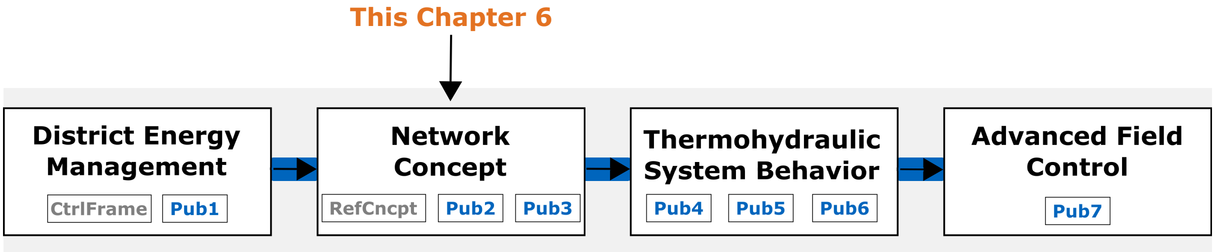


Figure 6.1: Position of this chapter within the overall structure of the main part of this dissertation.

**Chapter 6: Network Concept**
A reference network concept for PBDH networks is derived. It uses decentralized pumps on the network side of prosumer substations and adopts the return-to-supply (RS) principle for the feed-in. This reference network concept is practically implemented into a sector-coupled microgrid laboratory at TUM, enabling experimental testing of advanced control strategies in an emulated real-world environment. First laboratory experiments reveal special pump requirements due to high hydraulic resistances at low volume flows. Further, a new dimensioning method is developed to determine the decisive operating point for component dimensioning in PBDH networks, as in these systems, the hydraulic circuits and critical points can change dynamically. The proposed reference network concept provides a foundation for further technical and operational investigations of PBDH networks.

## 6.1 Reference Network Concept

To technically implement the concept of PBDH networks, a reference network concept is required. This comprises an hydraulic infrastructure and associated operational principles. In Section 2.1, PBDH networks are oulined as a specific form of smart thermal grids consisting only of prosumers that can flexibly exchange heat across the network infrastructure.
To the best of the author's knowledge, at the time this dissertation was conducted there was no specific reference network concept for PBDH networks existing in literature, as these kind of networks are not

yet broadly investigated. However, there are suggestions for infrastructure concepts of networks that incoporate certain aspects of PBDH networks. Therefore, in this section, through literature review on related concepts and comprehensive reasoning, a conceptual common ground is derived and condensed to a reference network concept for PBDH networks. This forms the basis for further investigations in the context of this thesis.

### 6.1.1 Literature Review

As introduced in Section 3.3, we categorize PBDH under 4GDH, making it a successor of TDH systems. A literature review and reference network concept for traditional DH systems is described in Section 3.2. To keep PBDH networks in line with the evolution of generations, several aspects can be adopted from TDH systems, while others have to be added and adapted.

#### Network Configuration

A two-pipe system with a hot supply line and a cold return line can be considered for PBDH. Following the underlying idea described in Section 2.1, PBDH networks are meant to operate without central elements. That means on the network side, only pipes connect the prosumers as network participants. In order to facilitate short transport paths between the distributed prosumers that change their modes dynamically, additional to the traditional radial topologies also meshed topologies, as well as combinations of both are reasonable to be considered.

#### Substation Connection Principles

Without central units, the distributed prosumer substations are core components, responsible for implementing and controlling the bidirectional heat exchange between the primary and secondary sides as well as within the network. For the connection of the substations to the network, there are four principles explored in literature (see Figure 6.2): supply-to-return (SR), supply-to-supply (SS), return-to-return (RR), RS.

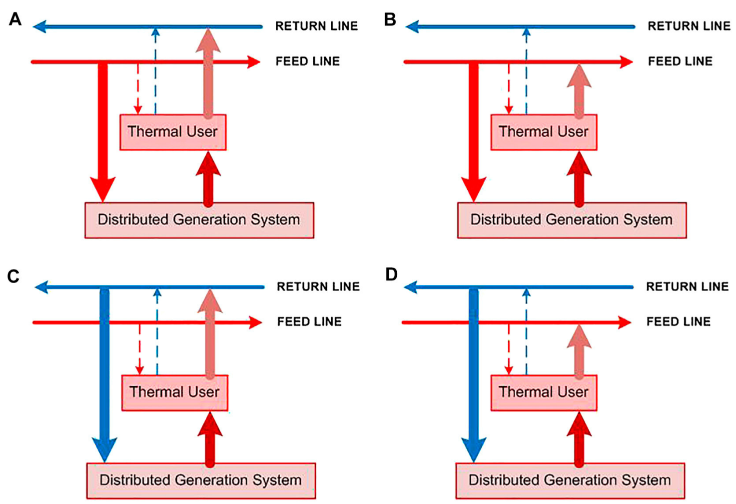


Figure 6.2: Schematic representation of volume flow interaction principles between substations and network: supply-to-return (A), supply-to-supply (B), return-to-return (C), return-to-supply (D). [80]

For the heat extraction from the network of prosumers in consumption mode, the SR principle can be adopted from TDH networks: warm water is drawn from the supply line, heat is transferred to the secondary side by the substation and the cooled water is released to the return line. Together with the SR principle, the actuators introduced in Section 3.2 for extraction can also be adopted. This includes the CV on the primary side and the CP on the secondary side.

The CV on the primary side for the extraction implies that the supply line must be pressurized in order for water to flow along the pressure gradient through the valve and the substation into the return line. In TDH networks, this pressure gradient is created by the central pumping station. To create the pressure gradient in a network consisting solely of prosumers without central units, the prosumers themselves must create the pressure difference. To do so, the SR principle is the only feasible option for feed-in. A feed-in pump (FP) on the primary substation side is employed to create the differential pressure between supply and return line. Cold water is drawn from the return line, heat is transferred from the secondary to the primary side to heat up the water in the substation and the warm water is injected to the supply line.

Concepts with two pumps on the primary side, including an extraction pump instead of the CV, are considered in some sources in the context of 5GDHC networks [94]. In this case there is no fixed pressurized line needed. However, also here a primary side FP is required for the production mode.

Initial studies on the feed-in to DH networks come from the context of distributed solar thermal plants and mostly assume TDH networks as context, where the solar plants serve as supplementary supply [69]–[80]. With TDH networks having central pumping stations that pressurize the supply line, various feed-in principles can be considered side by side, as done in the early solar thermal literature. It was only lately that the upcoming thermal prosumer principle integrated well with the research on decentralized feed-in to heat networks [95], [96]. In PBDH networks without central units, the RS principle is the only option to assure a pressurized supply line so that the SR extraction principle including its control can be adopted from TDH networks.
Nevertheless, also in the solar thermal research area, the RS principle has become established as prevalent choice. Options that feed into the return line are sub-optimal, as the return-line temperature increases, which decreases the operating efficiency of generation devices, like boilers [72]. Drawing from the supply line requires high temperature levels provided by the heat source to be able to feed in energy. Also, the RS principle represents the natural reversal of the SR extraction principle. Ref. [74] finds that for a high solar fraction, meaning a high penetration of decentral generation in the network, the RS feed-in is beneficial.

### Heat Exchanger Setup

As decentralized solar thermal generation is often seen as an retrofitted additional system, separate heat exchangers are usually planned for extraction and feed-in. However, shared hydraulic circuits for extraction and feed-in, allow to reduce the number of components and can increase economic efficiency [97].
Adopted from TDH networks with unidirectional substations, counter-current flow plate heat exchangers are the established solution, also for bidirectional substations. In the case of using a common heat exchanger for feed-in and extraction, the flow direction on the secondary side must be reversed. This requires either an additional production pump (PP) on the secondary side or a suitable hydraulic switch, using three-way valves. Some configurations additionally use a bypass between supply- and return-line on the primary side to circulate and heat up the medium before feeding in, when switching between modes [97].

**Prosumer-side configuration**

For the prosumer side, various configurations are possible: Bidirectional heat transfer stations, heat generators, the consumption system, and storages can be interconnected in numerous ways. In Ref. [98], the author of this dissertation co-authored a paper that delves into and examines these distinct configurations. In the publication, typical system components on the secondary side are abstracted into classes and arranged in various ways relative to one another, thus deriving potential prosumer-side configurations. In a preliminary selection, out of 14 configurations, 5 are excluded due to high estimated exergy losses, limited flexibility, or their incompatibility with PBDH [99]. The performance of the remaining 9 configurations is assessed using Modelica-based simulations, evaluating exportable excess heat, network temperatures, and the overall efficiency of the heat supply. These configurations are explored across different scenarios, varying in heat generation type (e.g., heat pump, solar thermal collectors, or combustion device) and the required supply temperatures for both the prosumer and network side. The study reveals that different configurations offer distinct benefits depending on specific boundary conditions. Thereby, Ref. [98] serves as a guide, assisting in the selection of the most suitable prosumer-side configuration given the desired district heating network and consumption temperatures. One learning from this paper is, that the technical arrangement of the secondary side can have significant impact on the prosumer behavior and performance. To exclude this impact from the network-oriented focus of this dissertation, the prosumer side beyond the substation is abstracted as an ideal heat source (production modes) or sink (consumption mode), having constant inflow temperatures from the prosumer system to the substation.

### 6.1.2 Reference Concept

A reference network concept for PBDH networks is derived by condensing the conclusions of the preceding literature review to a minimal configuration. In the following the features of the proposed reference network concept for PBDH are listed. Additionally, Figure 6.3 illustrates this reference network concept, while Figure 6.4 details the according reference configuration for bidirectional substations in PBDH networks.

- district heating network with warm water as carrier medium
- two-pipe system with warm supply and cold return line, supply line has higher pressure than return line
- radial, meshed or mixed network topologies allowed
- no central units in the pipe network, i.e. no network pumps, no central plant or storages, no hydraulic or thermal balancing unit
- all network participants are prosumers in the sense that they can switch over time between production and consumption mode w.r.t. the network; no dominant participant, but peer prosumers
- substations indirectly connect the prosumer side via a heat exchanger
- the same heat exchanger is used in production and consumption mode: plate heat exchanger, always operated in counter-current flow mode, reversal of flow directions on both sides when operation mode changes
- heat feed-in in production mode via volume flows from return to supply line (RS), extraction in consumption mode via volume flows from supply to return line (SR)
- production mode: feed-in pump (FP) on the primary side and production pump production pump (PP) on the secondary side drive the volume flows; FP pressurizes the supply line

- consumption mode: control valve (CV) on the primary side regulates volume flow, consumption pump (CP) on the secondary side drives the volume flow
- control valves and variable-speed pumps are used, controlled by an external signal to modulate the opening or speed respectively
- no shortcut between supply and return line for low / no demands, this implies: for any prosumer to interact with the network, at least one other prosumer in opposite mode must be active to have a closed hydraulic circuit, no buffering function of the network itself, network infrastructure is meant just for transmission
- secondary side prosumer system is not specified (system agnostic investigations), the prosumer is an idealized heat source (production mode) or sink (consumption mode), providing specific constant inflow temperatures to the substation from the secondary side

This proposed reference network concept still allows different variations for specific network implementations, but fixes some basic architecture and functional principles.
In principle rhe reference network concept can be used for DH and DC networks, also an implementation for DHC is possible, as heat consumers are cold producers and vice versa. In the context of this dissertation the focus is on DH.
Further, the presented concept is open to be used at different temperature levels. Here no specifications on the temperature levels are made on purpose: the functional principles relevant for the further investigations remain basically the same independent from the temperature level. As a small note, it should nevertheless be pointed out again that in the context of this dissertation, PBDH networks are assigned to 4GDH, which already delineates the range of temperatures (see Section 3.3). This applies similarly to other technical specifications, like the type of pipelines etc. Moreover, installations for a safe and reliable operation, like pressure relief valves or expansion vessels are not mentioned or shown here for the sake of conciseness.

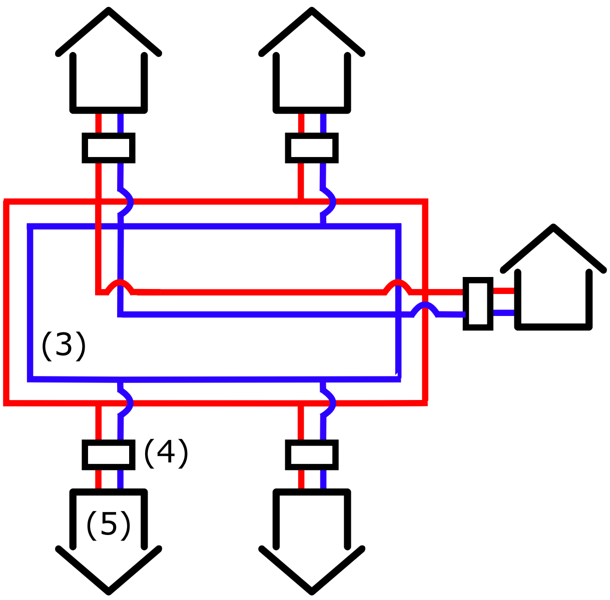


Figure 6.3: Simplified exemplary scheme of the proposed reference network concept for PBDH: (3) pipe network, warm supply line in red, cold return line in blue; (4) bidirectional prosumer substations, see Figure 6.4; (5) prosumer systems.

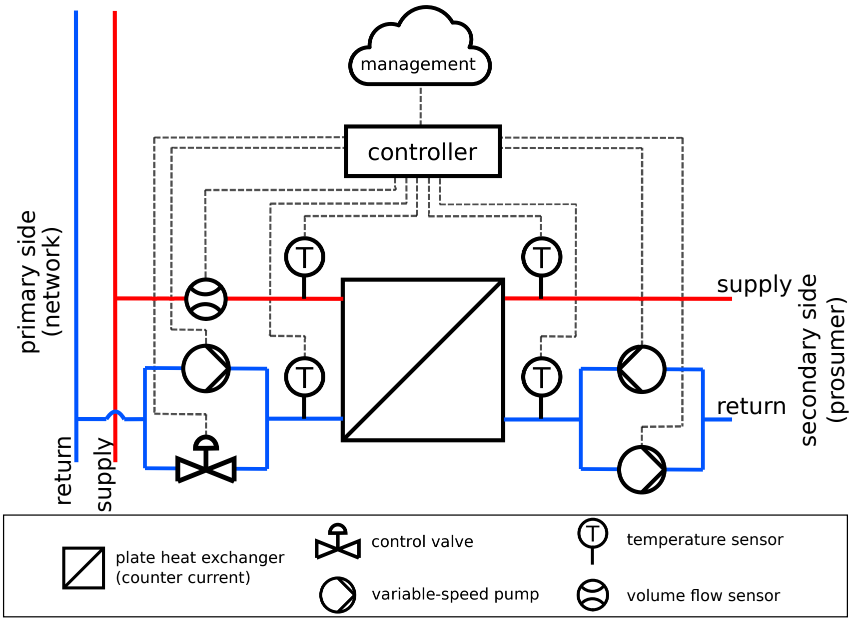


Figure 6.4: Proposed reference concept of bidirectional substations for thermal prosumers.

## 6.2 Pub2: A prosumer-based sector-coupled district heating and cooling laboratory architecture

### 6.2.1 Context

The concept of PBDH networks is relatively new and not yet broadly investigated, although studies on it have the potential to lead to valuable insights for smart thermal grids in general (as elaborated in Section 2.1). In addition to theoretical and simulation-based studies, practical experimental investigations with real hardware are crucial to observe phenomena that simplified modeling cannot capture. The construction of heat networks in the field is very complex and costly, and users (e.g., in buildings) can experience significant comfort disruptions during the prototype operation of unexplored network concepts. Therefore, prior to field tests, a laboratory setup is as an ideal environment for the practical examination of network concepts. Parallel to the considerations on reference network concepts for PBDH within the scope of this dissertation, the laboratory for Combined Smart Energy Systems (CoSES) was planned and commissioned at the TUM (see Figure 6.5). The reference network concept for PBDH described in Section 6.1 is practically implemented in this laboratory environment.

The primary motivation for the CoSES laboratory is to explore and analyze smart operation and control strategies for future small-scale thermal and electrical networks, also called 'microgrids'. Therefore it is aimed to replicate a neighborhood of five buildings, focusing on their energy technology setups, covering both layers, the electricity and thermal energy supply. To enhance the implementation of smart operating strategies, computation and communication is the third essential layer. Apart from testing operation and control strategies and investigating the system behavior (e.g. [100], [101]), the laboratory environment is used for the characterization of components (e.g. [102]–[105]) and for the parameterization, calibration and validation of simulation models (e.g. [106], [107]).
A detailed documentation of the laboratory implementation can be found on the public Wiki[1] of the associated research group. A brief overview on the general architecture can be found in Ref. [108].

[1]https://collab.dvb.bayern/display/TUMcoseslab/CoSES+Laboratory+Documentation (work in progress, visited on 2023/11/11)

Figure 6.5: Picture of the CoSES Laboratory, view from the top floor. Status: 2019. ©Stefan Hobmaier / TUM

Information on the electrical side of the laboratory and on the attached internet of things (IoT) infrastructure can be found in Ref. [109]–[112]. More detailed information on the electrical side at its design as an active distribution grid laboratory is given in the complementary dissertation of Anurag Mohapatra and his further work.

On the thermal side, the laboratory implements the proposed reference network concept for PBDH. The unique selling point is that the laboratory environment is designed to practically study systemic interactions in smart thermal grids with prosumers, covering all levels of operation and control (see automation pyramid in Figure 5.2), as well as the interconnection to the electrical layer (sector coupling). Various scenarios can be investigated independently of the real environment. By employing commercial generation devices and utilizing actual hardware like heat exchangers, this approach, in contrast to pure simulations, also considers the impact of real system dynamics.
In combination with simulation models and a sophisticated communication and control framework, this complements to a thermal power hardware in the loop (PHiL) setup. Boundary conditions, such as thermal demands, ambient conditions, pipe delays and losses are calculated and communicated in real-time between the simulation and the emulating hardware.

The implementation of the proposed PBDH reference network concept from Section 6.1 in the CoSES laboratory environment covers particularly two core modules: bidirectional substations and grid emulator modules.

Figure 6.4 showed the abstract concept drawing of the proposed bidirectional prosumer substation configuration. For comparison, a detailed technical drawing in Figure 6.6 illustrates exemplarily how the reference network concept is implemented in the CoSES laboratory. The commissioning and characterization of this bidirectional substation, is described in a bachelor thesis document, including the faced challenges (see Ref. [113]). The substations in the laboratory environment are designed with three temperature levels, to facilitate the investigation of 4GDH networks that are used for both heating and cooling. The medium temperature level can be used as the colder return line of the warm supply line for heating. At the same time, the medium temperature level can be used as warmer return line of the cold supply line, used for cooling purposes. Therefor, the substations in the laboratory have two heat exchanger with the medium temperature line as common return line.

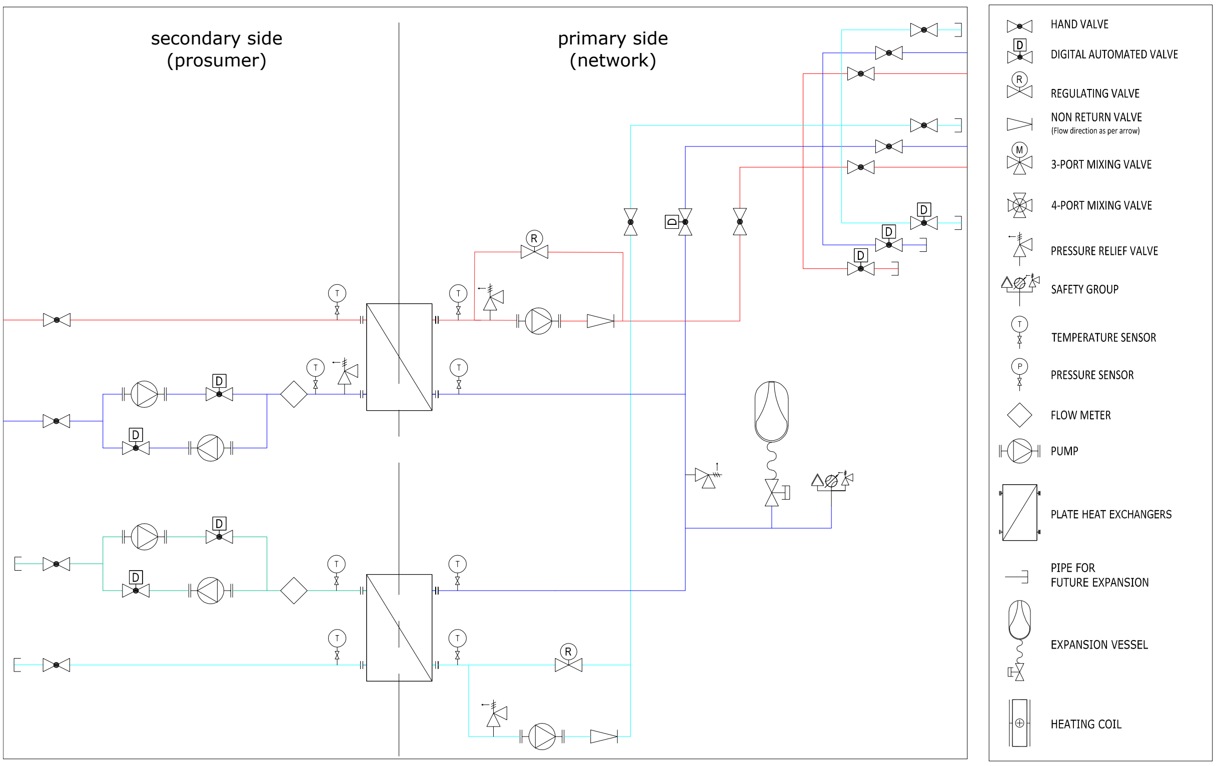


Figure 6.6: Technical drawing of a bidirectional substation as implemented in the CoSES laboratory at TUM. To be seen complementing and in comparison to the abstract bidirectional substation concept in Figure 6.4.

The thermal grid emulator modules allow to emulate the key physical behavior of the interconnecting network pipes in a PBDH network. This covers i.e. heat losses and time delays for the transportation of heat. By controlled extraction of water from the pipelines and injection of water with a specifically warmer or cooler temperature, the delay and thermal losses to the surroundings of various pipe lengths can be replicated, without modifying the actual lengths of the pipes in the laboratory.

The subsequent publication describes the architecture and setup of the thermal side of the CoSES laboratory in detail and presents first experimental results. The setup of this testbed allows to practically investigate PBDH and smart thermal grids in general.

### 6.2.2 Paper

| | |
|---|---|
| **Title** | **A prosumer-based sector-coupled district heating and cooling laboratory architecture** |
| **Authors** | Daniel Zinsmeister, Thomas Licklederer, Stefan Adldinger, Franz Christange, Peter Tzscheutschler, Thomas Hamacher, Vedran S. Perić |
| **Publication medium** | Smart Energy, Volume 9, February 2023, 100095 |
| **Copyright** | Included under Elsevier's copyright terms of 2023, which permit the inclusion in a thesis or dissertation provided the thesis is not published commercially. (https://www.elsevier.com/about/policies/copyright, Status: August 2023) |
| **Identifier / URL** | https://doi.org/10.1016/j.segy.2023.100095 |
| **Author contributions** | according to the Contributor Roles Taxonomy (CRediT, see [93]) |
| Daniel Zinsmeister | Conceptualization, Visualization, Writing - Original Draft and Editing. |
| Thomas Licklederer | Conceptualization, Writing - Original Draft, Review and Editing. |
| Stefan Adldinger | Writing - Original Draft. |
| Franz Christange | Conceptualization, Writing - Review. |
| Peter Tzscheutschler | Conceptualization, Writing - Review, Supervision, Project administration, Funding acquisition. |
| Thomas Hamacher | Conceptualization, Supervision, Funding acquisition. |
| Vedran S. Perić | Conceptualization, Writing - Review, Supervision, Project administration, Funding acquisition. |

Smart Energy 9 (2023) 100095

Contents lists available at ScienceDirect

Smart Energy

journal homepage: www.journals.elsevier.com/smart-energy

# A prosumer-based sector-coupled district heating and cooling laboratory architecture

Daniel Zinsmeister [a,*], Thomas Licklederer [a], Stefan Adldinger [b], Franz Christange [c], Peter Tzscheutschler [a], Thomas Hamacher [a], Vedran S. Perić [a]

[a] Technical University of Munich, Arcisstrasse 21, Munich, 80333, Bavaria, Germany
[b] Stadtwerke Neuburg an der Donau, Heinrichsheimstrasse 2, Neuburg an der Donau, 86633, Bavaria, Germany
[c] Triowatt GmbH, Falkenstr. 12c, Stephanskirchen, 83071, Bavaria, Germany

ARTICLE INFO

*Keywords:*
District heating
District cooling
Decentralized feed-in
Prosumer
Sector coupling
Power-hardware-in-the-loop
Laboratory

ABSTRACT

New control strategies for thermal systems and innovative district heating and cooling grids can help to decarbonize the thermal sector. Before implementing these new concepts, they should be validated, ideally with commercial hardware but without influencing user comfort. For this reason, the laboratory at the research center for Combined Smart Energy Systems (CoSES) at the Technical University of Munich (TUM) was designed. By combining commercial hardware with Power Hardware in the Loop simulations, the laboratory enables research in a controllable, but realistic setting without affecting real users. It consists of five prosumers equipped with heat generators and thermal storages. All prosumers are linked with an adjustable district heating and cooling grid. The modular hardware and control architecture presented in this paper covers management-, automation-, field-level control and offers interfaces to external control. A case study shows that prosumer integration into flexible district heating grids can reduce overall heating costs but requires intelligent control concepts for transfer stations and heat generators. The conducted experiments emphasize the importance of validating control strategies in laboratory environments. They allow the analysis of phenomena that are difficult and impractical to model accurately with existing simulation tools. The structure and capabilities of the laboratory are presented in order to foster collaboration with other researchers.

## 1. Introduction

Around half of the global final energy consumption is caused by heating and cooling [1]. 46% of the heating and cooling energy is used in residential and commercial buildings, mainly for space heating and domestic hot water (DHW) [1]. Currently, most of the energy used for heating comes from fossil fuels or biomass [1] while space cooling is typically provided by electrically powered fans or air conditioners [2]. To decarbonize this sector, district heating and cooling (DHC) grids can be a key element [3–6]. In recent years, the development of DHC grids has been focused on the following key aspects:

- Grid temperatures for district heating grids are reduced to minimize transport losses and enable the integration of low temperature heat sources [7].
- DHC, electric and gas grids are combined to exploit synergies. Those synergies can increase energy flexibility needed for balancing intermittent and volatile renewable energy sources and achieve the optimal efficiency of the overall energy system [8–11].
- Formerly unused energy sources are integrated into DHC grids, by using booster heat pump transfer stations that feed excess cold into the DHC grid during heating and vice versa [9,12,13] or by integrating decentralized heat sources and prosumers analog to the electric grid [14–16].
- Control strategies are improved to reduce grid return temperatures, e.g. by motivation tariffs [17] or by integrating low temperature district heating grids into an existing district heating grids [18]. In addition, energy sources can be integrated in a more intelligent way, e.g. by introducing new market mechanisms to district heating systems [19,20] or by implementing Model Predictive Control (MPC) to improve waste heat utilization [21].

When developing and evaluating new approaches in DHC research, simulation models are often used. However, simulations do not always

* Corresponding author.
*E-mail address:* d.zinsmeister@tum.de (D. Zinsmeister).

https://doi.org/10.1016/j.segy.2023.100095
Received 5 December 2022; Received in revised form 27 February 2023; Accepted 27 February 2023
Available online 5 March 2023

adequately represent realistic behavior, like the dynamic behavior or the internal control of components. Laboratories are still useful to emulate commercial products, map interactions of different control layers (management, automation, field control) and to validate control strategies without influencing user comfort. The requirements for a smart energy laboratory with a focus on district heating systems are:

- a detailed emulation of prosumer behavior in smart energy systems including heat and cooling rates within the building must be possible,
- commercial equipment for heat generators and storages shall be used,
- the boundary conditions and all components must be completely controllable, independent from external influences and the environment (climate, weather etc.),
- sector coupling must be featured to enable investigations on the interaction of the thermal sector with other sectors, such as electricity or mobility.

Several laboratories for heating or DHC systems test individual components, like heat pumps [22], booster heat pump transfer stations [23] or decentral feed-in stations [24,25]. In order to test the behavior of DHC grids, other laboratories consider complete, small-scale DHC grids. The Energy Exchange Lab at Eurag Research [26] in Bozen emulates the behavior of a small low temperature district heating grid with different generators (combined heat and power, condensing boiler and solar thermal) and a configurable grid length. Heat pumps emulate prosumers that extract heat or feed it into the grid. The District LAB of Fraunhofer IEE is being built and will feature a flexible heating grid, a pipe test bench for mechanical tests and different control concepts [27]. The NODES laboratory investigates the effects of thermal cross-linking, in unidirectional, bidirectional, or meshed grid topologies. It consists of a simplified district heating grid with three consumers, a seasonal storage and a heat source [28].

Although these laboratories focus on the investigation of DHC grids, prosumers and consumers are not emulated in detail, neglecting effects within buildings. Moreover, the synergy between DHC grids and electric grids cannot be analyzed in detail in these laboratories. In order to fill this gap, the research center for Combined Smart Energy Systems (CoSES) at Technical University of Munich (TUM) was developed [29]. The CoSES laboratory enables research on innovative concepts of DHC grids and smart energy systems. It emulates five houses, one multi-family house (MF) and four single-family houses (SFs), equipped with decentralized electricity and heat generators, electric vehicle charging stations and controllable thermal and electricity loads. A configurable electric and DHC grid connects the houses. The setup allows a holistic investigation of sector coupling in the building domain and supplements the existing laboratories with its detailed emulation of prosumers and their impact on DHC and power grids.

This paper describes the architecture of the CoSES laboratory, with focus on a detailed description of the thermal subsystem. The proposed design of the laboratory can be used as an architecture template for other DHC laboratories. The goal is to present the design, capabilities and limitations of the laboratory, as well as the operation principles in order to share the experience, help in designing similar laboratories and foster collaboration and exchange with similar laboratories as well as with other research institutions and companies in this field. The laboratory is designed to test control strategies for new generation DHC grids, analyze new concepts for bidirectional heat and cold transfer, generate data to validate simulation models and quantify the sector coupling potential of different setups.

The laboratory can be used for research on 3rd and 4th generation and ambient temperature heat grids. Older generations cannot be tested as they require temperatures above 100 °C. Moreover, research on 2nd, 3rd and 4th generation cooling grids is possible. The classification into

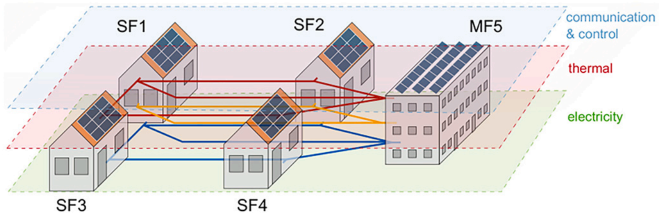


**Fig. 1.** Different layers of the CoSES laboratory. Five prosumers are connected by a district heating and cooling grid.

the different generations is based on Lund et al. [8] and Østergaard et al. [30].

A case study is conducted with the target demonstrating how the laboratory works. The case study shows that the laboratory provides insights into DHC systems that are hard to simulate. This includes the behavior of commercial equipment. Heat generators, for example, are influenced by their internal control and external influences that can hardly be captured, while pumps and valves behave non-linearly. In addition, we were able to gain first findings on the operation of prosumer-based DHCs.

The paper is structured as follows: Chapter 2 describes the hardware components of the laboratory. The communication and control structure is presented in chapter 3. Chapter 4 shows a case study before chapter 5 discusses the strength, limitations and research potential of the laboratory. In chapter 6 the conclusions are drawn.

## 2. Thermal energy system

Fig. 1 shows the layout of the CoSES laboratory, which can be divided into three layers:

- The electricity layer consists of a flexible electric grid, battery storages, electric vehicle charging stations and emulates distributed generators and consumption at household level. The electric side is described in detail by Mohapatra et al. [31] and Christange [32].
- The thermal layer consists of five thermal prosumers that are connected with an adjustable DHC grid and is described in detail in the following section.
- The communication and control layer controls and monitors the experiments and is described in detail in section 3.

The laboratory consists of five houses which are connected with a DHC grid. The length of the grid between the houses can be adjusted with a DHC grid emulator according to the experiment setting (see Subsection 2.1). This module is necessary since the houses in the CoSES laboratory are located with a maximum distance of 10 meters. It emulates heat losses and the time delay of temperature changes between two houses over variable distances, as will be explained in the later subsection. The modules can also be used to add additional emulated houses into the system by mimicking the dynamics of a house through cooling or heating the water in the pipe.

The laboratory components were selected with the aim of covering as wide a range of household technologies as possible. A catalog of criteria was prepared for this purpose; among other things, all heat generators had to be controllable by an energy management system. In addition, heat generators were selected to cover a broad range of applications:

- Heat generators with a low purchase price: condensing boiler
- Conventional technology for sector coupling: combined heat and power units (CHPs)
- Renewable technology for sector coupling: Heat Pumps (HPs), with different heat sources
- Volatile renewable heat generators: solar thermal emulators

**Table 1**
Overview of the heat modules of each house.

| | SF1 | SF2 | SF3 | SF4 | MF5 |
|---|---|---|---|---|---|
| Heat Generator | CHP (2 $kW_{el}$, 5.2 $kW_{th}$)<br>Condensing boiler (20 $kW_{th}$)<br>Solar thermal (9 $kW_{th}$) | Condensing boiler (20 $kW_{th}$)<br>Air source HP (10 + 6 $kW_{heat}$, 9 $kW_{cold}$)<br>Solar thermal (9 $kW_{th}$) | Ground source HP (10 + 6 $kW_{heat}$)<br>Solar thermal (9 $kW_{th}$) | Stirling engine (1 $kW_{el}$, 6 $kW_{th}$)<br>Integrated auxiliary boiler (20 $kW_{th}$)<br>Integrated electric heating rod (6 $kW_{th}$) | CHP (5 $kW_{el}$, 11.9 $kW_{th}$)<br>CHP (18 $kW_{el}$, 34 $kW_{th}$)<br>Condensing boiler (50 $kW_{th}$) |
| Thermal Storage | 800 l | 785 l | 1000 l | 1000 l | 2000 l |
| Domestic Hot Water | Fresh water storage (500 l) | Fresh water station | Fresh water station | Internal heat exchanger | Fresh water station |
| Transfer Station | Bidirectional HCTS (30 $kW_{th}$)<br>bHPTS (19 $kW_{heat}$, 14 $kW_{cold}$) | Bidirectional HCTS (30 $kW_{th}$) | Bidirectional HCTS (30 $kW_{th}$) | Bidirectional HCTS (30 $kW_{th}$) | Bidirectional HCTS (60 $kW_{th}$) |
| Thermal load emulator | 30 $kW_{heat}$, 9 $kW_{cold}$ | 30 $kW_{heat}$, 9 $kW_{cold}$ | 30 $kW_{heat}$, 9 $kW_{cold}$ | 30 $kW_{heat}$ | 60 $kW_{heat}$ |

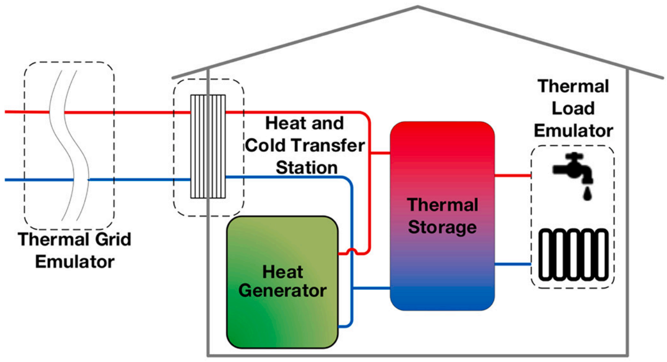


**Fig. 2.** General structure of the houses, the red line indicates the supply pipe, blue the return pipe.

Furthermore, thermal storage systems are used to decouple generation and demand. For this purpose, different sizes, designs and connections were selected for the storage units. Fig. 2 and Table 1 show the general structure of each house, which consist of the following elements:

- Heat and cold transfer stations (HCTS, see Subsection 2.2):
  Each house is equipped with a bidirectional HCTS. SF1 has an additional booster heat pump transfer station (bHPTS).
  The bidirectional HCTS connects the house to the DHC grid. With this module, heat or cold can be extracted from or fed into the grid. It is designed for a return-to-supply feed-in, since this is the most efficient feed-in setup [33]. Other setups, like supply-to-supply or return-to-return feed-in as described by Lamaison et al. [33] could be realized with minor modifications.
  The bHPTS can be used for both, heating and cooling. It consists of a standard heat exchanger and a booster heat pump (BHP), a water-source heat pump, using the DHC grid as the heat source. If grid temperatures are higher than the water in the heating system, a heat exchanger is used to extract heat from the grid. If grid temperatures are too low for direct usage, the BHP operates. The cold extraction operates in a similar way.
- Heat generators (see Subsection 2.3):
  In order to have realistic behavior, the laboratory uses real heat generators. Solar thermal heat generators are emulated with controllable electric heaters, to run experiments independent of outdoor weather conditions. Table 1 provides an overview of the technical specifications of the different heat generators and in which house they are installed.
- Thermal load emulators (see Subsection 2.4):
  Since no real consumers are connected in the CoSES laboratory, the heat and cold consumption is emulated. Setpoints can be provided by PHIL or from predefined data, e.g. from field test measurements.
- Thermal storages and domestic hot water (DHW) systems (see Subsection 2.5):
  Thermal storages of different sizes from 500 l to 2000 l are used in the laboratory. All storages have several inlet and outlet ports at different heights. Three storages are connected to solar thermal systems with an internal heat exchanger and the storage in SF4 is equipped with an internal electric heating rod.
  Since DHW has very high hygiene requirements as compared to the heating system, the two circuits are separated. DHW is heated by the thermal storage tank using heat exchangers.

The CoSES laboratory uses a modular system architecture, which allows easy adaptations and expansions according to specific experiment requirements.

### 2.1. District heating and cooling grid emulator

Fig. 3 shows the structure of one pipe of the DHC grid emulator, which heats or cools the water in the DHC grid according to the desired pipe temperature for supply or return. The pipe temperature is provided by the user or a PHIL simulation model. Check valves are used to rectify the flow in the active part of the emulator, allowing it to be used in both flow directions (①). The DHC grid emulator has two operation modes:

- If the desired pipe temperature is higher than the inlet temperature, the water is heated up by an electric heating rod (⑤).
- If the desired pipe temperature is lower than the inlet temperature, the 4-way-mixer is used to exchange hot water from the grid with cooling water (②). A control valve on the cooling water inlet is used to match the cooling water pressure to the grid pressure (③). Another control valve at the cooling water pipe controls the water flow, to ensure that the flow rates in the DHC grid, upstream and downstream of the mixer, are identical (④). The electric heating rod has a high thermal mass, which has a negative effect on the dynamic response. For this reason, a bypass is included. A 3-way mixing valve controls whether the flow goes through the bypass or the heating rods (⑥).

### 2.2. Heat and cold transfer station

Two different types of HCTS are installed at the CoSES laboratory, bidirectional HCTS and a bHPTS.

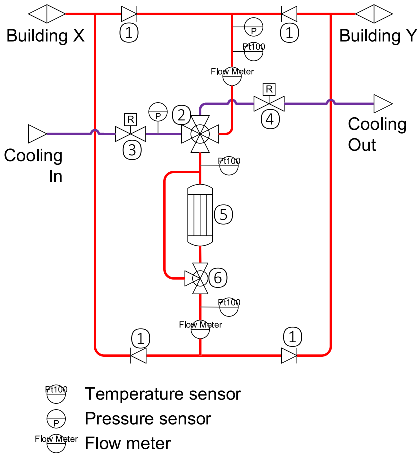


(a)

(b)

**Fig. 3.** District heating and cooling grid emulator: a) schematic drawing; b) setup at the CoSES laboratory.

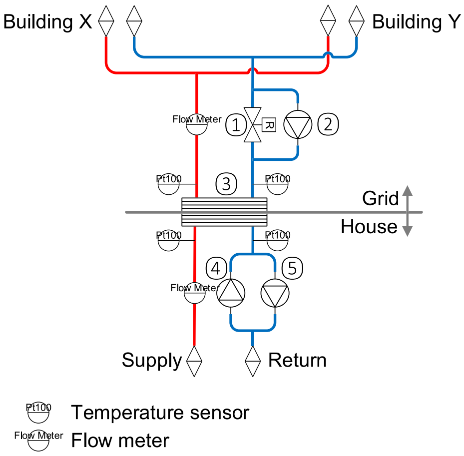


(a)

(b)

**Fig. 4.** Bidirectional heat and cold transfer station: a) schematic drawing; b) setup at the CoSES laboratory.

### 2.2.1. *Bidirectional heat and cold transfer station*

Each bidirectional HCTS has two circuits that can be used in a district heating grid with three different temperature levels or a DHC grid. Fig. 4 shows one circuit of the bidirectional HCTS. A heat exchanger separates the DHC grid and the house circuit (③). Due to the pressure difference between the supply pipe (red) and return pipe (blue), the water flow for heat or cold extraction from the grid can be controlled by a control valve (①), while a grid pump is required for feed-in (②). On the house side, the flow is controlled by two separate pumps (④ and ⑤).

### 2.2.2. *Booster heat pump transfer station*

In the laboratory, the bHPTS 'WP Grid HiQ F14' from Ratiotherm [34] is installed and its schematic is shown in Fig. 5. The heat exchanger (①) and the BHP (②) separate the grid from the house.

Inside the house, the flow can be channeled through the heat exchanger or the HP by the electric ball valves (④). The flow rate is controlled by the pump (⑤) and an electric heating rod is installed as an auxiliary heater (⑥).

On the grid side, the flow through the heat exchanger or BHP is controlled by another set of control valves (③). In standard configuration, water flows from the warm supply pipe to the cold return pipe for both heat and cold extraction. The pressure in the supply pipe is higher and therefore, no additional pump is needed to generate water flow for cold extraction. More efficient options for cold extraction, where the flow direction changes, can be investigated with the additional pump that generates the volume flow from the return to the supply pipe (⑦). Electric ball valves are used to include or bypass the pump (⑧).

## 2.3. *Heat generators*

The installed heat generators are connected to a higher-level energy or building management system which provides the generation setpoints. The internal structure and control of these heat generators is not modified to preserve the behavior of commercially available products.

Two different types of HPs are installed in the laboratory. An air source heat pump (ASHP) with a nominal heating/cooling rate of 10 kW/9 kW and a ground source heat pump (GSHP) for heating only with a nominal heat rate of 10 kW. Both HPs have a 6 kW electric heater as an auxiliary heater that is activated when the heat output is too low.

The commercial HPs installed in our laboratory are operated with a constant temperature difference between supply and return. This means that the supply temperature can not be specified as a setpoint to the HP, but depends on the return temperature from the thermal storage. In order to efficiently provide DHW at a high temperature and heating at a low temperature, the stratification within the thermal storage is used.

Fig. 6 shows the schematic of the HP testbed in the laboratory. Two 3-way valves (①) allow the HP to change the connection to the thermal storage and switch between the high temperature at the top and the

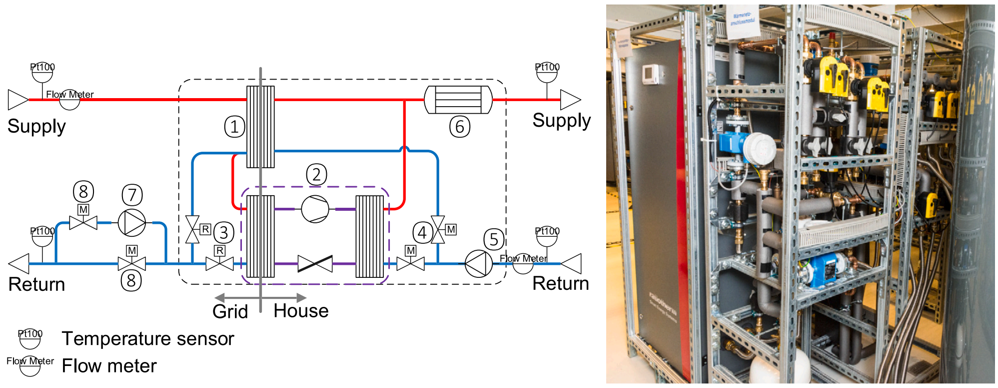


(a) (b)

**Fig. 5.** Booster heat pump transfer station: a) schematic drawing; b) setup at the CoSES laboratory.

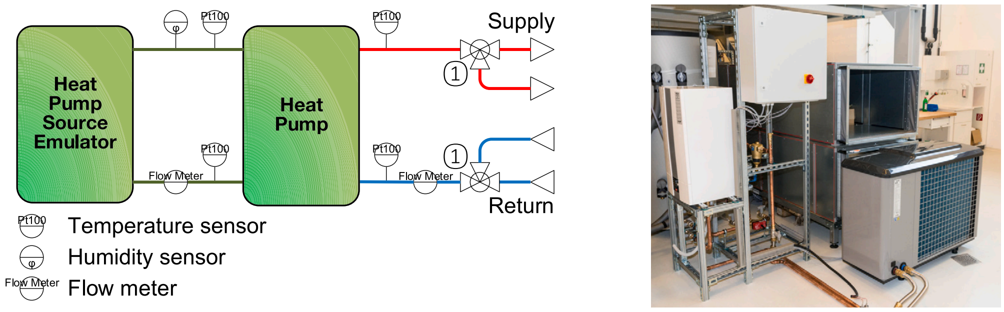


(a) (b)

**Fig. 6.** Heat pump emulator: a) schematic drawing; b) setup of the air source heat pump at the CoSES laboratory.

low temperature at the bottom. The ambient heat source is provided according to experiment specifications by heating up brine for the GSHP or setting the air humidity and temperature in a heating, ventilation and air conditioning (HVAC) system for the ASHP.

The laboratory is further equipped with gas powered CHPs and condensing boilers. Four different CHPs are used, three gas engine CHPs and one Stirling CHP. Three different Wolf ‘CGB’ condensing boilers are installed with a thermal output of 14, 20 and 50 kW [35].

Solar thermal heat generators are emulated in the laboratory, to run experiments independent of outdoor weather conditions. The heat source is a 9 kW electric heating rod, which corresponds to a solar thermal system of up to 15 $m^2$. The water flow is controlled by a pump. Solar thermal systems are usually filled with brine to prevent freezing and are therefore connected to a separate circuit. They are integrated into the heating system through an internal heat exchanger in the thermal storage tanks.

## 2.4. Thermal load emulator

For experiments, it is necessary to emulate heat and cold consumption in detail. Therefore, thermal load emulators for heat and cold are used and controlled according to setpoints defined by the PHIL setup (see chapter 3.2) or field test data.

### 2.4.1. Heat consumption

The heat consumption module is constructed similar to the testbed described by El Baz et al. [22] and is shown in Fig. 7.

A commercially available mixing module is installed, which consists of a 3-way mixer (①) and a pump (②). The 3-way mixer is used to reduce the supply temperature according to the setpoint of the heating system, e.g. 40 °C for space heating. In real houses, the pump generates the pressure difference to enable the water flow in the heating system and the flow rate is controlled by thermostatic radiator valves in each room. Since those valves are not installed in the emulator, a controllable pump is used to control the volume flow according to the target flow rate. The consumed heat is extracted by a heat exchanger (③). A control valve in the cooling circuit controls the cooling water flow, to reach the target return temperature in the heating circuit (④).

The DHW circuit uses three solenoid valves to emulate the opening and closing of different DHW consumers (⑤). The flow rate through the solenoid valves is set corresponding to different consumers, e.g. taps or showers, by three needle valves (⑥). The cold water flow is supplied by the cooling circuit. As prevalent in houses these days, a circulation pump is used to prevent the DHW pipe from cooling down (⑦). The resulting losses are extracted by a heat exchanger (⑧) and a control valve (⑨), the same way as in the heating circuit.

### 2.4.2. Cold consumption

The cold consumption is emulated with the solar thermal module. As a pump is already installed in the cold generator, the pump in the module is bypassed when used as a cold consumer. The electric heater is controlled to match the cold consumption.

## 2.5. Thermal storage and domestic hot water system

The thermal storage is integrated differently for each house and is equipped with 10 temperature sensors on its surface at different heights, to measure the temperature profile in the thermal storage. Fig. 8 shows the storage integration of SF2. Simulations showed that this is the most efficient configuration [36]. The ASHP is connected to four ports at different heights and the solar thermal module is connected to an internal heat exchanger. DHW is provided by a fresh water station. Ball valves (not illustrated in the figure) are connected at each port of the thermal storage, allowing a simple reconfiguration.

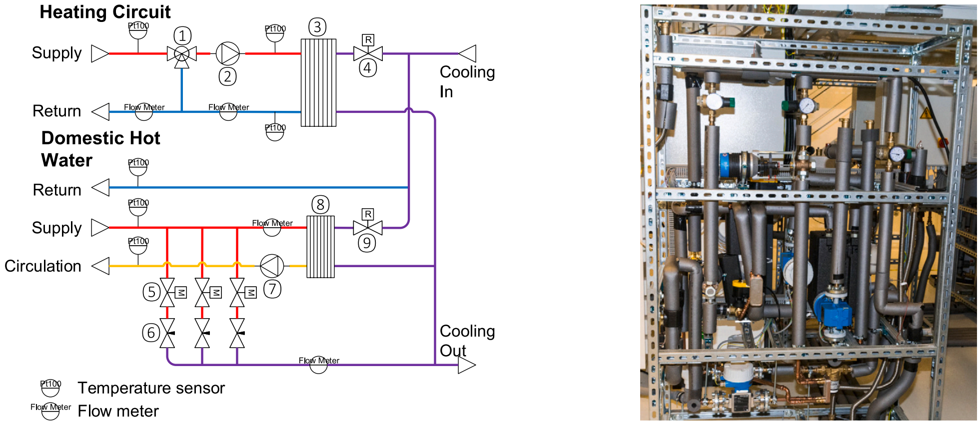


**Fig. 7.** Heat consumption emulator: a) schematic drawing adapted from [22]; b) setup at the CoSES laboratory.

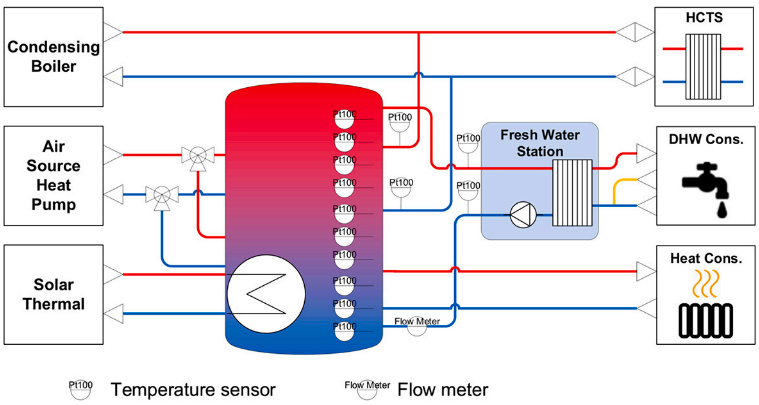


**Fig. 8.** Thermal storage connection of SF2.

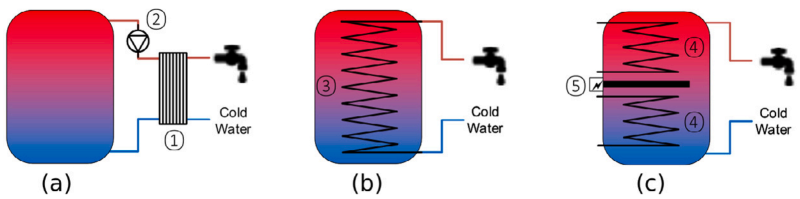


**Fig. 9.** Schematics of different domestic hot water installations: a) fresh water station, b) combined thermal storage and c) a separate domestic hot water storage.

At the CoSES laboratory, the DHW preparation is always connected to the thermal storage. Fig. 9 shows the three implemented options to provide DHW:

- Fig. 9.a: Fresh water station — The two circuits are separated by an external heat exchanger (①). An additional pump is necessary to pump hot water through the heat exchanger on the thermal storage side (②).
- Fig. 9.b: Combined thermal storage — An internal heat exchanger separates the heating and DHW circuit (③). In this case, no additional pump is necessary.
- Fig. 9.c: DHW storage tank — DHW is heated by one or more internal heat exchangers (④), which can be connected to the heating side or solar thermal collectors with an additional pump. An internal electrical heating rod can also be used to provide heat (⑤).

## 3. Monitoring and control system

The monitoring and control of the laboratory meets various requirements, such as processing more than 600 sensors and 300 actuators, a high operation frequency and real-time control. This is realized with the NI VeriStand software environment that enables easy management of real time experiments. NI VeriStand can configure input/output (IO) channels, log data, and communicate in real time with hardware [37]. It also offers the possibility to include external simulation models as dynamic link libraries (dll). These simulation models can be used for PHIL applications.

Table 2 gives an overview of the sensors for the equipment of the thermal side of the CoSES laboratory.

### 3.1. General control structure

In order to manage the high number of IO signals and the various hardware modules, a modular control software is developed. This allows intuitive understanding, modification and expansion of the control software. Necessary software modules are then combined for each house according to hardware specifications.

Each house is controlled by two controllers of National Instruments, an Industrial Controller (IC) for the thermal subsystem and a PXI for the electric subsystem. A compactRIO (cRIO), connected to the IC, acquires

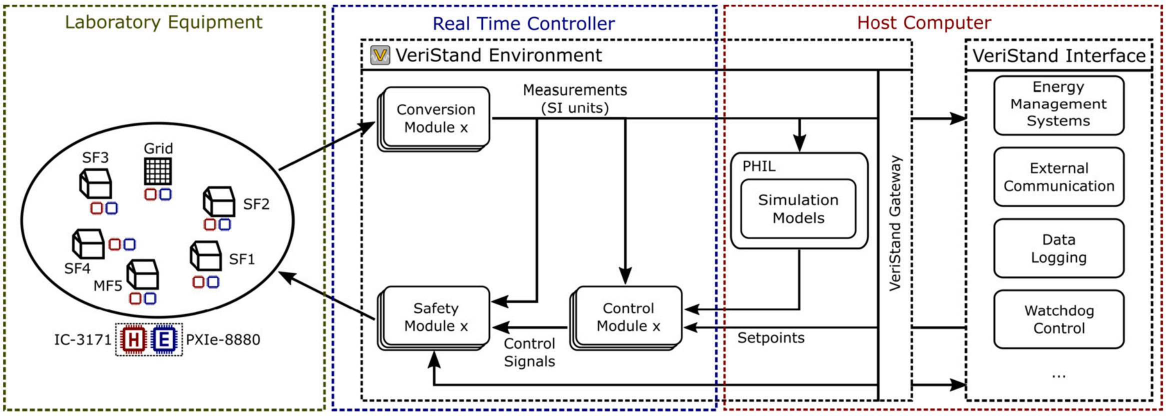


**Fig. 10.** Control structure of the thermal system: The laboratory equipment with its sensors and actuators exchanges information with the VeriStand environment. The VeriStand environment is divided into two parts, one running on the real time controller, the other on the host computer.

**Table 2**
Overview of sensors used in the CoSES laboratory.

| Parameter | Sensor type | Accuracy | Source |
|---|---|---|---|
| Temperature | 4-wire PT100 resistance sensors of quality class A | $\pm(0.15 + 0.002 \cdot \|T\|)$ | [38] |
| Humidity | Combined air and humidity sensor | $\pm 2\%$ | [39] |
| Water flow | Magnetic flow meter 'Proline Promag E / H 100' with different diameters | $\pm 0.5\% \pm 1$ mm/s | [40][41] |
| Gas flow | Calibrated bellows gas meter GR 2.5 from WDV Molliné | | [42] |
| Air flow | Hot film anemometer | $\pm 0.04$ m/s + 2% | [43] |
| Voltage | LEM CV 3-1000 | $\pm 0.2\%$ | [44] |
| Current | LEM LF210-S/SP3 | $\pm 0.2\%$ | [45] |

temperatures, counter signals (e.g. from the gas flow meter) and digital inputs, while the Remote I/O (REM IO) system measures analog input signals. Analog and digital output signals are sent from the REM IO system to the components. The execution rate of the controller of the thermal subsystem is 100 Hz. Fig. 10 shows the control structure of the thermal subsystem.

The control structure can be divided into 5 parts, 'Conversion', 'Logic', 'Control' and 'Safety' are deployed directly on the IC while the 'VeriStand Interface' runs in LabVIEW on the host PC and uses an API to interact with NI VeriStand [46]:

1. The 'Conversion' block converts raw measurement data such as 0-10 V signals, counter signals, and resistance measurements into the corresponding standard unit values. Additional values such as heat rate or state of charge can be calculated.
2. The 'Logic' block generates setpoints for the laboratory. The setpoints can come from PHIL simulation models, an energy management system, external inputs, or direct inputs from the operator.
3. The 'Control' block converts setpoints into the respective analog or digital output signals, typically using PID and bang-bang controllers.
4. The 'Safety' block checks whether signals can be implemented safely and if the communication between the host PC and the laboratory is active. If thresholds are violated or the connection is lost, a safe value, usually '0' or 'off' is passed. All safety interventions are recorded with error codes.
5. The 'VeriStand Interface' in LabVIEW is used for data logging, the integration of energy management systems and external communication. Common communication protocols enable the communication to other software or applications such as internet-of-things (IoT) as implemented by Mayer et al. [47].

### 3.2. Power hardware in the loop

The PHIL approach is a key concept for the design of the CoSES Laboratory. PHIL simulation systems are designed based on the hybrid configuration of simulation tools and real hardware and interface through digital and analog input/output signals [48]. This allows to simulate parts of real systems without losing critical information, which simplifies the laboratory setup. At the same time, the coupling of software and hardware can ensure that deviations from setpoints in the experiment are taken into account in the simulation through the feedback loop and thus influence the future reaction of the experiment. Furthermore by combining physical and simulated systems, environmental conditions and user behavior can be integrated into experiments. Compared to field tests, this allows PHIL experiments to be more easily adapted and better reproducible, while not compromising user comfort.

PHIL models can be easily integrated or replaced in the monitoring and control concept of the CoSES laboratory. First, a model for NI VeriStand must be created in dll format. The model must run at a constant step size that is a multiple of the execution rate of the controller or host computer. As shown in Fig. 10, the PHIL model is integrated into the NI VeriStand project, where it is connected to 'Measurements' and 'Setpoints'.

PHIL and simulation models are used for several modules that are otherwise hard to emulate in the laboratory:

- Heating and DHW system: A detailed description of the PHIL approach for this system is described below.
- Cooling system: Set values for supply temperature and volume flow are generated to keep the room temperature at its set value. The measured supply temperatures and volume flow are used to calculate the set return temperature of the cooling system. This setpoint is sent to the cold consumption emulator described in 2.4
- DHC pipes: The outlet temperature setpoint of the pipe is calculated in a simulation model based on the measured inlet temperature and flow rate. The simulation model considers losses and gains caused by the environment. The emulator described in subsection 2.1 is controlled so that the set outlet temperature is met.
- ASHP: The setpoints for air temperature and humidity are determined based on the environment conditions of the PHIL simulation. An HVAC system with an electric heating rod and steam humidifier is controlled to emulate the setpoints accordingly.
- GSHP: The set value for supply temperature of the brine is calculated in a simulation model based on the measured return temperature and flow rate. The simulation model calculates heat gains for different types of ground collectors depending on the environment. The brine is then heated up to reach the set temperature. A more detailed description of the PHIL system can be found in [22].

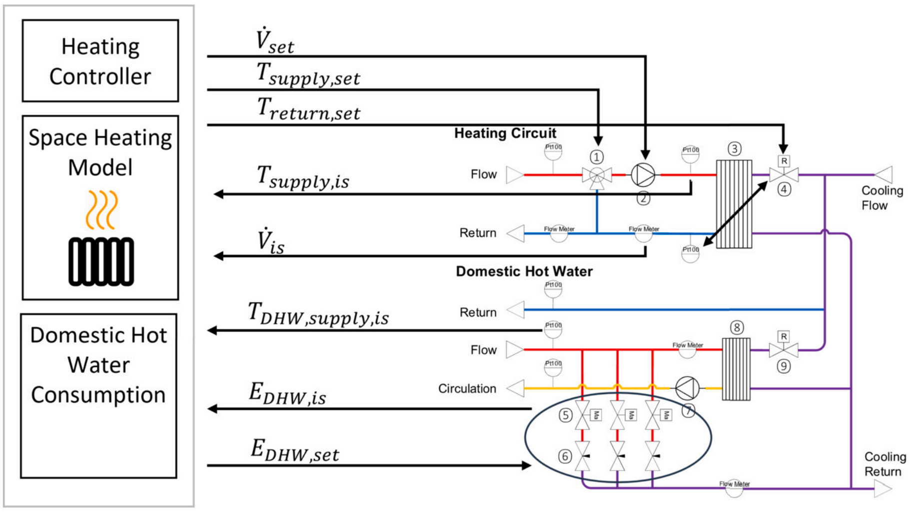


**Fig. 11.** PHIL setup of the CoSES laboratory. The simulation models generate setpoints for the laboratory considering inputs from laboratory measurements.

- Solar thermal modules: An electric heater emulates the behavior of solar thermal modules as described in subsection 2.3. The electric heater setpoint is calculated based on the measured return temperature and flow rate, solar thermal panel type, irradiance and ambient temperature.

As an example, Fig. 11 shows the application of the PHIL concept in the CoSES laboratory for the heat consumption emulator similar to [49]. The simulation model of the building is implemented in the Modelica-based program SimulationX. It simulates the heating controller and the heating and DHW consumption.

The heating controller defines the set water flow through the heating system ($\dot{V}_{set}$) and the supply temperature ($T_{sup,set}$) based on the current room and outdoor temperature. The setpoints are sent to the 3-way mixer and pump (① and ② in Fig. 7).

The actual flow rate ($\dot{V}_{is}$) and supply temperature ($T_{sup,is}$) are measured in the testbed and then sent to the simulation model, where the set return temperature from the heating system ($T_{ret,set}$) is calculated. The water of the heating system is cooled by a heat exchanger. The cooling water flow is controlled by a control valve (④ in Fig. 7) to follow the return temperature setpoint.

If setpoints cannot be met, e.g. because the thermal storage is too cold or the pumping power is too low, this will be considered in the simulation model and lead to a reduction of the room temperature. This reduction of the room temperature has to be compensated at a later point. Due to this feed-back loop, results are more realistic when using PHIL.

The DHW consumption model works in a similar way. The simulation model defines the set heat demand of the DHW system ($E_{DHW,set}$) based on load profiles. If the DHW supply temperature ($T_{DHW,sup,is}$) is below a chosen minimum temperature, the DHW consumption cannot be fulfilled and has to be either fulfilled at a later point and/or the results highlight those times.

## 4. Results

In the previous sections, we showed a detailed description of the laboratory infrastructure and the control setup. In this section, we validate the PHIL system for some selected cases to show the functionality of the laboratory. We further present a case study with three houses to demonstrate capabilities of the laboratory and provide insights into prosumers behavior in DHC systems that are difficult to accurately model in existing simulation tools.

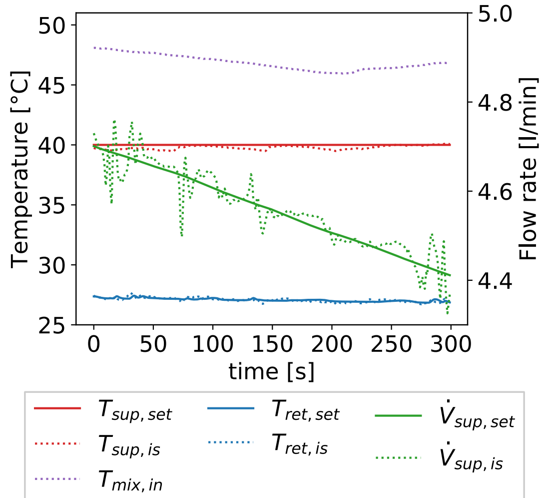


**Fig. 12.** Validation of the PHIL system of the heating system.

### 4.1. Validation of the power hardware in the loop system

The goal of this section is to demonstrate that the PHIL emulators can follow the provided setpoints similar to [49]. All controllers used for the PHIL emulators were tuned and validated by step test experiments. The results of these experiments are not included in this paper as they are trivial. We will not validate the underlying models, as they can be replaced and are ideally already validated in the simulation library.

Fig. 12 shows the validation of the PHIL emulator of the heating system as described in subsection 3.2. As can be seen, the setpoints can be followed well. The 3-way mixer (① in Fig. 7) mixes cold water from the return ($T_{ret}$) with the inlet water ($T_{mix,in}$) and follows the setpoint for the supply temperature ($T_{sup}$) well. The pump (② in Fig. 7) and the control valve (④ in Fig. 7 also follow the setpoints for the flow rate ($\dot{V}_{sup}$) and return temperature ($T_{ret}$) accurately.

The heat consumption for DHW is specified as an energy setpoint ($E_{DHW}$) instead of a setpoint of the water flow. This allows minor deviations in the water flow to be neglected as long as the drawn heat is the same after a short time period. Therefore, Fig. 13 shows the drawn heat for DHW over time. We can see that there is a small delay during strong consumption rates, but the total consumption stays the same. We can further see that the supply temperature is above the minimum domestic hot water temperature during consumption. It cools down slightly

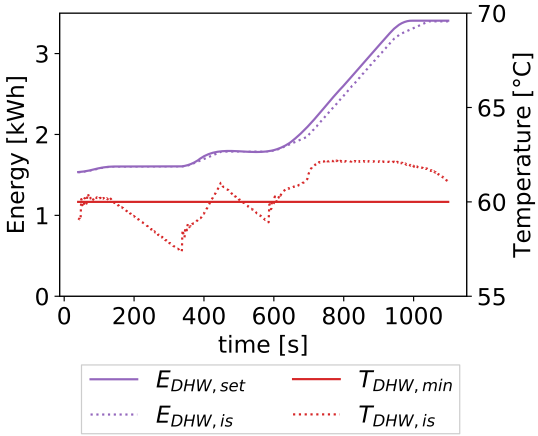


**Fig. 13.** Validation of the PHIL system of the DHW system.

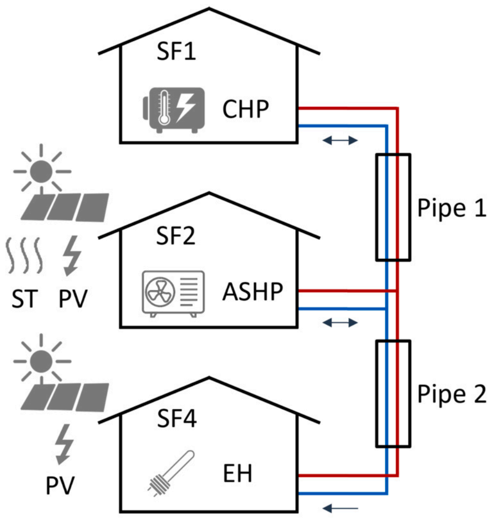


**Fig. 14.** Setup of the case study.

when no water is drawn. This effect can be prevented if the circulation pump is activate.

### 4.2. Case study with three houses

A case study analyzes the integration of prosumers in a DHC system. For this purpose, 3 houses are used, equipped according to Table 1 and as specified in Fig. 14:

- SF1 uses a radiator heating system. Heat is generated by a CHP and can be stored in an 800 l thermal storage. DHW is provided by a 500 l DHW storage, which is connected to the thermal storage and CHP.
- SF2 uses a space heating system. Heat is generated by an ASHP and solar thermal panels and can be stored in a 785 l thermal storage. DHW is provided by a fresh water station. It is further equipped with PV panels.
- SF4 uses a radiator heating system. Heat is drawn from the grid or generated with a back-up electric heating rod and can be stored in a 1000 l combined thermal storage for heating and DHW. It is equipped with PV panels that can be used to directly generate heat with the heating rod.

SF1 and SF2 are heat prosumers, meaning that they can feed-in or extract heat from the grid, while SF4 is a pure consumer.

In the first step, setpoints are generated with a MPC. A cost optimization is conducted for the 3 houses over 24 hours in 15-minute steps with the optimization tool urbs [50]. The optimization goal was to minimize the total costs for heating and electricity. The costs consist of expenses for gas (0.14 EUR/kWh) and electricity (0.32 EUR/kWh) and revenues from the sale of electricity produced by PV (0.06 EUR/kWh) and the CHP (0.16 EUR/kWh). Electricity and heat demand as well as solar radiation are provided as time series to the model. The same optimization is conducted as a benchmark without a heat grid.

The optimization results are shown in Fig. 15. The top graph shows the generated and consumed heat. The CHP operates mostly during the night, when there is no heat from solar thermal and electricity from PV. After the sun rises, heat from renewable sources becomes cheaper and dominates the production mix. At this time the thermal storage is recharged. Looking at the feed-in and extraction rates, we can see that at night, SF1 exports heat to SF4 and during the day to SF4.

The optimization showed cost savings of 30% compared to individual heating systems, mainly due to better usage of the equipment and the high individual heating costs of SF4.

In the morning and evening hours, when the PV production picks up or declines, heat is transferred to SF4 both from SF1 and SF2 in

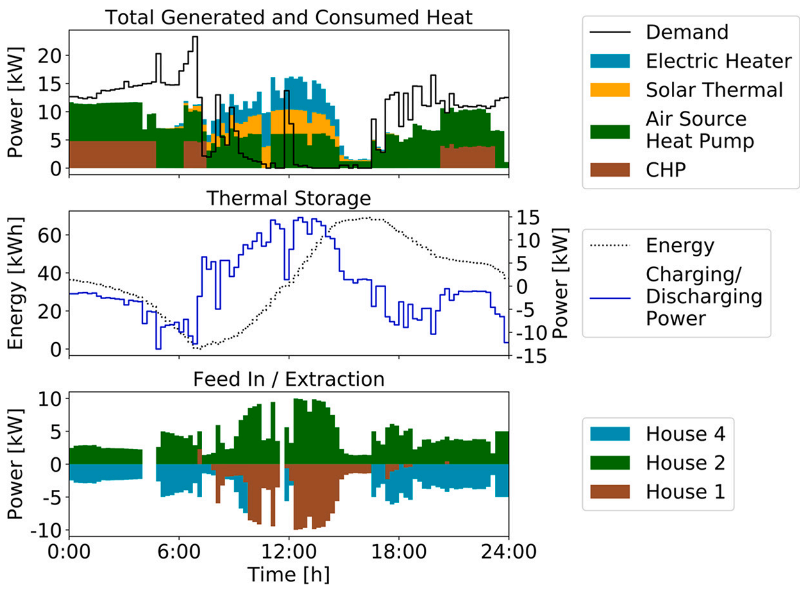


**Fig. 15.** Optimal heat flow between buildings.

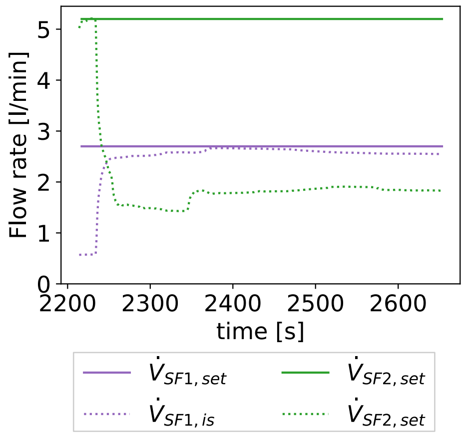


**Fig. 16.** Pump blocking: The pump in SF1 has to overcome a higher pressure difference and is blocked by the pump in SF1. A better control strategy could avoid this problem as demonstrated by manually reducing the power of the pump in SF2 after 2230 s.

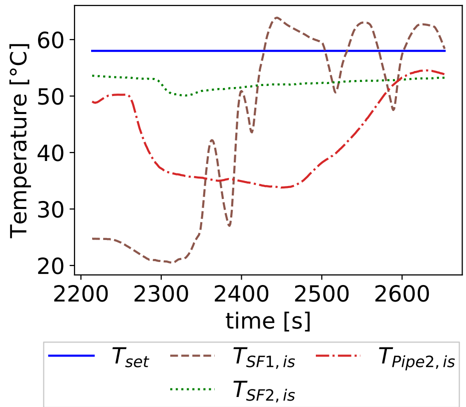


**Fig. 17.** Mixing of hot and cold water in district heating pipes: Pipe 1 between SF1 and SF2 cooled during the down time. When SF1 starts to feed in, the water in pipe 2 cools down at the beginning until pipe 1 is warm.

a short time period. This means that we have 2 sources at the same time. With multiple feed-in pumps, the pumps might block each other as mentioned by Licklederer et al. [51]. Fig. 16 shows this effect, when SF1 and SF2 should feed in and SF4 extracts heat. Since SF1 is further away from SF4, its pump has to overcome a higher hydraulic resistance. This results in SF2 being able to provide the required heat while SF1 provides only a small volume flow and is almost blocked. At 2250 s, the power of the pump in SF2 was manually reduced to show that a better control strategy could prevent this and result in a better distribution of the volume flow.

Another challenge arises due to the fact that there was no flow between SF1 and SF2 before SF1 starts feeding in. This means that the temperature in the pipe is at ambient temperature. Fig. 17 shows problems that can occur in this situation. When SF1 starts feeding in, cold water from pipe 1 mixes with hot water from SF2, which results in a reduction of the temperature in pipe 2. This destroys exergy and means that SF4 cannot extract heat from the grid in that time period due to too low temperatures. The delay and oscillation of the feed-in temperature of SF1 are caused by its controller, which could be further improved. One option to prevent the grid cooling would be to flush pipe 1 with hot water from SF2, before SF1 feeds in. However this has to be considered in the resource scheduling.

The case study also showed that the chosen MPC is inaccurate. It simplifies the thermohydraulic system to heat only and neglects temperature and pressure constraints. This results in two problems: The thermal storage in SF2 is fed by a HP with high volume flow and low temperature difference between supply and return, which resulted in strong mixing. Although the state of charge of the thermal storage is according to the optimization results, the outlet temperature and thus the feed-in temperature of SF2 are too low (see Fig. 17). Hou et al. [21] introduced a detailed MPC for prosumers in a DHC system with a thermal storage and waste heat from a data center. They achieved more robust results than rule-based control. They show that MPCs can be suitable to provide good control for prosumer-based DHC systems when the models are detailed enough.

Furthermore, neglecting pressure and temperature in the heat network model can lead to setpoints for the volume flow, which cannot be reached and might result in feed-in pumps blocking each other. A more accurate model of the heat network can reduce the impact of this problem.

The findings of the case study show that the laboratory is able to reproduce the behavior of district heating systems. The results further show that the laboratory is a good complement to simulation models, as it allows validation of control algorithms on real hardware and highlights phenomena that may have been neglected in simulation models. It allows researchers to test their algorithms in a real-world environment, providing another step toward implementing innovative approaches from research in practice.

## 5. Discussion

The focus of the thermal side of the CoSES laboratory is on a detailed study of thermal prosumer systems in DHCs as well as heating solutions for individual homes. Because of this focus, the laboratory has different strengths, limitations, and use cases, which are discussed in this chapter.

### 5.1. Strength

The strengths of the laboratory lie in the very detailed replication of the five prosumers by using commercial devices. In combination with PHIL, a close to reality operation of the thermal system can be emulated. The modular design allows a simple exchange of components depending on the research purpose, e.g. experimental heat transfer stations can be replaced by commercial ones to analyze and replicate the behavior of field experiments. Since most pumps and valves can be controlled by the user, novel control strategies can be tested at field level.

Another strength is the integration of the thermal and electric energy system. This allows to analyze and optimize sector coupling of thermal and electric systems, including real electrical components such as PV, batteries or electric vehicles. By measuring the experimental electric grid of the CoSES laboratory, effects of different control strategies on the electric grid can be determined.

The use of PHIL allows to emulate environmental conditions in a controlled laboratory environment without affecting user comfort, as would be the case in field tests. In addition, experiment results are independent of environmental conditions and thus reproducible.

### 5.2. Limitations

Several limitations of the laboratory come from its design. Due to the short distance between the buildings, a PHIL emulator for the thermal grid is used to replicate temperature losses and dynamic temperature changes. However, this setup cannot reproduce the pressure behavior in the pipes of the thermal network. The design with standard pipes limits its research to 3rd and 4th generation and ambient temperature heat grids as well as 2nd, 3rd and 4th generation cooling grids. Older generations for heat grids cannot be tested as they require temperatures above 100 °C.

The PHIL approach also has drawbacks, as it is only as good as the simulation models used for it. Ideally, these simulation models should be validated against real data. This was the motivation of using commercial hardware as much as possible in the initial laboratory design.

Furthermore, the components of the SFs are designed for typical household size. This means that they can only feed a small amount of excess heat into the grid when the buildings are integrated as prosumers. As a result, the flow rates during feed in are low. At the same time, feeding heat into the DHC grid requires a high differential pressure. Since there are no commercially available pumps that have their ideal operating point at low flow rates and high pressure, this results in poor efficiency of the pumps used in the laboratory. However, the same problem occurs with prosumers in practice at similar small heat rates. The size of the components leads to a further limitation, as heat pumps and CHPs have little influence on the experimental electric grid.

### 5.3. Research potential

Since the entire system is simulated in detail and all components can be controlled, the laboratory is well suited for validating new control strategies. These include control strategies at field level, e.g. the control of pumps and control valves of bidirectional heat transfer stations as well as EMS. EMS can be tested under real conditions and in a reproducible way to identify unforeseen influences.

By characterizing components installed in the CoSES laboratory (as done for a CHP [52] and a thermal storage [53]), simulation models can be validated. This has already been done for the Modelica-based simulation library CoSES ProHMo [49] and a hybrid one dimensional multi-node model of a thermal storage [54].

The impact of sector coupling on the electric grid can be analyzed and optimized with workarounds, even though the heat generators in the CoSES laboratory are too small:

- The voltage and current profile of the heat pump or CHP is measured in detail, scaled and emulated in real time by the Egston load emulator.
- The Egston load emulator artificially creates further burdens on the grid.
- In a joint experiment with other laboratories, the voltage and current profile can be measured externally and emulated by the Egston load emulator. This can be done in real time or sequentially.

In addition, the CoSES laboratory can be used to prequalify control strategies and components prior to a field test. The laboratory includes commercial heat generators that are affected by their internal control and external influences, as well as pumps and valves that behave nonlinearly. Prequalification of control strategies can help to detect errors in advance, reducing the time required for the field tests while increasing the significance of the results. Similarly, problems that occur in reality can be reproduced and addressed in a controlled laboratory environment.

The open communication interface allows the laboratory to be combined with other facilities. The CoSES laboratory can be used by other facilities, for instance, to provide detailed information about the behavior in the building or in the electricity grid. Likewise, other facilities can provide information for experiments in the CoSES laboratory, for example about the hydraulics in the DHC grid as setpoints for the DHC grid emulator.

## 6. Conclusion and outlook

This paper presents the CoSES laboratory at TUM that bridges between simulation models and field tests in the evaluation and analysis of innovative DHC and smart energy systems. The detailed description of the architecture can serve as an example for the design of other DHC laboratories. It consists of five thermal and electric prosumer houses that are connected with a thermal and electric grid. The laboratory replicates dynamics and efficiencies of commercial components and their internal control, of which generic simulation models are sometimes lacking. In contrast to field tests, weather conditions and user behavior are emulated, improving reproducibility and allowing it to run independently from external influences without affecting user comfort. Due to its modular design, the configuration can be adapted to individual experiment requirements, thus enabling a wide range of experiments. The CoSES laboratory is therefore well suited for a broad spectrum of research areas:

- Commercial equipment can be characterized to generate data for the validation of simulation models. So far, data for a thermal storage [53] and a CHP [52] are published.
- Control strategies for HCTS and a bHPTS can be improved and validated with a focus the interaction of multiple sources, their pump control and effects from flexibly operating DHC grids.
- Energy management systems for individual houses or whole districts can be tested under the influence of commercial components and their internal control.
- The interaction between different control structures from high level control to field level control can be analyzed.
- The influence of the thermal side on smart energy systems and vice versa through sector coupling can be analyzed.

A case study demonstrates the functionality of the laboratory and the advantage of the PHIL approach. The case study showed that prosumer integration into flexible district heating grids can reduce overall heating costs but requires intelligent control concepts for transfer stations. Simple control concepts might lead to problems, when multiple houses feed in at the same time. It further showed that a simple MPC that neglect temperatures and pressure constraints might be too inaccurate for flexible operation of prosumer based DHC systems.

Experimental case studies are a good complement to simulation models as they replicate phenomena that are difficult to capture in generic simulation models, such as internal control strategies of commercial components, delayed and inaccurate implementation of setpoints, and the behavior of the thermohydraulic system.

The presented laboratory can contribute to further improve DHC grids, to decarbonize the heating and cooling sector and to further develop smart energy systems. Its modular structure allows the expansion of the setup for new research questions. Currently planned expansions include equipment for cooling concepts of houses and the analysis of electrolyzer/fuel cell systems for long-term storage of surplus electricity. The CoSES laboratory welcomes collaborations with other researchers and companies optimizing the thermal and electric system at the house or district level.

## CRediT author statement

**Daniel Zinsmeister:** Conceptualization, Visualization, Writing - Original Draft and Editing. **Thomas Licklederer:** Conceptualization, Writing - Original Draft, Review and Editing. **Stefan Adldinger:** Writing - Original Draft. **Franz Christange:** Conceptualization, Writing - Review. **Peter Tzscheutschler:** Conceptualization, Writing - Review, Supervision, Project administration, Funding acquisition. **Thomas Hamacher:** Conceptualization, Supervision, Funding acquisition. **Vedran S. Perić:** Conceptualization, Writing - Review, Supervision, Project administration, Funding acquisition.

## Declaration of competing interest

The authors declare that they have no known competing financial interests or personal relationships that could have appeared to influence the work reported in this paper.

## Data availability

Data will be made available on request.

## Acknowledgements

This project was funded by the Federal Ministry for Economic Affairs and Climate Action, Germany (FKZ: 03EN3032). The work of Vedran S. Perić was supported by Deutsche Forschungsgemeinschaft (DFG), Germany through "Optimal Operation of Integrated Low-Temperature Birdirectional Heat and Electric Grids (IntElHeat)" under project number 450821044. The construction of the CoSES laboratory was supported by Deutsche Forschungsgemeinschaft (DFG) through the project "Flexible reconfigurable microgrid laboratory" under project number 350746631.

## References

[1] Ferroukh Rabia, Frankl Paolo, Abid Rana. Renewable energy policies in a time of transition: heating and cooling. https://www.irena.org/-/media/Files/IRENA/Agency/Publication/2020/Nov/IRENA_IEA_REN21_Policies_Heating_Cooling_2020.pdf, 2020.

[2] Dean Brian, Dulac John, Morgan Trevor, Remme Uwe. The future of cooling: opportunities for energy-efficient air conditioning. https://iea.blob.core.windows.net/assets/0bb45525-277f-4c9c-8d0c-9c0cb5e7d525/The_Future_of_Cooling.pdf, 2018.

[3] Kavvadias K, Jiménez Navarro JP, Thomassen G. Decarbonising the eu heating sector: integration of the power and heating sector (2019). https://doi.org/10.2760/072688. https://op.europa.eu/en/publication-detail/-/publication/208e7048-b406-11e9-9d01-01aa75ed71a1/language-en.

[4] Connolly D, Lund H, Mathiesen BV, Werner S, Möller B, Persson U, et al. Heat roadmap Europe: combining district heating with heat savings to decarbonise the eu energy system. Energy Policy 2014;65:475–89. https://doi.org/10.1016/J.ENPOL.2013.10.035.

[5] Clean energy for all europeans package. https://ec.europa.eu/energy/topics/energy-strategy/clean-energy-all-europeans_en, 2021.

[6] Lund H, Duic N, Østergaard PA, Mathiesen BV. Future district heating systems and technologies: on the role of smart energy systems and 4th generation district heating. Energy 2018;165:614–9. https://doi.org/10.1016/j.energy.2018.09.115.

[7] Lund H, Østergaard PA, Chang M, Werner S, Svendsen S, Sorknæs P, et al. The status of 4th generation district heating: research and results. Energy 2018;164:147–59. https://doi.org/10.1016/j.energy.2018.08.206.

[8] Lund H, Werner S, Wiltshire R, Svendsen S, Thorsen JE, Hvelplund F, et al. 4th generation district heating (4gdh): integrating smart thermal grids into future sustainable energy systems. Energy 2014;68:1–11. https://doi.org/10.1016/j.energy.2014.02.089.

[9] Lund H, Østergaard PA, Connolly D, Mathiesen BV. Smart energy and smart energy systems. Energy 2017;137:556–65. https://doi.org/10.1016/j.energy.2017.05.123.

[10] Edtmayer H, Nageler P, Heimrath R, Mach T, Hochenauer C. Investigation on sector coupling potentials of a 5th generation district heating and cooling network. Energy 2021;230:120836. https://doi.org/10.1016/j.energy.2021.120836.

[11] Gudmundsson O, Thorsen JE, Brand M. The role of district heating in coupling of the future renewable energy sectors. Energy Proc 2018;149:445–54. https://doi.org/10.1016/j.egypro.2018.08.209.

[12] Bünning F, Wetter M, Fuchs M, Müller D. Bidirectional low temperature district energy systems with agent-based control: performance comparison and operation optimization. Appl Energy 2018;209:502–15. https://doi.org/10.1016/j.apenergy.2017.10.072.

[13] Zarin Pass R, Wetter M, Piette MA. A thermodynamic analysis of a novel bidirectional district heating and cooling network. Energy 2018;144:20–30. https://doi.org/10.1016/j.energy.2017.11.122.

[14] Brange L, Englund J, Lauenburg P. Prosumers in district heating networks – a Swedish case study. Appl Energy 2016;164:492–500. https://doi.org/10.1016/j.apenergy.2015.12.020.

[15] Kauko H, Kvalsvik KH, Rohde D, Nord N, Utne Å. Dynamic modeling of local district heating grids with prosumers: a case study for Norway. Energy 2018;151:261–71. https://doi.org/10.1016/j.energy.2018.03.033.

[16] Rosemann T, Löser J, Rühling K. A new dh control algorithm for a combined supply and feed-in substation and testing through hardware-in-the-loop. Energy Proc 2017;116:416–25. https://doi.org/10.1016/j.egypro.2017.05.089.

[17] Lund H, Thorsen JE, Jensen SS, Madsen FP. Fourth-generation district heating and motivation tariffs. ASME Open J Eng 2022;1. https://doi.org/10.1115/1.4053420.

[18] Volkova A, Reuter S, Puschnigg S, Kauko H, Schmidt R-R, Leitner B, et al. Cascade sub-low temperature district heating networks in existing district heating systems. Smart Energy 2022;5:100064. https://doi.org/10.1016/j.segy.2022.100064.

[19] Huynh T, Schmidt F, Thiem S, Kautz M, Steinke F, Niessen S. Local energy markets for thermal-electric energy systems considering energy carrier dependency and energy storage systems. Smart Energy 2022;6:100065. https://doi.org/10.1016/j.segy.2022.100065.

[20] Frölke L, Sousa T, Pinson P. A network-aware market mechanism for decentralized district heating systems. Appl Energy 2022;306:117956. https://doi.org/10.1016/j.apenergy.2021.117956.

[21] Hou J, Li H, Nord N, Huang G. Model predictive control for a university heat prosumer with data centre waste heat and thermal energy storage. Energy 2023;267:126579. https://doi.org/10.1016/j.energy.2022.126579.

[22] El-Baz W, Tzscheutschler P, Wagner U. Experimental study and modeling of ground-source heat pumps with combi-storage in buildings. Energies 2018;11(5):1174. https://doi.org/10.3390/en11051174.

[23] Thorsen JE, Ommen T, Meesenburg W, Smith KM, Oliver EM. Energylab nordhavn (d10.1c): heat booster substation and circulation booster for domestic hot water. https://backend.orbit.dtu.dk/ws/portalfiles/portal/245670581/d10.1c_heat_boosters_for_hot_tap_water_and_heating.pdf, 2019.

[24] Heymann M, Rosemann T, Rühling K, Tietze T, Hafner B. Concept and measurement results of two decentralized solar thermal feed-in substations. Energy Proc 2018;149:363–72. https://doi.org/10.1016/j.egypro.2018.08.200.

[25] Schäfer K, Schmidt T. Experimental plant for analyzing the technical feasibility of decentralized solar heat feed-in. In: EuroSun 2018 conference proceedings; 2018.

[26] Fedrizzi R. Energy exchange lab: facility for tests on advanced district heating and cooling networks. https://webassets.eurac.edu/31538/1621456833-energyexchangelaben-2020.pdf, 2020.

[27] Kallert A, Lottis D, Shan M, Schmidt D. New experimental facility for innovative district heating systems—district lab. Energy Rep 2021;7:62–9. https://doi.org/10.1016/j.egyr.2021.09.039.

[28] Messmer C, Ackermann C, Spoerri R, Dahinden C, Afjei T, Sulzer M. Virtual test bench by linking the 'fhnw - energy research lab' and the 'hslu - nodes lab'. http://hpc2017.org/wp-content/uploads/2017/05/P.2.3.4-Virtual-test-bench-by-linking-the-FHNW-Energy-Research-Lab-and-the-HSLU-NODES-Lab.pdf, 2017.

[29] Perić VS, Hamacher T, Mohapatra A, Christiange F, Zinsmeister D, Tzscheutschler P, et al. Coses laboratory for combined energy systems at TU Munich. In: 2020 IEEE power & energy society general meeting (PESGM). IEEE; 02.08.2020 - 06.08.2020. p. 1–5.

[30] Østergaard PA, Werner S, Dyrelund A, Lund H, Arabkoohsar A, Sorknæs P, et al. The four generations of district cooling - a categorization of the development in district cooling from origin to future prospect. Energy 2022;253:124098. https://doi.org/10.1016/j.energy.2022.124098.

[31] Mohapatra A, Hamacher T, Perić VS. Phil infrastructure in coses microgrid laboratory. In: 2022 IEEE PES innovative smart grid technologies conference Europe (ISGT-Europe). IEEE; 2022. p. 1–6.

[32] Christange F. The combined smart energy systems laboratory. Dissertation. Technical University of Munich; 2021. http://mediatum.ub.tum.de/?id=1540691.

[33] Lamaison N, Bavière R, Cheze D, Paulus C. A multi-criteria analysis of bidirectional solar district heating substation architecture. In: Romero M, Mugnier D, Renné D, Guthrie K, Griffiths S, editors. Proceedings of SWC2017/SHC2017, international solar energy society; 29.10.2017 - 02.11.2017. p. 1–11.

[34] District heating transfer station wp grid-hiq. https://ratiotherm-systems.com/waermepumpen/nahwaerme-waermepumpen/wp-grid-hiq/, 2022.

[35] Wall mounted gas condensing boiler cgb-2. https://www.wolf.eu/en/products/gas-heating-systems/wall-mounted-gas-condensing-boiler-cgb-2/, 2021.

[36] Zinsmeister D, Licklederer T, Christange F, Tzscheutschler P, Perić VS. A comparison of prosumer system configurations in district heating networks. Energy Rep 2021;7:430–9. https://doi.org/10.1016/j.egyr.2021.08.085.

[37] What is veristand? https://www.ni.com/en-us/shop/data-acquisition-and-control/application-software-for-data-acquisition-and-control-category/what-is-veristand.html, 2021.

[38] DKE Deutsche Kommission Elektrotechnik Elektronik Informationstechnik in DIN und VDE, Industrielle platin–widerstandsthermometer und platin–temperatursensoren.

[39] Sensorshop24. Kanalkombifühler für temperatur und feuchte (0-10v/4-20ma). https://www.sensorshop24.de/kanalkombifuehler-fuer-temperatur-und-feuchte-0-10v-4-20ma.

[40] Endress + Hauser. Technical information proline promag h 100. https://portal.endress.com/dla/5000612/9225/000/06/TI01101DEN_0717.pdf.

[41] Endress + Hauser. Technical information proline promag e 100. https://portal.endress.com/dla/5000883/5389/000/02/TI01159DEN_0317.pdf, 1.10.2021.

[42] Molliné WDV. Balgengaszähler gr. https://www.molline.de/fileadmin/content/content/Bilder/produkte_gaszaehler/Balgengaszaehler_GR/DB0300_Balgengaszaehler-GR.pdf.

[43] E + E. Sensor for very low air velocity: Ee660. https://www.epluse.com/products/air-velocity-instrumentation/air-flow-transmitters-and-probes/ee660, 2023.

[44] LEM International SA. Cv3. https://www.lem.com/en/cv-31000.

[45] LEM International SA. Lem lf210-s. https://www.lem.com/en/lf-210ssp3.

[46] National Instruments Corp. Apis in veristand. https://www.ni.com/documentation/en/veristand/latest/manual/api-veristand/, 2021.

[47] Mayer M, Mohapatra A, Perić VS. Iot integration for combined energy systems at the coses laboratory; 2021. p. 195–200.

[48] Lauss G, Faruque MO, Schoder K, Dufour C, Viehweider A, Langston J. Characteristics and design of power hardware-in-the-loop simulations for electrical power systems. IEEE Trans Ind Inform 2016;63(1):406–17. https://doi.org/10.1109/TIE.2015.2464308.

[49] Zinsmeister D, Perić VS. Implementation of a digital twin of the coses district heating prosumer laboratory. In: 14th international conference on applied energy - ICAE2022; 08.08.2022 - 11.08.2022.

[50] Dorfner Johannes, Schönleber Konrad, Dorfner Magdalena, sonercandas, froehlie, smuellr, et al. tum-ens/urbs: urbs v1.0.1. https://doi.org/10.5281/zenodo.594200, 2019.

[51] Licklederer T, Zinsmeister D, Elizarov I, Perić V, Tzscheutschler P. Characteristics and challenges in prosumer-dominated thermal networks. J Phys Conf Ser 2021;2042(1):012039. https://doi.org/10.1088/1742-6596/2042/1/012039.

[52] Zinsmeister Daniel, Licklederer Thomas. Characterization of a combined heat and power unit at the coses laboratory. https://doi.org/10.13140/RG.2.2.31035.34089/1, 2021.

[53] Zinsmeister Daniel, Licklederer Thomas. Characterization of a thermal storage at the coses laboratory. https://doi.org/10.13140/RG.2.2.13461.19687, 2022.

[54] de La Cruz-Loredo I, Zinsmeister D, Licklederer T, Ugalde-Loo CE, Morales DA, Bastida H, et al. Experimental validation of a hybrid 1-d multi-node model of a hot water thermal energy storage tank. Appl Energy 2023;332:120556. https://doi.org/10.1016/j.apenergy.2022.120556.

### 6.2.3 Learnings from Laboratory Integration

In the following, some general challenges and key learnings from the integration of the PBDH concept into the laboratory environment are described.

#### Implementation Principles

Guiding principles for the planning and implementation of the CoSES laboratory were:

- Creating a realistic emulation of a MES across a five-building neighborhood.
- Ensuring independence from ambient conditions to facilitate diverse scenario testing.
- Enabling safe and secure testing of prototype algorithms and critical operating points without impacting users or their comfort.
- Ensuring modularity to allow for interchangeable hardware and software components and to support diverse testing approaches.
- Using as generic interfaces as possible, thereby enhancing extendability and cooperations.

More information on the conceptualization of the CoSES lab can be found in [114].

In addition to its potential for scientific contributions, the laboratory environment proofs high value in the practical training of students through guided tours, internships, student assistant jobs or theses.

#### Implementation Challenges

Setting up and commissioning the thermal side of the laboratory came along with various challenges. A selection of them is summarized in the following.

Very specific requirements for the setup made outsourcing the construction of the thermal laboratory infrastructure to external companies impossible. The hardware- and software-setup was implemented by doctoral students, facing a steep learning curve. To facilitate the operation of the heat side, a comprehensive peripheral setup must be installed and managed, necessitating both, specialized knowledge and a high level of commitment. This pertains to several aspects, including amongst others:

- handcrafting for heating system installations
- managing the water supply and maintaining water quality amidst the challenges of various metal combinations
- operating a re-cooling system (e.g. for water in the heat sinks)
- operating gas supply and exhaust systems
- dealing with space limitations while ensuring the flexibility of the setup
- upholding operational and workplace safety within the laboratory environment

The laboratory is not a single testbed for individual devices, but is intended to test the interaction of multiple devices across sectors. This leads to a very extensive and large facility. The complexity is manageable only through a modular setup - both hardware and software-wise. Thermal components do not have a standardized interface to external controls, as each manufacturer uses individual solutions. This makes the integration of diverse devices complex and necessitates a unifying software framework. Further, the high inertia of the thermal system compared to the electrical system leads to very different relevant time scales. While for the control of thermal systems sampling rates in the range of 0.01-1 Hz are enough, the electrical system requires 10Hz - 10kHz. Both ranges must be covered simultaneously to allow for a real sector-coupled smart grid laboratory behavior. The computation and communication layer of the CoSES laboratory relies mostly on hardware and software by National Instruments (NI) [2]. Almost the complete range of the NI product sortiment is combined in order to fullfill the requirements. A large number of analog and digital input/output (I/O) signals has to be managed - more than 1700 data points on the thermal side. NI VeriStand is a powerful tool for the realtime operation with industrial controllers, but complex to handle with large scale systems. To make this manageable, strict rules concerning the modular structure of the software were formulated to ensure similar structures for all modules. This enhances interchangeability and compatability. Further, an Application Programming Interface (API) between LabVIEW and VeriStand is used to compensate for weaknesses of VeriStand, such as simple data logging, watchdog functionality, interfaces to external systems (e.g. via OPC UA), etc.

### Experimental Insights

The first experiments with the PBDH setup in the CoSES laboratory showed that the pumps in the laboratory run at an unfavorable area on the characteristic curve due to high network resistances paired with small volume flows. In the flow-pressure diagram this expresses in steep resistance curves, resulting in operating points close to the pressure-axis (compare Figure 3.1b). This is problematic due to several aspects, elaborated in the following:
First of all, operating points located on the boundaries of the characteristic pumping curve have low pumping efficiency (see Figure 6.7). The efficiency is highest for a balanced ratio between pressure difference and volume flow, around the design point of a pump.
Second, the controllability of the pumps is limited - operational states with low flow rates cannot be reached, the range of reachable flow rates is considerably reduced overall and specific operating points are difficult to approach due to an over-sensitivity in relation to control signals. The pumps in the bidirectional substations are variable-speed circulating pumps, controlled by an external input signal that modulates the speed and associated with that the corresponding pumping power, e.g., with a signal of $0 - 10V$, reflecting $0 - 100\%$. In general, the pumps need to overcome a start-up resistance, which is composed of the rotor's inertia, the static pressure of the water, the hydraulic resistance of the circuit and other factors. Consequently, a minimal pumping power is required, which typically restricts the modulation of the pumps to a certain range, such as $20 - 100$ %. This is associated with a minimal flow rate and, according to the characteristic curve, a minimal pressure difference. In the CoSES laboratory we observed that, the more valves wore closed and the steeper the characteristic curve became thereby, the higher was the minimal necessary pumping power to overcome the start-up resistance. This was measured in form of a reduced modulation range (e.g., only between $60 - 100$ %) and an increased minimum volume flow rate. This can lead to the FP of a prosumer not being able to overcome the resistance at all, resulting in zero flow. A similar effect occurs when the pump speed is downregulated - at some point far away from minimum speed the pump can't overcome the hydraulic resistance anymore. Moreover, a steeper resistance curve substantially limits the maximum attainable flow rate. In addition, the emerging operating points are highly sensitive to changes in the control signals for high system resistances.

Typical centrifugal circulating pumps, like those used in the heating sector, are usually not designed

[2]https://www.ni.com/de.html (visited on 2023/10/10)

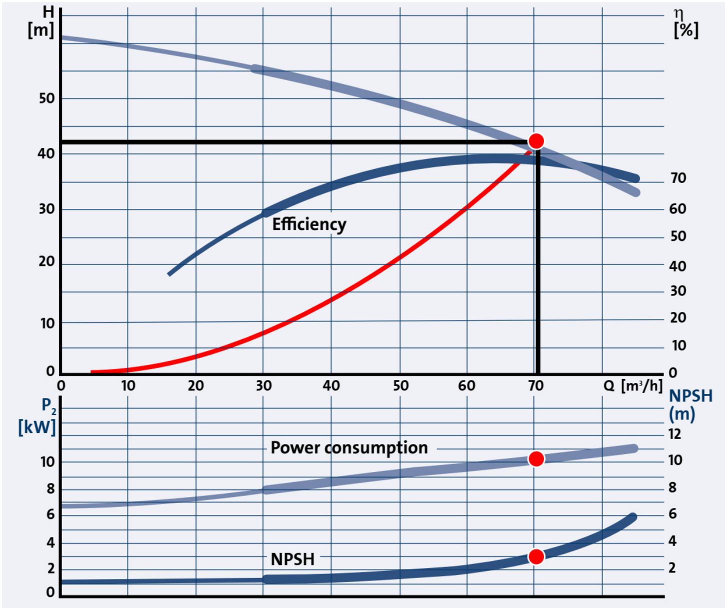


Figure 6.7: Typical performance curves for a centrifugal pump. Head $H$ $[m]$ (proportional to pressure difference $\Delta p$), power consumption $P_2$ $[kW]$, efficiency $\eta$ $[\%]$ and Net Positive Suction Head $NPSH$ $[m]$ are shown as a function of the flow $Q$ $[m^3/h]$ [115].

for the operation with high pressure differences (due to high system resistances) at low volume flows. In the laboratory, therefore, an upgrade to more powerful, oversized pumps was done to be able to operate them in an efficient and well-controllable operating area and to achieve sufficient volume flows for the desired power transfer, despite the high hydraulic system resistance. An alternative solution would have been the installation of two pumps in series. Reasons for the extraordinary high hydraulic resistances of the emulated PBDH network in the CoSES laboratory are: a high amount of installed measuring equipment with high hydraulic resistances, numerous bends in the pipe routing within short distances, installations such as check valves that have a minimum cracking pressure, small pipe diameters (22 mm) due to the microgrid character associated with low heat transfer capacity.

Of course, the hydraulic network characteristics for real PBDH networks in the field will differ from these in the laboratory environment. Nevertheless, it is anticipated that strong pumps will be needed. For every prosumer to be able to exchange heat with each other prosumer in the network, every prosumer's FP must be capable of overcoming the total network length's resistance and maintaining the necessary minimum differential pressure. Thus, each FP would have to be dimensioned similiar to the central network pumps in TDH networks in terms of the pumping pressure. In contrast to central network pumps of TDH networks, the FPs of PBDH networks require significantly lower volume flows, as each prosumer represents a distributed generation source, unlike the central power plants in TDH networks that supply the entire network. For PBDH networks in the field, this implies that distributed pumps would either operate at inefficient points or need substantial overdimensioning. The subsequent Section 6.3 will delve deeper into component dimensioning for PBDH networks. This leads to substantial economic implications in form of high overall investments for the FPs. To alleviate these issues, minimizing the hydraulic resistance of the network is crucial. Alternatively, restricting network energy exchange to neighboring prosumers could be considered, requiring pumps to be dimensioned only for this scope. Further, this suggests that the PBDH concept may be more suited to smaller network sizes. Another implication can be that low prosumer volume flow rates are problematic. As these are associated with low prosumer feed-in power, restricting the feed-in to producers with high power capacities can be a circumvention of the observed pump operation challenges.

A potential technical solution for these challenges might involve serially connecting smaller pumps, operated uniformly by a common signal. Analogous to how voltage sources work, the pumping pressures will add up, while a common volume flow will establish. This would enable each pump to handle a smaller differential pressure, allowing the use of smaller, cost-efficient, standard pumps operating with high efficiency. However, this proposed solution needs further detailed investigation for the specific application case.

## 6.3 Pub3: Dimensioning radial prosumer-based thermal networks

### 6.3.1 Context

For an efficient practical implementation of PBDH networks, an appropriate dimensioning of the relevant components is essential. This pertains in particular to the distributed actuators in form of pumps and valves, as the laboratory implementation has shown (see subsection 6.2.3). The conventional dimensioning procedure as described in subsection 3.2.3 is not sufficient for PBDH networks anymore, due to their highly flexible and dynamic operation, caused by changing prosumer modes and distributed actuators in the substations. In sharp contrast to TDH networks, PBDH networks show bidirectional volume flows and varying hydraulic circuits over time. Consequently, which hydraulic circuit a network segment is part of, can change over time.
As explained in subsection 3.2.3, the max. volume flow (associated with the max. power flow) through each network segment is the basis for the dimensioning the network components. Therefore, the variability introduces a significant challenge for component dimensioning, as it is not a priori evident which hydraulic circuit should be considered when dimensioning the components of a distinct network segment. Additionally, for dimensioning the decentral pumps in the network, the network critical point is relevant (see subsection 3.2.2). When several prosumers are in producer mode, more than one FP in the network is active, each with its critical point at which a minimal hydraulic pressure must be guaranteed at all time. That individual critical points of the different circuits can additionally migrate, depending on the overall operation of the network. That behavior was also observed by Ref. [71] in the context of solar-thermal feed-in. Ref. [71] states that the critical consumer changes its location dependant on a) the feed-in point and b) the demand of all other consumers. Thus, the high flexibility of PBDH rises the need for adapted methods to dimension the distributed components.

The subsequent paper presents a method to dimension linear PBDH networks, despite the a priori unknown closed hydraulic circuits, which are relevant for dimensioning. Key aspect of the presented method is the determination of the maximal power flows that have to be transported trough each network segment, considering any reasonable operating condition of the network. These maximal power flows depend on the prosumer modes, demand situations and the resulting hydraulic circuits in the network. Having determined the max. power flows through each network section, the associated hydraulic circuits are known and conventional methods from subsection 3.2.3 can be used for dimensioning the components such as pipes, valves and pumps. The presented method follows a rule-based and iterative approach and is limited to linear networks as a subcategory of radial networks. We provide a freely accessible Excel-spreadsheet where the method is automated and allows to dimension the components by specifying only some nominal and maximal values for the secondary prosumer sides. Thus, the tool allows to dimension flexible and linear PBDH networks with limited information during early-stage economic analyses and variant comparisons.

### 6.3.2 Paper

| | |
|---|---|
| **Title** | **Dimensioning radial prosumer-based thermal networks** |
| **Authors** | Fabian Speer, Thomas Licklederer, Daniel Zinsmeister, Vedran S. Perić |
| **Publication medium** | online, proceedings of the 13. Internationale Energiewirtschaftstagung an der TU Wien |
| **Copyright** | open access |
| **Identifier 1 / URL 1** | https://iewt2023.eeg.tuwien.ac.at/download/contribution/fullpaper/104/104_fullpaper_20230210_224423.pdf |
| **Identifier 2 / URL 2** | https://www.researchgate.net/publication/369480633_Dimensioning_radial_prosumer-based_thermal_networks |
| **Associated repositories** | https://github.com/FabianSpeer/PBN_Dimensioning_Tool |
| **Author contributions** | according to the Contributor Roles Taxonomy (CRediT, see [93]) |
| Fabian Speer | Writing - Original Draft, Methodology, Software, Investigation, Validation |
| Thomas Licklederer | Writing - Review & Editing, Supervision, Conceptualization, Methodology |
| Daniel Zinsmeister | Writing - Review & Editing, Conceptualization |
| Vedran S. Perić | Resources, Supervision, Writing - Review & Editing |

# Dimensioning radial prosumer-based thermal networks

**Fabian SPEER (1), Thomas LICKLEDERER (1), Daniel ZINSMEISTER (1), Vedran S. PERIĆ (1)**

(1)Technical University of Munich (TUM)
Munich Institute of Integrated Materials, Energy and Process Engineering (MEP), Lichtenbergstraße 4a, 85748 Garching b. München, fabian.speer@tum.de

**Abstract:**

The energy flows in prosumer-based based thermal networks are volatile, thus the problem of dimensioning the network infrastructure is more challenging than in the case of conventional unidirectional thermal networks. This paper introduces a rule-based method to determine the relevant design parameters of network pipes, control valves, and circulation pumps in radial prosumer-based networks. The dimensioning is performed based on the calculated maximal power flows through each pipe section of the network. The required inputs for the method are secondary side prosumer characteristics. The method is implemented in Excel and its application is demonstrated on a case study with a network with five residential prosumers. The method's accuracy and the functionality of dimensioned components were benchmarked under different energy exchange scenarios with a detailed thermohydraulic grid model implemented in Modelica using *Dymola*. The validation criteria were (i) the accuracy of the calculated maximal power flows in the network pipes, (ii) supply of consumers with the designed power and supply temperature (iii) the actuator operating points. Criterium (i) was achieved with a maximal error of *0.7 %*. Criterium (ii) was met in all exchange scenarios with maximal deviations of *3.3 %* for delivered power and *0.58 K* for supply temperature. In criterium (iii), control errors in the primary temperature spread lead to deviations in the operating points. However, they remained in an operable range and did not impair the network's functionality. Thus, the introduced method allows to dimension flexible prosumer-based networks with limited information during early-stage economic analyses and variant comparisons.

**Keywords:** district heating, prosumer-based network, dimensioning method, planning tool, network components

# 1 Introduction

## 1.1 Motivation

Conventional thermal networks (*CNs*) use a central generation unit to provide thermal energy. Central circulation pump(s) in a network of supply and return pipes drive a unidirectional mass flow to distribute the energy to consumers. Due to the unidirectional flows in *CN*s, each network section (pipe, substation) is part of a fixed hydraulic circuit (see Figure 1, A and B). Various tools and guides exist to dimension *CN*s with state of the art methods [1–6]. In those guides, the worst conditions for each network section in its hydraulic circuit build the design state for dimensioning.

Including prosumers in *CN*s can be advantageous for energy efficiency and network flexibility [7, 8]. This paper considers the most extreme form of prosumer integration: a prosumer-based thermal network (*PBN*) comprised only of prosumers without any dominating central unit. Decentral actuators (pumps and control valves) in the substations enable bidirectional mass and energy flow in the network for load-balancing between prosumers [9]

In *PBN*s, in contrast to *CN*s, each specific network section is part of varying hydraulic circuits. This phenomenon is caused by bidirectional flows in the network and influenced by changing prosumer modes and load scenarios (see Figure 1, C and D). Thus, the question arises of how to dimension such networks.

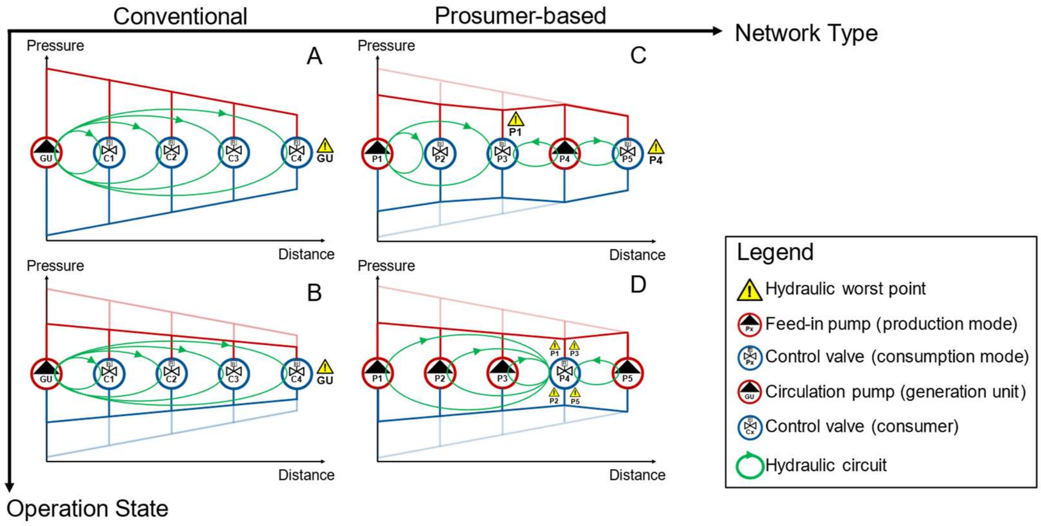


**Figure 1: Comparison of pressure curves and hydraulic circuits in different operation states of a thermal network (A and B) with central generation unit vs. prosumer-based network (C and D).**

Various models and simulations have been built to optimize the operation and design of components in thermal networks with bidirectional mass flow [10–12]. However, to the best of the authors knowledge, there is no tool for dimensioning such networks, while the number of planners with experience in pilot projects is very limited [7, 13]. Thus, comparisons between *CN* and *PBN* for variant decisions in early project stages require simulations and are prone to inconsistency [7, 14]

The basis for thermal dimensioning procedures is the design power flow. Due to the hydraulic flexibility of *PBN*s described earlier, the design power in the network components depends on other prosumers. Thus, determining the significant power flows is the necessary preliminary stage for component design in radial *PBN*s.

In this paper we propose a method to identify the hydraulic circuit, power flows and prosumer load situations relevant to the design of primary side network components in radial *PBN*s. It is structured as follows: First the considered network structure is characterized. An algorithm to determine the relevant power flows for dimensioning in this network structure is proposed. An Excel tool for dimensioning the core network components, i.e. feed-in pumps (*FIP*s), control valves (*CoV*s), and network pipes is introduced. In a case study a network with 5 prosumers is dimensioned with the tool and a simulation with different exchange scenarios is used to validate the functionality of the dimensioned components.

## 1.2 Network concept

The structure and the main components of the considered *PBN* are depicted in Figure 2. The *FIP* and *CoV* are the decentral actuators, which influence the pressure and mass flow on the primary network side, while the production pump (*ProP)* and the consumption pump (*ConP)* control the mass flow on the secondary side. When the prosumer is in production mode, *FIP* and *ProP* are active; *CoV* is closed, and *ConP* is inactive. In consumption mode, FIP and ProP are inactive, while CoV is open and ConP is active. In this paper, to prove the concept of the method, only a radial network configuration with a main distribution line and direct connection lines is considered.

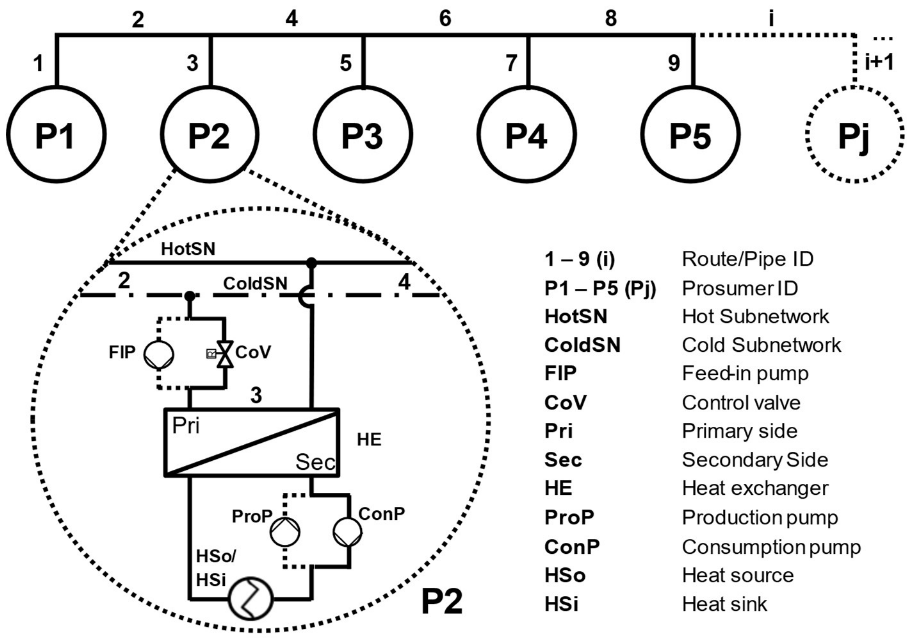


**Figure 2: Structure of a radial prosumer-based network**

# 2 Dimensioning Method

The dimensioning method was developed for two flexibility design premises to give upper and lower boundaries for component dimensioning depending on the targeted operation flexibility:

- All-Neighbor-Exchange (*ANE*): Each prosumer can exchange energy with each of the other prosumers in the network.
- One-Neighbor-Exchange (*ONE*): Each prosumer can only exchange energy with directly neighboring prosumers.

Throughout this paper the design premise *ANE* is assumed.
Table 1 lists the necessary input parameters and the values used for the case study.

**Table 1: User input parameters and values applied in the case study**

| Description | Symbol | Value | Unit |
|---|---|---|---|
| Medium in the network pipes | Medium | Water | – |
| Type of network pipes | Piping type | Plastic jacket pipes | – |
| Length of the route sections | $l_{route}$ | see Table 6 | $m$ |
| Maximum flow velocity in connection pipes | $u_{max}^{pipe,cct}$ | 1 | $m/s$ |
| Maximum flow velocity in distribution pipes | $u_{max}^{pipe,dis}$ | 1.5 | $m/s$ |
| Maximum pressure gradient in connection pipes | $R_{max}^{pipe,cct}$ | 250 | $Pa/m$ |
| Maximum pressure gradient in distribution pipes | $R_{max}^{pipe,dis}$ | 250 | $Pa/m$ |
| Target temperature in the hot subnetwork | $\vartheta_{hot,tar}^{prim}$ | 65 | $°C$ |
| Target temperature in the cold subnetwork | $\vartheta_{cold,tar}^{prim}$ | 50 | $°C$ |
| Targeted valve authority | $a_{tar}^{CoV}$ | 0.5 | – |
| Assumed pressure gradient in individual resistors (e.g. fittings) | $R_{ir}$ | 10 | % |
| Maximal prosumer consumption power | $P_{max}^{pros,con}$ | see Table 3 | $kW$ |
| Maximal prosumer production power | $P_{max}^{pros,pro}$ | see Table 3 | $kW$ |
| Target secondary supply temperature consumption mode | $\vartheta_{hot,tar}^{sec,con}$ | 60 | $°C$ |
| Set secondary return temperature in consumption mode | $\vartheta_{cold,set}^{sec,con}$ | 45 | $°C$ |
| Pressure loss through heat exchangers in design conditions | $\Delta p_{HE}^{prim}$ | 20 | $kPa$ |
| Design temperature difference in the heat exchangers | $\Delta T_{HE}$ | 3 | $K$ |

| **Symbols** | | **Sub- and superscripts** | | **Abbreviations** | |
|---|---|---|---|---|---|
| l | Length | $cct$ | Connection | PBN | Prosumer-based network |
| u | Velocity | $dis$ | Distribution | CN | Conventional network |
| $R$ | Pressure gradient | $con$ | Consumption | FIP | Feed-in pump |
| $\Delta p$ | Pressure loss | $pro$ | Production | CoV | Control valve |
| H | Pump head | $tar$ | Target | DHC | Design hydraulic circuit |
| $\vartheta$ | Temperature °C | $prim$ | Primary side | Sc | Exchange scenario |
| $T$ | Temperature K | $sec$ | Secondary side | ANE | All-Neighbor-Exchange |
| $a$ | Valve authority | $pros$ | Prosumer | ONE | One-Neighbor-Exchange |
| $P$ | Prosumer power | $HE$ | Heat exchanger | P1 | Prosumer with ID 1 |
| $\dot{Q}$ | Transported power | $ir$ | Individual resistors | DHW | Domestic hot water |
| $D$ | Diameter | $pipe$ | Network pipe | | |
| $K$ | Flow coefficient | $max$ | Maximal | | |
| | | $set$ | Set point | | |

## 2.1 Determining the design power flows - algorithm

In Figure 3, an example application of the proposed algorithm to determine the maximal power flows $\dot{Q}^{i}_{max}$ in the network pipes as design conditions is depicted. The algorithm is built for radial *PBN* with a network structure and nomenclature as shown in Figure 2.

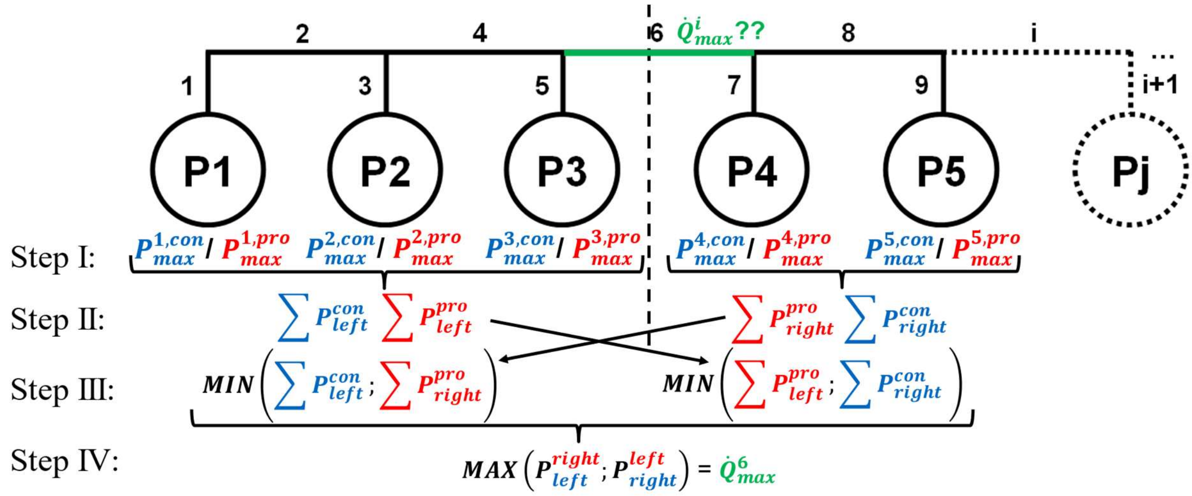


**Figure 3: Algorithm for determining the design power flows in an example distribution pipe**

The algorithm describes four main steps to determine the maximum power flow through the network pipes of a radial *PBN*. In *Step I* the network is split into two sides, relative to the considered pipe (i.e. pipe 6). The maximal consumption power $P^{j,con}_{max}$ and the maximal production power $P^{j,pro}_{max}$ are set for each prosumer. In *Step II* the available demand and supply power of both network sides are calculated by adding up the consumption and production power of the prosumers. With this, the relevant demand and supply from the left and the right side of the network are determined. The power flow in the pipe is characterized by the energy exchange from one side to another. Thus, in *Step III* the possible power exchanges between the two sides is determined. This is done by comparing the maximum supply power of one side to the maximum demand power from the other side. The smaller value between those describes the possible power exchange. Finally, in *Step IV* the maximum of the two possible power exchanges is calculated to result in the design power flow $\dot{Q}^{6}_{max}$ of pipe 6. A more detailed flow chart for determining the power flow in all network pipes is included in the appendix (see Figure 10).

## 2.2 Component dimensioning

The remaining dimensioning procedure follows established methods described in Ref. [3]. The flow chart describing the main dimensioning steps and target values is depicted in Figure 4.

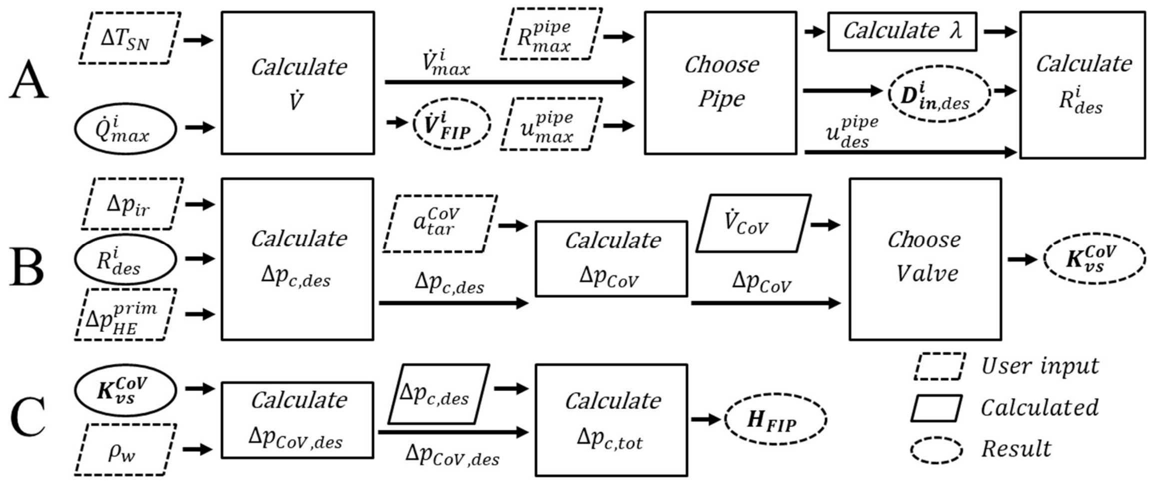


**Figure 4: Flow chart for the component dimensioning**

### 2.2.1 Pipe Dimensioning

The procedure for pipe dimensioning is depicted in **A** (see Figure 4). The pipes are dimensioned, based on the maximum transported power $\dot{Q}^i_{max}$ determined in subsection 2.1. The user-defined values for the maximum conditions in connection and distribution pipes (see Table 1) are considered.

The friction factor $\lambda$ is calculated using the approximation of the Colebrook's equation described in [15].

### 2.2.2 Control valve Dimensioning

The procedure for *CoV* dimensioning is depicted in **B** (see Figure 4). The hydraulic circuit with the maximum pressure loss $\Delta p_{c,des}$ between a consuming and a producing substation (*CoV* excluded) is the design hydraulic circuit (*DHC*) for the *CoV*. The theoretical *CoV* pressure drop is calculated with $\Delta p_{c,des}$ and $a^{CoV}_{tar}$ set in Table 1 (eq. (1)). To limit the pressure losses, the next larger available *CoV* is chosen.

$$a^{CoV}_{tar} = \frac{\Delta p_{CoV,th}}{\Delta p_{CoV,th} + \Delta p_{c,des}} \tag{1}$$

### 2.2.3 Pump Dimensioning

The $\Delta p_{CoV,des}$ is calculated with $K^{CoV}_{vs}$ determined in **B** [3]. The head for the *FIP* $H^{FIP}_{des}$ (see **C** Figure 4) is then specified by the resulting total pressure drop in the *DHC* $\Delta p_{c,tot}$. The volume flow $\dot{V}^{FIP}_{des}$ is determined in **A** (see Figure 4) along with the volume flows in the network pipes.

# 3 Dimensioning Tool

An Excel tool was built to automate the dimensioning process. The parameters, algorithm and dimensioning procedure from section 2, alongside the nomenclature from Figure 2 are implemented in the tool.

It is published at: https://github.com/FabianSpeer/PBN_Dimensioning_Tool. It provides the structure to dimension a *PBN* with a maximum of 20 prosumers (with limits to the available product sizes).

Example products are used for dimensioning, as shown in Table 2. The relevant values from the manufacturer data sheets of the product lines are included in the tool.

**Table 2: Product lines and manufacturers of primary network components used in the case study**

| Component | Manufacturer | Product line |
|---|---|---|
| **Pipes** | ISOPlus [16] | Plastic jacket pipes (standard) |
| **Control valves** | Sauter [17] | VUN |
| **Circulation pumps** | Grundfos [18] | CR – inline pumps |

For each component, the calculated dimensioning results are considered the minimum requirements.

# 4 Case study

The dimensioning method is validated by implementing its results in a thermohydraulic simulation and comparing the results.

The validation criteria are:

i. Accuracy of the predicted design power flows in network pipes ($\dot{\boldsymbol{Q}}^{i}_{max}$)
ii. Sufficient consumer supply with power demand ($\dot{\boldsymbol{Q}}^{j}_{con}$) and supply temperature ($\boldsymbol{\vartheta}^{sec}_{hot}$)
iii. Actuator states: valve opening ($\boldsymbol{\kappa}^{CoV}_{set}$), pump speed ($\boldsymbol{u}^{FIP}_{set}$) and operating state $\Delta\boldsymbol{p}(\dot{\boldsymbol{V}})$

## 4.1 Setup

The introduced dimensioning tool is used to dimension the network components, as described in sections 2 and 3. The dimensioned components are implemented into a thermohydraulic grid model. The *ProsNet* [20] library was used to build the model in the Modelica-based software *Dymola* [19]. During the simulation, the actuators are controlled by a specially modeled weighted PID controller [20] to achieve the temperatures and power flows specified in Table 1.

### 4.1.1 Prosumer side

The prosumers are based on the five residential houses emulated in the *CoSES*-laboratory [21]. Due to the proposed early-stage application of the dimensioning method, the houses are categorized into TABULA building typologies [22] to determine their heat demands. Their properties and resulting demands are listed in Table 3.

Ventilation and transmission losses of the houses were calculated according to the simplified procedure of the *DIN EN 12831-1* for the climate in Munich, using the respective heat transfer coefficients stated in the TABULA typologies.

For the power demand for domestic hot water (DHW), the peak flows were determined according to the *DIN 1988-300*. The required additional power was calculated for temperatures described in *DIN 12831-3 A100*. A DHW storage with a discharge time of 10 min (*DIN 4708-1*) and a recharge time of 60 min was assumed.

All prosumers are assumed to be equipped with heat sources capable of generating 100 % of their total heat demand, as suggested in [23].

**Table 3: Prosumer characteristics in the case study**

| | ***P1*** | ***P2*** | ***P3*** | ***P4*** | ***P5*** |
|---|---|---|---|---|---|
| *Living Area [m²]* | 300 | 400 | 300 | 750 | 300 |
| *No. of Apartments* | 1 | 3 | 2 | 4 | 2 |
| *Age Class* | 1995 - 2002 | From 2016 | 2007 – 2009 | 1995 – 2002 | 2007 - 2009 |
| *TABULA Code* | SFH.09.Gen | SFH.12.Gen | SFH.10.Gen | MFH.09.Gen | SFH.10.Gen |
| *TABULA Standard* | Improved | Improved | Improved | Improved | Improved |
| *Heat loss transmission [kW]* | 13.0 | 9.9 | 8.9 | 16.7 | 8.9 |
| *Heat loss ventilation [kW]* | 5.2 | 1.1 | 4.3 | 13.0 | 4.3 |
| *Heat demand DHW [kW]* | 7.1 | 10.5 | 8.1 | 12.2 | 8.1 |
| *Total heat demand [kW]* | 25.3 | 21.5 | 21.2 | 41.8 | 21.2 |

### 4.1.2 Network side

The parameters of primary side components are chosen according to the results from the dimensioning tool with the conditions described in Table 1 and Table 2. The selected component sizes are documented in the appendix (see Table 6-Table 8).

### 4.1.3 Scenarios

The exchange scenarios (*Sc*) were chosen to create a consumption design state and production design state for each prosumer at least once. Two criteria must be fulfilled for a prosumer to be in its design state. First, it must operate with its maximum production or consumption power (see Table 3). Second, the transported power flow in their design hydraulic circuit (DHC) (see Figure 5) is maximal, as defined by the algorithm in subsection 2.1.

In Figure 5 the qualitative pressure curves and set prosumer powers in two example scenarios are shown. In scenario 1 the production design states for the *FIP*s 1 and 2, and the consumption design state for the *CoV*s 4 and 5 are observed. Prosumer 3 is operating in part-load, since the prosumer powers set in Table 3 do not allow all prosumers to be in a design state simultaneously. Consequently a separate scenario is required to achieve the design states described above for prosumer 3. The chosen design scenario for the *FIP3* is also shown in Figure 5, where prosumers 1,2 and 3 operate under maximum loads, while prosumers 4 and 5 operate in part-load.

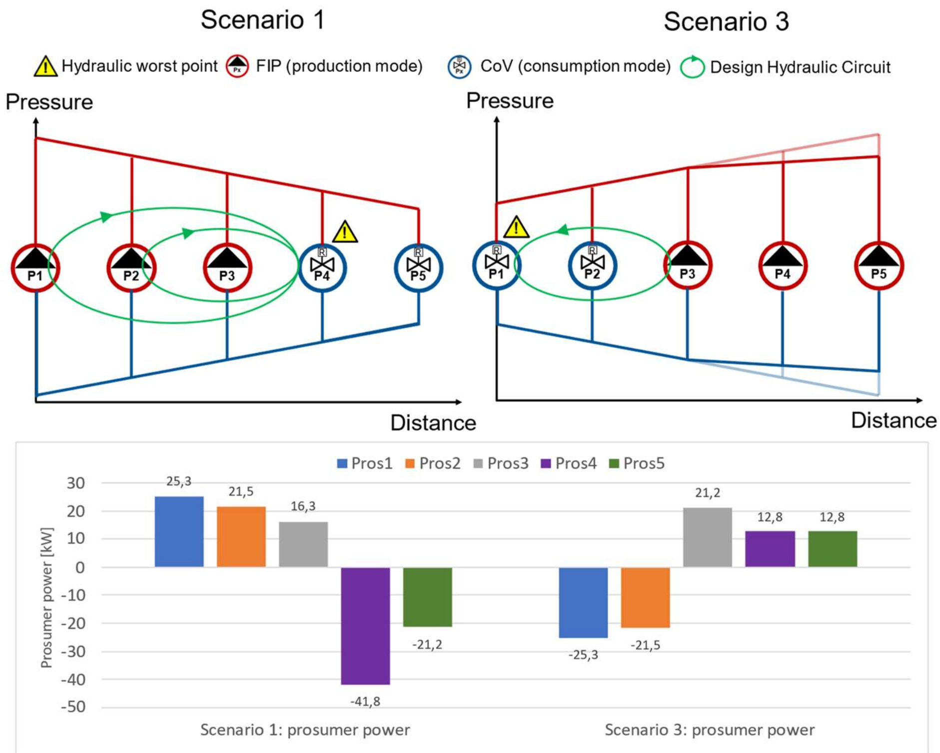


**Figure 5: Qualitative pressure curves and prosumer power in example exchange scenarios 1 and 3 with design conditions for FIP1&2 and CoV4&5 in scenario 1 and for FIP3 in scenario 3**

Since the consumption power is as high as the production power for all prosumers, the missing design states can be achieved by inverting the power flow of all prosumers during scenarios 1 and 3. By doing so the production design scenario for the *FIP* of a prosumer turns into the consumption design scenario for the *CoV* of the prosumer.

The inverted *Sc1* is named *Sc2* and the inverted *Sc3* describes *Sc4*. The relevant design scenarios for all actuators are listed in Table 4.

**Table 4: Design scenarios for the actuators**

| | Scenario 1 | | Scenario 2 | | Scenario 3 | | Scenario 4 | |
|---|---|---|---|---|---|---|---|---|
| **Design scenario for:** | FIP | 1 & 2 | FIP | 4 & 5 | FIP | 3 | FIP | - |
| | CoV | 4 & 5 | CoV | 1 & 2 | CoV | - | CoV | 3 |

Additionally, the observation of the network behavior in part-load situations is desired. Thus, 2 additional scenarios (5 and 6) are created, which correspond to half the power flows of scenario 1 and 2 respectively.

The secondary supply temperature $\boldsymbol{\vartheta_{hot,pro}^{sec}} = \boldsymbol{\vartheta_{hot,tar}^{prim}} + \Delta \boldsymbol{T_{HE}}$ is set according to the inputs from Table 1 to *68 °C* during production, and the return temperature $\boldsymbol{\vartheta_{cold,con}^{sec}}$ is set to *45 °C* during consumption for every prosumer to exclude the performance of the secondary heat source/sink from the analysis.

Each scenario is simulated for 1 hour with simulation steps of 10 seconds. Before and after each scenario, transition states with half the power are set for 15 minutes.

## 4.2 Simulation results

For evaluating the proposed dimensioning method, only the steady-state operation is relevant. Thus, the following values are read at the end of each 1-hour simulation section when the operation state has stabilized.

The design values for the error analyses of pipes and actuators are documented in the appendix (see Table 6 - Table 8). The design values for prosumers can be extracted from Table 3.

The absolute errors ($\boldsymbol{\varepsilon}$) for the maximum simulated power flows $\boldsymbol{\dot{Q}_{max,sim}^{i}}$ and the maximum volume flow $\boldsymbol{\dot{V}_{max,sim}^{i}}$ in the 9 pipe sections are shown in Figure 6.

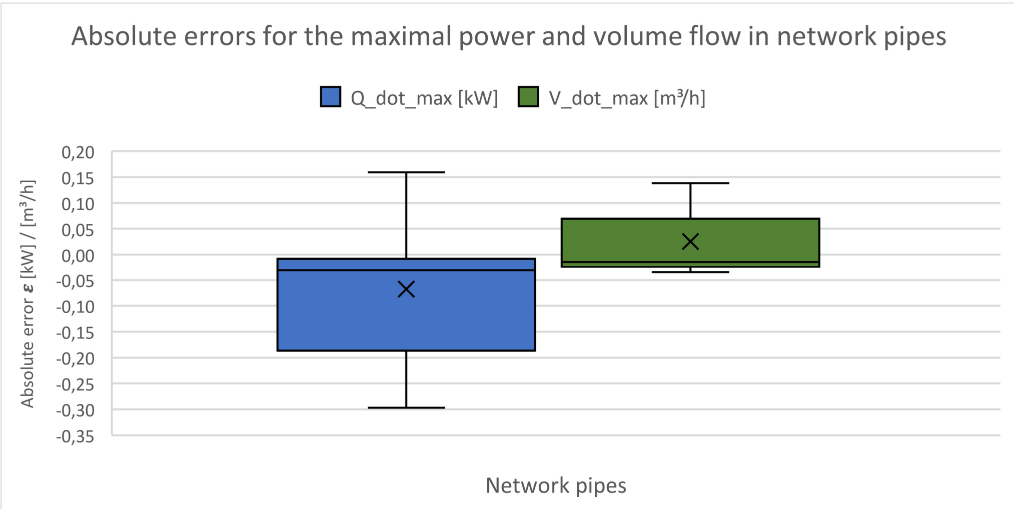


**Figure 6: Absolute errors for simulated $\dot{Q}_{max,sim}^{i}$ and $\dot{V}_{max,sim}^{i}$ compared to design $\dot{Q}_{max}^{i}$ and $\dot{V}_{max}^{i}$ in the network pipes**

The maximal relative deviation for $\boldsymbol{\dot{Q}_{max}^{i}}$ is *0.7 %* and occurs during Sc3. The small errors for $\boldsymbol{\dot{Q}_{max}^{i}}$ indicate, that the algorithm presented in 2.1 can accurately predict the design power flows in the network pipes. Thus, the first (i) validation criterium is fulfilled. The maximal relative deviation for $\boldsymbol{\dot{V}_{max}^{i}}$ is *5.5 %* in pipe sections 8 and 9 during Sc1. This increases the pressure gradient in the pipe compared to the design value. However, with the chosen pipe dimensions (see Table 6) the pressure gradient is still below the set maximum of *250 pa/m*.

Figure 7 depicts the absolute errors for $\dot{Q}_{con}^{j}$ and $\vartheta_{hot}^{sec}$ that resulted from the simulation of the prosumers during their design (*des*) scenario and during part load (*pl*) scenarios *Sc5* and *Sc6* as defined in subsection 4.1.3.

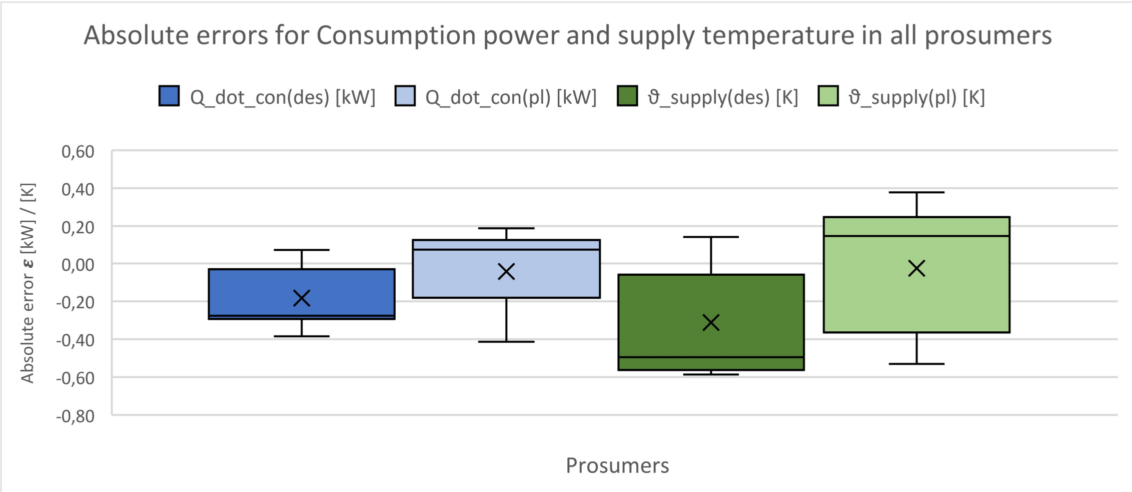


**Figure 7: Simulated and design values for $\dot{Q}_{con}^{j}$ and $\vartheta_{hot}^{sec}$ during design and part load consumption scenarios**

The maximal relative error for $\dot{Q}_{con}^{j}$ is *1.5 %* during design conditions in Sc2 and *3.3 %* in the part-load scenario 6. The maximal relative deviation of $\vartheta_{hot}^{sec}$ is *-0.58 K* during design conditions in Sc4 and *-0.53 K* in the part-load scenario 6. The recorded errors have no significant not impact on the operation of the connected prosumers with a setpoint supply temperature of $\vartheta_{hot}^{sec} = 60\,°C$. Consequently, the consumption demands of all prosumers are met during every scenario. Thus, the second (ii) validation criterium can also be regarded as fulfilled.

In the third (iii) criterium, the actuator operating states are considered. The operating states are defined by volume flow $\dot{V}$ through and the pressure difference $\Delta p$ over the actuator. Since the differential pressure and the volume flow depend on each other, a volume flow error also causes deviations from the designed differential pressure of the actuator. Volume flow errors were already recorded in the network pipes (see Figure 6). These deviations must result from an error in the temperature spread $\Delta T_{set}^{prim} = \vartheta_{hot,set}^{prim} - \vartheta_{cold,set}^{prim}$, since the power flows in the pipes matched the design nearly perfectly and the two values are connected by eq. (2).

$$\dot{Q}_{des}^{pipe} = c * \dot{V} * \Delta T_{set}^{prim} \tag{2}$$

Where $c$ is a combined constant of the density and heat capacity of the medium.

With the described impact on the volume flow, the errors for $\boldsymbol{\Delta T_{set}^{prim}}$ shown in Figure 8, have direct impact on the operating point deviations of the actuators.

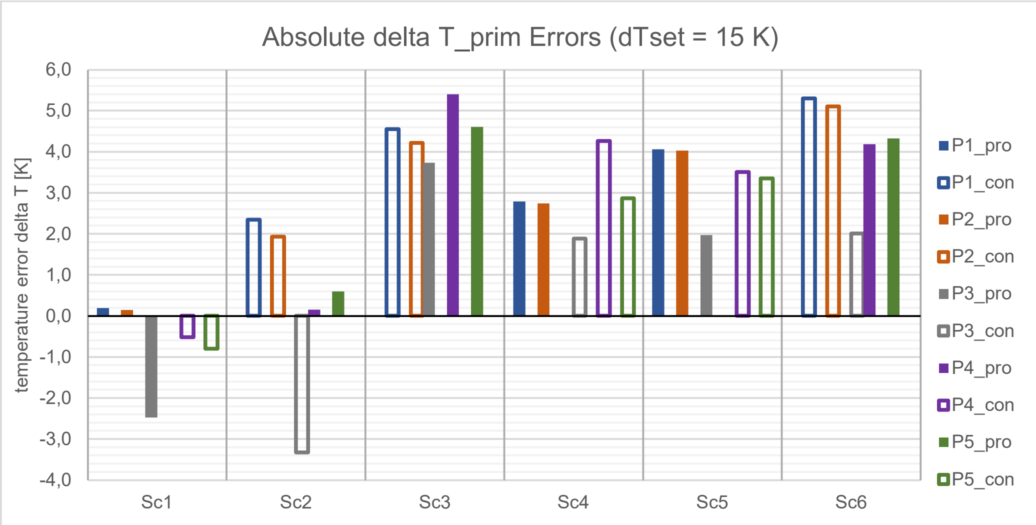


**Figure 8: Absolute error $\varepsilon(\Delta T_{set}^{prim})$ across all scenarios**

It is noticeable, that the errors in Figure 8 are mostly positive and thus cause a reduced volume flow. The errors are at their lowest, during the scenarios 1 and 2, when the energy exchange in the network is the highest. The control objectives of the used weighted PID controller [20] are still undergoing research. Thus, control errors are likely to be the cause of the deviations.

Table 6 shows the normalized control values for the *FIP* speed, and the *CoV* opening in a range from *0* to *1* during their respective design scenarios.

**Table 5: Normalized speed of FIPs $u_{set}^{FIP}$ and opening of CoVs $\kappa_{set}^{CoV}$ at their operating points**

| Normalized values | P1 | P2 | P3 | P4 | P5 |
|---|---|---|---|---|---|
| $u_{set}^{FIP}$ [0..1] | 0.80 | 0.74 | 0.56 | 0.80 | 0.70 |
| $\kappa_{set}^{CoV}$ [0..1] | 1.00 | 0.80 | 1.00 | 1.00 | 0.93 |

The maximum $u_{set}^{FIP}$ value of *0.8* in Table 5 shows that the designed pumps allow for expansion of the *PBN* at hand. The $\kappa_{set}^{CoV}$ is *1* for the prosumers at the critical point during their consumption design scenario (see Figure 5), as intended to minimize pressure losses. For *P2* and *P5* $\kappa_{set}^{CoV} < \mathbf{1}$ to adjust to the pressure conditions created by the remaining prosumers in *Sc1* and *Sc2* (see Figure 5). Thus, the actuator control in general works as intended, but the errors in Figure 8 suggest the built in prioritization of the controller causes deviations from the set conditions during part-load situations.

In Figure 9, the dimensioned operating point of each actuator is compared to the operating point resulting from the simulation of their design scenario (see Table 4). Additionally, the pump curves of the two *FIP* types (see Table 8) at maximum speed ($\boldsymbol{u_{max}^{FIP}}$) are displayed.

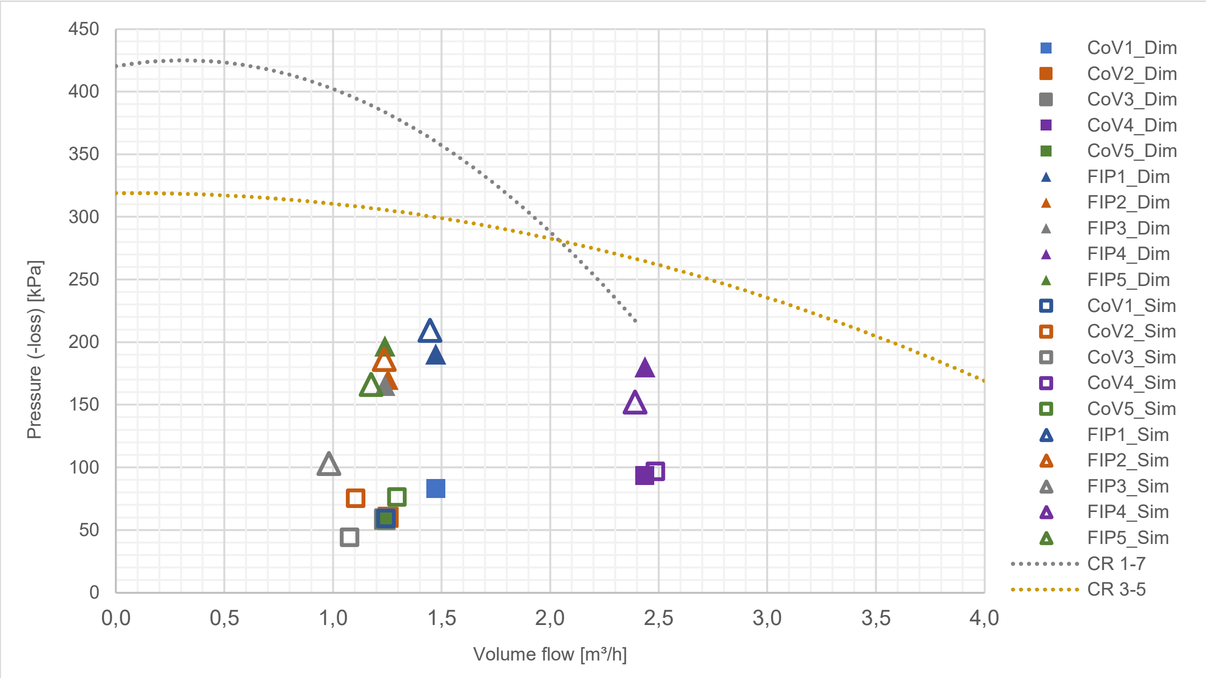


**Figure 9: Pump curves ($\boldsymbol{u_{max}^{FIP}}$) and dimensioned and simulated operation states of FIPs and CoVs during design states**

The operating point deviations of the actuators (*FIP3*, *CoV3*, *FIP5*, *FIP4* and *CoV1*) can be explained by the positive $\boldsymbol{T_{set}^{prim}}$errors at the consuming *P1* in *Sc1* and Sc3 and the consuming *P4* in *Sc4*. It is notable that *FIP1,* despite a positive $\boldsymbol{T_{set}^{prim}}$error during *Sc1* features a higher pressure increase than expected. That is because in *Sc1* the $\boldsymbol{T_{set}^{prim}}$error at the *CoV4* in the *DHC* of *FIP1* is negative due to the large negative $\boldsymbol{T_{set}^{prim}}$error at the part load *FIP3*. The difference between the simulation and design for *CoV2* and *CoV5* stems from a combination of $\boldsymbol{T_{set}^{prim}}$errors and the partially closed state of the *CoV*s $\boldsymbol{\kappa_{set}^{CoV2} = 0.8}$ during *Sc2* and $\boldsymbol{\kappa_{set}^{CoV5} = 0.93}$ in *Sc1* (see Table 5).

Due to the $\boldsymbol{T_{set}^{prim}}$errors, the predicted network states are not recreated fully in the simulation. However, since the deviations at the design load scenarios *Sc1* and *Sc2* are relatively small, the case study still yields relevant results for the validating the dimensioning method under the third (iii) criterium. Furthermore, the positive outcomes in the second (ii) validation criterium showed, that the different operating points did not impair the network's functionality.

A pump blocking effect, described in previous work [24] on *PBN*s could not be observed in the simulated exchange scenarios. Pump blocking is likely mitigated by the used design method for the pump, which considers the pressure conditions created by other prosumers at the feed-in location.

# 5 Conclusion and outlook

The simulation results showed that the dimensioning tool is well suited to dimension *PBN* components with limited information. Thus, the proposed method can be used in early-stage dimensioning, to dimension components capable of a functional network operation during different load scenarios.

The proposed method in its current state has a few limitations: It is restricted to a radial heat network. More complex networks with interconnections are not implemented yet. Additionally, the demand and temperatures of the secondary heat sources and sinks were assumed as static inputs. Furthermore, the provided tool is currently limited to two exchange premises.

Additional research regarding *PBN* dimensioning should aim to advance the dimensioning method towards more complex network typologies and conduct tests for different distributions of source and sink powers at the prosumers. The combination of the *PBN* structure with principles of $5^{th}$ generation district heating and cooling networks could provide additional benefits for flexibility and efficient energy exchange. The coupling with secondary load and production models for a dynamic simulation with included environmental influences on the prosumer side should be targeted to represent the networks' robustness precisely.

The provided dimensioning tool in its current state offers a quick way to dimension the core network components of small-scale radial *PBN*s. Thus, our developed method allows to include this innovative network type for neighborhood solutions in early-stage variant comparisons and provides realistic component sizes for planners to use in economic analyses.

# 6 Appendix

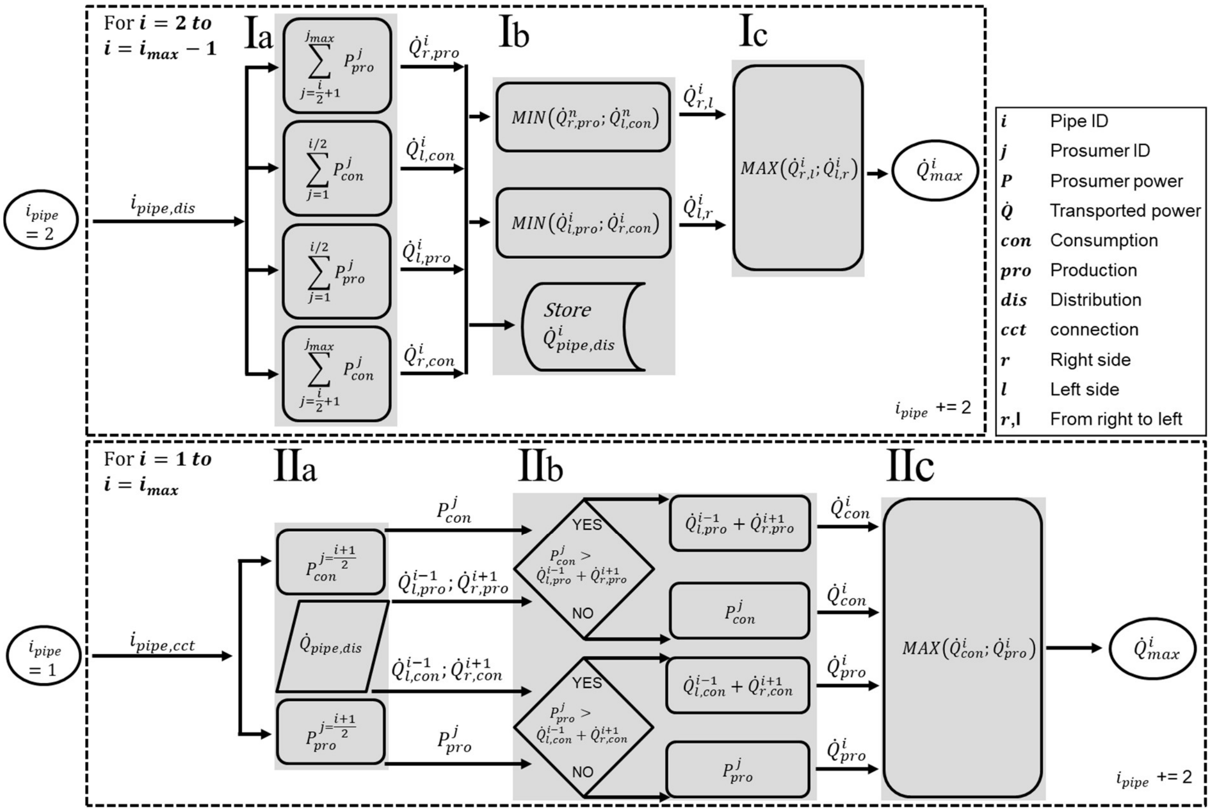

**Figure 10: Detailed flow chart for the power determination algorithm: In Ia – Ic the maximum power exchange in distribution pipes is determined; in Iia - IIc the maximum transported power in the connection pipe is determined under consideration of the maximum power flows in the distribution pipes**

**Table 6 Pipe dimensions and designed power and volume flows**

| Pipe ID | DN | $D_{in,des}^{pipe}$ [mm] | $u_{des}^{pipe}$ [m/s] | $l_{route}$ [m] | $R_{des}^{pipe}$ [Pa/m] | $\dot{Q}_{max}^{i}$ [kW] | $\dot{V}_{max}^{i}$ [m³/h] |
|---|---|---|---|---|---|---|---|
| **1** | 25 | 27.3 | 0.70 | 10 | 215.51 | 25.27 | 1.47 |
| **2** | 25 | 27.3 | 0.70 | 40 | 215.51 | 25.27 | 1.47 |
| **3** | 25 | 27.3 | 0.59 | 10 | 160.58 | 21.51 | 1.25 |
| **4** | 32 | 36 | 0.74 | 40 | 171.35 | 46.78 | 2.72 |
| **5** | 25 | 27.3 | 0.59 | 10 | 157.03 | 21.24 | 1.24 |
| **6** | 40 | 41.9 | 0.74 | 49.5 | 140.80 | 63.07 | 3.67 |
| **7** | 32 | 36 | 0.66 | 10 | 139.58 | 41.83 | 2.44 |
| **8** | 25 | 27.3 | 0.59 | 46.5 | 157.03 | 21.24 | 1.24 |
| **9** | 25 | 27.3 | 0.59 | 10 | 157.03 | 21.24 | 1.24 |

**Table 7 Control valve dimensions and designed operating points**

| Pros ID | Type | $\dot{V}_{des}^{CoV}$ [m³/h] | $\Delta p_{CoV,des}$ [kPa] | $K_{vs}^{CoV}$ [m³/h] | $a_{des}^{CoV}$ [-] |
|---|---|---|---|---|---|
| 1 | VUN015F320 | 1.47 | 83.36 | 1.6 | 0.42 |
| 2 | VUN015F320 | 1.25 | 60.37 | 1.6 | 0.39 |
| 3 | VUN015F320 | 1.24 | 58.91 | 1.6 | 0.41 |
| 4 | VUN015F310 | 2.44 | 93.53 | 2.5 | 0.48 |
| 5 | VUN015F320 | 1.24 | 58.91 | 1.6 | 0.34 |

**Table 8 Pump dimensions and designed operating points**

| Pros. ID | Type | $\dot{V}_{des}^{FIP}$ [m³/h] | $H_{des}^{FIP}$ [mH₂O] | $H_{des}^{FIP}$ [kPa] |
|---|---|---|---|---|
| 1 | CR 1-7 A-A-A-E-HQQE | 1.47 | 19.45 | 190.72 |
| 2 | CR 1-7 A-A-A-E-HQQE | 1.25 | 17.39 | 170.54 |
| 3 | CR 1-7 A-A-A-E-HQQE | 1.24 | 16.89 | 165.60 |
| 4 | CR 3-5 A-A-A-E-HQQE | 2.44 | 18.41 | 180.55 |
| 5 | CR 1-7 A-A-A-E-HQQE | 1.24 | 20.09 | 197.00 |

# 7 Literature


[1] isoplus Fernwärmetechnik Vertriebsgesellschaft mbH, *Planungshandbuch: Kapitel 1 - Allgemein.* [Online]. Verfügbar unter: https://www.isoplus.de/download/planungshandbuch.html (Zugriff am: 8. Juni 2022).

[2] J. Krimmling, *Energieeffiziente Nahwärmesysteme: Grundwissen, Auslegung, Technik für Energieberater und Planer*. Stuttgart: Fraunhofer-IRB-Verl., 2011.

[3] T. Nussbaumer, S. Thalmann, A. Jenni und J. Ködel, *Planungshandbuch Fernwärme,* 1. Aufl. Ittigen: EnergieSchweiz Bundesamt für Energie BFE, 2021.

[4] *Verenum.* [Online]. Verfügbar unter: http://www.verenum.ch/Dokumente_QMFW.html (Zugriff am: 10. Februar 2023).

[5] ASHRAE, *District Heating and Cooling Guides.* [Online]. Verfügbar unter: https://www.ashrae.org/technical-resources/bookstore/district-heating-and-cooling-guides (Zugriff am: 20. November 2022).

[6] Hochschule-Luzern, *Software Tools.* [Online]. Verfügbar unter: https://www.hslu.ch/de-ch/technik-architektur/ueber-uns/organisation/kompetenzzentren-und-forschungsgruppen/bau/gebaeudetechnik-und-energie/software-tools/ (Zugriff am: 10. Februar 2023).

[7] F. Bünning, M. Wetter, M. Fuchs und D. Müller, „Bidirectional low temperature district energy systems with agent-based control: Performance comparison and operation optimization", *Applied Energy*, Jg. 209, S. 502–515, 2018, doi: 10.1016/j.apenergy.2017.10.072.

[8] L. Brange, J. Englund und P. Lauenburg, „Prosumers in district heating networks – A Swedish case study", *Applied Energy*, Jg. 164, Nr. 1, S. 492–500, 2016, doi: 10.1016/j.apenergy.2015.12.020.

[9] T. Licklederer, T. Hamacher, M. Kramer und V. S. Perić, „Thermohydraulic model of Smart Thermal Grids with bidirectional power flow between prosumers", *Energy*, Jg. 230, 2021, doi: 10.1016/j.energy.2021.120825.

[10] Hanne Kauko, Karoline Husevåg Kvalsvik, Daniel Rohde, Natasa Nord und Åmund Utne, „Dynamic modeling of local district heating grids with prosumers: A case study for Norway", *Energy*, Jg. 151, S. 261–271, 2018, doi: 10.1016/j.energy.2018.03.033.

[11] G. Schweiger, P.-O. Larsson, F. Magnusson, P. Lauenburg und S. Velut, „District heating and cooling systems – Framework for Modelica-based simulation and dynamic optimization", *Energy*, Jg. 137, Nr. 3, S. 566–578, 2017, doi: 10.1016/j.energy.2017.05.115.

[12] J. Lindhe, S. Javed, D. Johansson und H. Bagge, „A review of the current status and development of 5GDHC and characterization of a novel shared energy system", *Science and Technology for the Built Environment*, Jg. 28, Nr. 5, S. 595–609, 2022, doi: 10.1080/23744731.2022.2057111.

[13] Marco Wirtz, Thomas Schreiber und Dirk Müller, „Survey of 53 5th Generation District Heating and Cooling (5GDHC) Networks in Germany", 2022.

[14] Stephan-Arved Bröcker, „Ökologische und wirtschaftliche Bewertung von gebäudeübergreifenden Energiekonzepten für ein Quartier in München". Masterthesis, Hochschule Augsburg, Augsburg, 2020.

[15] D. J. Zigrang und N. D. Sylvester, „Explicit approximations to the solution of Colebrook's friction factor equation", *AIChE J.*, Jg. 28, Nr. 3, S. 514–515, 1982, doi: 10.1002/aic.690280323.

[16] *ISOPlus-Website.* [Online]. Verfügbar unter: https://www.isoplus.de/home.html (Zugriff am: 26. Januar 2023).

[17] Fr. Sauter AG, *2-Way Valve with Male Thread, PN16 - VUN On Fr. Sauter AG.* [Online]. Verfügbar unter: http://bim.sauter-controls.com/viewitems/regulating-valves/2-way-valve-with-male-thread--pn16---vun (Zugriff am: 26. Januar 2023).

[18] Grundfos Germany, *CR > Vertikale mehrstufige Kreiselpumpen / GG/1.4301.* [Online]. Verfügbar unter: https://product-selection.grundfos.com/de/products/cr?tab=products (Zugriff am: 26. Januar 2023).

[19] *Dymola – Dassault Systèmes®.* [Online]. Verfügbar unter: https://www.3ds.com/de/produkte-und-services/catia/produkte/dymola/ (Zugriff am: 24. Januar 2023).

[20] T. Licklederer, D. Zinsmeister und V. S. Perić, „A field-level control approach for bidirectional heat transfer stations in prosumerbased thermal networks: simulation and experimental evaluation: Presentation at “8th International Conference on Smart Energy Systems.“, S. 62–63. [Online]. Verfügbar unter: https://smartenergysystems.eu/wp-content/uploads/2022/09/BoA_SESAAU2022.pdf

[21] D. Zinsmeister *et al.,* „A Prosumer-Based Sector-Coupled District Heating and Cooling Laboratory Architecture“, *SSRN Journal*, 2022, doi: 10.2139/ssrn.4003819.

[22] *TABULA WebTool.* [Online]. Verfügbar unter: https://webtool.building-typology.eu/#bm (Zugriff am: 24. Januar 2023).

[23] M.-H. Kim, D.-W. Kim, D.-W. Lee und J. Heo, „Experimental Analysis of Bi-Directional Heat Trading Operation Integrated with Heat Prosumers in Thermal Networks“, *Energies*, Jg. 14, Nr. 18, S. 5881, 2021, doi: 10.3390/en14185881.

[24] T. Licklederer, D. Zinsmeister, I. Elizarov, V. Perić und P. Tzscheutschler, „Characteristics and Challenges in Prosumer-Dominated Thermal Networks“ (en), *J. Phys.: Conf. Ser.*, Jg. 2042, Nr. 1, 2021, doi: 10.1088/1742-6596/2042/1/012039.

**Credit author statement**

Fabian Speer: Writing - Original Draft, Methodology, Software, Investigation, Validation. Thomas Licklederer: Writing - Review & Editing, Supervision, Conceptualization, Methodology. Daniel Zinsmeister: Writing - Review & Editing, Conceptualization. Vedran Perić: Resources, Supervision, Writing - Review & Editing.

## 6.4 Chapter Conclusion

For the narrative of this dissertation, several conclusions from this chapter shall be highlighted:

Based on literature review and comprehensive reasoning, a reference network concept for PBDH networks was proposed, building the basis for further technical investigations of these archtypical smart thermal grids. This reference network concept was implemented in a laboratory environment at the TUM, allowing for the safe and flexible testing of advanced control strategies for smart thermal grids as a part of a smart energy system and in interaction with real hardware under close-to reality conditions. To dimension pipes, pumps, valves and heat exchangers as the most relevant components of PBDH networks, a method for linear topologies was presented and implemented in an open source Excel tool.

Adopting from TDH the SR extraction principle with a pressurized supply line, the RS principle is found to be the only grid-forming feed-in principle for PBDH networks without central pumping station. To facilitate the decentralized feed-in, decentralized pumps in the substations are necessary. The proposed reference network concept for PBDH will be used as the foundation for investigating the systemic impacts of the prosumer interaction in smart thermal grids.

Essential key learnings from the first experiments with the PBDH setup in the CoSES laboratory were: The pumps in the laboratory run in an inefficient operating area on the characteristic curve, due to high hydraulic resistances in combination with low required volume flows. This limits also the controllability of the pumps. For real PBDH networks in the field, similiar challenges can be anticipated: The decentralized pumps must drive only small volume flows through the individual substations, compared to the central pumping stations in TDH networks. At the same time each pump must have enough power to overcome the pressure difference of the whole network in order to potentially be able to exchange heat with each other participant in the network (all-neighbor-exchange). Restricting the energy exchange to closely located prosumers, considering only small PBDH networks, restricting the feed-in to big producers or using serially installed pumps might be appropriate solution approaches.

The dimensioning of network components is further complicated by the variability in the emerging hydraulic circuits of PBDH networks. It is a priori not evident which overall network state is the determining one for dimensioning purposes. The proposed approach determines for each network segment the maximal volume flow, considering all possible hydraulic circuits each segment can be a part of during the dynamic network operation and all possible exchange scenarios. Although a solution for linear PBDH was presented, the challenge of appropriate and efficient dimensioning remains for general topologies.

# Chapter 7

# Thermohydraulic System Behavior

With the proposed reference network concept at hand, this chapter investigates the thermohydraulic system behavior of PBDH. A particular focus is on the relation between distributed actuator operation and the emerging overall system state, having RQ2 (see Section 2.2) in mind. Therefore, in Section 7.1 (Pub4), a mathematical model is formulated that interlinks the control inputs of the distributed actuators in the prosumer substations and the thermohydraulic network state of PBDH networks. Section 7.2 (Pub5) presents a specialized library in the established Modelica modeling language, developed to facilitate the thermohydraulic modeling of PBDH networks. Based on these available models, in Section 7.3 (Pub6), technical characteristics and challenges of PBDH are deduced and compiled. Altogether, this chapter tackles especially RQ2 from Section 2.2.

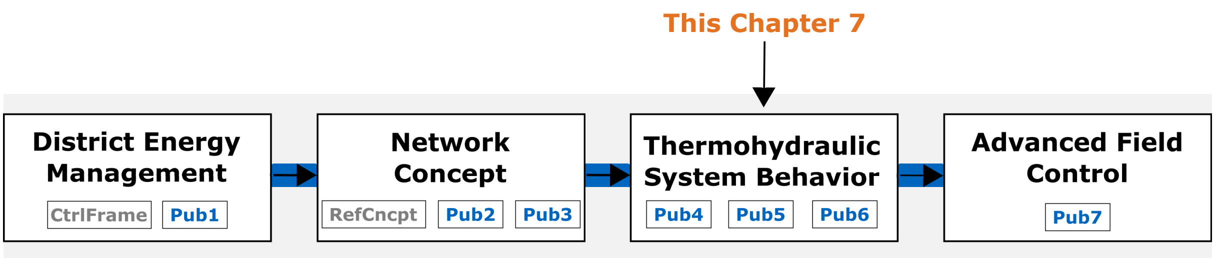


Figure 7.1: Position of this chapter within the overall structure of the main part of this dissertation.

**Chapter 7: Thermohydraulic System Behavior**
Based on the established reference network concept, a closed-form mathematical model is formulated to investigate the thermohydraulics of PBDH networks. The model captures relationships between power flows, temperature, volume flows, pressures, and actuator behavior. An open-source Python tool implements this model for steady-state simulation, complemented by a Modelica-based library that facilitates dynamic simulation across diverse PBDH network configurations. An exponential increase in modeling complexity is observed with growing network size. Using the developed models, the nonlinear sensitivity of the overall network state to actuator control variations is uncovered. Resulting systemic phenomena like 'pump blocking' and hydraulic network splitting are highlighted. Challenges in inverting the mathematical model for control purposes lead to a strategic shift towards an alternative control framework. This circumvents the need for a direct technical network model formulation and has several other benefits.

## 7.1 Pub4: Thermohydraulic model of Smart Thermal Grids with bidirectional power flow between prosumers

### 7.1.1 Context

Complementing experimental investigations, model-based simulations can serve as a groundwork, allowing to gain generalizable insights by studying various scenarios in a flexible, time efficiency, risk-free and controlled manner. To address RQ2 (Section 2.2), a network model is needed that relates the actuator control to the thermohydraulic network state and thereby to the overall network operation. As outlined in Section 5.1, control framework A suggests utilizing a network model at the automation layer. For this purpose, it is desirable that a suitable model for PBDH networks can not only be used for simulations, but is invertible to be used as a control model. An equation-based model is particularly suitable for use as an internal model for a MPC, as introduced in subsection 4.1.2. Such a control model reflecting also the technical behavior can determine the necessary control input signals to the actuators in order to enforce the desired power flows calculated by the management layer (see Section 6.2).

However, as concluded in Section 4.2, there are no suitable models of PBDH networks existing for the application purposes outlined above. Therefore, the subsequent publication derives a thermohydraulic model for PBDH networks. The following aspects distinguish the derived model from existing ones: The model considers the individual component behavior and at the same time captures the systemic network interactions by interlinked equation systems for the hydraulic and the thermal system behavior (see Figure 7.2). It incorporates the hydraulic behavior of pumps and valves as distributed actuators in prosumer substations, controlling the overall thermohydraulic network state. Further, the derived model considers the thermal heat exchanger behavior and thereby the influence of the return temperatures from the secondary side prosumer system. With its systematized mathematical description, the model can be used as basis for an open-loop network controller that determines the necessary control inputs for desired thermal power flows. For simulation purposes the mathematical model is implemented in a Python-based[1] open-access tool. The tool is named *ProHeatNet_Sim* and is publically available on https://github.com/thomaslicklederer/ProHeatNet_Sim.

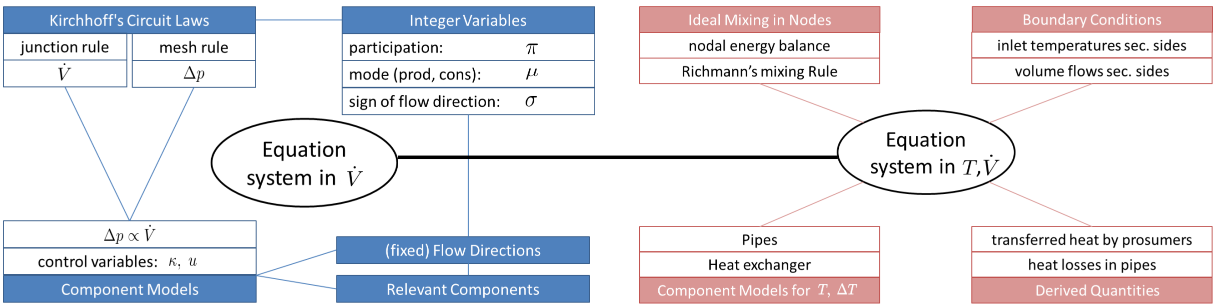


Figure 7.2: Hydraulic (left) and thermal (right) modeling aspects of the mathematical model for PBDH networks, as derived in Ref. [116] (Pub4).

[1] https://www.python.org/

### 7.1.2 Paper

| | |
|---|---|
| **Title** | **Thermohydraulic model of Smart Thermal Grids with bidirectional power flow between prosumers** |
| **Authors** | Thomas Licklederer, Thomas Hamacher, Michael Kramer, Vedran S. Perić |
| **Publication medium** | Energy, Volume 230, 1 September 2021, 120825 |
| **Copyright** | Included under Elsevier's copyright terms of 2023, which permit the inclusion in a thesis or dissertation provided the thesis is not published commercially. (https://www.elsevier.com/about/policies/copyright, Status: August 2023) |
| **Identifier / URL** | https://doi.org/10.1016/j.segy.2023.100095 |
| **Associated repositories** | https://github.com/thomaslicklederer/ProHeatNet_Sim |
| **Author contributions** | according to the Contributor Roles Taxonomy (CRediT, see [93]) |
| Thomas Licklederer | Conceptualization, Methodology, Software, Validation, Investigation, Writing - Original Draft, Writing - Editing, Visualization, Project administration. |
| Thomas Hamacher | Resources, Supervision. |
| Michael Kramer | Project administration, Conceptualization. |
| Vedran S. Perić | Writing - Review, Supervision. |

Energy 230 (2021) 120825

Contents lists available at ScienceDirect

Energy

journal homepage: www.elsevier.com/locate/energy

# Thermohydraulic model of Smart Thermal Grids with bidirectional power flow between prosumers☆,☆☆

Thomas Licklederer*, Thomas Hamacher, Michael Kramer, Vedran S. Perić

*Technical University of Munich, Munich School of Engineering, Lichtenbergstrasse 4a, 85748, Garching near Munich, Germany*

ARTICLE INFO

*Article history:*
Received 30 November 2020
Received in revised form
29 March 2021
Accepted 28 April 2021
Available online 6 May 2021

*Keywords:*
Smart energy system
District heating network
Network analysis
Optimal control
Infrastructure concept
Variable speed pump

ABSTRACT

Part of Smart Energy Systems are Smart Thermal Grids, which enable bidirectional power flow between prosumers. To facilitate this feature, the network architecture and intelligent control of the decentralized actuators are a major challenge. Therefore, methods for the analysis of prosumer-dominated thermal networks are needed, including the hydraulic actuators and the heat transfer to the prosumers. This paper derives a holistic mathematical system representation that allows to investigate the relations between the control variables of such networks and their thermohydraulic steady-state. At first a suitable network architecture concept is introduced. Based on this, balance equations are combined with common physical models for the network components. Explicitly considered are the heat transfer to the secondary side, flexible prosumer modes and the behavior of decentralized control pumps and valves depending on their control inputs. The resulting system of equations is discussed in the context of two use cases: a) simulation of the system state for given control inputs and b) determining the necessary control inputs for target heat exchanges (optimal control). Exemplary simulation results are presented. For the simulation use case a Python code is provided on Github under open source license, based on the derived model.



## 1. Background

### 1.1. Introduction

A paradigm shift in the last years brought Smart Thermal Grids as integrated parts of Smart Energy Systems into focus [1,2]. This holistic perspective is accompanied by new requirements for thermal networks. They shall be more efficient, renewable, integrated, decentralized and flexible. In this context also the concept of prosumers became increasingly important. Prosumers are entities that can act as power consumer or producer to the superordinate energy system and over time switch between these modes. Inspired by the electricity sector, the possibility of bidirectional energy exchange also between thermal prosumers via suitable infrastructures became a desired feature. In thermal networks the bidirectional power flows go along with bidirectional volume flows, which conventional district heating and cooling systems do not feature. Distributed actuators are necessary, such as control pumps and valves. These distributed actuators mutually influence their operating points and define together the overall system state.

As an equivalent to Smart Electrical Grids, we propose thermal networks without central units, where (almost) all participants are prosumers (pro-sumer-dominated) and the bidirectional power flows are controlled by distributed actuators only. Typical application cases can be e.g. in dense and mixed urban and industrial areas, neighbourhoods or local ”energy communities”.

In order to draw generalizable conclusions on the behavior, operation and control of such systems, various different setups and scenarios must be studied. This includes e.g. varying numbers of prosumers, network sizes, topologies, but also the flexible switching of prosumers between modes and control inputs of pumps and valves. To the best of our knowledge no real systems matching our proposed concept are in operation yet. Experimental setups replicating whole neighborhoods are big, costly and inflexible. Therefore a model is needed that describes this type of networks and

☆ While conducting the research for this document, the first and the third author were in a position funded by the German Federal Ministry for Economic Affairs and Energy (BMWi) [FKZ: 03ET1413B].

☆☆ While supporting the research for this document, the fourth authorwas in a position funded by the Bavarian Government and the German Research Foundation (DFG) [project nr. 350746631].

* Corresponding author. (T. Licklederer).
*E-mail address:* thomas.licklederer@tum.de (T. Licklederer).

https://doi.org/10.1016/j.energy.2021.120825

**Nomenclature**

*Symbols*

| | |
|---|---|
| $a$ | hydraulic parameter |
| $b$ | thermal parameter |
| $c_p$ | specific heat capacity of fluid |
| $e$ | edge |
| $G', G$ | (un)directed graph as network representation |
| $\dot{m}$ | mass flow |
| $\Delta p$ | pressure difference |
| $P$ | Prosumer |
| $\dot{Q}$ | heat flow |
| $r$ | aggregated hydraulic resistance |
| $T, \Delta T$ | temperature, temperature difference |
| $u$ | control variable for pump speed |
| $\dot{V}$ | volume flow |
| $v, w$ | vertex, node |
| $y$ | aggregated offset for pressure difference |
| $\gamma$ | aux. variable for altern. operation of pump or valve |
| $\kappa$ | control variable for valve opening |
| $\mu$ | integer variable for prosumer mode |
| $\pi$ | integer variable for participation of prosumer |
| $\varrho$ | density of fluid |
| $\sigma$ | integer variable for sign/direction of volume flow |

*indices*

| | |
|---|---|
| $c$ | cold (level) |
| $h$ | hot (level) |
| $hc$ | interconnecting hot and cold level |
| $ij, k$ | iterators |
| $P$ | Prosumer |

*Sets*

| | |
|---|---|
| $\mathbb{E}$ | edges |
| $\mathbb{P}$ | Prosumers |
| $\mathbb{V}$ | vertices, nodes |

*Matrices and Vectros*

| | |
|---|---|
| $\mathbf{B}$ | incidence matrix |
| $\mathbf{C}$ | matrix for temperature differences |
| $\mathbf{E}$ | matrix representing thermal component models |
| $\mathbf{L}$ | matrix for ideal mixing in nodes |
| $\mathbf{M}$ | matrix for nodal energy balance |
| $\mathbf{O}$ | cycle basis matrix |
| $\mathbf{S}_{T,in}$ | matrix for secondary sides' inlet temperatures |
| $\mathbf{S}_{V}$ | matrix for secondary sides' volume flows |
| $\underline{R}$ | vector representing thermal component models |

*Sub-/Superscripts*

| | |
|---|---|
| $hx$ | heat exchanger |
| $hy$ | hydraulic |
| $pi$ | pipe |
| $prim$ | primary (side), network (side) |
| $pu$ | pump |
| $sec$ | secondary (side), prosumer (side) |
| $set$ | setpoint, desired or given value |
| $th$ | thermal |
| $trnsf$ | transferred between prim. and sec. side |
| $va$ | valve |

interlinks the energy management level (power flows), the technical level (temperatures, volumes flows, pressures) and the control level (control inputs, actuator behavior). The aim of this paper is to derive a suitable model fulfilling these criteria. The model has to be flexible to adjust with low effort for different setups and must explicitely incorporate the prosumer modes (producer or consumer), control signals and behavior of pumps and valves.

This paper suggestes an architecture concept and functional principle for prosumer-dominated Smart Thermal Grids. Based on this, a system of mathematical equations is derived that maps the control inputs to the thermohydraulic steady-state and thereby to power flows of the network. To do so, validated component models are combined with balance equations from network analysis. The inlet conditions on the prosumers' secondary sides are considered as boundary conditions. The emerging model can be applied for two use cases: a) simulation of the resulting system state and power flows for given control inputs and b) determining the necessary control inputs for target heat exchanges (optimal control). Both cases are discussed in this paper. A Python code using the derived model for simulation purposes is provided on Github[1] under open source license.

The rest of the paper is organized as follows: Section 1.2 discusses relevant literature and outlines the scope of this paper in distinction to it. In section 2 the network concept in combination with the suggested network architecture and functional principle is explained. After that, in section 3.1 the modeling assumptions and variables are introduced. In section 3.2 the used hydraulic and thermal component models are presented. In section 3.3 the governing hydraulic and thermal equation systems for the steady-state in the network are derived. Subsequently the derived equation system is discussed in section 4 in the context of the application for simulation and for optimal control. Section 5 presents a short simulation case study. In section 6 a conclusion on the contribution and findings completes the paper.

### 1.2. Literature review

Under terms like "Smart Thermal Grids" [1,3] and "5th Generation District Heating and Cooling" [4,5] the research on thermal energy systems wants to make use of synergies within and between sectors, integrate fluctuating renewable energy sources, include distributed and low temperature heat sources, combine heating and cooling in a single infrastructure, increase efficiency, add flexibility and provide services to the overarching energy system.

On the energy management level, the possibility of bidirectional energy exchange between prosumers often is axiomatically assumed. The energy hub approach and variations of it [6,7] take place only at the level of power flows (e.g. Ref. [8]). However, for the thermal sector it is mostly unconsidered and unclear how these calculated power setpoints can be implemented in terms of temperatures, volume flows and pressures by according control signals.

On the technical level, multiple substation configurations for the feed-in have been investigated [9–13] and the feed-in from return to supply line was found the most promising for a broad range of operation. Expanding this local focus, studies were done on the impact of decentral producers feeding into heat networks [14,15].

[1] https://github.com/thomaslicklederer/ProHeatNet_Sim.

However, most literature in this context assumes conventional, unidirectional thermal networks and sees the decentral feed-in only as support of central generation units.

For bidirectional networks, the main trends in literature are towards combined heating and cooling networks with (ultra) low temperature levels that exploit simultaneous heating and cooling demands by using distributed heat pumps and chillers in the substations [16–18]. The literature investigates and proves benefits of bidirectional thermal networks, like energy and cost savings by the usage of synergies. The control and thermohydraulic behavior of the thermal networks is not in the focus. In literature, control aspects are mostly discussed from the substation point of view [19,20] or connected with market-related principles [21], but not with a focus on the overall thermohydraulic network behavior.

To formulate equation systems describing the hydraulic and thermal behavior of district heating systems, combining graph theory and network analysis is a common approach, e.g. used in Refs. [22–24]. Building up on this mathematical formulation of the thermohydraulics, different frameworks are used for purposes like model calibration by measurements and genetic algorithms [25] or design optimization [26]. Literature with a more hydraulic focus considers additionally the behavior of decentral actuators, like variable speed pumps. Ref. [27] and [28] find that compared to conventional central hydraulic approaches, decentral pumps can save electricity in operation, but mutually influence each other. Therefore in Ref. [29] it is stated, that the simultaneous adjustment of the decentral actuators is necessary to avoid oscillations and water hammers. In Ref. [30] it is found, that in optimal system operation mode at least one substation edge always has its minimum pressure head (max. pump speed or valve opening). Although these existing approaches formulate the thermohydraulics in mathematical equation systems, they do not consider the mode switching of prosumers in their formulation, nore have models for decentral actuators or the influence of their control inputs on the thermohydraulics.

None of the reviewed approaches in literature formulate a model that is compatible with our proposed network concept under investigation and at the same time allows to study the relation between the energy management level, the thermohydraulics and the control level.

## 2. Network concept

We propose a type of thermal networks that differs from other approaches and is characterized mainly by the following points:

- no central generation units
- no central actuators (e.g. no network pumps), instead decentral actuators in substations
- only prosumers as participants (prosumer-dominated)
- prosumers can switch between producer and consumer mode flexibly
- featuring bidirectional power flows between the prosumers
- allowing meshed, radial and mixed topologies
- a specific substation design

In the following paragraphs, a basic architecture concept and functional principle for type of thermal networks is presented. All following explanations are given for the usage of the thermal grid as a heat network, but apply analogously for heating networks, cooling networks and even mixed operation.

A hot and a cold temperature level form subnetworks, which are connected by the prosumers with their substations (see Fig. 1). A prosumer can in principle operate in three modes: consumption, production, idle mode. For heating consumption of a prosumer the classic functional principle remains: water from the hot level flows through the substation, where heat is extracted and the water is injected to the cold level. For the feed-in, the return-to-supply principle is chosen. That means water from the cold network level flows trough the substation, heat input takes place and the water is injected into the hot level. For a prosumer in idle mode, there is no volume flow through its substation.

The described behavior for the consumption and production (feed-in) mode of a prosumer can be implemented with different hydraulic configurations for the substations. Fig. 1 shows a simple hydraulic scheme to implement prosumer behavior for a substation. This is in principle also used in the laboratory for Combined Smart Energy Systems (CoSES) at the Technical University of Munich [31]. In producer mode a variable speed pump is used to pump the water from the cold level to the hot level, while the control valve is completely closed. The resulting overpressure in the hot level forces hot water through the substation of neighboring prosumers in consumption mode. In consumption mode the pump in the substation is switched off and blocked (check-valve). For a prosumer in idle state its control valve is closed and the pump is blocked. The volume flows and pressure differences in the network are controlled by adjusting the opening of the control valves in the consumers and the speed of the variable speed pumps in producers. These volume flows directly influence the heat flows between the network and the prosumers, but also within the network. Additional influencing factors are the inlet temperatures and volume flows on the secondary sides (prosumer sides). In substations of heat networks, counter-current heat exchangers have proven to be effective. To keep up the counter-current flow, the flow direction on the secondary side of the heat exchanger has to be reversed as the flow direction on the network side (primary side) changes with the prosumer mode. For this, there are different hydraulic configurations that allow to implement the flow reverse through the secondary side of the heat exchanger.

It must be stressed that by the presented functional principle the direction of the volume flows in the interconnecting edges including the substations are predescribed by the prosumer modes. At the same time the flow directions within the subnetworks are not predescribed, but emerge from the operation of the pumps and valves. Another major difference to conventional heating networks is that temperatures can vary over time and even spatially. Further, conventional district heatings systems are usually radial networks with (at most) a few loops. This results from the unidirectional heat distribution between a central generation unit to the consumers. With the step towards flexibly changing prosumer modes, meshed topologies with few radial branches are more reasonable, as they can provide shorter distances between the prosumers and more flexibility for the emerging flow states and directions. Immanent to the described architecture concept is the fact, that in order to run a prosumer as producer or consumer, the hydraulic balance requires at least one other prosumer to run in the opposite mode or a hydraulic shortcut without prosumer is needed between the hot and the cold subnetworks. That means, the different substations and prosumers are hydraulically and thereby also thermally coupled and the manipulation of a control variable in a single substation influences the operation mode of the other substations and the whole network.

## 3. Modeling

### 3.1. Basics

It is assumed that the network is used as heating network. The usage as cooling network or for mixed operation can be investigated analogously. The fluid in the network is assumed to be

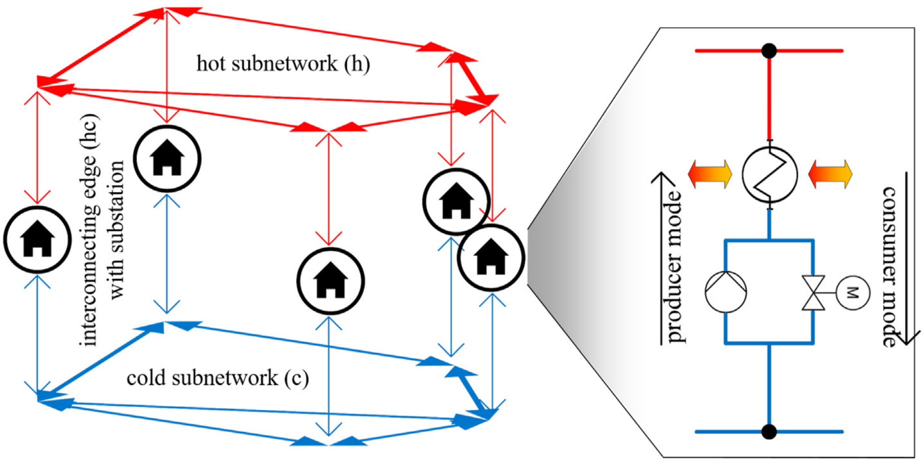


**Fig. 1.** Scheme of an exemplary bidirectional prosumer heat network with the substations connecting the hot and cold subnetworks.

incompressible liquid water with constant density $\varrho = const.$ and constant specific heat capacity $c_p = const.$ This assumption decouples the hydraulic investigations from those on temperatures in the network. The temperature of the soil surrounding the network pipes is assumed to be constant. It is reasonable to assume, that the hot and the cold subnetwork have the same topology. The inlet temperatures and volume flows to the secondary side of the substations' heat exchangers are assumed to be known (e.g. measured). The hydraulic and the thermal dynamic behavior of heat networks take place on different time scales. Hydraulic dynamics propagate with the speed of sound ($\approx 1480\frac{m}{s}$), while thermal dynamics propagate with the velocity of the volume flow ($\approx 1\frac{m}{s}$). Compared to this, the timescales used in the context of energy management in district heating networks are typically much bigger (15 min - 1 h) and the resulting power flow setpoints can be seen as stationary. Therefore dynamics are neglected and the investigations are restricted to steady-states.

For modelling, the network is represented by a directed mathematical graph $G$. $G$ consists of the ordered pair $(\mathbb{V}, \mathbb{E})$, compromising the set $\mathbb{V}$ of vertices $v_i$ (also called nodes) together with the set $\mathbb{E}$ of directed edges $e_j$. Volume flows against an edge direction are counted as negativ. The hot and cold subnetworks form subgraphs $G_h = (\mathbb{V}_h, \mathbb{E}_h)$ and $G_c = (\mathbb{V}_c, \mathbb{E}_c)$, where $\mathbb{V}_h, \mathbb{V}_c \subset \mathbb{V}$ and $\mathbb{E}_h, \mathbb{E}_c \subset \mathbb{E}$. The edges that connect these two subgraphs can be seen as a third subgraph $G_{hc} = (\mathbb{V}_{hc}, \mathbb{E}_{hc})$, where $\mathbb{V}_{hc} \subset \mathbb{V}$, $\mathbb{E}_{hc} \subset \mathbb{E}$ and $\mathbb{E}_{hc} \notin \{\mathbb{E}_h, \mathbb{E}_c\}$. With each prosumer $P \in \mathbb{P}$ exactly one edge $e_j \in \mathbb{E}_{hc}$ is associated. This edge includes the substation of the prosumer. By convention, the direction for edges $e \in \mathbb{E}_{hc}$ shall be defined positive from the hot to the cold subnetwork. The graph representation allows to use several metrics associated with the graph, such as its incidence matrix $\mathbf{B}$ or its cycle basis matrix $\mathbf{O}$.

The relevant physical quantities in the heat networks under investigation are temperatures, mass or volume flows and pressure differences as their driving force. Mass and volume flows are directly proportional by the (constant) density $\varrho$. With each network edge $e$ connecting the nodes $v$ and $w$ the following variables are associated: mass flow $\dot{m}_e$, volume flow $\dot{V}_e$, pressure difference $\Delta p_e$, two temperatures $T_{e,v}$ and $T_{e,w}$ and the transferred heat $\dot{Q}_e$. The temperatures $T_{e,v}$ and $T_{e,w}$ refer to the temperatures at the two ends of the edge. That means depending on the amount of edges that intersect at a certain node, there can be multiple temperatures at different sides of this node. This is relevant for the modeling of the mixing of flows with different temperatures in the nodes. Assuming the direction of edge $e$ from node $v$ to node $w$, the according temperature difference is denoted as

$$\Delta T_e = T_{e,w} - T_{e,v} \tag{1}$$

In an analog manner the sign of pressure difference $\Delta p_e$ is defined. Additionally, for the secondary side of the prosumer substations, there are two temperatures $T_{P,h}$, $T_{P,c}$, the according temperature difference $\Delta T_P$, one volume flow $\dot{V}_P$ and the transferred heat $\dot{Q}_P$ associated with each prosumer $P \in \mathbb{P}$. $\Delta T_P$ is defined as

$$\Delta T_P = T_{P,h} - T_{P,c} \tag{2}$$

The volume flow at the secondary side is defined positive from $T_{P,h}$ to $T_{P,c}$. Accordingly the transferred heat $\dot{Q}_P$ is positive for the prosumer in production mode.

$$\dot{Q}_P = \varrho \cdot \dot{V}_P \cdot c_p \cdot \Delta T_P \tag{3}$$

The variables can be grouped into vectors $\underline{\dot{V}}$, $\underline{\Delta p}$, $\underline{T}$, $\underline{\Delta T}$, $\underline{\dot{Q}}$. The variables for the secondary sides are included and appended at the end of the vectors (apart from pressure differences).

### 3.2. Component models

Relevant components to be modelled are variable speed pumps, control valves, pipes and heat exchangers.

***Hydraulic component models***

The hydraulic component models describe the relation between the volume flow trough and the pressure head over a component, including the influence of control variables (if applicable). The general relation between volume flow and pressure head is quadratic.

***Variable speed pumps***

The considered type of pumps are centrifugal circulator pumps with variable speed drives. The controlled parameter is the speed $n^{pu}$, expressed by the unified control variable $u^{pu}$. From the hydraulic affinity laws [32], the following model equations can be derived:

$$u^{pu} = \frac{n^{pu}}{n^{pu}_{nom}} \tag{4}$$

$$\Delta p^{pu} = a^{pu}_1 \cdot \left(\dot{V}^{pu}\right)^2 + a^{pu}_2 \cdot (u^{pu})^2 \tag{5}$$

By knowing at least two representative operating points in terms of the variables $u^{pu}_{ref}$, $\Delta p^{pu}_{ref}$, $\dot{V}^{pu}_{ref}$, the parameters $a^{pu}_1$ and $a^{pu}_2$ can be calculated (see Appendix A.1).

***Control valves***

The considered type of control valves consists of two parts: The actual valve and the valve drive. The drive is typically addressed by a control signal, that is transformed and controls the stroke of the valve. The stroke influences the volume flow $\dot{V}^{va}$ through the valve and the pressure head $\Delta p^{va}$ at the same time. This is expressed by the flow factor $K_v$ (see equation (6)) [33]. As the relation between the control signal and the flow factor strongly depends on the used configuration of the valve drive, the flow factor ratio $\kappa^{va}$ is used to describe the operation status of the control valves. $\kappa^{va}$ describes the ratio between the current flow factor $K_v$ and the nominal flow factor $K_{vs}$ at nominal valve stroke. Neglecting leakage flows leads to equation (7) as model equation.

$$K_v = \dot{V}^{va} \cdot \sqrt{\frac{-10^3 hPa}{\Delta p} \cdot \frac{\varrho}{1000 \frac{kg}{m^3}}} \tag{6}$$

$$\Delta p^{va} = a^{va}_1 \cdot (\kappa^{va})^{-2} \cdot \left(\dot{V}^{va}\right)^2 \tag{7}$$

$$\kappa^{va} = \frac{K_v}{K_{vs}} \tag{8}$$

$$a^{va}_1 = -10^3 hPa \cdot \frac{\varrho}{1000 \frac{kg}{m^3}} \cdot \frac{1}{K^2_{vs}} \tag{9}$$

***Pipes***

The Darcy-Weisbach equation is a widely-used empiric equation, that gives a relation between the pressure loss along a pipe due to friction and the volume flow through this pipe [34,35]. The involved Darcy-Weisbach friction factor $f_D$ can be calculated by implicit semi-empirical equations, such as the Colebrook-White equation [36] or explicit approximations of them [37] (see also Appendix A.2). The friction factor depends on the flow velocity and profile, therefore it is dependent on the volume flow trough the pipe. Since the volume flow through a particular pipe in the network is not known in advance, $f_D$ is calculated for a nominal volume flow and assumed to be constant in order to avoid the need for iterative calculations. This can lead to small inaccurancies. For installations in pipes, such as junctions, bends, etc., empirically derived pressure loss coefficients $\zeta^{inst}_i$ can be used. Elevation differences between the two ends of a pipe do not have an effect in a closed system. This leads to a simple model equation for pipes, where the parameter $a^{pi}_1$ summarizes the factors from the above equations:

$$\Delta p^{pi} = a^{pi}_1 \cdot \left(\dot{V}^{pi}\right)^2 \tag{10}$$

For a pipe with circular cross-section of inner diameter $d^{pi}$ and length $L^{pi}$, the parameter $a^{pi}_1$ can be calculated in accordance with Darcy-Weisbach as follows:

$$a^{pi}_1 = -\frac{8}{\pi^2} \cdot \varrho \cdot \frac{1}{\left(d^{pi}\right)^4} \cdot \left[\frac{L^{pi}}{d^{pi}} \cdot f_D + \sum_i \zeta^{inst}_i\right] \tag{11}$$

***Heat exchanger***

The hydraulics of heat exchangers is modelled by a quadratic regression to the nominal point. For the nominal volume flow rate $\dot{V}^{hx}_{nom}$ the according nominal pressure loss $\Delta p^{hx}_{nom}$ is usually given in the technical specifications. With these values a proportionality constant can be calculated and the modelling equation results:

$$\Delta p^{hx} = a^{hx}_1 \cdot \left(\dot{V}^{hx}\right)^2 \tag{12}$$

$$a^{hx}_1 = -\frac{\left|\Delta p^{hx}_{nom}\right|}{\left(\dot{V}^{hx}_{nom}\right)^2} \tag{13}$$

***Thermal component models***

The thermal component models describe the relation between the volume or mass flows and the temperature differences. Relevant thermal phenomena to model are heat losses in pipes, heat transfer by the heat exchangers in the substations and mixing of volume flows with different temperatures in nodes. Mixing has to be taken into account during the network analysis.

***Pipes***

Heat losses in pipes occur across the overall thermal resistance per unit length $R^{pi}$ separating the temperature difference between the fluid flowing trough the pipe and the soil surrounding the pipe. It is a common assumption for the temperature $T^{soil}$ of the surrounding soil and the overall thermal resistance $R^{pi}$ to be constant. In reality the overall thermal resistance $R^{pi}$ is highly depending on the volume flow. With the presented assumptions the underlying stationary differential equation for the temperature distribution along the longitudinal pipe coordinate $x$ is in accordance with Ref. [38]:

$$C^{pi} \cdot \frac{dT^{pi}}{dt} = -\frac{1}{R^{pi}} \cdot \left(T^{pi} - T^{soil}\right) \tag{14}$$

$C^{pi}$ is the heat capacity of the water per unit length. The infinitesimal time $dt$ can be substituted by an infinitisimal length $dx$ using the flow velocity expressed by the volume flow and the pipe geometry.

$$C^{pi} = \frac{\pi}{4} \cdot \varrho^{wat} \cdot c_p \cdot \left(d^{pi}\right)^2 \tag{15}$$

$$dt = \frac{\pi}{4} \cdot \frac{\left(d^{pi}\right)^2}{\dot{V}^{pi}} \cdot dx \tag{16}$$

with the inlet temperature $T^{pi}_{in}$ at $x = 0$ and the outlet temperature $T^{pi}_{out}$ at $x = L^{pi}$, the differential equation can be solved and reformulated to

$$\begin{pmatrix} b^{pi}_1 & b^{pi}_2 \end{pmatrix} \begin{pmatrix} T^{pi}_{in} \\ T^{pi}_{out} \end{pmatrix} = b^{pi}_3 \tag{17}$$

$$b^{pi}_1 = e^{\left(s^{pi}\right)} \tag{18}$$

$$b^{pi}_2 = -1 \tag{19}$$

$$b^{pi}_3 = \left(e^{\left(s^{pi}\right)} - 1\right) \cdot T^{soil} \tag{20}$$

The quantity $s^{pi}$ depends on the volume flow, the geometry of the pipe and the thermal resistance per unit length $R^{pi}$.

$$s^{pi} = -\frac{L^{pi}}{\varrho^{wat} \cdot c_p \cdot R^{pi} \cdot \dot{V}^{pi}} \tag{21}$$

The thermal resistance per unit length can either be calculated with the geometry and material properties of the pipe and its insulation or can directly be obtained from technical specification sheets.

***Heat exchanger***

Plate heat exchangers operating with counter current flow are the most common configuration for substations in heat networks. The mathematical model is based on the equations for ideal pure counter current flow, as they can be found in the VDI Heat Atlas [39]. The heat transfer surface $A^{hx}$ and the overall heat transfer coefficient $k^{hx}$ are assumed to be constant at the value of the design state. This a common simplification. Nevertheless it leads to inaccurancies, as the overall heat transfer coefficient in reality is highly depending on the volume flow. To be able to derive a reduced set of equations that combines the producer and the consumer mode, a different notation is chosen (see Fig. 2). Index "1" represents the heat source side, index "2" the heat sink side. Quantities with one dash are associated with inflowing streams, double-dashed quantities are outflowing from the heat exchanger. The specific heat capacities $c_{p,1}$ and $c_{p,2}$ are assumed to be equal at both sides. In general the following holds

$$T_1{'} > T_1{''} > T_2{''} > T_2{'} \tag{22}$$

Depending on the operating mode of a prosumer, either the network side or the prosumer side are the heat source (see Table 1).

With the assumptions, that $\varrho_1 = \varrho_2 = const.$, $c_{p,1} = c_{p,2} = const.$, abbreviation variables can be defined:

$$\dot{W}_i = \varrho_i \cdot \dot{V}_i \cdot c_{p,i} \text{ for } i = 1, 2 \tag{23}$$

$$R_1 := \frac{\dot{W}_1}{\dot{W}_2} = \frac{\dot{V}_1}{\dot{V}_2} \tag{24}$$

$$R_2 := \frac{\dot{W}_2}{\dot{W}_1} = \frac{1}{R_1} = \frac{\dot{V}_2}{\dot{V}_1} \tag{25}$$

$$NTU_i = \frac{k^{hx} \cdot A^{hx}}{\dot{W}_i} \text{ for } i = 1, 2 \tag{26}$$

Then according to the formulas for ideal pure counter current flow, the following holds:

$$(1 - X_1) \cdot T_1{'} - T_1{''} + X_1 \cdot T_2{'} = 0 \tag{27}$$

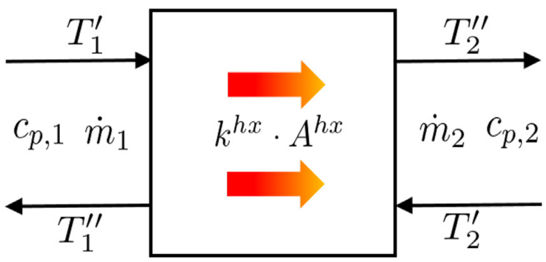


**Fig. 2.** Scheme with nomenclature for the heat exchanger model.

**Table 1**
Assignment of heat exchanger notation to the different modes of prosumers.

| | consumer mode | producer mode |
|---|---|---|
| $T_1{'}$ | network hot | prosumer hot |
| $T_1{''}$ | network cold | prosumer cold |
| $T_2{'}$ | prosumer cold | network cold |
| $T_2{''}$ | prosumer hot | network hot |

$$-X_2 \cdot T_1{'} + (X_2 - 1) \cdot T_2{'} + T_2{''} = 0 \tag{28}$$

$$X_i = \begin{cases} \dfrac{1 - exp[(R_i - 1) \cdot NTU_i]}{1 - R_i \cdot exp[(R_i - 1) \cdot NTU_i]} & , R_i \neq 1 \\ \dfrac{NTU_i}{1 + NTU_i} & , R_i = 1 \end{cases} \tag{29}$$

These relations between the temperatures can be brought into the following form:

$$\begin{pmatrix} b_{11}^{hx} & b_{12}^{hx} & b_{13}^{hx} & 0 \\ b_{21}^{hx} & 0 & b_{23}^{hx} & b_{24}^{hx} \end{pmatrix} \begin{pmatrix} T_1{'} \\ T_1{''} \\ T_2{'} \\ T_2{''} \end{pmatrix} = \begin{pmatrix} 0 \\ 0 \end{pmatrix} \tag{30}$$

Each of the parameters is highly nonlinear in the volume flows of both heat exchanger sides. This arises from the nonlinearity of the logarithmic mean temperature difference (LMTD). On top of that, there is a definition gap in the formulas of the parameters for $R_1 = R_2 = 1$, which can be closed with a different set of equations for this specific case. So, a case distinction is necessary (see equation (29)).

### 3.3. System model

***Hydraulic system model***

To mathematically describe the hydraulic steady-state in a bidirectional heat network that is built according to the concept proposed in section 2, a network analysis similar to electric circuit analysis can be used. Taking into account the presented models, together with additional variables representing the prosumer modes, this leads to the set of equations built by equation 31–49. In the following these equations will be explained and derived step-by-step.

Kirchhoff's circuit laws are the basis for the network analysis. The junction rule in this case refers to the volume flows and equals the volume balance and mass conservation for the closed system. Using the incidence matrix of the network graph, equation (31) describes Kirchhoff's junction rule. The mesh rule refers to the pressure differences along a cycle of the network. Making use of cycle basis matrix **O**, Kirchhoff's mesh rule applied to the heat network can be expressed as seen in equation (32). Equation (31) and equation (32) are coupled by the relations between the volume flows and the pressure differences that are expressed in the hydraulic component models. All hydraulic component model equations are axisymmetric to $\Delta p_e = 0$ and thereby insensitive to the sign of the volume flow. For equation (32) to hold, it's important, that the pressure difference over a certain edge is sensitive to the sign of the volume flow. That means the relation has to be axisymmetric to $\Delta p_e = -\dot{V}_e$. Therefore the integer variable $\sigma_e$ is introduced for each edge (see equation (47)). As expressed by equation (39), $\sigma_e$ is positive for volume flows along the edge direction and negative for volume flows in opposite direction. For each edge, the relation between $\Delta p_e$ and $\dot{V}_e$ can be broken down to a quadratic equation with the parameters $r^{hy}$ and $y^{hy}$. In order to make the relations axisymmetric to $\Delta p_e = -\dot{V}_e$, $\sigma_e$ is added as a factor (see equation (33)). For the calculation of the parameters in equation (33), the parameters of the component equations are used. $r^{hy}$ and $y^{hy}$ depend on the components that are included and active along the specific edge. Here two cases can be distinguished: While in the hot and the cold subnetworks only the pipes play a role, in the edges that are connecting the two subnetworks also the heat exchanger, the pump and the valve have to be taken into account. In producer mode the valve is inactive and the pump is active, while in consumer mode it's vice versa. Another integer variable $\mu_P$ for each prosumer $P \in \mathbb{P}$ is needed to cover this (see Table 2 and equations (36), (37) and (48)). As the edge direction for the interconnecting edges $e \in \mathbb{E}_{hc}$ is predefined by convention from the hot to the cold network, the correct volume flow direction (sign) determined by the prosumer state must be ensured. This is done by equation (38). Further, the idle state of a prosumer has to be covered. Here another integer variable $\pi_P$ per prosumer is used: For a participating prosumer it's 1, otherwise 0 (see equation (49)). In case a prosumer does not participate, the volume flow through its interconnecting edge (substation) has to be fixed to 0, which is done by the equations (40) and (41). In fact the equations (40) and (41) convert the volume flow through the interconnecting edges to a limited mixed-integer variable using the introduced integer variables $\sigma_e$, $\mu_P$ and $\pi_P$. The equations (34) and (35) describe how the parameters for equation (33) are calculated. The equations (34) and (35) result from the hydraulic component models. Again it has to be destinguished between edges in the hot and cold subnetworks and interconnecting edges $e \in \mathbb{E}_{hc}$. All together the decision variables are $\dot{V}_e$, $\Delta p_e$ and $\sigma_e$ for each edge $e \in \mathbb{E}$ and $\pi_P$, $\mu_P$, $\kappa_P^{va}$, $u_P^{pu}$ for each prosumer $P \in \mathbb{P}$ in the network.

$$\mathbf{B}\underline{\dot{V}} = 0 \tag{31}$$

$$\mathbf{O}\underline{\Delta p} = 0 \tag{32}$$

$$\Delta p_e = \sigma_e \cdot \left[ r_e^{hy} \cdot \left(\dot{V}_e\right)^2 + y_e^{hy} \right] \forall e \in \mathbb{E} \tag{33}$$

$$r_e^{hy} = \begin{cases} a_1^{pi,e} & \forall e \in \{\mathbb{E}_h, \mathbb{E}_c\} \\ a_1^{pi,e} + a_1^{hx,e} + & \\ +\gamma^{pu} \cdot a_1^{pu,e} + & \\ +\gamma^{va} \cdot a_1^{va,e} \cdot \left(\kappa_P^{va}\right)^{-2} & \forall e \in \mathbb{E}_{hc}, P \in \mathbb{P} \end{cases} \tag{34}$$

$$y_e^{hy} = \begin{cases} 0 & \forall e \in \{\mathbb{E}_h, \mathbb{E}_c\} \\ \gamma^{pu} \cdot a_2^{pu,e} \cdot \left(u_P^{pu,e}\right)^2 & \forall e \in \mathbb{E}_{hc}, P \in \mathbb{P} \end{cases} \tag{35}$$

**Table 2**
Mathematical modelling of alternating operation of pump and valve depending on prosumer mode.

| | valve ($\gamma^{va}$) | pump ($\gamma^{pu}$) |
|---|---|---|
| consumption, $\mu_P = -1$ | 1 | 0 |
| production, $\mu_P = +1$ | 0 | 1 |
| | $0.5 \cdot (1 - \mu_P)$ | $0.5 \cdot (1 + \mu_P)$ |

$$\gamma^{pu} = 0.5 \cdot (1 + \mu_P) \tag{36}$$

$$\gamma^{va} = 0.5 \cdot (1 - \mu_P) \tag{37}$$

$$\sigma_e \cdot \mu_P \le 0 \, \forall e \in \mathbb{E}_{hc}, P \in \mathbb{P} \tag{38}$$

$$-\sigma_e \cdot \dot{V}_e \le 0 \, \forall e \in \mathbb{E} \tag{39}$$

$$-\sigma_e \cdot \dot{V}_e - (1 - \pi_P) \cdot \dot{V}_{e,min} \le -\dot{V}_{e,min} \, \forall e \in \mathbb{E}_{hc}, P \in \mathbb{P} \tag{40}$$

$$\sigma_e \cdot \dot{V}_e + (1 - \pi_P) \cdot \dot{V}_{e,max} \le \dot{V}_{e,max} \, \forall e \in \mathbb{E}_{hc}, P \in \mathbb{P} \tag{41}$$

$$\Delta p_{e,min} \le \Delta p_e \le \Delta p_{e,max} \, \forall e \in \mathbb{E} \tag{42}$$

$$u_{P,min}^{pu} \le u_P^{pu} \le u_{P,max}^{pu} \, \forall P \in \mathbb{P} \tag{43}$$

$$\kappa_{P,min}^{va} \le \kappa_P^{va} \le \kappa_{P,max}^{va} \, \forall P \in \mathbb{P} \tag{44}$$

$$0 \le \dot{V}_{e,min} \, \forall e \in \mathbb{E}_{hc} \tag{45}$$

$$0 \le \dot{V}_{e,max} \, \forall e \in \mathbb{E}_{hc} \tag{46}$$

$$\sigma_e \in \{-1, 1\} \, \forall e \in \mathbb{E} \tag{47}$$

$$\mu_P \in \{-1, 1\} \, \forall P \in \mathbb{P} \tag{48}$$

$$\pi_P \in \{0, 1\} \, \forall P \in \mathbb{P} \tag{49}$$

***Thermal system model***

The first effect to be considered in the thermal network analysis is mixing in nodes. Ideal mixing is assumed. For each node the energy balance holds. Under consideration of constant densities and specific heat capacities:

$$\sum_i \left( \left| \dot{V}_{in,i} \right| \cdot T_{in,i} \right) = \sum_j \left( \left| \dot{V}_{out,j} \right| \cdot T_{out,j} \right) \tag{50}$$

It is necessary to determine which volume flows enter a node and which ones leave the node. For this two factors must be considered: a) direction of the edge - is the considered node at the head or at the tail of an edge, b) sign of the volume flow - is the streaming direction along or against the edge direction. For a), the incidence matrix **B** of the graph is helpful. Considering node $v$ and edge $e$, the matrix entry $B_{ve}$ of **B** tells if $e$ enters $(+1)$ or leaves $(-1)$ node $v$. For b), the sign of the volume flows is directly included in their values. So, a matrix **M** can be built, where each row of **M** represents a node in the graph. For each edge connected to this node, the nonzero column-entries of **M** give the volume flow including its true sign with respect to the node ($+$ for inflowing, - for outflowing). The entries of **M** can be calculated as:

$$M_{v,j} = B_{ve} \cdot \dot{V}_e \cdot \varrho \, \forall v \in \mathbb{V}, T_{v,e} \in \underline{T} = (T)_j \tag{51}$$

For the nodal energy balance, the temperatures of the flows must be considered. For each edge $e$, there are two temperatures $T_{v,e}$ and $T_{w,e}$ associated with the two nodes $v$ and $w$ that border the edge. By indexing these temperatures, a vector representation $\underline{T} = (T)_j$ is possible. By using **M** and $\underline{T}$, the abstract nodal energy balance (see equation (50)) can be formulated as in equation (53).

Ideal mixing is assumed, so all outflowing volume fluxes of a node must have the same temperature.

$$T_{out,j} = T_{out,k} \forall j,k \tag{52}$$

This is only relevant for nodes with multiple (more than one) truely outflowing volume flows. So for each row of $\mathbf{M}$ with $l > 1$ non-zero elements, a set of $l-1$ equations can be formulated, which states that all temperatures belonging to the nonzero elements in this row of $\mathbf{M}$ are equal. These equation sets for all nodes can be formulated in matrix form depending on the vector $\underline{T}$ with matrix $\mathbf{L}$. Then the ideal mixing is represented by equation (54) together with equation (53).

For edges within the subnetworks $e \in \{\mathbb{E}_h, \mathbb{E}_c\}$ heat losses in the pipes towards the environment can be considered as formulated in equation (17). For the edges including the substations and interconnection the subnetworks, heat losses in the pipes can be neglected compared to the active heat transfer by the heat exchangers. The heat transfer by the heat exchangers can be considered as formulated in equation (30). A matrix $\mathbf{E}$ and a vector $\underline{R}$ can be formed that summarize the matrix formulations of the component models for the pipes and heat exchangers (see equation (17)). Together with the temperature vector $\underline{T}$ this leads to equation (55). To describe the relation between the temperature differences and the temperature values at the two ends of each edge, a matrix $\mathbf{C}$ is used. By using $\mathbf{C}$, equation (1) is incorporated in matrix form for all $\Delta T$ (see equation (56)).

As a boundary condition, the inlet temperatures and the mass flow on the secondary side of the heat exchangers must be set. Depending on the operation mode of the specific prosumer, either $T_{P,h}$ or $T_{P,c}$ can be the inlet temperature at a prosumers secondary side. A matrix $\mathbf{S}_{T,in}$ can be formed to choose only the secondary sides' inlet temperatures from $\underline{T}$ and assign them pre-set values in form of the vector $\underline{T}_{sec,in}$ (see equation (57)). In the same manner the secodary sides' volume flows are set with a matrix $\mathbf{S}_V$ and the vector $\underline{\dot{V}}_{sec}$ (see equation (58)). The mass flows in the network are known from the hydraulic model, while the inlet temperatures and mass flows of the secondary sides emerge from the heating system and can be measured. The resulting outlet temperatures $\underline{T}_{sec,out}$ of the secondary sides are also included in $\underline{T}$. Finally, the heat transferred by the heat exchangers in the substations and the heat losses to the environment can be calculated (see equations (59) and (60)). All together, the decision variables are $T_{e,v}, T_{e,w}$ and $\dot{Q}_e$ for each edge $e \in \mathbb{E}$ with adjacent nodes $v,w \in \mathbb{V}$, while the network volume flows $\dot{V}_e$ and the conditions on the secondary sides must be given by $\underline{T}_{sec,in}$ and $\underline{\dot{V}}_{sec}$.

$$\mathbf{M}\underline{T} = 0 \tag{53}$$

$$\mathbf{L}\underline{T} = 0 \tag{54}$$

$$\mathbf{E}\underline{T} = \underline{R} \tag{55}$$

$$\mathbf{C}\underline{T} = \underline{\Delta T} \tag{56}$$

$$\mathbf{S}_{T,in}\underline{T} = \underline{T}_{sec,in} \tag{57}$$

$$\mathbf{S}_V\underline{\dot{V}} = \underline{\dot{V}}_{sec} \tag{58}$$

$$\dot{Q}_{P,trnsf} = \varrho \cdot \dot{V}_e \cdot c_p \cdot \Delta T_e \quad \forall e \in \mathbb{E}_{hc}, P \in \mathbb{P} \tag{59}$$

$$\dot{Q}_{e,loss} = \varrho \cdot \dot{V}_e \cdot c_p \cdot \Delta T_e \quad \forall e \in \{\mathbb{E}_h, \mathbb{E}_c\} \tag{60}$$

## 4. Discussion

The hydraulic and the thermodynamic equation systems ((53)–(60) and (31)–(49)) together with the presented component models form a set of governing equations for bidirectional prosumer heat networks. It represents the relations between the prosumer modes $(\pi_P, \mu_P)$, the control variables of actuators $(\kappa_P^{va}, u_P^{pu})$, inlet temperatures and volume flows at the secondary prosumer sides $\left(\underline{T}_{sec,in}, \underline{\dot{V}}_{sec}\right)$, the thermohydraulic steady-state of the network $(\dot{V}_e, \Delta p_e, T_{e,v})$ and the outlet temperatures and heat flows $\left(\underline{T}_{sec,out}, \dot{Q}_{P,trnsf}, \dot{Q}_{e,loss}\right)$.Two application cases for this equation system shall be distinguished: a) simulation, b) control. For both use cases first of all the setup has to be specified in order to build the modelling equations. A setup consists of configuration and parametrization. The configuration specifices e.g. the number of prosumers and the topology of the subnetworks. The parametrization specifies the properties of the devices. By a scenario the specification of certain flexible parameters is meant, such as the modes of the prosumers and the secondary sides inlet conditions. The simulation use case and the control use case are kind of inverted application cases. This is illustrated in Fig. 3. The inputs and outputs for these two cases are named in Table 3 and explained more detailed in the individual subsections for the use cases.

### 4.1. Simulation use case

The aim of the simulation use case is to simulate the emerging thermohydraulic system state including the heat flows to the prosumers for a given scenario and given specific control inputs for the decentral actuators. Therefore $\kappa_P^{va}, u_P^{pu}$ are specified as an input (see Table 3). The thermohydraulic network state and the prosumer outlet temperatures and heat flows are outputs.

In the simulation case, the hydraulic and the thermodynamic equation systems can be solved separately in sequence: Solving the hydraulic equations leads to the volume flows in the network, which then determine the thermal state according to the thermodynamic equation system (see Fig. 4). There may not be a unique solution for the hydraulic equation system. The reason for that is, that especially in highly meshed grids, multiple combinations of volume flow directions in the subnetworks could fullfill the steady-state equations. By adding a suitable objective function, the equation system becomes an optimization problem with either a unique

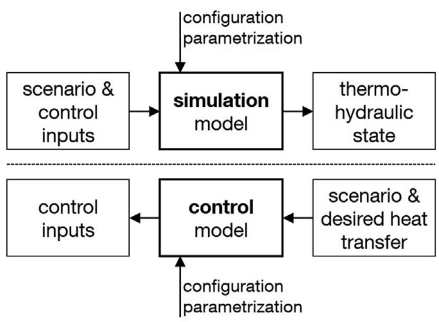


**Fig. 3.** Illustration of application cases a) simulation (top) and b) control (bottom).

**Table 3**
Inputs and outputs for application cases "simulation" and "control" of the derived equation system.

| | inputs | outputs |
|---|---|---|
| simulation | $\pi_P$, $\mu_P$, <br> $\underline{T}_{sec,in}$, $\underline{\dot{V}}_{sec}$, <br> $\kappa_P^{va}$, $u_P^{pu}$, <br> $\dot{V}_{e,min}$, $\dot{V}_{e,max}$ | $\dot{V}_e$, $\Delta p_e$, $T_{e,\nu}$, $\sigma_e$ <br> $\underline{T}_{sec,out}$, <br> $\dot{Q}_{P,trnsf}$, $\dot{Q}_{e,loss}$ |
| control | $\pi_P$, $\mu_P$, <br> $\dot{Q}_{P,trnsf,set}$, <br> $\underline{T}_{sec,in}$, $\left(\underline{\dot{V}}_{sec}\right)$, <br> $\dot{V}_{e,min}$, $\dot{V}_{e,max}$, <br> $\underline{T}_{sec,out,min}$, <br> $\underline{T}_{sec,out,max}$ | $\kappa_P^{va}$, $u_P^{pu}$, <br> $\dot{V}_e$, $\Delta p_e$, $T_{e,\nu}$, $\sigma_e$, <br> $\underline{T}_{sec,out}$, $\left(\underline{\dot{V}}_{sec}\right)$ <br> $\dot{Q}_{e,loss}$, $\dot{Q}_{P,trnsf}$ |

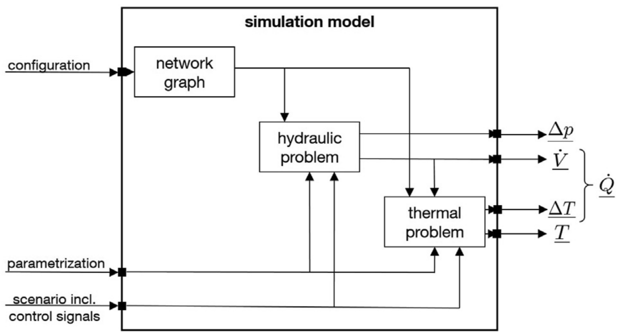


**Fig. 4.** Solving scheme of the governing equation systems for the simulation case.

or no solution. As water is taking the path of lowest resistance, it's assumed that in real systems the solution with minimal pressure heads will emerge as a system state. An according objective function creates a quadratic optimization problem:

$$\min_{\Delta p_e} \sum_e (\Delta p_e)^2 \tag{61}$$

While the signs $\sigma_e$ of the volume flows $\dot{V}_e$ are fixed by the prosumer modes $\mu_e$ for the edges $e \in \mathbb{E}_{hc}$ that connect the two subnetworks (see equation (38)), the signs of the volume flows along the edges $e \in \{\mathbb{E}_h, \mathbb{E}_c\}$ within the subnetworks are free variables of the optimization. Therefore the multiplication of $\sigma_e$ and $(\dot{V}_e)^2$ makes equation (33) a mixed-integer cubic constraint and the limiting factor for solving the hydraulic problem. However, a way to relax this is the reduction to a quadratically constrained problem by branching for different combinations of $\sigma_e$. As $\sigma_e$ is unspecified for the subnetwork edges, several optimization problems for all combinations of flow directions have to be solved (if feasible) for $\dot{V}_e$ and $\Delta p_e$. The one with the best objective function is the final solution. Making use of the symmetry between the hot and cold subnetwork, for a network with $E$ edges per subnetwork, there are $2^E$ combinations and the same amount of optimization problems to be solved. This is quite inefficient. Here further research is necessary. The optimizer Gurobi 9.0 is able to handle non-convex mixed-integer quadratically constrained problems (MIQCP) by applying the McCormick relaxation [40,41].

The thermal equation system is linear in the temperatures. For known volume flows given by the hydraulic calculations also all matrices of the thermal problem can be calculated. So the thermal problem can be solved quite easily for the simulation case.

The exponentially growing complexity of solving the equation set for the simulation case arises from the undetermined flow directions in the pipes of the subnetworks. Exactly this undirected flow distinguishes the presented thermal network concept from conventional district heating systems.

### 4.2. Control use case

The aim of the control use case is to determine the necessary control inputs for a desired system state in terms of heat transfer to/from the individual prosumers. This is the intersection point of this paper with optimization approaches and investigations on smart energy systems, sector coupling, demand side management, flexibility services etc. Either the derived model can be directly integrated into the optimization approaches or for example a superordinate energy management application determines the perfect heat exchange between the prosumers in the network in terms of target heat flows that each prosumer has to feed into the network or withdraw from it. So, additional to the scenario, target heat flows ($\dot{Q}_{P,trnsf,set}$) of each prosumer are inputs together with constraints for the secondary sides' outlet temperatures (see Table 3). Outputs in this application case are the necessary control variables for the pumps and valves, the emerging thermohydraulic network state and the secondary side outlet conditions that result.

A reasonable objective function for the control use case is:

$$\min_{\dot{Q}_{P,trnsf}} \sum_P \left( \dot{Q}_{P,trnsf} - \dot{Q}_{P,trnsf,set} \right)^2 \tag{62}$$

At the same time the inlet temperatures $\underline{T}_{sec,in}$ are assumed to be determined by the prosumers' internal heating systems and can be measured. The secondary sides volume flows $\underline{\dot{V}}_{sec}$ can either be assumed to be also determined by the prosumer or to be free variables of the optimization, if they can be controlled. For the outlet temperatures at the secondary sides some constraints are given and have to be satisfied. E.g. the different heating technologies such as radiators are designed for specific (minimal) supply temperatures. This can be formulated as additional equations.

$$\mathbf{S}_{T,out}\underline{T} \le \underline{T}_{sec,out,max} \tag{63}$$

$$-\mathbf{S}_{T,out}\underline{T} \le -\underline{T}_{sec,out,min} \tag{64}$$

Of course also the derived hydraulic and thermal equations (31)–(49) and (53)–(60) have to be fulfilled as constraints.

For the control use case, the hydraulic and the thermal equation systems can not be solved subsequently. Instead, the equations (31)–(49), (53)–(60) and (63)-(64) together form the constraints for a joint optimization problem with the objective function in equation (62). In difference to the simulation case, the control variables ($\kappa_P^{va}, u_P^{pu}$) as well as the hydraulic variables ($\dot{V}_e, \Delta p_e, \sigma_e$) are free variables of the optimization. This means that the hydraulic system status is not determined and the volume flow including its sign is free to vary also within the thermal equations. This leads to the problem, that the matrices $\mathbf{M}$ and $\mathbf{L}$ representing the thermal mixing as well as the matrices and vectors $\mathbf{S}_{T,in}$, $\mathbf{S}_{T,out}$, $\underline{T}_{sec,in}$, $\underline{T}_{sec,out,max}$, $\underline{T}_{sec,out,min}$ become ambiguous. The entries (and for $\mathbf{L}$ even the dimension) of these arrays depend on the values and the signs of the volume flows (see section 3.3). Also the parameters of the heat exchangers and the pipes that are represented in matrix $\mathbf{E}$ depend on the volume flows (see equations (17)–(21) and (24))-(30)). The volume flows are free to vary within the optimization. So the matrices would have to be created dynamically for each evaluated set of $\left(\underline{\dot{V}}, \underline{\sigma}\right)$. This means high computational effort, the application of heuristics and no guarantee to find (if feasible at all) the optimal solution of the problem. So further investigations on the relaxation and simplification of the problem formulation have to be done.

### 4.3. Limitations

In section 4.1 and section 4.2 the suitability of the derived model for the simulation and control use cases was already discussed from a mathematical and technical feasibility point of view. In this subsection some remarks are made on limitations concerning the model quality and its predictive power.

Limitations in this context are mainly set by the modeling assumptions, that can be found in section 3.1 of the paper. The most relevant is that it's a steady-state model and therefore dynamics are not described. Dynamics of the system can not be investigated. This is argued also in the assumptions section by the fact, that the power flow setpoints coming from district energy management systems can be seen as stationary in relation to the thermohydraulic timescales.

Further, in the component models several parameters that in reality depend on the volume flow through a component are assumed to be constant and calculated by using a nominal volume flow. This is true e.g. for the friction factor of pipes, the heat transfer coefficient of the heat exchangers or the heat transfer coefficient between the inner of a pipe and the environment. However, this is a common assumption, that is widely used. Without it, iterative calculations would be necessary, as the volume flows are not known apriori, but needed to calculate these parameters.

Also the specific representation of pumps and valves is a simplification, as e.g. for pumps pure quadratic behavior is assumed, while real pumps follow characteristic curves that deviate from that. However, this is a widely used assumption based on ideal pump behavior.

As discussed in the context of the network concept (see section 2), the prosumer mode has to determine the flow direction trough the prosumers substation. In the hydraulic system model this is guaranteed by equation (38) and is explained in section 3.3. For the simulation case this hard mathematical constraint leads to a limitation, such that e.g. an overpushing of a pump by another pump can not be modelled and leads to a simulation error. However, for the control case this behavior is wanted, as there the prosumer mode shall force an according flow direction through the substation. If this flow direction is not possible, the controller gives the feedback, that the desired system state can not be reached with any control inputs under the given conditions. This will be referred to also in the analysis of the case study in the next section.

## 5. Case study

For the simulation case the presented mathematical model was implemented in Python. The implementation is kept flexible, so that different setups and scenarios can be investigated quite easily. The source code is provided under open source license on Github.[2] The code was tested with Linux 5.4.0–54-generic on a AMD Ryzen 5 PRO 3500U 8 × 2.1 GHz 16 GB RAM with Radeon Vega Mobile Gfx. Scenarios with 5 prosumers took about 5 s to solve, whereas scenarios with 10 prosumers took about 5 min.

Fig. 5 illustrates a very small network configuration with three participating prosumers and a radial network. In this specific scenario, prosumer 1 acts as consumer, while prosumer 2 and 3 are producers. All prosumers are assumed to have the same components. The component parameterization is based on the laboratory setup of the CoSES laboratory of the TU Munich. For the sake of brevity the detailed parametrization is not presented. Table 4 shows the inputs of the scenario and an excerpt of the simulation results for two variations of the scenario. At first, the control input (nominalized speed) of the pump at prosumer 3 is set to 0.7. Although prosumer 2 and 3 now have the exact same setting, prosumer 3 contributes with 4.7 kW only half as much as prosumer 2 to the supply of prosumer 1. The reason is the higher hydraulic resistance in the closed loop of prosumer 3 due to its greater distance from prosumer 1. After speeding up the pump at prosumer 3 from 70% to 80%, the power supply of prosumer 3 to the network almost doubles. At the same time prosumer 2 only feeds in half as much power as before, although its control values haven't changed. The reason is, that prosumer 3 with the higher pump speed now increases the pressure difference between the hot and the cold level and therefore the operation point of the pump at prosumer 2 shifts to a lower volume flow obtaining the same pump speed. A minimal change of the actuating variable of prosumer 3 changed the feed-in ratio to the network completely. For even lower pump speeds of prosumer 2 and higher pump speeds of prosumer 3, the model would not be feasible any more at some point. The reason is, that due to the pressure built by prosumer 3, the fluid would be pushed also through prosumer 2 from the hot to the cold level. But in the mathematical problem formulation prosumer 2 is defined as producer ($\mu_2 = 1$) and therefore its volume flow direction is fixed from the cold to the hot level. This is conflicting with the network state that would fullfill the steady-state conditions for the given control inputs and therefore the problem becomes infeasible.

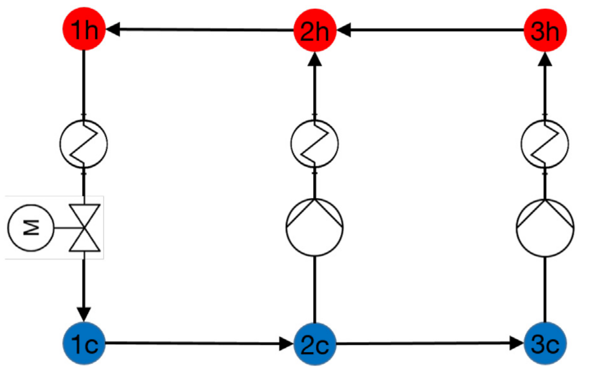


**Fig. 5.** Setup for an example simulation with three prosumers: prosumer 1 in producer mode and prosumer 2, 3 in consumer mode.

**Table 4**
Scenario inputs for example simulation and simulation results for two variations.

| | PSM1 | PSM2 | PSM3 | |
|---|---|---|---|---|
| $\mu$ | − 1 | 1 | 1 | $[-]$ |
| $\dot{V}_{sec}$ | 8.0 | − 5.0 | − 5.0 | $\left[\frac{l}{min}\right]$ |
| $T_{sec,in}$ | 40.0 | 65.0 | 65.0 | $[C^{\circ}]$ |
| $u^{pu}$ | 0.0 | 0.7 | $u_3^{pu}$ | $[-]$ |
| $\kappa^{va}$ | 1.0 | 0.0 | 0.0 | $[-]$ |
| $u_3^{pu} = 0.7$ | | | | |
| $T_{sec,out}$ | 59.6 | 42.1 | 51.7 | $[C^{\circ}]$ |
| $\dot{Q}_{trnsf}$ | − 11.0 | 8.0 | 4.7 | $[kW]$ |
| $u_3^{pu} = 0.8$ | | | | |
| $T_{sec,out}$ | 60.1 | 51.3 | 41.8 | $[C^{\circ}]$ |
| $\dot{Q}_{trnsf}$ | − 11.3 | 4.8 | 8.1 | $[kW]$ |

[2] https://github.com/thomaslicklederer/ProHeatNet_Sim.

This example shows how a local change influences the whole network and how sensitive the thermohydraulic steady-state is to small changes in the control variables. Therefore smart control based on models as the one that was presented is inevitable.

## 6. Summary, conclusion and Outlook

Subject of the investigations in this paper are decentralized and flexible thermal networks. The considered network type has no central units, is dominated by prosumers with flexible modes and characterized by bidirectional power flows controlled by distributed actuators only. An architecture concept and functional principle was presented for this type of networks. Based on that, a model describing the thermohydraulic steady-state was derived in form of a system of equations. The system of equations was analysed with regard to its applicability for simulation and optimal control. For simulation purposes a fully functional open source software framework was coded and is provided on Github.[3]

The main advantages of the derived model are:

- The model creates an interlink between the high-level energy management (power flows) and the thermohydraulic system state (temperatures, pressures, volume flows) of the considered thermal networks. By incorporating a model for the heat transfer to the secondary sides, also the thermohydraulic conditions (temperatures, volume flows) at the prosumer sides are part of the model.
- At the same time, the model creates an interlink between the thermohydraulic system state and the control inputs for operation. In contrast to existing approaches, the nonlinear behavior of the pumps and valves as well as the flexible prosumer behavior are incorporated directly in the model formulation. The flexible prosumer modes and control inputs for the distributed actuators are model variables. This allows to evaluate different control strategies from a thermohydraulic point of view.
- The presented model itself can be the basis for the formulation of a model-based open-loop controller. The model provides a comprehensive description of the thermal network including the inputs and behavior of the actuators in the substations. Even though such systems can be simulated in general modeling tools like Modelica, our model provides a systematized mathematical description that can be later used for the design of an open-loop network controller where the goal is to determine the necessary control inputs for given target heat flows. In this controller the system model is intrinsically part of the controller in form of constraints, whereas general modeling tools would require iterative simulations within a MPC-framework for such a problem.
- The presented model allows to flexibly investigate different setups without much effort. The formulation is scalable and changes in the settings can be done very easy and can even be automated with simple scripts. This is the basis for consecutive studies to gain insights in the general behavior of this network type.
- The derived model and its underlying network concept is compatible with recent trends in the research on thermal networks. E.g. for investigations with distributed heat pumps in substations, the considered heat exchanger just has to be seen as the corresponding evaporator of the heat pump.

The main findings of the paper are:

- For thermal networks with bidirectional power and volume flows, the complexity of modeling the hydraulic network state increases exponentially with the number of network connections. This holds not only for our model, but for all models that want to cover bidirectional thermal networks. The reason for that are the apriori unknown flow directions in the network pipes of prosumer-dominated thermal networks. In conventional, unidirectional district heating systems this is not the case and therefore modeling is less complex.
- The thermohydraulic network state shows high sensitivity and nonlinear behavior towards small changes in the actuators control inputs. A strong interdepency and mutual influence between the decentralized actuators and prosumers in the network was observed in the case study. This underlines the necessity of a holistic control approach considering the whole system on the technical level instead of decentral control approaches of individual substations.
- The apriori undetermined flow directions as well as the high nonlinearities between the volume flows and the heat transfer parameters are a big challenge for control approaches that explicitely incorporate the thermohydraulic system model in the controller. The volume flows including their directions are variables of the optimization, but also needed in advance to formulate the balance equations for the control-model. Here further research has to be done.

For future work, a validation of the provided simulation tool with simulation results from established environments like Modelica will be done. Consecutive simulation studies are expected to generate insights on general characteristics and challenges of this type of prosumer-dominated Smart Thermal Grids. By using reformulations and relaxations it is aspired to derive a model-based controller from the presented system of equations. In the medium term, the gained knowledge will be verified and applied in an laboratory environment that replicates a prosumer-dominated thermal network within a neighborhood of five buildings.

## Credit author statement

Thomas Licklederer: Conceptualization, Methodology, Software, Validation, Investigation, Writing - Original Draft, Writing - Editing, Visualization, Project administration. Thomas Hamacher: Resources, Supervision. Michael Kramer: Project administration, Conceptualization. Vedran S. Perić: Writing - Review, Supervision.

## Declaration of competing interest

The authors declare that they have no known competing financial interests or personal relationships that could have appeared to influence the work reported in this paper.

## A. Appendix

### A.1. Pump model

For given reference operation points $(u^{pu}_{ref1}, \dot{V}^{pu}_{ref1}, \Delta p^{pu}_{ref1})$ and $(u^{pu}_{ref2}, \dot{V}^{pu}_{ref2}, \Delta p^{pu}_{ref2})$, the hydraulic pump parameters can be calculated by

[3] https://github.com/thomaslicklederer/ProHeatNet_Sim.

$$a_1^{pu} = \frac{\Delta p_{ref1}^{pu} - \left(\frac{u_{ref1}^{pu}}{u_{ref2}^{pu}}\right)^2 \cdot \Delta p_{ref2}^{pu}}{\left(\dot{V}_{ref1}^{pu}\right)^2 - \left(\frac{u_{ref1}^{pu}}{u_{ref2}^{pu}}\right)^2 \cdot \left(\dot{V}_{ref2}^{pu}\right)^2} \tag{A.65}$$

$$a_2^{pu} = \left(\frac{1}{u_{ref2}^{pu}}\right)^2 \cdot \left[\Delta p_{ref2}^{pu} - \left(\dot{V}_{ref2}^{pu}\right)^2 \cdot a_1^{pu}\right] \tag{A.66}$$

### A.2. Pipe model

*Approximation of the Colebrook-White relation*

$$Re_{nom} = \frac{\varrho \cdot u_{nom} \cdot d^{pi}}{\mu^{fluid}} \tag{A.67}$$

for lsaminar flow ($Re_{nom} \leq 2000$) according to the equation of Hagen-Poiseuille:

$$f_D = \frac{64}{Re_{nom}} \tag{A.68}$$

For turbulent flow ($Re_{nom} \geq 4000$) according to Ref. [42]:

$$f_D = \frac{0.25}{\left[\log\left(\frac{\varepsilon}{3.7 \cdot d^{pi}} + \frac{5.74}{Re_{nom}^{0.9}}\right)\right]^2} \tag{A.69}$$

for transition regime ($2000 < Re_{nom} < 4000$):

Linear interpolation between $f_D$ for laminar flow at $Re_{nom} = 2000$ and turbulent flow at $Re_{nom} = 4000$ with the given pipe properties $\varepsilon$ and $d^{pi}$.

Calculation of the thermal resistance per unit length with form factors and material properties [43].

$$R^{pi} = \frac{1}{h_{ir} \cdot \pi \cdot d^{pi}} + \sum_j \left(\frac{ln\left(\frac{d_{j,or}^{pi}}{d_{j,ir}^{pi}}\right)}{2 \cdot \pi \cdot \lambda_j}\right) + \frac{1}{h_{or} \cdot \pi \cdot D^{pi}} \tag{A.70}$$

## References


[1] Lund H, Østergaard PA, Connolly D, Mathiesen BV. Smart energy and smart energy systems. Energy 2017;137:556–65.
[2] Lund H, Werner S, Wiltshire R, Svendsen S, Thorsen JE, Hvelplund F, Mathiesen BV. 4th Generation District Heating (4GDH). Integrating smart thermal grids into future sustainable energy systems. Energy 2014;68:1–11.
[3] Mathiesen BV, Lund H, Connolly D, Wenzel H, Ostergaard PA, Möller B, Nielsen S, Ridjan I, KarnOe P, Sperling K, Hvelplund FK. Smart Energy Systems for coherent 100% renewable energy and transport solutions. Appl Energy 2015;145:139–54.
[4] Buffa S, Cozzini M, D'Antoni M, Baratieri M, Fedrizzi R. 5th generation district heating and cooling systems: a review of existing cases in Europe. Renew Sustain Energy Rev 2019;104:504–22.
[5] Abugabbara M, Javed S, Bagge H, Johansson D. Bibliographic analysis of the recent advancements in modeling and co-simulating the fifth-generation district heating and cooling systems. Energy Build 2020;224:110260.
[6] Geidl M, Andersson G. Optimal power flow of multiple energy carriers. IEEE Trans Power Syst 2007;22:145–55.
[7] Mohammadi M, Noorollahi Y, Mohammadi-ivatloo B, Yousefi H. Energy hub: from a model to a concept – a review. Renew Sustain Energy Rev 2017;80: 1512–27.
[8] Bytschkow D, Capone A, Mayer J, Kramer M, Licklederer T. An OPC UA-based energy management platform for multi-energy prosumers in districts. In: 2019 IEEE PES Innovative Smart Grid Technologies Europe (ISGT-Europe); 2019. doi:10.1109/ISGTEurope.2019.8905725, https://ieeexplore.ieee.org/document/8905725/.
[9] Ancona M, Branchini L, Di Pietra B, Melino F, Puglisi G, Zanghirella F. Utilities substations in smart district heating networks. Energy Procedia 2015;81: 597–605.
[10] Beckenbauer D, Ehrenwirth M, Klärner M, Zörner W, Cheng V. Validation of a district heating system model and simulation-based investigation of bidirectional heat transport by decentralised solar thermal plants. In: Proceedings of SWC2017/SHC2017. International Solar Energy Society; 2017.
[11] Heymann M, Rosemann T, Rühling K, Tietze T, Hafner B. Concept and measurement results of two decentralized solar thermal feed-in substations. Energy Procedia 2018;149:363–72.
[12] Lamaison N, Bavière R, Cheze D, Paulus C. A multi-criteria analysis of bidirectional solar district heating substation architecture. In: Proceedings of SWC2017/SHC2017. Freiburg, Germany: International Solar Energy Society; 2017. p. 1–11.
[13] Paulus C, Papillon P. Substations for decentralized solar district heating: design, performance and energy cost. Energy Procedia 2014;48:1076–85.
[14] Brand L, Calvén A, Englund J, Landersjö H, Lauenburg P. Smart district heating networks – a simulation study of prosumers' impact on technical parameters in distribution networks. Appl Energy 2014;129:39–48.
[15] Brange L, Englund J, Lauenburg P. Prosumers in district heating networks - a Swedish case study. Appl Energy 2016;164:492–500.
[16] Zarin Pass R, Wetter M, Piette M. A thermodynamic analysis of a novel bidirectional district heating and cooling network. Energy 2018;144:20–30.
[17] Blacha T, Mans M, Remmen P, Müller D. Dynamic simulation of bidirectional low-temperature networks - a case study to facilitate the integration of renewable energies. In: Proceedings of building simulation 2019: 16th conference of IBPSA, vol. 16. International Building Performance Simulation Association; 2020. p. 3491–8.
[18] Wirtz M, Kivilip L, Remmen P, Müller D. 5th Generation District Heating: a novel design approach based on mathematical optimization. Appl Energy 2020;260:114158.
[19] Rosemann T, Löser J, Rühling K. A new DH control algorithm for a combined supply and feed-in substation and testing through hardware-in-the-loop. Energy Procedia 2017;116:416–25.
[20] Hassine IB, Eicker U. Control aspects of decentralized solar thermal integration into district heating networks. Energy Procedia 2014;48:1055–64.
[21] Bünning F, Wetter M, Fuchs M, Müller D. Bidirectional low temperature district energy systems with agent-based control: performance comparison and operation optimization. Appl Energy 2018:502–15.
[22] Guelpa E, Sciacovelli A, Verda V. Thermo-fluid dynamic model of large district heating networks for the analysis of primary energy savings. Energy 2019;184:34–44.
[23] Guelpa E, Verda V. Compact physical model for simulation of thermal networks. Energy 2019;175:998–1008.
[24] Huang S, Tang W, Wu Q, Li C. Network constrained economic dispatch of integrated heat and electricity systems through mixed integer conic programming. Energy 2019;179:464–74.
[25] Wang J, Zhou Z, Zhao J. A method for the steady-state thermal simulation of district heating systems and model parameters calibration. Energy Convers Manag 2016;120:294–305.
[26] Wang H, Wang H, Haijian Z, Zhu T. Optimization modeling for smart operation of multi-source district heating with distributed variable-speed pumps. Energy 2017;138:1247–62.
[27] Yan A, Zhao J, An Q, Zhao Y, Li H, Huang YJ. Hydraulic performance of a new district heating systems with distributed variable speed pumps. Appl Energy 2013;112:876–85.
[28] Wang Y, You S, Zhang H, Zheng W, Zheng X, Miao Q. Hydraulic performance optimization of meshed district heating network with multiple heat sources. Energy 2017a;126:603–21.
[29] Wang H, Wang H, Zhu T. A new hydraulic regulation method on district heating system with distributed variable-speed pumps. Energy Convers Manag 2017b;147:174–89.
[30] Wang H, Wang H, Zhou H, Zhu T. Modeling and optimization for hydraulic performance design in multi-source district heating with fluctuating renewables. Energy Convers Manag 2018;156:113–29.
[31] Peric VS, Hamacher T, Mohapatra A, Christiange F, Zinsmeister D, Tzscheutschler P, et al. CoSES laboratory for combined energy systems at TU Munich. In: 2020 IEEE Power & Energy Society General Meeting (PESGM); 2020.
[32] da Costa Bortoni E, Almeida RA, Viana ANC. Optimization of parallel variable-speed-driven centrifugal pumps operation. Energy Efficiency 2008;1:167–73.
[33] Association of German Engineers (VDI). Fluidic characteristic quantities of control valves and their determination. 2018.
[34] Brown GO. The history of the Darcy-weisbach equation for pipe flow resistance. In: Environmental and Water Resources History, vol. 40650. Reston, VA: American Society of Civil Engineers; 2002. p. 34–43. https://doi.org/10.1061/40650(2003)4.
[35] Weisbach J. Lehrbuch der Ingenieur- und Maschinen-Mechanik, vol. 1. Braunschweig: Theoretische Mechanik, Vieweg und Sohn; 1845.

[36] Colebrook C, White C. Experiments with fluid friction in roughened pipes. Proceedings of the Royal Society of London. Series A - Mathematical and Physical Sciences 1937;161:367–81.
[37] Brkić D. Review of explicit approximations to the Colebrook relation for flow friction. J Petrol Sci Eng 2011;77:34–48.
[38] van der Heijde B, Fuchs M, Ribas Tugores C, Schweiger G, Sartor K, Basciotti D, Müller D, Nytsch-Geusen C, Wetter M, Helsen L. Dynamic equation-based thermo-hydraulic pipe model for district heating and cooling systems. Energy Convers Manag 2017;151:158–69.
[39] Roetzel W, Spang B. C1 thermal design of heat exchangers. In: VDI heat Atlas. Berlin, Heidelberg: Springer Berlin Heidelberg; 2010. p. 31–66.
[40] Achterberg T. Products of variables in mixed integer programming. Webinar: Gurobi Optimization, LLC.; 2019. https://www.gurobi.com/resource/products-of-variables-in-mixed-integer-programming/; 2021. [Accessed 30 November 2020].
[41] Gurobi LLC. Optimization, Gurobi optimizer reference manual. 2020. http://www.gurobi.com.
[42] Swamee PK, Jain AK. Explicit equations for pipe-flow problems. J Hydraul Div 1976;102:657–64.
[43] Stephan P. B1 fundamentals of heat transfer. In: VDI heat Atlas. Berlin, Heidelberg: Springer Berlin Heidelberg; 2010. p. 15–30.

**M.Sc. Thomas Licklederer** is a research associate and PhD student at the Technical University of Munich (TUM). His work focuses on the management of cross-sectoral energy systems on a neighborhood scale. In his doctoral thesis he focuses on the operation of prosumer-dominated Smart Thermal Grids. His research interests are mathematical modelling, optimization, and optimal control in Smart Energy Systems.

**Prof. Dr. Thomas Hamacher** is professor at the Chair of Renewable and Sustainable Energy Systems and head of the Munich School of Engineering at the Technical University of Munich (TUM). He researches in the field of energy and systems analysis. His research focuses on urban energy systems and the integration of renewable energies into the power grid. Further focal points of his work are methods and fundamentals of energy system models.

**M.Sc. Michael Kramer** Michael Kramer was head of the research group on Energy Efficient and Smart Cities at the Technical University of Munich (TUM). He researches in the field of urban energy systems with a focus on scalable solutions for planning and provision of cross-sectoral flexibility. His research interests include, distributed optimization and optimal control of distributed energy systems in smart grids.

**Dr.-Ing. Vedran S. Perić** is head of the Research Center for Combined Smart Energy Systems (CoSES) at the TUM Munich School of Engineering. His research interests include topics related to power systems dynamic stability, as well as the operation and control of smart grids, with the focus on the integration of electric systems with district heating/cooling grids.

## 7.2 Pub5: ProsNet – a Modelica library for prosumer-based heat networks: description and validation

### 7.2.1 Context

In order to enhance the dynamic modeling of PBDH networks and to improve the compatibility of PBDH modeling with the existing MES modeling community, the Modelica library *ProsNet* is developed. Modelica is a widespread multi-purpose modeling language with some distinguishing features. As outlined in subsection 4.1.2, Modelica models are often used as 'digital twins' and external system models in the MPC context.

Pub5 presents the *ProsNet* library which is specifically designed for PBDH networks and facilitates the user-friendly setup of various network configurations. In this context, the library contains the necessary component models, which are based on open-source libraries and have been adapted in accordance with Pub4 for use in PBDH networks. Included are, amongst others, a model for the idealized system-agnostic secondary prosumer side and a bidirectional substation model that adheres to the reference concept from Figure 6.4. The library incorporates built-in control logics that enable automatic switching between the respective pumps/valves, depending on the specified prosumer mode, and allows for the control of these actuators by external input control signals. Several models, such as those for liquid-to-liquid heat exchangers or pipes with heat losses, have been adapted to ensure a user-friendly, but realistic representation of PBDH. While the models from Pub4 and the *ProHeat-Net_Sim* tool in Python utilize quasi steady-state considerations, the *ProsNet* library, implemented in Modelica, further permits the simulation of transient processes. To accomplish this, dynamic energy and mass balances must be chosen for the individual components, and time constants for the filters in the component models must be specified. The *ProsNet* library is publically available under https://github.com/thomaslicklederer/ProsNet. As a complement to the *ProsNet* library, the *ProHMo*[2] library developed by Daniel Zinsmeister models several secondary prosumer side configurations in SimulationX [117], [118].

[2] https://github.com/DZinsmeister/CoSES_thermal_ProHMo (visited on 2023/11/14)

### 7.2.2 Paper

| | |
|---|---|
| **Title** | **ProsNet – a Modelica library for prosumer-based heat networks: description and validation** |
| **Authors** | Ilya Elizarov, Thomas Licklederer |
| **Publication medium** | Journal of Physics: Conference Series, Volume 2042, 012031; CISBAT 2021 Carbon-neutral cities - energy efficiency and renewables in the digital era 8-10 September 2021, EPFL Lausanne, Switzerland |
| **Copyright** | Published under licence by IOP Publishing Ltd with the permission to reuse in accordance with the terms of the applicable Creative Commons Attribution (CC BY) licence (see https://creativecommons.org/licenses/by/4.0/). |
| **Identifier / URL** | https://doi.org/10.1088/1742-6596/2042/1/012031 |
| **Associated repositories** | https://github.com/thomaslicklederer/ProsNet |
| **Author contributions** | according to the Contributor Roles Taxonomy (CRediT, see [93]) |
| Ilya Elizarov | Conceptualization, Methodology, Software, Validation, Investigation, Writing - Original Draft, Visualization |
| Thomas Licklederer | Conceptualization, Resources, Writing - Review & Editing, Supervision, Project administration, Funding acquisition |

# ProsNet – a Modelica library for prosumer-based heat networks: description and validation

**I Elizarov, T Lickledederer**

Munich School of Engineering, Technical University of Munich, Lichtenbergstr. 4a, 85748 Garching, Germany

E-mail: ilya.elizarov@yahoo.com

**Abstract.** Prosumer-based heat networks are a new concept in district heating systems that uses the ability of prosumers to operate as either producers or consumers. This type of network allows for utilizing distributed heat generation, including renewable energy sources. A broad range of individual operating modes, heat generation technologies, and topologies determine complex thermo-hydraulic behavior of such networks. Simulations help gain insights into their properties. In this paper, a Modelica library *ProsNet* is presented for such simulations. It is designed to set up a prosumer-based heat network to investigate their dynamic and steady-state performance in a user-friendly way. Important models of the library are described in more detail. Finally, a successful validation of the developed components was performed by comparing results for different scenarios with another software for modeling bidirectional heat networks in steady-state.

## 1. Introduction

District heating could contribute to the decarbonization of energy production and improve supply security by integrating renewable sources, storage, and energy coupling between different sectors. These features are commonly found in the newer generation of district heating systems. Implementations of such systems also includes an ability for bidirectional energy flow [1]. This means that the participants, or in other words prosumers, can produce or consume heat with respect to the heat network depending on a current operating mode. Prosumer-based heat networks promote distributed heat generation including renewables. Furthermore, they exploit the synergy between users and increase flexibility of the heat supply. Potentially, customers in such network could shift a market paradigm from a production-centralized model to a decentralized one where substations can freely exchange energy for a price [1]. Considering the complexity mainly associated with operation strategy and pressure difference limitations [2], there is a need for a toolbox that can effortlessly simulate this type of network. This will allow users to focus on the thermohydraulic operation, investigating new control concepts and various types of generation that are compatible with these heat network. The paper describes the Modelica library *ProsNet* that was developed for this purpose.

The underlying scheme of a prosumer is shown in figure 1. It is based on an actual experimental setup at the CoSES lab at the Technical University of Munich. The prosumer is in production mode when the net heat flow rate on the secondary side $\dot{Q}_{\text{net}}$ [W] is positive and vice versa for consumption mode. The net heat flow rate, in turn, is formed by heat supply $\dot{Q}_{\text{source}}$ [W] and demand $\dot{Q}_{\text{sink}}$ [W]:

$$\dot{Q}_{\text{net}} = \dot{Q}_{\text{source}} - \dot{Q}_{\text{sink}} \text{ [W]} \tag{1}$$

The plate heat exchanger hydraulically separates the secondary side from the primary side. The primary side is connected to a two-pipe heat network. The direction of the flow in the network is defined by control elements on the primary side: a control valve and a feed-in pump in parallel. They are active depending on the operating mode: in production mode, the feed-in pump is active, and the control valve is closed, for the consumption mode, the feed-in pump is shut down, but the control valve maintains the flow. On the secondary side, the direction of the flow is established by a pair of circulation pumps operating in opposite directions: production and consumption pump. At least one customer must be in production mode to maintain a pressure difference in the network.

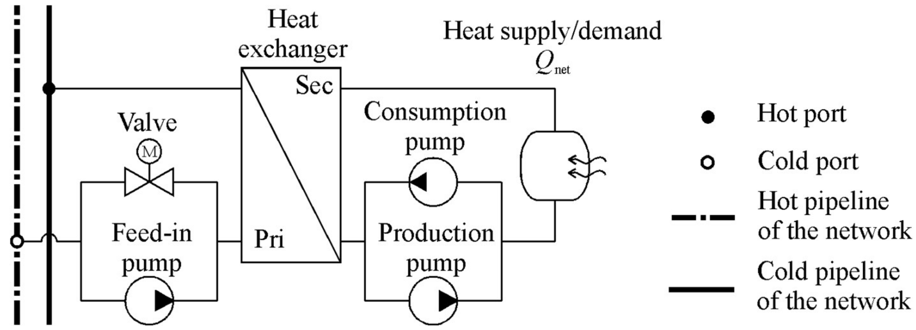


**Figure 1.** The underlying scheme of a prosumer.

## 2. Arrangement of the ProsNet library

The models in the library inherit components from the *IBPSA* library (version 3.0.0) and the *Modelica Standard Library* (version 3.2.3). Necessary components of the *IBPSA* library were copied to the library so it can be used with the default workspace available for every simulation environment. All fluid components are initialized with the incompressible water media model.

The overall structure of the library is given in figure 2. A prosumer model, as well as its base classes, are included in the *Prosumers* package. The *Controls* package contains control-related elements. The *Fluid* package consists of models for thermo-fluid flow. A liquid-to-liquid heat exchanger model *(LiquidToLiquid)*, a control volume with prescribed outlet temperature independent of the flow direction *(Heater_Cooler_T)*, and a pipe model with thermal losses *(InsulatedPipe)* were developed for the library. Examples of prosumer-based heat networks are provided in the *Examples* package. Important models of the library are described below.

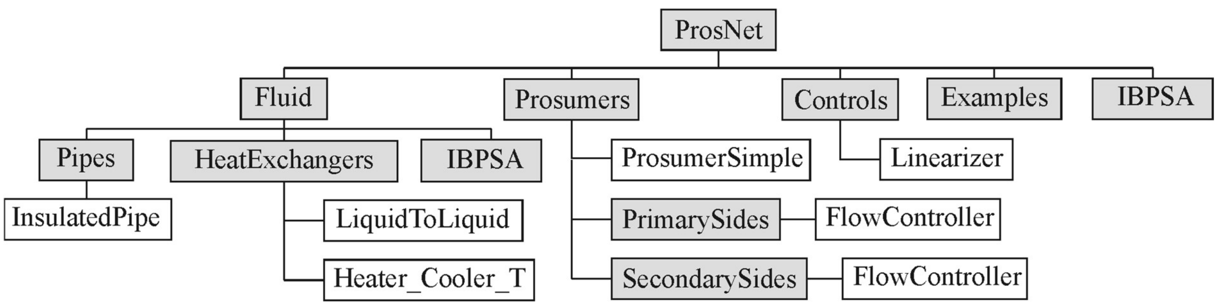


**Figure 2.** The overall structure of the *ProsNet* library.

### 2.1. Heat exchanger model

The *IBPSA* library does not contain a model or a function for calculating the overall heat transfer coefficient for liquid-to-liquid heat exchangers. This coefficient must be defined by the end-user. The *LiquidToLiquid* heat exchanger model extends from the *PartialEffectivenessNTU* partial model and provides the required value in *ProsNet*.

The derived expression for the overall heat transfer coefficient is based on the following assumptions. First, thermal resistance through the wall $L/\lambda$ [(m$^2$·°C)/W] is negligible compared to thermal resistance of convection on primary $1/\alpha_1$ [(m$^2$·°C)/W] and the secondary $1/\alpha_2$ [(m$^2$·°C)/W] side:

$$h = \frac{1}{\frac{1}{\alpha_1} + \frac{L}{\lambda} + \frac{1}{\alpha_2}} \approx \frac{1}{\frac{1}{\alpha_1} + \frac{1}{\alpha_2}} \ [\mathrm{W/(m^2 \cdot {}^\circ C)}] \tag{2}$$

Second, flow conditions predominantly determine the heat transfer for nominal and actual values of the convective coefficients:

$$\frac{\alpha}{\alpha_{\mathrm{nom}}} = \frac{\mathrm{Nu}}{\mathrm{Nu}_{\mathrm{nom}}} \sim \left(\frac{\dot{m}}{\dot{m}_{\mathrm{nom}}}\right)^b \tag{3}$$

where $\alpha$ is the actual convective heat transfer [W/(m$^2$·°C)], $\alpha_{\mathrm{nom}}$ is the nominal heat transfer coefficient [W/(m$^2$·°C)], Nu and $\mathrm{Nu}_{\mathrm{nom}}$ are the Nusselt numbers for actual and nominal conditions [-], $\dot{m}$ and $\dot{m}_{\mathrm{nom}}$ are actual and nominal mass flow rates [kg/s].

Combining formulas (2) and (3), the actual overall heat transfer coefficient can be computed for any new value of mass flow rate other than the nominal one. The exponent $b$ in formula (3) can be taken from an appropriate correlation for the Nusselt number for plate heat exchangers [3]:

$$\mathrm{Nu} = A \cdot \mathrm{Re}^b \mathrm{Pr}^c \ [-] \tag{4}$$

where Re is the Reynolds number [-], Pr is the Prandtl number [-].

### 2.2. *Flow controller*

This model generates control signals for pumps and actuators depending on the operating mode and participation. The valve receives zero opening signal for production mode, while the production and feed-in pumps are active and vice versa for consumption mode.

### 2.3. *Linearizer*

When only a small pressure drop is allowed by a control valve, the most used valve type has an equal percentage inherent characteristic. The volumetric flow rate through such a valve can be expressed as:

$$\dot{V} = K_{\mathrm{v}} \cdot f(op) \left(\frac{\Delta p}{\mathrm{SG}}\right)^{1/2} \ [\mathrm{m^3/h}] \tag{5}$$

where $K_{\mathrm{v}}$ is the flow factor $[\mathrm{m^3/(h \cdot bar^{1/2})}]$; $f(op)$ is the inherent characteristic, which is a function of the opening [-], $op$ is the opening of the valve [-], $\Delta p$ is pressure drop at the valve [bar], and SG is the specific gravity of the fluid.

The inherent valve characteristic is non-linear. To linearize the flow rate with respect to the valve characteristic, the opening is substituted with its inverse:

$$op = f^{-1}(\kappa) \tag{6}$$

where $\kappa$ is the actual flow coefficient, which varies between zero and one [-].

The flow coefficient $\kappa$ serves as one of the inputs of the prosumer model. The function (6) is provided by the block *Linearizer* of the *ProsNet* library and is calculated as an inverse of the equal percentage valve characteristic from the *IBPSA* library.

### 2.4. *Prosumer model*

The prosumer model, shown in figure 3, is composed of primary and secondary side submodels. Seven inputs control the prosumer: operating mode $\mu$, participation $\pi$, the normalized velocity of the feed-in pump $u$, valve flow coefficient $\kappa$, mass flow rate on the secondary side $\dot{m}_{\mathrm{sec}}$, and the outlet temperature of the heat supply/demand block $T_{\mathrm{sec}}$,. They can be individually set as parameters instead of accepting input signals.

The secondary side submodel represents technology-dependent heat generation and demand implementation. In the current release of the library, a prescribed outlet temperature control volume model is available.

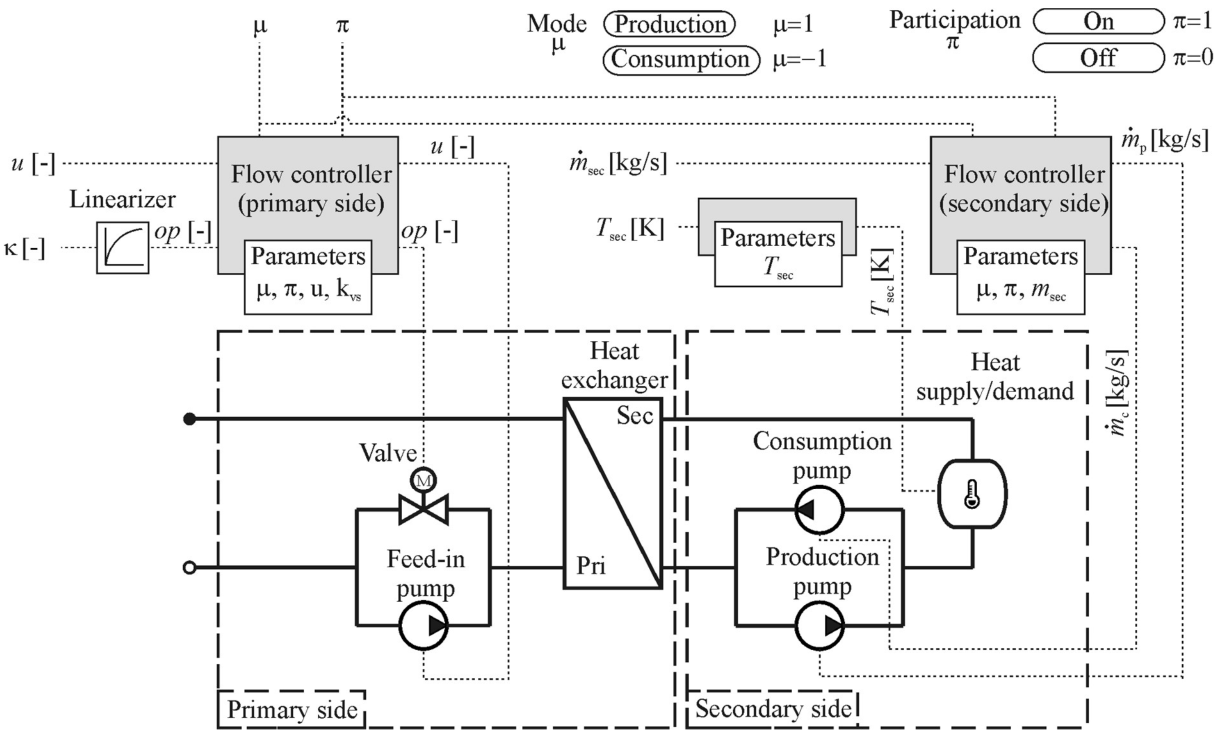


**Figure 3.** The prosumer model in the library.

## 3. Validation

To determine the accuracy of the developed models, validation was performed with the results acquired from the *ProHeatNet_Sim*, a Python framework for simulating bidirectional heat networks [4]. In addition, the absolute and relative errors between the two were calculated. Three prosumer models were put together to form a radial heat network (see figure 4). A corresponding model for validation is provided in the library's *Examples* package.

The following essential parameters are set for components of the library and the framework. For the pipeline section, length is 10 m, diameter is 0.022 m, and local pressure loss factor $\zeta$ is 3.5. For prosumers, the quadratic feed-in pump's performance curve has a shut-off head at $402.21 \cdot 10^2$ Pa and a maximum flow rate of 55.33 l/min. The valve's nominal flow coefficient $K_v$ is 2.5 $m^3/h$. The heat exchanger's nominal heat flow rate is 30 kW, inlet temperatures are 70 °C and 45 °C on the primary and secondary side, respectively. For both sides, nominal flow rates are 21.48 kg/min with a pressure loss of $155 \cdot 10^2$ Pa. The ambient temperature for simulating thermal losses in the pipes is 12 °C, the thermal resistance of the insulation is 3.78 (K·m)/W.

To acquire comparative results from *ProsNet* and *ProHeatNet_Sim*, two sets of operating modes are given in table 1. For both cases, the flow rate on the secondary side $\dot{m}_{sec}$, was kept 10 kg/min, and two values of the inlet temperatures on the secondary side $T_{sec}$ were applied: 65 °C for production mode and 45 °C for consumption mode.

The *ProsNet* library can perform both dynamic and steady-state simulations, while *ProHeatNet_Sim* is only capable of steady-state simulations. For this reason, the tested components were initialized in steady-state. There are minor differences in flow models of pipes and heat exchangers as well: the Darcy-Weisbach friction factor and the overall heat transfer coefficient in *ProHeatNet_Sim* are defined for nominal conditions and kept constant. For this reason, some discrepancies between the results were expected.

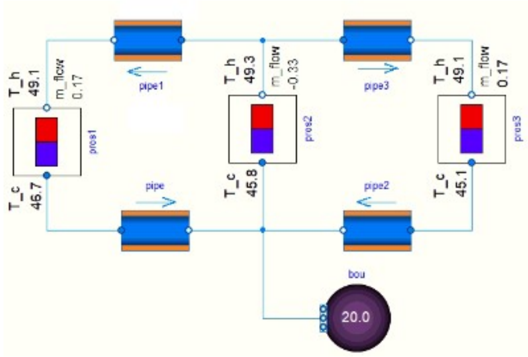


**Figure 4.** The prosumer-based heat network for validation.

**Table 1.** Operating modes and inputs for validation.

| Case | Prosumer no. 1 | Prosumer no. 2 | Prosumer no. 3 |
|---|---|---|---|
| A | Cons., $\kappa$=0.9 | Prod., $u$=0.6 | Cons., $\kappa$=0.6 |
| B | Cons. $\kappa$=0.6 | Prod., $u$=0.9 | Prod. $u$=0.9 |

The compared pressure difference and flow rate for *ProsNet* and *ProHeatNet_Sim* is shown in figure 5. The *ProHeatNet_Sim* framework underestimates pressure losses due to the simplified flow model. The pressure difference at the connecting ports is lower for *ProsNet* because of the actual Darcy-Weisbach friction factor for internal hydraulic losses. For case A, maximal relative error for pressure difference between the models was found for prosumers 1 and 3: 11.7% and 11.6%, respectively. For case B, the relative error for prosumer 2 is 4.9%, and for prosumer 3 – 4.4%. Due to the quadratic law between the flow rate and pressure drop, the relative error for the volumetric flow rate is lower: in case A, 6.4%, 7.1% for prosumers 1, 3. For the same prosumers in case B 3.2% and 3.7%.

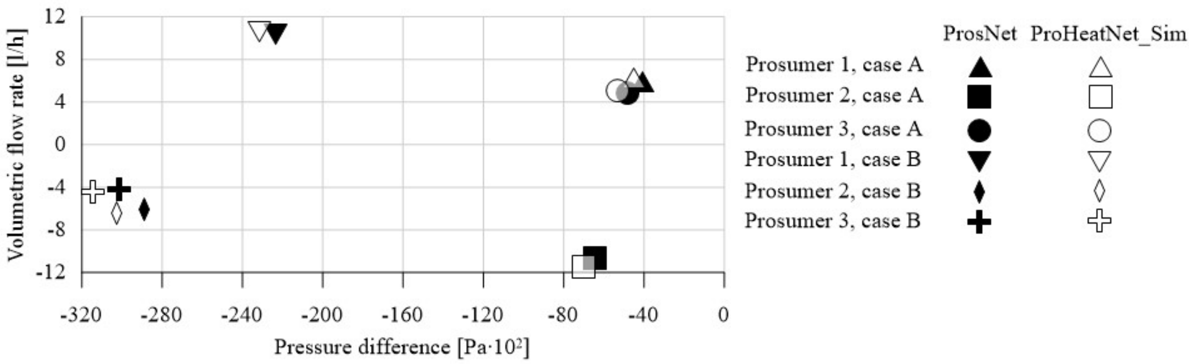


**Figure 5.** The plot of flow rate and pressure difference at prosumers.

The heat flow rate through the heat exchanger of each prosumer is shown in figure 6. The flow rate through the heat exchanger for all the cases is significantly less than for the nominal value. A change in the flow conditions is not considered for *ProHeatNet_Sim*, as a result, the heat flow is overestimated. On the contrary, *ProsNet* determines the change in the overall heat transfer coefficient. This, along with the decreased flow rates, explains lower thermal power for *ProsNet*. The calculated relative error between the results varies in the interval 10.4% - 9.9% for case A, and 9.45% - 8.16% for case B.

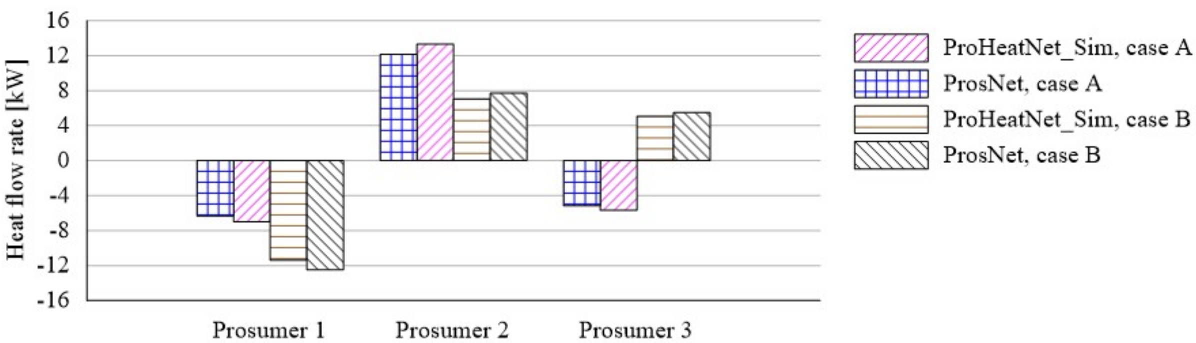


**Figure 6**. The plot of heat flow rate transferred to the network from prosumers.

The temperatures on the primary side of the prosumers are shown in figure 7. Note that due to the thermal losses in the pipelines, the temperature at the hot ports of the prosumers in consumption mode is lower than that for production mode. The error estimation showed that the maximal absolute error between the results for *ProsNet* and *ProHeatNet_Sim* is 0.27 K and 0.65 K for prosumer 1 in case A and B for the cold port.

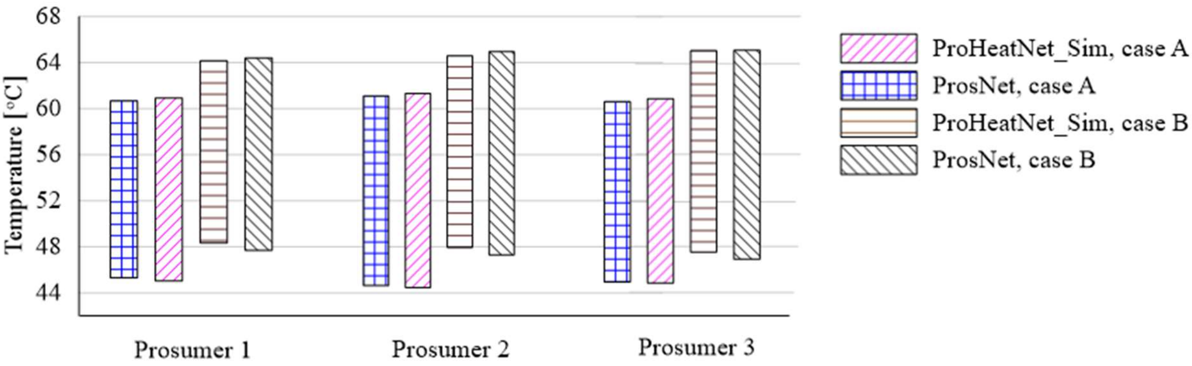


**Figure 7**. The plot of temperature at hot ports (top of the bars) and cold ports (bottom of the bars) at prosumers on the primary side.

## 4. Conclusion

For the validation of the library, the comparison between the results from the *ProsNet* library and the *ProHeatNet_Sim* framework was made. Although the results demonstrated a certain discrepancy in the heat flow rate and pressure drop, the reasons for the differences were explained. In principle, the two approaches align and can predict the outcome of one another, but the distinctive features of both must be taken into consideration. The *ProsNet* library contains essential models to simulate prosumer-based heat networks. It allows for a dynamic and steady-state simulation of such networks in a user-friendly way. *ProsNet* is available at: https://github.com/ilyaelizarov/ProsNet.

## References


[1] Buffa S, Cozzini M, D'Antoni M, Baratieri M and Fedrizzi R 2019 *Renewable and Sustainable Energy Reviews* **104** 504-522

[2] Elizarov I 2020 Master's thesis: Analysis, modelling, and control strategy development for prosumer-based heat networks DOI: 10.13140/RG.2.2.24851.71206

[3] Yang J, Jacobi A and Liu W 2017 *Applied Thermal Engineering* **113** 1547-1557

[4] Licklederer T, Hamacher T, Kramer M and Perić V 2020 Accepted preprint submitted to Energy – The International Journal DOI: 10.13140/RG.2.2.16914.68803

## 7.3 Pub6: Characteristics and Challenges in Prosumer-Dominated Thermal Networks

### 7.3.1 Context

Employing the developed thermohydraulic models for PBDH networks, along with the corresponding software artifacts, comprehensive tools are available to explore the interplay between actuator control and network status in smart thermal grids. This facilitates the development and testing of dedicated control strategies, which consider the peculiarities in network behavior and the associated challenges. As described in Section 4.3, challenges are expected especially resulting from the distributed actuators and the flexibility of the prosumers.

The subsequent publication presents a comprehensive compilation of characteristics and challenges in PBDH networks, derived from studies on the relation between actuator inputs and thermohydraulic behavior. Case studies are used and supported by literature references together with logical reasoning. Two types of case studies are conducted, steady-state scenarios using the tool *ProHeatNet_Sim* (see Section 7.1) and dynamic simulations using the *ProsNet* library in Dymola (see Section 7.2). Although some of the aspects have been anticipated in earlier publications, they have not been thoroughly examined within the overall network context, nor have they been compiled and contextualized in a broader framework.

### 7.3.2 Paper

| | |
|---|---|
| **Title** | **Characteristics and Challenges in Prosumer-Dominated Thermal Networks** |
| **Authors** | Thomas Licklederer, Daniel Zinsmeister, Ilya Elizarov, Vedran S. Perić, Peter Tzscheutschler |
| **Publication medium** | Journal of Physics: Conference Series, Volume 2042, 012039; CISBAT 2021 Carbon-neutral cities - energy efficiency and renewables in the digital era 8-10 September 2021, EPFL Lausanne, Switzerland |
| **Copyright** | Published under licence by IOP Publishing Ltd with the permission to reuse in accordance with the terms of the applicable Creative Commons Attribution (CC BY) licence (see https://creativecommons.org/licenses/by/4.0/). |
| **Identifier / URL** | https://doi.org/10.1088/1742-6596/2042/1/012031 |
| **Author contributions** | according to the Contributor Roles Taxonomy (CRediT, see [93]) |
| Thomas Licklederer | Conceptualization, Methodology, Software, Validation, Investigation, Writing - Original Draft, Visualization |
| Daniel Zinsmeister | Conceptualization, Investigation, Writing - Review & Editing |
| Ilya Elizarov | Methodology, Software |
| Vedran Perić | Validation, Writing - Review & Editing, Supervision |
| Peter Tzscheutschler | Project administration, Funding acquisition |

# Characteristics and Challenges in Prosumer-Dominated Thermal Networks

**Thomas Licklederer, Daniel Zinsmeister, Ilya Elizarov, Vedran Perić and Peter Tzscheutschler**

Technical University of Munich, Munich School of Engineering (MSE), Lichtenbergstr. 4a, 85748 Garching near Munich, Germany

E-mail: `thomas.licklederer@tum.de`

**Abstract.** Prosumer-dominated thermal networks interconnect distributed prosumers. These networks form the infrastructure that allows to execute the trading of thermal energy as desired in the context of local energy markets. However, the significantly different behavior of such networks compared to conventional district heating and cooling networks has not yet been comprehensively investigated. This paper provides a compilation of instrinsic characteristics of prosumer-dominated thermal networks and discusses challenges that arise from these characteristics. As a basis for the investigations an underlying reference concept for the considered type of networks is described. Simulative case studies are combined with scientific deduction and literature references to gain new insights on the design and operation of this type of networks. It is found that due to the variability in these networks, the definition of a design case is a challenge for the dimensioning of concrete network implementations. To anticipate the strong coupling between prosumers and the nonlinear network behavior, it is concluded that centralized control combined with a model of the physical network behavior is necessary. The discussion of characteristics and challenges in prosumer-dominated thermal networks indicates open points in this field and thus provides a starting point for consecutive studies.

## 1. Introduction

Prosumers are entities that can act as consumers or producers to the network and switch between these modes over time. Inspired by microgrids and virtual power plants in the electricity sector, the most exhaustive adaption to the thermal sector are thermal networks that consist only or predominantly of prosumers. Linked to the idea of local multi-energy markets, a prosumer-dominated network allows to physically execute the trade of thermal energy between prosumers. The behavior of such networks however differs a lot from conventional district heating and cooling systems, that were characterized by dominant central generation units. Even though some papers compare different concepts for specific applications, to the best of our knowledge there are no investigations on the general characteristics and challenges of prosumer-dominated thermal networks.

Therefore, this paper aims to give a comprehensive compilation by combining scientific deduction with simulative case studies and references to literature where applicable. For the sake of simplicity, all discussions are performed subject to heating networks, but in principle they can also be transferred to cooling networks as well as to combined heating and cooling networks.

**Nomenclature**

**Symbols**

| | |
|---|---|
| $\dot{Q}$ | thermal power flow, transferred heat |
| $\dot{V}$ | volume flow |
| $T$ | temperature |
| $u$ | normalized pump speed as control (input) variable of variable speed pumps |
| $\kappa$ | normalized flow coefficient as control (input) variable of control valves, proportional to valve opening |

**Indices**

| | |
|---|---|
| *cold* | cold subnetwork, return line |
| *hot* | hot subnetwork, supply line |
| *in* | inflowing (into substation) |
| *out* | outflowing (out of substation) |
| *prim* | primary side, network side |
| *sec* | secondary side, prosumer side |

**Abbreviations**

| | |
|---|---|
| cons | consumption mode (of prosumer) |
| prod | production mode (of prosumer) |
| pros | prosumer |

## 2. Reference Concept and Case Studies

### *2.1. Reference network concept*

Since there is no unified standard network concept for prosumer-dominated networks, a reference architecture is needed as a basis for the investigations and simulation studies. This paper focuses on the network side while the internal prosumer side is considered only by a net heat flow in form of an accordingly heated or cooled fluid flow. Further investigations on different prosumer side configurations in the context of thermal networks are presented in [1]. Figure 1 illustrates a setup with three prosumers using the reference network concept the paper at hand is based on. The used reference concept is a 2-pipe-system with counter-flow plate heat exchangers in the heat transfer stations. Prosumers feed-in from the cold subnetwork (return line) to the warm subnetwork (supply line) and extract in consumption mode vice versa. The network is controlled by distributed actuators in the substations: variable speed pump (production mode), control valve (consumption mode). Radial, meshed and mixed topologies are allowed.

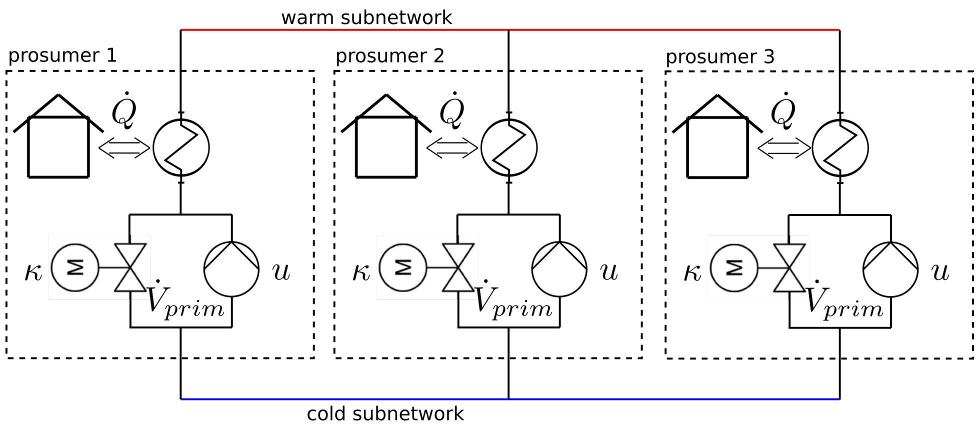


**Figure 1.** Setup of three prosumers in a radial topology following the reference network concept

This reference network concept is quite generic and applicable for heating, cooling networks or combined heating & cooling networks. It is compatible with recent trends in literature, like decentral booster heat pumps in substations. For this application case the heat exchanger can be substituted by a booster heat pump. The generality of the proposed reference network concept allows the derivation of general statements regarding the operation of prosumer-dominated thermal networks.

*2.2. Case studies*

In this section, the considered simulation scenarios are explained. The discussion of the results takes place in the following sections. Four scenarios were simulated, all using the setup of figure 1 and parameters (e.g. pipe diameters, pump dimensioning etc.) from the *CoSES* laboratory environment [2]. The scenarios I & II are steady-state scenarios that were simulated with the tool *ProHeatNet_Sim*[1]. With the scenarios III & IV dynamic behavior is investigated using the modelica-based simulation tool *Dymola* together with the library *ProsNet*[2].

In scenario I, prosumer 1 consumes while the prosumers 2 and 3 produce. The pumps of prosumer 1 and 2, both run on 80% speed. Scenario II is the same as scenario 1, but the pump speed of prosumer 2 is reduced to 60%. In scenario III, the thermal network is cold ($30°C$), as prosumers 1 and 2 start to exchange energy with prosumer 2 being the consumer. Scenario IV starts from the steady-state of scenario 1. Then prosumer 2 switches from production to consumption mode and after some time back to production mode.

Table 1 shows the steady-state simulation results of the scenarios I & II. Figure 2 shows for the scenarios III and IV the dynamic simulation results over time.

**Table 1.** Simulation results of the scenarios I and II (described above). $u$ is the control input for pumps in producers, $\kappa$ the control input for valves in consumers (100% is max speed / open).

| | | parameters | | | | simulation results | | |
|---|---|---|---|---|---|---|---|---|
| scenario | | mode | $\dot{V}_{sec}\left[\frac{l}{min}\right]$ | $T_{sec,in}\,[°C]$ | control | $T_{sec,out}\,[°C]$ | $\dot{V}_{prim}\left[\frac{l}{min}\right]$ | $\dot{Q}\,[kW]$ |
| I | pros1 | cons | 8 | 40 | $\kappa = 100\%$ | 59.8 | 8.8 | $-11.1$ |
| | pros2 | prod | $-5$ | 65 | $u = \mathbf{80}\%$ | 42.8 | $-5.8$ | 7.8 |
| | pros3 | prod | $-5$ | 65 | $u = 80\%$ | 50.7 | $-3.0$ | 5.0 |
| II | pros1 | cons | 8 | 40 | $\kappa = 100\%$ | 54.2 | 6.9 | $-7.9$ |
| | pros2 | prod | $-5$ | 65 | $u = \mathbf{60}\%$ | 63.5 | $-0.3$ | 0.5 |
| | pros3 | prod | $-5$ | 65 | $u = 80\%$ | 39.5 | $-6.6$ | 8.9 |

## 3. Characteristics

*3.1. Bidirectionality*

A central characteristic for prosumer-dominated thermal networks is the bidirectionality of both, energy and mass flows. This bidirectionality occurs within the network as well as between the individual prosumers and the network.

*3.2. Temporal and spatial fluctuations of temperatures*

Conventional district heating system typically have fixed desired fluid temperatures for the whole warm and cold subnetwork. Prosumer-based thermal networks can consist of different prosumers with various generation technologies and demand profiles. They might exchange heat

[1] `https://github.com/thomaslicklederer/ProHeatNet_Sim`

[2] `https://github.com/ilyaelizarov/ProsNet`

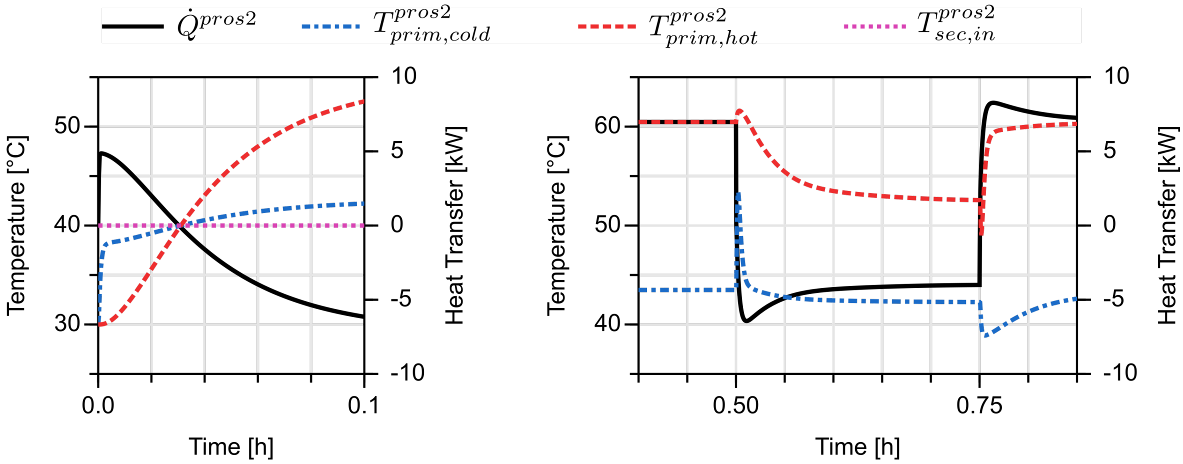


**Figure 2.** Simulation results of scenario III (left) and scenario IV (right) in form of heat flows (solid) between the network and prosumer 2, together with the corresponding primary side temperatures (hot dashed, cold dash-dotted) and secondary side inlet temperatures (dotted).

on different temperature levels, best fitting to the current requirements and in order to minimize losses. Additionally, the variable mass flow rates through the individual substations influence the local temperature levels. If not inhibited by specific control concepts, the temperature levels can fluctuate not only temporally, but also spatially within in the network.

### *3.3. Mutual influence of actuators*

The distributed pumps and valves control the whole network. They are mutually coupled. Each change on the operation of a pump or valve influences the overall network state including temperatures and energy flows. This can be observed in the simulation results of table 1. When reducing the speed of the pump of prosumer 2 from 80% in scenario I to 60% in scenario II, the volume flow and thereby the heat transfer of prosumer 2 decreases. Without any other changes in the system, prosumer 1 and 3 are also significantly influenced as it can be seen at the changes in their temperatures, volume flows and transferred heat.

### *3.4. High sensitivity on control inputs*

Comparing the simulation results of scenario I and II in table 1 makes clear that the network state shows a very high sensitivity on changes in the control inputs. While the pump of prosumer 2 is only slowed down from 80% to 60% speed, the volume flow trough the substation of prosumer 3 more than doubled and its heat transfer raised from 5 kW to 8.9 kW. This is a nonlinear behavior caused by the mutual influence of the distrubed actuators and the nonlinear relations between pressure differences, volume flows and heat transfer coefficients.

### *3.5. Pump blocking*

Another nonlinear effect is the pump blocking as described in [3]. In the simulation results of scenario II (table 1) the volume flow through the substation of prosumer 2 is almost zero. The pump of prosumer 3 runs on 80% speed and holds the pressure difference between hot and cold subnetwork at a level at which the pump of prosumer 2 is not able to generate significant volume flow. That means pump 2 is effectively blocked by pump 3 and prosumer 2 therefore can not contribute to the network. How and when this effect occurs is depending on the dimensioning of the pumps and the distances and hydraulic resistances in the network.

*3.6. Supply frontier and hydraulic network splitting*
In a thermal network with multiple feed-in points another effect, similar to pump blocking occurs: the creation of a supply frontier. When there are prosumers in consumption mode topologically between two or more prosumers in production mode, then the producers "compete" for the supply of the consumers. The colliding opposite flows annihilate at a certain point to no flow. This is described as supply frontier by [4]. The supply frontier can shift over time, due to the operation point of the individual pumps and valves. If it does not shift over a longer period of time, the network can cool down locally at the supply frontier. From an hydraulic system perspective, the network is effectively split into two or multiple hydraulic subsystems by the supply frontier.

*3.7. Energ flow reversal for network heat-up*
In prosumer-dominated networks that are operated with flexible temperatures and a local energy market, the network can (locally) cool out. This can happen e.g. when the network is not used because prosumers operate self supplying over a longer period of time or because previous heat exchange was at a lower supply temperature. The simulation results in figure 2 (left) show the case of prosumer 2 that wants to consume from the cooled out network while prosumer 1 feeds in. It can be seen that the inlet temperature on the prosumer side is higher than the temperature on the network side. Therefore prosumer 2 feeds in heat to the network in the beginning, although it wanted to consume. When the hot subnetwork is heated up to a temperature above the inlet temperature on the prosumer side, prosumer 2 starts to consume, as intended.

*3.8. Network behavior during prosumer mode switching*
Figure 2 (right) shows the network behavior when prosumer 2 switches its mode. When switching from production to consumption, the local temperature in the cold subnetwork rises significantly. At the same time, the local temperature in the warm subnetwork rises slightly. These observations are caused by the following effects: The mass flow directions are inverted quite fast, while the inlet temperature on the secondary side sinks gradually. That means, in the beginning the network side flow is not significantly cooled by the prosumer side. So the temperature in the cold subnetwork rises. At the same time, warmer water from prosumer 3 (production) is now pushed trough substation 2 where the local temperature in the warm subnetwork rises. After some time, the prosumer side inlet temperature is cold enough to cool the network side flow and the steady-state begins to settle. When switching back from production to consumption mode the opposite effects can be observed. The magnitude of these effects depends on the volume of water in the substations, the rate of temperature change on the secondary side and various other aspects.

## 4. Challenges
*4.1. Challenges in network design*
The planning of conventional district heating systems is based on representative design cases. It affects aspects like the topology, design temperatures as well as the dimensioning of pipes and pumps. In prosumer-dominated thermal networks there are no representative design cases due to the high variability in operation. Therefore, new procedures for the network planning are needed. Further, new challenges for the network design come up related to the characteristics discussed in section 3 : mixed topologies (meshed and radial), temperature control, substation dimensioning, pressure difference between the subnetworks etc. For the dimensioning of the pumps and pipes the decisive question is over which distance the supply of other prosumers should be possible. Oversizing the distributed pumps for the supply over long distances is uneconomical and inefficient. Therefore either the whole network must be geographically compact or the energy exchange must be restricted to local groups of prosumers within the network.

### *4.2. Challenges in network control*

The type of networks under consideration is controlled only by distributed actuators in the prosumers' substations. As discussed in section 3 these actuators mutually influence each other and the overall thermohydraulic network state behaves sensitive and nonlinear to changes in the control variables. This is a big challenge for the network control, as prosumers with their substations cannot be controlled independently. Ref. [5] warns that the mutual influence of the actuators can lead to hydraulic oscillations and water hammers. In order to prevent this, ref. [5] proposes to adjust all actuators simultaneously. Further, ref. [6] shows that in order to minimize the pumping power, the control valve of at least one consuming point has to be completely opened, while the other valves are adjusted relatively to it.

The previous points argue for a central network controller for prosumer-dominated thermal networks. Such a central controller must consider power setpoints for the feed in or extraction of each prosumer as well as temperature requirements and other specifications. Also, the central controller must take into account and anticipate described phenomena like pump blocking, the supply frontier or network heat-up. For this, the central control approach must rely on some kind of model of the underlying physical network behavior. In ref. [7] a thermohydraulic model is presented in form of a system of equations that can be the basis for such a central network controller. Further, ref. [7] shows that the complexity of simulating and controlling a prosumer-dominated thermal network increases exponentially with the number of interconnections, which is usually proportional to the number of prosumers in the network.

### *4.3. Challenges for thermal markets*

Related to the characteristics discussed in section 3, the following challenges must be faced by heat markets in the context of prosumer-dominated thermal networks: How to allocate costs for heating up or cooling down the network? How to integrate variable temperatures into the market? How to reflect the restriction of energy exchange only within local groups by the market? What is the general market design and market clearing process? It can be seen that compared to local electricity markets, for the thermal sector the technical implementation & control level strongly influences and limits possible local energy market concepts.

## 5. Conclusion

Prosumer-dominated thermal networks are the infrastructure that physically allows to exchange thermal energy between prosumers, as this is desired in the context of local energy markets. This paper shows, that the technical execution of the thermal energy trading has several challenges. Previously used procedures for the design of district heating networks cannot be adopted directly. Further research is necessary on how to determine reasonable design cases for such networks with high variability. For the control of prosumer-dominated networks it was deduced that a central controller with an underlying model of the relations and physical network behavior is necessary. Based on the technical insights, challenges are named for heat markets in the context of prosumer-dominated networks. It becomes clear that for the development of local thermal energy market concepts the feedback between the market level and the technical level is an important and limiting factor. As an overarching hypothesis, it is stated that energy exchange between thermal prosumers is technically more reasonable over small distances and is very complex to control with higher numbers of prosumers exchanging energy simultaneously.

Summarized, the higher flexibility of prosumer-dominated thermal networks and their compatibility with the idea of local market is bought with higher complexity in design and operation. The presented compilation of characteristics and challenges is to be extended and provides a basis for consecutive studies in this innovative field of thermal networks.

**Acknowledgments**
The research for this paper was founded by the German Federal Ministry for Economic Affairs and Energy *BMWi* (FKZ: 03ET1413B and FKZ: 03EN3032A) and the German Research Association *DFG* (project nr. 450821044).

## References

[1] Zinsmeister D, Licklederer T, Christange F, Tzscheutschler P and Perić V S 2021 A Comparison of Prosumer System Configurations in District Heating Networks *Manuscript submitted to 17th International Symposium on District Heating and Cooling*
[2] Peric V S, Hamacher T, Mohapatra A, Christiange F, Zinsmeister D, Tzscheutschler P, Wagner U, Aigner C and Witzmann R 2020 CoSES Laboratory for Combined Energy Systems At TU Munich *2020 IEEE Power & Energy Society General Meeting (PESGM)* November (IEEE) pp 1–5 ISBN 978-1-7281-5508-1
[3] Elizarov I 2020 Master's Thesis "Analysis , modelling, and control strategy development for prosumer-based heat networks" (Technichal University of Munich) URL `http://doi.org/10.13140/RG.2.2.24851.71206`
[4] Heymann M, Rosemann T, Rühling K, Tietze T and Hafner B 2018 *Energy Procedia* **149** 363–372 ISSN 18766102
[5] Wang H, Wang H and Zhu T 2017 *Energy Conversion and Management* **147** 174–189 ISSN 01968904
[6] Wang H, Wang H, Zhou H and Zhu T 2018 *Energy Conversion and Management* **156** 113–129 ISSN 01968904
[7] Licklederer T, Hamacher T, Kramer M and Perić V S 2021 *Energy* **230** 120825 ISSN 03605442 URL `https://linkinghub.elsevier.com/retrieve/pii/S0360544221010732`

## 7.4 Chapter Conclusion

For the narrative of this dissertation, several conclusions from this chapter shall be highlighted:

A closed-form mathematical model of the thermohydraulics in PBDH networks was derived. It interlinks the energy management level (power flows), the technical level (temperatures, volumes flows, pressures) and the control level (control inputs, actuator behavior), considering also heat transfer from / to the secondary side. The mathematical model was implemented in an open-source python tool that solves an optimization problem for steady-state simulation of the PBDH network under investigation. Further, a Modelica-based modeling library has been developed, enabling rapid setup and dynamic simulation of various PBDH network configurations. Through the application of the developed models in case studies, alongside a synthesis of literature review and logical reasoning, a comprehensive paper describes eight key technical characteristics of PBDH networks from which challenges with respect to the network design, network control and the integration with thermal energy markets are derived.

One key observation is the high sensitivity and nonlinear behavior of the overall thermohydraulic network state in response to changes in control inputs from distributed actuators. Associated with that, the interdependence of operation points of these actuators was predicted and confirmed by simulations. A challenging phenomenom resulting from that is 'pump blocking', where the FP of one prosumer rises the differential pressure to a level that the FP of another prosumer is not able to overcome and therefore is blocked from feeding in. This blocking can also lead to hydraulic network splitting, forming smaller subnetworks. Pump blocking was examined in this chapter through simulations and has been validated experimentally in the CoSES lab, described in Pub2 (subsection 6.2.2). This specific effect is addressed also in the subsequent Chapter 8.

Pub6 notes also minor characteristic aspects of PBDH networks: One of them is transient cooling of the supply line and heating of the return line during prosumer mode switching. This is addressed in the literature by a bypass on the primary substation side, circulating the water within the substation until it reaches the appropriate temperature to be injected to the respective network line [77]. Another discussed aspect are the influence and limitation of local thermal energy market concepts, by the technical network implementation and control. Some technical details, such as temperature have to be considered in market (or other management) concepts to make meaningful and feasible decisions. This was also one conclusion from Pub1 (subsection 5.2.2), leading to a necessity to reflect some technical aspects within the control framework (see Section 5.1).

Another key obeservation are challenges associated with the a priori unknown flow directions in PBDH networks, due to their bidirectional nature and the (potentially) meshed topologies.
It was shown that this causes the modeling complexity to grow exponentially with the network size in terms of number of connections, which is usually proportional to the number of network participants. Further, it is stated that the beforehands unknown flow directions imply the need for adopted component dimensioning methods, which was already addressed by Pub3 (Section 6.3).
The observed mutual influence of prosumers argues for a central network controller. However, the inversion of the formulated mathematical simulation model to a control model was not accomplished, as the formulated optimization problem could not be solved analytically. Reasons are high nonlinearities in the heat transfer equations of the heat exchanger and the a priori unknown flow directions. For control purposes, the hydraulic and thermal subproblems cannot be the solved subsequently anymore, as the volume flows become variables of the thermal problem. There are approaches to solve this problem using simplifications, relaxations or heuristics. However, this leads to the flexibilties and intricacies of PBDH networks not being reflectled accurately enough for control purposes.

The inversion of the formulated mathematical simulation model for control purposes would have been necessary to derive a network model as a part of the originally targeted control framework A (presented in Section 5.1). Since this was not successful within the timeframe of the dissertation, the selection of control framework A was re-evaluated, leading to a shift of focus on control framework B. A more detailed argumentation with further aspects will be given in Section 8.1. The tasks of the network model in control framework A must therefore be taken over by the remaining layers in control framework B (see Section 5.1). For this purpose, advanced control algorithms at the field level are needed. This is discussed in the subsequent Chapter 8.

# Chapter 8

# Advanced Field Control

To leverage synergies within the network, the diverse participants in smart thermal grids, and specifically in PBDH networks, must be orchestrated by smart management. For this, substations are crucial, acting as the connection between the network and prosumer sides. An advanced field control for bidirectional prosumer substations is developed in Section 8.1 (Pub7) to facilitate compatibility with the coordinative management while pragmatically anticipating systemic interactions in a bidirectional network. Thus, in conjunction with Chapter 5, this chapter addresses the operational framework for smart thermal grids and, in particular, PBDH networks. Thereby, it focuses mainly on RQ3 from Section 2.2.

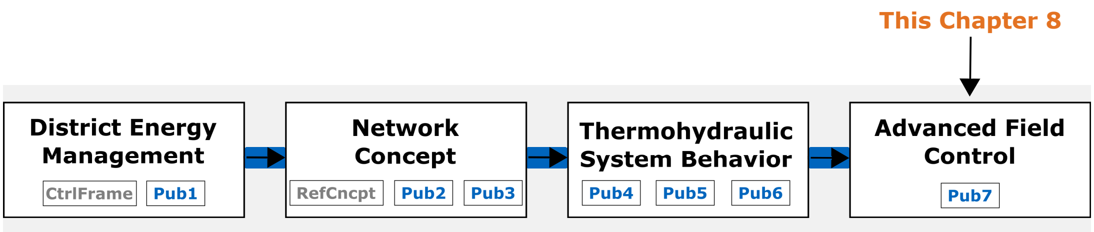


Figure 8.1: Position of this chapter within the overall structure of the main part of this dissertation.

**Chapter 8: Advanced Field Control**
The shift to a control framework without an explicit technical network model necessitates advanced control methods on the field level. For this purpose, a new field-level controller for bidirectional substations is developed and validated. This controller is engineered to interpret and execute directives from a management system, while managing the technical interactions among prosumers in the network. It combines weighted error functions with PID controllers, a strategy that balances multiple control objectives efficiently. Crucially, the controller anticipates the mechanics and systemic behaviors of the network. This allows for a seamless operation without relying on a technical network model or establishing direct communication links between substations. This pragmatic solution bridges the gap between high-level management and real-time operations on the field level. It ensures that PBDH networks can be operated cohesively and efficiently, aligning with the overarching objectives of smart thermal grid management while remaining flexible to the dynamic nature of network interactions.

## 8.1 Pub7: Control of bidirectional prosumer substations in smart thermal grids: A weighted proportional-integral control approach

### 8.1.1 Context

The preceding investigations revealed some disadvantages of the three-layer control framework A (see Section 5.1) that includes a technical network model at the automation layer:

- Computational complexity: Considering the thermohydraulic behavior and systemic interaction through a detailed network model leads to high computational complexity or the necessity of simplifications, i.e. the mathematical simulation model from subsection 7.1.2 could not be inverted analytically for control purposes.
- Modeling dynamics: Network models with acceptable computational complexity for control purposes do not capture dynamics. However, for the operation and control of real systems, especially the transient behavior is critical, therefore system dynamics need to be modeled.
- Communication effort: If distributed actuators are controlled with a central network model, ongoing communication between the actuators and the model-based controller is required. The more detailed the system dynamics are that the control anticipates, the higher the communication rate must be, which immensely increases the effort.

Due to the aforementioned reasons, control framework A was deemed impractical.

Control framework B, as introduced in Section 5.1, represents a bi-layer control approach [32], where on the management layer for the global operation, multi-energy optimal power flow problems are solved or market approaches are used. The resulting power setpoints for the feed-in or extraction to/from the network are communicated to the thermal prosumers, which have to implement them on the technical field layer. This offers the advantage of not requiring an explicit and computationally demanding network model at the automation layer. This leads to reduced computational complexity and communication efforts. As noted in Ref. [79], communication links are highly prone to errors and are a common cause of poor system performance in practical applications. So, a reduction of required communication is desirable. Furthermore, the dynamic behavior can be more effectively anticipated by controllers at the field level, since these local controllers are anyways engaged in high-frequency, iterative communication with the hardware.
However, with the elimination of the middle automation layer in the transition from control framework A to framework B, the tasks of this layer need to be redistributed among the remaining layers. This primarily involves considering technical requirements and limitations, as well as anticipating systemic network interactions and dynamic system behavior at the technical level.

The consideration of technical temperature limitations can be simply addressed by universally setting or assuming uniform temperature levels for both feed-in and consumption across the network. A certain temperature difference (e.g., 5 Kelvin) between these levels should be considered to account for for losses in the network and the necessary driving temperature difference of heat exchangers. Only producers who exceed the minimum feed-in temperature, or consumers who can operate with the minimum desired consumption temperature, should be allowed to participate in the network and be considered in the optimization of the district EMS. Similarly, requirements for achieving return temperatures can be set for consumers to ensure efficient operation of the producers. This approach is a simple and pragmatic solution, similar to that used in TDH networks. For various potential producers and consumers with different temperature requirements or characteristics, selecting appropriate temperature levels represents a distinct research question that requires further investigation. Objective functions could include enabling the largest possible energy exchange over the year or achieving the highest possible coverage of consumer demands in the district through the network.

Integrating the thermohydraulic aspects of prosumer interaction in detail into the district EMS would lead to similar effects as observed with the network model and the computational burden would rise drastically. Therefore, systemic interactions of prosumers on the technical level must be anticipated by the local controllers on the field level, when using control framework B. A key challenge is that controllers at the field level only possess local information in form of measurements but are required to anticipate network-wide interactions.
When using control framework B from Section 5.1, power setpoints from the district EMS must be processed directly at the field level. Here, a challenge is that the power setpoints from the EMS are composite quantities, affected by both, volume flows and temperatures (see Equation 3.10). These quantities are related, e.g. by the heat exchanger equations (Equation 3.8 - Equation 3.7). Further, the power setpoints have to be considered additionally to the traditional technical setpoints (temperatures) for the substation control, leading to the challenge that multiple quantities must be controlled with a limited number of actuators.

The subsequent Pub7 derives an advanced control method for bidirectional prosumer substations, in order to enhance the field-level controller for the main challenges introduced above: anticipates technical interactions of prosumers over the network and directly processing power setpoints from the overarching management. As context for the controller development, the reference network concept for PBDH from Section 6.1 is used, including the bidirectional substation configuration illustrated in Figure 6.4.

### 8.1.2 Paper

| | |
|---|---|
| **Title** | **Control of bidirectional prosumer substations in smart thermal grids: A weighted proportional-integral control approach** |
| **Authors** | Thomas Licklederer, Daniel Zinsmeister, Lorenz Lukas, Fabian Speer, Thomas Hamacher, Vedran S. Perić |
| **Publication medium** | Applied Energy, Volume 354, Part A, 15 January 2024, 122239 |
| **Copyright** | Included under Elsevier's copyright terms of 2023, which permit the inclusion in a thesis or dissertation provided the thesis is not published commercially. (https://www.elsevier.com/about/policies/copyright, Status: August 2023) |
| **Identifier / URL** | https://doi.org/10.1016/j.apenergy.2023.122239 |
| **Author contributions** | according to the Contributor Roles Taxonomy (CRediT, see [93]) |
| Thomas Licklederer | Conceptualization, Methodology, Software, Validation, Investigation, Writing - Original Draft, Visualization. |
| Daniel Zinsmeister | Conceptualization, Methodology, Validation, Writing - Review & Editing. |
| Lorenz Lukas | Investigation, Writing - Review & Editing. |
| Fabian Speer | Software, Writing - Review & Editing. |
| Thomas Hamacher | Resources, Supervision, Funding acquisition. |
| Vedran S. Perić | Writing - Review & Editing, Project administration. |

Applied Energy 354 (2024) 122239

Contents lists available at ScienceDirect

# Applied Energy

journal homepage: www.elsevier.com/locate/apenergy

# Control of bidirectional prosumer substations in smart thermal grids: A weighted proportional-integral control approach☆

Thomas Licklederer *, Daniel Zinsmeister, Lorenz Lukas, Fabian Speer, Thomas Hamacher, Vedran S. Perić

*Technical University of Munich (TUM), Center for Combined Smart Energy Systems (CoSES), Lichtenbergstraße 4a, 85748 Garching near Munich, Germany*

ARTICLE INFO

Dataset link: https://github.com/thomaslicklederer/ProsNet

*Keywords:*
District heating
Prosumer
Bidirectional
Substation
Heat transfer station
Control

ABSTRACT

In future smart thermal grids, decentralized prosumers shall supply each other over the network, optimized by an overarching management system. For this, the substation control must be able to directly process optimal power flow setpoints from the management, while considering the mutual influence of prosumers on the technical level. Addressing these requirements, this paper develops a control approach for bidirectional prosumer substations. Therefore, we identify the objectives and characteristics of the control problem, before relaxing it by reformulation. This enables to keep proportional–integral–derivative controllers (PIDs) for operating the pumps and valves as decentral actuators in the substations. We propose a control approach, exploring the combination of two key aspects: (1) The assignment of temperature objectives to actuators. (2) Weighted error functions that linearly combine temperature and power errors as input for the PIDs, allowing to handle multiple objectives with limited actuators. Through case studies, we validate the suitability of our proposed objective–actuator assignment and demonstrate the necessity and benefits of the weighted error functions. Like this, we conclude with a control approach for bidirectional prosumer substations that aims for the relevant temperature objectives, directly considers heat transfer setpoints, replicates and exploits the coupling within the network, effectively manages conflicting objectives, copes with prosumer interference, and is pragmatic for real-time operation. Our approach can be transferred to different network concepts, bridging the gap between decentralized field-level operation and the management level.

## 1. Introduction

Traditional district heating (DH) and district cooling (DC) systems are based on a centralized perspective; their control is demand driven with a focus on security of supply [1]. Central plants combined with a pumping station feed-in enough heat to compensate for the extraction and to keep the boundary conditions for the substation supply as constant as possible [2,3]. Consumer substations extract heat from the network by transferring it unidirectionally from the network (primary side) to the consumer (secondary side).

New concepts under the terms “4th and 5th generation district heating and cooling systems” (4&5GDHC) try to meet the upcoming requirements for future smart thermal grids [1,4,5]. Apart from lower network temperatures, two main trends can be observed: (1) A shift towards a decentralized perspective with prosumers in focus [1]. (2) A shift towards a holistic perspective with thermal grids being operated in an optimized way as an integrated part of a smart energy system (SES) [6]. These trends have significant impact on the operation of thermal grids.

Prosumers are decentral entities that can act as power consumer or producer to the network, evoking bidirectionality in thermal grids. Therefore, in 4GDH and 5GDHC systems bidirectional substations are equipped with decentral actuators (pumps and valves) [7,8]. With an increasing penetration of prosumers in the network, no longer the central plant and circulating pump determine the thermohydraulic network behavior. Instead, the overall system state is significantly influenced by the operation of the substations incl. their decentralized actuators. The most extreme case are networks only based on prosumers, with no central plant or pumping unit. The bidirectional substations are thermohydraulically coupled over the network, causing mutual influence on their operation states [9,10]. Therefore, substation

☆ The paper content was developed within the research project ‘Optimierte Sektorkopplung in Quartieren durch intelligente thermische Prosumernetze’, funded by the German Federal Ministry for Economic Affairs and Climate Action (FKZ:03EN3032A). The work of Vedran S. Perić was supported by Deutsche Forschungsgemeinschaft (DFG) through the project ‘Optimal Operation of Integrated Low-Temperature Birdirectional Heat and Electric Grids (IntElHeat)’ under Project number 450821044.

* Corresponding author.
*E-mail address:* thomas.licklederer@tum.de (T. Licklederer).

https://doi.org/10.1016/j.apenergy.2023.122239
Received 3 August 2023; Received in revised form 1 September 2023; Accepted 30 October 2023
Available online 8 November 2023

**Nomenclature**

**Symbols**

| | |
|---|---|
| $\alpha$ | weighting parameter |
| $\Delta$ | difference |
| $\dot{Q}$ | heat (power) flow |
| $\dot{V}$ | volume flow |
| $\varepsilon$ | weighted error |
| $p$ | pressure |
| $r$ | aggregated hydraulic resistance of attached circuit |
| $T$ | temperature |
| $u$ | system input (controller output) pump speed, valve opening |

**Sub-/Superscripts**

| | |
|---|---|
| 1 | primary side (network) |
| 2 | secondary side (building) |
| $con$ | consumption mode |
| $CP$ | consumption pump (secondary side) |
| $CV$ | consumption control valve (primary side) |
| $EP$ | extraction pump (primary side) |
| $FP$ | feed-in pump (primary side) |
| $norm$ | normalization value |
| $PP$ | production pump (secondary side) |
| $prim$ | primary side (network side) |
| $pro$ | production mode |
| $r$ | return line (cold) |
| $ref$ | reference, setpoint |
| $s$ | supply line (warm) |
| $sec$ | secondary side (prosumer side) |

coordination and control becomes an essential part of the network operation.

In traditional DHC, this substation control was limited to the technical level. For the optimized operation within SESs, the interaction of the substation control with the management level is essential to be compatible with hybrid control approaches [11]. On the management level for the global operation multi-energy optimal power flow problems are solved (e.g. [12,13]) or market approaches are used (e.g. [14–16]). The resulting power setpoints for the feed-in or extraction to/from the network are communicated to the thermal prosumers, which have to implement them on the technical field level. Therefore, substation controllers must be able to process and track optimal power flow setpoints from overarching management systems.

The changed requirements for network operation impose new challenges for bidirectional prosumer substation control, which are not yet adequately addressed in literature:

- The control needs to aim for multiple temperature objectives to meet consumer requirements in consumption mode and efficiently operate decentral heat generators in production mode. Despite the presence of multiple actuators in bidirectional substations, there is a lack of studies assessing the pros and cons of different ways to assign the objectives to these actuators.
- The substation control must anticipate dynamically changing and strongly intercoupled boundary conditions resulting from the mutual influence of prosumers. Undesired phenomena have to be handled, such as mutual blocking of feed-in pumps [9,17], supply frontiers with zero flow [18], and temporally as well as spatially fluctuating substation inlet temperatures [9]. Although a holistic network consideration is necessary for that, the literature on substation control mainly focuses on individual substations as the system boundary of investigations [7,8,19–24]. Thereby, the network states are assumed to be given as boundary conditions that are independent of the substation operation. Like this, in particular the hydraulic influence of prosumers over the network is neglected in the controller design.
- The substation control should be able to handle heat transfer setpoints from the management level. As the power objective and the temperature objectives are physically coupled, aiming for both at the same time can cause conflicting objectives due to a mismatch between them or due to unfavorable boundary conditions resulting from mutual prosumer influence. We are not aware of any studies that comprehensively address this aspect. Ref. [25] develops approaches to control heat flow and outlet temperature simultaneously, however assuming that the secondary side temperature difference is pre-known, thereby relaxing the control problem.
- The control approach should be versatile across various prosumer systems and network configurations. Existing approaches in literature are tailored for specific setups, like solar-thermal generation in traditionally operated networks [21,23,26], thus limiting their transferability. Further, controlling for pressure differences makes existing approaches dependent on the hydraulic characteristics and operation of the attached system, limiting the universality of the control behavior.
- For real-time control in a practical setting, a simple and fast reacting closed-loop method with little communication is needed. This argues for a decentralized and local control of the substations at the field level. A central controller for all actuators in a prosumer-network as attempted to derive in Ref. [27] can be seen more on the automation level, and is not pragmatic for the field operation.

Altogether, to the best of our knowledge, there is currently no comprehensive control approach for bidirectional prosumer substations that addresses the combined challenges of considering the mutual influence of prosumers in networks with high prosumer penetration and directly processing optimal power flow setpoints from the management level. Therefore, we aim to bridge this research gap by investigating suitable actuator-objective-assignments in combination with a proposed weighted error function approach for proportional–integral–derivative (PID) controllers. We consider a basic substation configuration representative for 4GDH systems and compliant with 5GDHC systems. We limit our scope to heat networks, assuming analogous transferability to cooling networks based on physical principles.

The remainder of the paper is structured as follows: In Section 2 we provide background on the substation thermohydraulics and introduce the network type under consideration. In Section 3 we outline the considered control system and identify the objectives as well as characteristics of the control problem. In Section 4 we propose a control approach with weighted PIDs and explore the objective–actuator assignment. In Section 5 we present case studies that evaluate the proposed control approach. In Section 6 a summary and conclusion on the findings & contribution completes the paper.

## 2. Background

This section introduces nomenclature, presents background on relevant thermohydraulics, outlines the network & substation configuration under consideration and provides related literature.

### 2.1. Thermohydraulics and nomenclature

Substations in DHC systems thermally couple and hydraulically decouple the primary side (network side, Index 1) from the secondary side (consumer/prosumer side, Index 2). The relevant quantities that determine the thermohydraulic state are (local) temperatures $T$, volume flows $\dot{V}$ and pressures $p$, as well as differences between these values. This is illustrated together with the main nomenclature in Fig. 1.

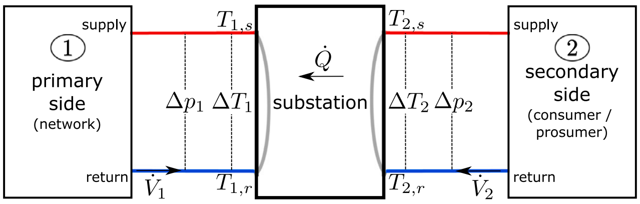


**Fig. 1.** Illustration of the main nomenclature.

We define the following sign convention:

$$\dot{V} > 0 \text{ for return } \rightarrow \text{ supply} \tag{1}$$

The temperature differences we define as:

$$\Delta T_1 = T_{1,s} - T_{1,r}; \quad \Delta T_2 = T_{2,s} - T_{2,r} \tag{2}$$

The pressure differences are defined accordingly.

Three elements dominate the substation behavior: heat exchanger, pumps and valves. Thus, the thermohydraulic substation behavior is covered by the following relations:

$$\dot{Q} = \dot{Q}_1 = \varrho_1 \cdot c_p \cdot \dot{V}_1 \cdot \Delta T_1 = -\dot{Q}_2 \tag{3}$$

$$\begin{bmatrix} T_{1,out} & T_{2,out} \end{bmatrix} = \mathcal{F}\left(T_{1,in}, T_{2,in}, \dot{V}_1, \dot{V}_2\right) \tag{4}$$

$$\dot{V} = \mathcal{G}(\Delta p) \tag{5}$$

$$\Delta p = \mathcal{H}\left(f_{pump}(\underline{u}), f_{valve}(\underline{u}), f_{hy-circ}\right) \tag{6}$$

The transferred heat results from the volume flows and temperature differences (Eq. (3)). The outlet temperatures of the heat exchanger are a function of the inlet temperatures of both sides and the volume flow on both sides (Eq. (4)). The heat exchanger behavior is linear in the inlet temperatures and highly nonlinear in the volume flow ratio of both sides [27]. For the exact equations, see Ref. [28]. The hydraulic operating state is described by the pressure differences and the volume flow in the attached circuits (Eq. (5)). It is determined by the intersection of the pressure source curve (i.e. pumps) and the pressure sink curve (i.e. valves and resistances), as represented in Eq. (6) and illustrated in Fig. 2.

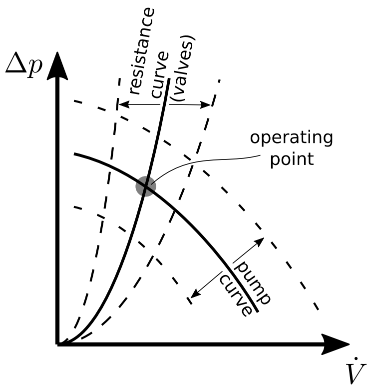


**Fig. 2.** Hydraulic operating point resulting from the intersection of the resistance curve and the pump curve of the respective hydraulic circuit.

These characteristic curves can be influenced by control signals $\underline{u} = [u_1\ u_2]^T$, opening or closing the valves and increasing or decreasing the pump speed. Like this, the hydraulic operating point in a circuit can be manipulated. Only certain hydraulic operating points are reachable, constrained by the characteristic behavior $f$ of the hydraulic circuit, the pumps and the valves (Eq. (6)). Through manipulation of the hydraulic operating point, volume flows can be controlled, thereby regulating the outlet temperatures and heat transfer of a heat exchanger in the circuit. Combining Eq. (4) with Eq. (3) relates the inlet temperatures and volume flows to the transferred heat. Higher volume flows lead to higher heat transfer, the same holds for a higher spread in the inlet temperatures. Only a certain set of combinations of transferred thermal power $\dot{Q}$ and outlet temperatures $T_{1,out}$ & $T_{2,out}$ are feasible, determined by the given inlet temperatures, the reachable volume flows and the heat exchanger physics.

### 2.2. Network and substation architecture

*Network architecture.* In prosumer-based networks, the effects of prosumer integration on the network and substation operation are maximal. Thus, these networks are ideal for investigating general control approaches for bidirectional prosumer substation operation that are then applicable also in networks with lower prosumer penetration. Prosumer-based networks can be seen as the thermal equivalent to smart electrical microgrids. The most relevant features for the following investigations are:

- all participants are prosumers (prosumer-dominated)
- no central units: no plant, no network pumps, no balancing units
- overarching management determines power setpoints for substations

We presented and modeled an underlying thermal network concept in Ref. [27].

*Substation architecture.* In the literature, various bidirectional substation designs [7,8,19] and associated variants for the feed-in to the network [29] are examined. Ref. [30] finds that for high fractions of decentral generation, specifically from solar panels, the return-to-supply feed-in principle is beneficial to others. Consequently, most studies covering bidirectional substations use similar functional principles for heat extraction and feed-in [19–24]. Based on the literature, we therefore consider in this paper a basic substation configuration (see Fig. 3) that features the commonly used functional principle:

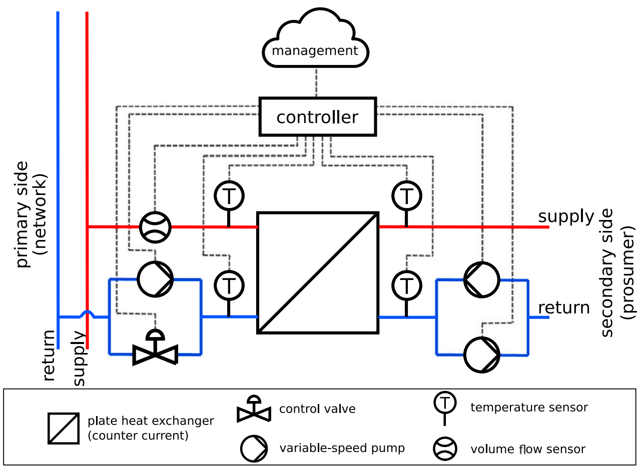


**Fig. 3.** Reference configuration for bidirectional substations of thermal prosumers. Simplified schematic, only relevant components for considerations in this paper are shown.

In consumption mode on the secondary side a consumption pump (CP) moves a flow from return to supply line of the prosumer system, while on the primary side the supply line is pressurized by producers in the network and a control valve (CV) regulates the flow through the substation from supply to return line. Some 5GDHC configurations use an extraction pump (EP) instead of the CV [31]. In production mode on the secondary side a production pump (PP) moves a flow from supply to return line of the prosumer system, while on the primary side a feed-in pump (FP) overcomes the differential pressure and regulates the flow through the substation from return to supply line.

In the following, prosumers that feed heat into the network at an observed point in time are called producers (pro), while those who extract heat from the network are called consumers (con), although each prosumer can switch between these modes over time.

### 2.3. Literature on bidirectional substation control

In traditional DH systems, the consumer substation control comprises mainly a PID-controlled valve on the primary side to achieve a secondary side outlet temperature Refs. [2,3]. On the secondary side, the heating circuit pump is operated at a constant speed in older systems or controlled according to the differential pressure in modern ones. Several papers aim to improve this conventional consumer substation control [32–36].

Concerning bidirectional substation control, the work most related to our paper is by Lottis et al. [25]. It develops two concepts to control substation heat flow and outlet temperatures simultaneously. Both use a feed-forward controller for the secondary side that converts the heat transfer setpoint into a mass flow setpoint, assuming the temperature difference on this side is known. However, usually both outlet temperatures are unknown and depending on the substation operation, as discussed in Sections 2.1 and 3.2.

In the context of decentral feed-in by solar thermal plants, several works explore bidirectional substation control strategies [19,21,23], with further applications seen in Refs. [20,22]. These strategies comprise traditional DH consumer substation control for consumption and tailored controls for solar thermal feed-in. Specifically, the PP control ensures that the temperature of the outflow is slightly above the desired network feed-in temperature, while the FP aims to achieve the primary side supply temperature.

Rosemann suggests [21] a cascaded closed-loop controller, with an inner loop for overcoming the differential pressure, while the outer loop controls the network supply temperature. Ref. [17] shows that the cascaded controller cannot cope with the challenge of pump blocking, when multiple prosumers interact in a network.

Ref. [37] proposes an agent-based control to track a constant supply temperature setpoint, while satisfying heat demands. A broker matches offers and demands from the agents centrally and gives a signal to the substations where decentral proportional controllers adjust valves and pumps. The controller behavior and the interaction of the controllers on the technical level remain unexplored.

Overall, few studies address generic control strategies for bidirectional substations and there is no established method. Most papers focus on determining optimized setpoints for the field-level control without detailing their technical implementation by actuator control. Further, the network behavior impacted by controller interactions is largely unexplored.

## 3. Problem statement

This section describes the targeted control problem for bidirectional substations in prosumer-based networks. The used nomenclature is illustrated in Fig. 1. The considered reference architecture for bidirectional substations was introduced in Section 2 and illustrated in Fig. 3. Due to the specific network concept, the entire network is operated by controlling the decentral prosumer substations.

### 3.1. Control loop

With the considered bidirectional substations, we face a multiple-input and multiple-output (MIMO) system (see Fig. 4). The principle functional relations of the system were outlined in Section 2.1. The exact transfer function is highly nonlinear, therefore considered as black box.

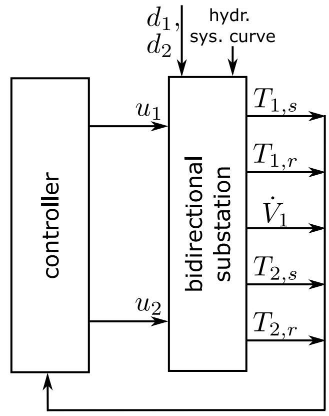


**Fig. 4.** Control loop with bidirectional substation as controlled system.

The manipulated variables of the system are the pump speed and valve opening in the substations. In each prosumer mode $(con,\ pro)$, one actuator (pump or valve) is active on each substation side $(1,\ 2)$, see also Fig. 3. The corresponding variables are controlled by the normalized control inputs $u_1$ and $u_2$. Output measurements are taken of the primary side volume flow and the four temperatures corresponding to the in- and outgoing flows on both substation sides. With these measurements, the temperature differences and the heat transfer can be calculated using Eqs. (2) and (3). The inflow temperatures to the substation are disturbances $d_1$, $d_2$ of the substation control system. For consumers, the secondary side return temperature $T_{2,r}^{con}$ is determined by the consumer's heating system, while for producers, the secondary side supply temperature $T_{2,s}^{pro}$ is influenced by the generation unit. The primary side inflow temperatures depend on the local thermohydraulic network state.

### 3.2. Control objective

The control objectives are summarized in Table 1 according to their priorities. There are three objectives for each prosumer mode: $T_{high\_prio}$, $\dot{Q}$, $T_{low\_prio}$. Aligning with this, two temperature control errors $e_{T,1}$ and $e_{T,2}$ for the primary and secondary side and a power control error $e_{\dot{Q}}$ can be defined in each mode. Ideally, the overall control objective is to bring these three errors to zero simultaneously.

**Table 1**
Control objectives for prosumers in different modes.

| Prio | Consumption | | Production | | gen. name |
|---|---|---|---|---|---|
| 1 | $T_{2,s} \overset{!}{=} T_{2,s}^{ref}$ | (7) | $T_{1,s} \overset{!}{=} T_{1,s}^{ref}$ | (8) | $T_{high\_prio}$ |
| 2 | $\dot{Q} \overset{!}{=} \dot{Q}^{ref}$ | (9) | $\dot{Q} \overset{!}{=} \dot{Q}^{ref}$ | (10) | $\dot{Q}$ |
| 3 | $\Delta T_1 \overset{!}{=} \Delta T_1^{ref}$ | (11) | $\Delta T_2 \overset{!}{=} \Delta T_2^{ref}$ | (12) | $T_{low\_prio}$ |

The individual control objectives can be understood most easily by looking at the simplest case of one producer supplying one consumer over the network. This is abstracted in Fig. 5 and will be explained in the following. An overarching management system defines the setpoint for heat transfer to/from the network as a reference that must be tracked by the substations (Eqs. 9 and 10). The technical systems of consumers (e.g. heating systems) usually require a certain minimum temperature for regular operation. High priority control objective for consumers is therefore to achieve a given secondary side supply temperature setpoint $T_{2,s}^{ref}$ (Eq. (7)). The supplying producer must ensure that the temperature provided to the network is high enough to meet the consumer's temperature requirements, accounting for potential losses at heat exchangers and within the network. High priority control objective for producers is therefore to achieve a given primary side supply temperature setpoint $T_{1,s}^{ref}$ (Eq. (8)). The generation units of producers

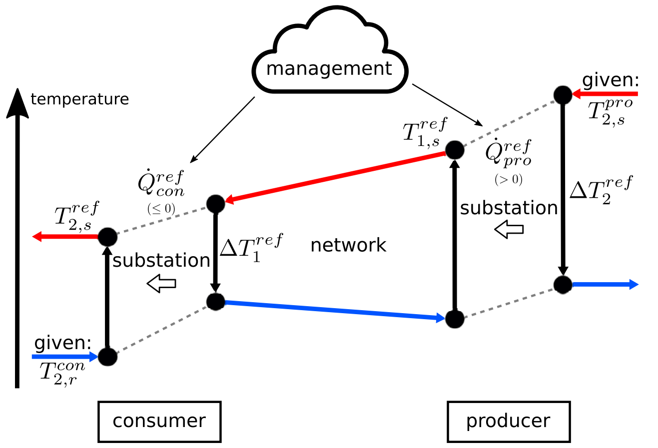


**Fig. 5.** Abstracted case of a producer supplying a consumer over the network: Illustration the control objectives and (given) disturbances for the operation of prosumer-dominated heat networks.

operate usually more efficiently at higher temperature differences. As the secondary side supply temperature is determined by the generation unit, the producer aims to achieve a certain secondary side temperature spread setpoint $\Delta T_2^{ref}$ (Eq. (12)). To be able to do so, the network return temperature needs to be low enough. This is influenced by the consumer. As the network supply temperature for the consumer is given, the consumer aims to achieve a certain primary side temperature spread setpoint $\Delta T_1^{ref}$ (Eq. (11)).

### 3.3. Characteristics

We want to highlight some characteristics of the control problem under investigation that a suitable control approach has to consider.

- There are multiple combinations of assigning the control objectives to the actuators on either the primary or secondary side. We identified three simultaneous objectives for each mode (Table 1), but there are only two actuators. Therefore, we cannot control one actuator for one objective to satisfy all objectives.
- There is a stiff coupling between the thermohydraulic states of all substations. Control actions in one substation affect the disturbances for the control of the others. Deviations from objectives in one substation are likely to cause deviations from objectives for other substations.
- The primary side inflow temperatures to the substations are disturbances for the individual substation control, but not for the closed producer–consumer system. The primary side temperature objectives (Eqs. 8 and 11) reflect this and interlink the different prosumers over the network.
- Achieving the different objectives of a single substation simultaneously can be conflicting, as the objectives are linked by Eqs. (3) and (4). In turn, deviations from one objective are likely to cause deviations from other objectives due to the interlink. Only certain combinations of transferred thermal power and outlet temperatures are feasible states, constrained by the disturbances and the thermohydraulic system properties (see Section 2.1).
- Unattainable power setpoints contribute to competing objectives. Heat losses and thermal inertia cause non-balancing heat transfer in the network, leading to deviations from ideal power flow calculations where often the determined heat transfer setpoints sum up to zero. The real-world physics results in producers meeting their setpoints while consumers cannot. If, on the other hand, losses and inertia are overestimated on the management level, the power setpoints for the producers are too high while the consumers extract just based on their demands — the producers cannot meet their setpoints.
- Individual pumps may be blocked from feeding in when multiple producers are involved, due to insufficient power to overcome the differential pressure caused by another producer and additional hydraulic losses caused by resistances. This phenomenon is known as pump blocking (see [9,17]).
- The control approach has to reflect the priority order of the temperature objectives (see Table 1).

## 4. Control approach

Heading for a suitable control approach, we start from the identified ideal control objective to reduce all three identified control errors $e_Q$, $e_{T,1}$ and $e_{T,2}$ to zero simultaneously. As we highlighted in the characteristics before, this might not be achievable for a significant range of operating conditions. Acknowledging that, we adopt a principle from the field of optimal control in order to shift to a relaxed formulation of the overall control objective: Minimizing an objective cost function $\varepsilon_{obj}$ that combines and weights multiple control errors:

$$\min_{\underline{u}} \quad \varepsilon_{obj}\left(e_Q, e_{T,1}, e_{T,2}\right) \tag{13}$$

The transferred heat $\dot{Q}$ is a common objective of both substation sides. We split the control for this common objective, resulting with individual control problems for each substation side.

$$\min_{\underline{u}} \varepsilon_1\left(e_Q, e_{T,1}\right) \quad \wedge \quad \min_{\underline{u}} \varepsilon_2\left(e_Q, e_{T,2}\right) \tag{14}$$

Instead of solving an optimization problem with an underlying system model, we combine the idea of weighted cost functions with proportional–integral–derivative (PID) controllers [38] as an established method for simple real-time control in the field. We propose to use one PID controller for each actuator in the controlled system, with a weighted error as input to each PID. This means there are four PIDs, of which two are always active depending on the respective prosumer mode. To account for the directional relation between control action and targeted control variable in the context of PIDs, we have to use weighted error functions that consider the signs of the incorporated errors. For the sake of simplicity we decide to use linear weighting using weights $K, G$. Thus, the weighted errors $\varepsilon$ can be calculated for the respective substation side $j$ and prosumer mode $i$ according to the following the scheme:

$$\varepsilon_j^i = \underbrace{K_j^i \cdot e_Q}_{E_Q} + \underbrace{G_j^i \cdot e_{T,j}^i}_{E_T} \;; \quad i \in \{con, pro\},\ j \in \{1,2\} \tag{15}$$

Fig. 6 illustrates the controller concept within the associated control loop.

The errors $e$ are calculated as the difference of the setpoint reference $r$ and the measurement feedback $f$. For the same behavior in consumption and production mode, despite negative heat transfer setpoints for consumption mode, $e_Q$ is defined as

$$e_Q = r_Q - f_Q = |\dot{Q}^{ref}| - |\dot{Q}| \tag{16}$$

The weights $K$, $G$ consist of two parts: a normalization part and a relative weighting part.

$$|K_j^i| = \frac{\alpha_j^i}{\dot{Q}^{nor}}, \qquad \dot{Q}^{nor} > 0,\ \alpha_j^i \in [0,1] \tag{17}$$

$$|G_j^i| = \frac{1-\alpha_j^i}{\Delta T^{nor}}, \qquad T^{nor} > 0,\ \alpha_j^i \in [0,1] \tag{18}$$

The signs of the weights $K$, $G$ in Eq. (15) depends on the directional relation between the controlled value and the control action — thereby they are related to assignment of objectives to actuators.

We propose to assign in both prosumer modes the transferred thermal power $\dot{Q}$ to the primary side actuators with higher priority, to reflect also the hydraulic coupling of different substations across the network. $T_{low\_prio}$ is assigned with lower priority to the primary side

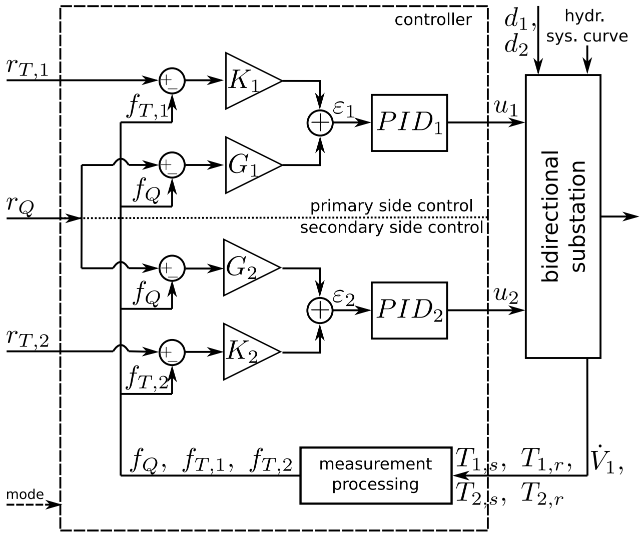


**Fig. 6.** Abstracted functional principle of the proposed controller within the according control loop. $r$ — references/setpoints, $\varepsilon$ — weighted error, $u$ — control input, $d$ — disturbance, $f$ — feedback, $K, G$ — weights.

**Table 2**
Proposed assignment of objectives to actuators for our control approach with weighted PIDs. Distinguishing from other variants, this assignment is called ctrl $D$ in the case studies.

| Mode | Actuator side | Proposed controller (D) | |
|---|---|---|---|
| con | **prim** | $\dot{Q}$ | $\Delta T_1$ |
| | **sec** | $T_{2,s}$ | $\dot{Q}$ |
| pro | **prim** | $\dot{Q}$ | $\Delta T_2$ |
| | **sec** | $T_{1,s}$ | $\dot{Q}$ |
| | | hi | lo |

actuator, while $T_{high\_prio}$ is assigned with higher priority and $\dot{Q}$ with lower priority to the secondary side actuator (see Table 2).

This leads to the following equations for our proposed controller to calculate the total weighted errors $\varepsilon_j^i$ depending on the prosumer mode $i \in \{con, pro\}$ and the substation side $j \in \{1, 2\}$:

$$\varepsilon_1^{con} = \underbrace{\left(+\frac{\alpha_1^{con}}{\dot{Q}^{nor}}\right)}_{K_j^i} \cdot \underbrace{\left(|\dot{Q}^{ref}| - |\dot{Q}|\right)}_{e_Q} + \tag{19}$$
$$+ \underbrace{\left(-\frac{1-\alpha_1^{con}}{\Delta T^{nor}}\right)}_{G_j^i} \cdot \underbrace{\left(\Delta T_1^{ref} - \Delta T_1\right)}_{e_{T,j}^i};$$

$$\varepsilon_2^{con} = \left(+\frac{\alpha_2^{con}}{\dot{Q}^{nor}}\right) \cdot \left(|\dot{Q}^{ref}| - |\dot{Q}|\right) + \tag{20}$$
$$+ \left(-\frac{1-\alpha_2^{con}}{\Delta T^{nor}}\right) \cdot \left(T_{2,s}^{ref} - T_{2,s}\right);$$

$$\varepsilon_1^{pro} = \left(+\frac{\alpha_1^{pro}}{\dot{Q}^{nor}}\right) \cdot \left(|\dot{Q}^{ref}| - |\dot{Q}|\right) + \tag{21}$$
$$+ \left(+\frac{1-\alpha_1^{pro}}{\Delta T^{nor}}\right) \cdot \left(\Delta T_2^{ref} - \Delta T_2\right);$$

$$\varepsilon_2^{pro} = \left(+\frac{\alpha_2^{pro}}{\dot{Q}^{nor}}\right) + \cdot \left(|\dot{Q}^{ref}| - |\dot{Q}|\right) + \tag{22}$$
$$+ \left(+\frac{1-\alpha_2^{pro}}{\Delta T^{nor}}\right) \cdot \left(T_{1,s}^{ref} - T_{1,s}\right);$$

In order to satisfy the objective priorities according to Table 2, the following must hold:

$$\alpha_1^{con}, \alpha_1^{pro} > 0.5; \tag{23}$$
$$\alpha_2^{con}, \alpha_2^{pro} < 0.5; \tag{24}$$

We suggest $\alpha_1^{con}, \alpha_1^{pro} = 0.75$ and $\alpha_2^{con}, \alpha_2^{pro} = 0.25$. In total, for the overall substation controller there are 6 parameters to be tuned additional to the 4 sets of PID gains.

### 4.1. Weighted error PIDs

In the following we elaborate on the rationale behind the weighted error functions. The basic idea behind the proposed weighted approach is to consider all three control objectives despite only two possible manipulated variables. By both substations aiming for the same transferred heat setpoint, the control approach mimics the physical thermal coupling of primary and secondary side across the heat exchanger. By taking into account the primary side temperature objectives, the thermal coupling across the network is also reflected in the control approach. The error weighting and summation is a relaxation of the stiff control problem that introduces elasticity to potentially conflicting objectives, one error can be compensated by others to reach an overall minimized weighted error. By the $\alpha$-parameters the relative importance of the objectives can be adjusted.

$\alpha > 0.5$ means that the according actuator is controlled with higher priority for the heat transfer power objective. Using extreme weights $\alpha \in \{0; 1\}$ leads to conventional PID-control with a single objective per actuator. By tuning the $\alpha$-values, also the relative weighting of the temperature objectives of the two substation sides can be adjusted. For this, the ratio of the $\alpha$-values of both substation sides is relevant: $\alpha_1/\alpha_2 < 1$ means that the temperature objective of the primary side actuator is weighted higher than the temperature objective that is assigned to the secondary side actuator. The normalization of the power and temperature errors with $\dot{Q}^{nor}$ and $\Delta T^{nor}$ makes the two errors dimensionless and defines the offset of how much a deviation of 1 K in the temperature control should affect the controller compared to a deviation of 1 kW in the heat transfer.

### 4.2. Objective–actuator assignment

Based on our research results, we proposed to assign in both prosumer modes the transferred thermal power $\dot{Q}$ to the primary side actuators with higher priority. However, there are in principle multiple ways to assign the different control objectives (Table 1) to the substation actuators on the two substation sides in the different modes. In the following we explore these possibilities, before in the next section we will compare our proposed approach through case studies to different controller variants in combination with the weighted error approach.

As a paradigm it is reasonable to set the substation side which controls for $T_{high\_prio}$ as the dominating side for temperature control ($\alpha < 0.5$), while the other side takes over the heat transfer power control with higher weighting ($\alpha > 0.5$). For the assignment of the $T_{high\_prio}$-objective to the two substation sides, two principles can be distinguished:

(a) Same-side control: The actuators are controlled for the temperature objective of the same substation side.
(b) Cross-over control: The actuators are controlled for the temperature objective on the opposite side of the substation.

Combined with the two prosumer modes (con, pro), there are four possibilities, resulting in four controller variants $A-D$ — see Table 3. Our proposed variant is $D$.

The signs of the weights $K$, $G$ in Eq. (15) for the weighted error depends on the directional relation between the controlled value and

**Table 3**
Controller variants with different assignments of the objectives to the substation side and thereby to the actuators. Variant D is highlighted as it is the proposed variant.

| Mode | Actuator side | A (cross-over cross-over) | | B (same-side same-side) | | C (cross-over same-side) | | D (same-side cross-over) | |
|---|---|---|---|---|---|---|---|---|---|
| con | **prim** | $T_{2,s}$ | $\dot{Q}$ | $\dot{Q}$ | $\Delta T_1$ | $T_{2,s}$ | $\dot{Q}$ | $\mathbf{\dot{Q}}$ | $\mathbf{\Delta T_1}$ |
| | **sec** | $\dot{Q}$ | $\Delta T_1$ | $T_{2,s}$ | $\dot{Q}$ | $\dot{Q}$ | $\Delta T_1$ | $\mathbf{T_{2,s}}$ | $\mathbf{\dot{Q}}$ |
| pro | **prim** | $\dot{Q}$ | $\Delta T_2$ | $T_{1,s}$ | $\dot{Q}$ | $T_{1,s}$ | $\dot{Q}$ | $\mathbf{\dot{Q}}$ | $\mathbf{\Delta T_2}$ |
| | **sec** | $T_{1,s}$ | $\dot{Q}$ | $\dot{Q}$ | $\Delta T_2$ | $\dot{Q}$ | $\Delta T_2$ | $\mathbf{T_{1,s}}$ | $\mathbf{\dot{Q}}$ |
| weight | | *hi* | *lo* | *hi* | *lo* | *hi* | *lo* | *hi* | *lo* |

**Table 4**
Signs of weights for calculating the weighted error $\varepsilon$.

| Mode | Actuator side | A (cross-over cross-over) | | B (same-side same-side) | | C (cross-over same-side) | | D (same-side cross-over) | |
|---|---|---|---|---|---|---|---|---|---|
| con | **prim** | + | + | + | − | + | + | + | − |
| | **sec** | + | + | + | − | + | + | + | − |
| pro | **prim** | + | + | + | − | + | − | + | + |
| | **sec** | + | + | + | − | + | − | + | + |
| | | $K$ $(e_Q)$ | $G$ $(e_T)$ | $K$ $(e_Q)$ | $G$ $(e_T)$ | $K$ $(e_Q)$ | $G$ $(e_T)$ | $K$ $(e_Q)$ | $G$ $(e_T)$ |

the control action — for example, if an increase in the pump speed increases or decreases the transferred heat. This relations result from the heat exchanger physics (see Section 2.1). Combining the heat exchanger physics with Table 3 leads to Table 4 which shows the signs of $G$ and $K$ for the respective controller variants.

Looking at high-priority objectives, the controller variant $A$ is comparable to the traditional control strategies of the district heating system. Yet, instead of controlling for $\dot{Q}$, the objective in the traditional systems is to achieve a certain reference pressure head $\Delta p_2$ (*con*) and $\Delta p_1$ (*pro*). The controller variant $C$ is related to the decentral feed-in control strategies for solar-thermal substations. However, traditionally in consumption mode again the pressure head is controlled instead of the transferred heat. In production mode, traditionally $T_{2,s}$ is controlled to avoid stagnation of the solar thermal panels, which is tailored to these specific systems. To the best of our knowledge, there are no comparable equivalents to controller variants B and D in existing thermal network control methods.

## 5. Case studies

In this section, we assess through case studies the performance of our proposed approach. We use simulations to compare the performance to the other possible controller variants (Table 3) and to assess the benefits of the weighted error functions (Eq. (15)) compared to a non-weighted approach. In the following, we present the case study setup, show and discuss results and finally evaluate the proposed approach.

For modeling and simulating we use the software tool *Dymola* in combination with the open-source library *ProsNet*[1] [39] which was adapted for this purpose. The performed simulations including setup and scenarios are integrated into the repository and therefore easily reproducible by the reader. The simulation results were analyzed with a resolution of 1 s. to capture the dynamic behavior. The dynamics of pumps and valves are considered by first-order filters in the models.

### 5.1. Setup

For the case studies we investigate a simple radial network with 3 prosumers, as illustrated in Fig. 7. This is the minimal setting to investigate the network behavior of multiple producers supplying one consumer over the network and vice versa. The four possible combinations in this setting are investigated by using the power setpoints timeseries shown in Table 5.

The component dimensioning is according to the set-up in the CoSES laboratory [24]. A methodology to dimension radial prosumer-based thermal networks is proposed by Speer et al. [40]. For the secondary side of all prosumers, we consider heating systems with design temperatures 50 °C / 30 °C. The secondary side generators are assumed to be designed for 55 °C / 35 °C. Assuming a temperature gradient of 1.5 $K$ across the heat exchanger, the objective primary side supply temperature in production mode results in 53.5 °C.

In the simulations, the hydraulic behavior of the primary side actuators (FP and CV) is replicated by detailed component models. The secondary side pumps (PP and CP) are modeled as ideal volume flow sources. This avoids detailed thermohydraulic simulation of a complete heating system and keeps the universality, as there are diverse options for secondary side configurations of prosumers (see [41]). To eliminate the thermal influence of the secondary side heating system, the secondary side inlet temperatures to the substation are artificially fixed to 55 °C/30 °C (prod/cons) depending on the prosumer mode. This means constant secondary side disturbances for the substation control, while the primary side disturbances change due to the mutual influence over the network.

Table 6 shows the default controller settings. The PID-tuning was done manually by trial-error, starting with time constants from technical data sheets of the pumps and valves. Further, for pump speed and valve openings we introduce lower boundary values that are greater than zero. This is meant to maintain temperature observability and to prevent the controllers from getting stuck. The controllers could get stuck, when incoming stream temperatures set boundary conditions that require decreasing volume flows to achieve desired outflow temperatures. If volume flows become too low or zero, temperatures stop changing as thermal energy is transported by the moving fluid and the controller cannot observe and control the system anymore, but also has

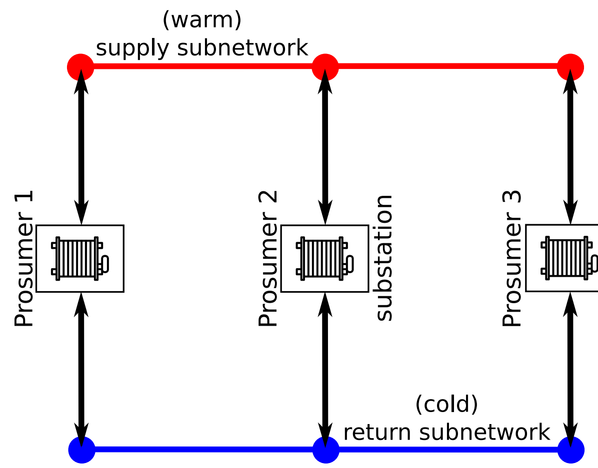


**Fig. 7.** Illustration of the considered network concept for prosumer-based heat networks. A simple exemplary network with 3 prosumers.

**Table 5**
Power setpoints and modes for case studies.

| Time [h] | Pros1 | | Pros2 | | Pros3 | |
|---|---|---|---|---|---|---|
| | [kW] | [mode] | [kW] | [mode] | [kW] | [mode] |
| 0–1 | −10 | (cons) | +4 | (prod) | +6 | (prod) |
| 1–2 | −6 | (cons) | +10 | (prod) | −4 | (cons) |
| 2–3 | +6 | (prod) | −10 | (cons) | +4 | (prod) |
| 3–4 | +10 | (prod) | −4 | (cons) | −6 | (cons) |

[1] https://github.com/thomaslicklederer/ProsNet

**Table 6**
Default controller settings for simulative case studies.

| Parameter | Value | Unit | Parameter | Value | Unit | Parameter | Value | Unit |
|---|---|---|---|---|---|---|---|---|
| General | | | Consumption | | | Production | | |
| $\dot{Q}^{nor}$ | 1 | kW | $T_{2,s}^{ref}$ | 50 | °C | $T_{1,s}^{ref}$ | 53.5 | °C |
| $\Delta T^{nor}$ | 3 | K | $\Delta T_1^{ref}$ | 20 | K | $\Delta T_2^{ref}$ | 20 | K |
| $\dot{V}_2^{max}$ | 8.5 | l/min | PID prim cons | | | PID prim prod | | |
| | | | $\alpha_1^{cons}$ | 0.75 | – | $\alpha_1^{prod}$ | 0.75 | – |
| | | | $k_1^{cons}$ | 1.5 | – | $k_1^{prod}$ | 1.5 | – |
| | | | $T_{i,1}^{cons}$ | 35 | s | $T_{i,1}^{prod}$ | 8 | s |
| | | | $T_{d,1}^{cons}$ | 0 | s | $T_{d,1}^{prod}$ | 0 | s |
| | | | PID sec cons | | | PID sec prod | | |
| | | | $\alpha_2^{cons}$ | 0.25 | – | $\alpha_2^{prod}$ | 0.25 | – |
| | | | $k_2^{cons}$ | 1.5 | – | $k_2^{prod}$ | 1.5 | – |
| | | | $T_{i,2}^{cons}$ | 8 | s | $T_{i,2}^{prod}$ | 8 | s |
| | | | $T_{d,2}^{cons}$ | 0 | s | $T_{d,2}^{prod}$ | 0 | s |

no incentive to move out of this state. The lower boundaries for the control signals avoid this.

For the case studies we vary different aspects:

- system configuration (1-3)
- controller variant (ctrl *A*- ctrl *D*)
- $\alpha$-value tuning (*a*-*c*)

By combination, this leads in total to 36 scenarios that are named accordingly, e.g. *'2.D.c'*.

The three different system configurations are:

1: without heat losses, properly dimensioned pumps
2: with heat losses, properly dimensioned pumps
3: without heat losses, smaller pumps

Configuration *1* is an idealized benchmark setting. Under configuration *2* the controller performance can be investigated under non-balancing heat transfer in the network.

In configuration *3*, the smaller pumps provoke the occurrence of pump blocking in the network. Like this, the suitability of the controllers for the identified characteristics of the control problem can be tested.

As introduced in Section 4, there are four possible controller variations with different assignments of the substation actuators to the temperature objectives (see Table 3). To compare their performance, all four controllers *A*–*D* were investigated.

Further, $\alpha$-values are varied, according to the following scheme to analyze the influence of the error weighting.

a: $\alpha_Q = 1.000$, $\alpha_T = 0.000$
(no weighting, single objective PID control)
b: $\alpha_Q = 0.666$, $\alpha_T = 0.333$
c: $\alpha_Q = 0.750$, $\alpha_T = 0.250$
(proposed tuning)

### 5.2. Results & discussion

We assess the performance of the controllers focusing on two aspects: (I) Which controller variant (objective–actuator assignment) is best? (II) What benefits or downsides does the error weighting have?

*Controller variants*

*Analysis method.* To analyze the simulation results, the deviations from the control objectives are particularly relevant. These are assessed using the Mean Absolute Errors (MAE) [42] for the power objective as well as the high- and low-priority temperature objectives, averaging across all prosumers in the simulated network and over time. This results in three metrics for each simulated scenario (see right graphs of Fig. 8).

To obtain a single key performance indicator (KPI) for the different tested controllers and parameter tunings, we first combine the three MAEs by building a Root Mean Square Error (RMSE) out of them (see left graph of Fig. 8). Averaging over all simulation configurations for one controller variant, including parameter tuning leads to the KPIs in Table 7.

**Table 7**
RMSE of the simulated scenarios for the different investigated controller variants (A, B, C, D) and parameter tunings (a, b, c) as key performance indicators (KPI) for the controllers.

| | *A* | *B* | *C* | *D* |
|---|---|---|---|---|
| *a* | 2.36 | 2.99 | 2.50 | 3.26 |
| *b* | 2.49 | 2.90 | 3.38 | 2.06 |
| *c* | 2.54 | 2.74 | 3.44 | 1.92 |

*Main result.* Table 7 shows that summarized across all simulated scenarios our proposed controller *D.c* outperforms the other controllers, as it achieves the lowest KPI. In the following, we analyze and explain the performance of the different controller variants and parameter tunings, based on the observed MAE illustrated in Fig. 8.

*Controller A.* (ctrl *A*) performs poorly under system configuration *2* with heat losses, showing high errors for $\dot{Q}$ and for $T_{high\_prio}$ compared to the other controllers. The main reason for that is the behavior of the consumers in the network: Due to the heat losses, the heat transfer setpoint $\dot{Q}^{ref}$ is unachievable for the consumers, therefore $|\dot{Q}^{ref}|-|\dot{Q}| < 0$. Using cross-over control in consumption mode, ctrl *A* speeds up the CP to raise $|\dot{Q}|$ by increasing $\dot{V}_2$. This decreases $T_{2,s}$, which is controlled by the CV on the network side. In the simulated cases, the max. achievable $\dot{V}_1$ by opening the CV is not enough to satisfy $T_{2,s}^{ref}$. Like this, ctrl *A* can neither achieve the heat transfer objective, nor the high-priority temperature objective with low errors. This is unexpected, as ctrl *A* (i.e. ctrl *A.a*) is related to control strategies that are successfully used in traditional DH. However, an essential difference between ctrl *A* and traditional DH control is that ctrl *A* controls for $\dot{Q}$, whereas in traditional DH the controlled variable in production mode is $\Delta p$. The (central) producer in traditional DH aims for a certain minimum differential pressure in the worst-point of the network, independently from the feed-in power. Thereby it provides higher volume flows $\dot{V}_1$ and allows the substation control to reach $T_{2,s}^{ref}$ by opening the CV. Our control approach uses power setpoints directly to be compliant with high level district energy management. The FP operates at medium level, as $\dot{Q}^{ref}$ is achieved for producers, leading to $\dot{V}_1$ being too low to reach $T_{2,s}^{ref}$. In other words, due to the control logic, the ratio $\dot{V}_1/\dot{V}_2$ is too low to achieve $T_{2,s}^{ref}$, resulting in the observed high errors for $T_{high\_prio}$.

*Controller B.* (ctrl *B*) performs poorly under system configuration *3* with small dimensioned pumps, showing high errors for all objectives, compared to the other controllers. The main reason for that is the behavior of the producers in the network: Ctrl *B* uses same-side control in production mode. To raise $T_{1,s}$ for achieving the setpoint reference, the FP is slowed down. One of the pumps is at the low speed not able to overcome the local differential pressure anymore. The pump is blocked from feeding in, as the volume flow $\dot{V}_1$ reaches zero. $T_{1,s}$ stays too low and the blocked FP is trapped in this operating point as the control logic says to slow down the speed further in order to increase $T_{1,s}$.

*Controller C.* (ctrl *C*) is a combination of the consumption control principle of ctrl *A* and the production control principle of ctrl *C*. Therefore it combines the negative effects and high errors, that ctrl *A* shows under configuration *2* with heat losses and the negative effects that ctrl *B* shows under configuration *3* with small dimensioned pumps. Ctrl *C* is related to the control strategies of decentral feed-in with solar thermal plants. Facing the pump-blocking challenge for feed-in, extra mechanisms are usually added here to overcome the local differential pressure.

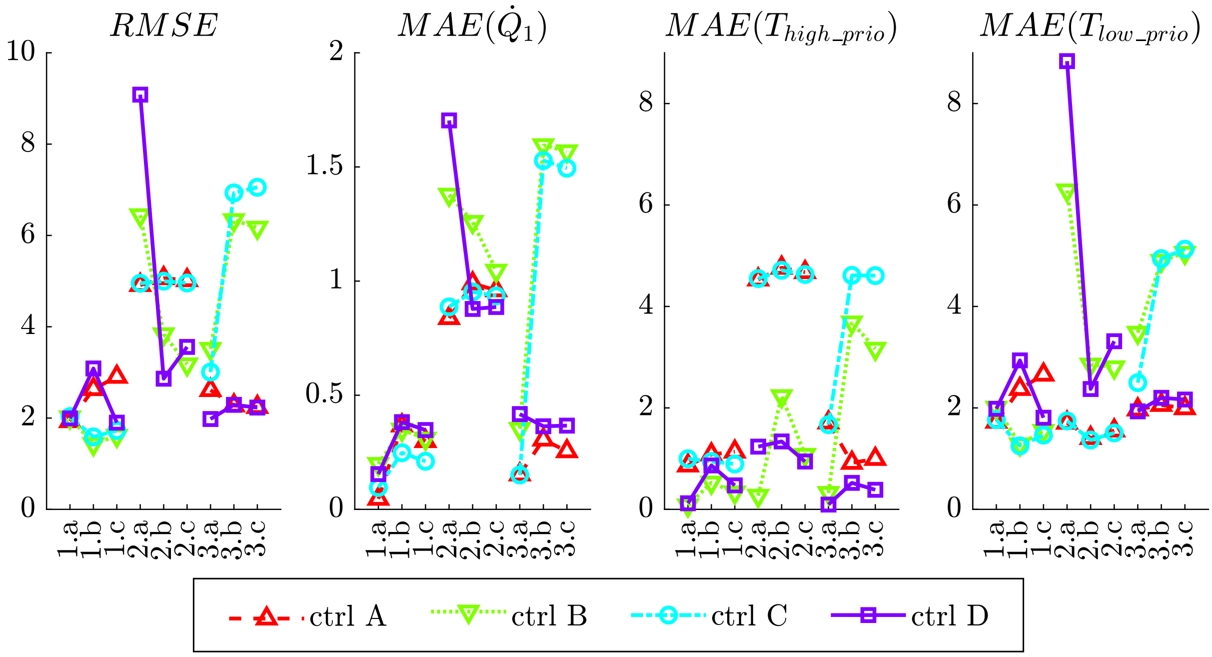


**Fig. 8.** Summarized errors of all simulated scenarios, averaged over time and over all three prosumers in the simulated network. Scenarios are named according to the explanation in Section 5. The three graphs on the right show the MAE values of the errors with respect to the three objectives. The left figure shows the RMSE error, composed of the errors of the three right graphs.

*Controller D.* (ctrl *D*) is our proposed controller variant. It is a combination of the production control principle of ctrl *A* and the consumption control principle of ctrl *C*. Therefore it combines the positive behavior of both controllers and compared to them shows low errors in all settings — except for tuning *D.a* without error weighting, which will be analyzed in detail in the next subsection. The main reason for the generally good performance of ctrl *D* is that it uses the primary side actuators to control for $\dot{Q}$ with higher priority in both modes. In consumption mode, the CV on the primary side opens widely to achieve $\dot{Q}^{ref}$. The CP on the secondary side can be operated independently from that to achieve $T_{2,s}$. In production mode, using the primary side actuators to control for $\dot{Q}$ with high weighting makes sure that the feed-in pump (FP) of a producer is speeded up as soon as its volume flow (and thus transferred heat) goes to zero — this avoids pump blocking. Like this, controller *D* makes use of the heat transfer reference $\dot{Q}$ being a coupling element of the producers and consumers in the network.

*Weighted error functions*

*Main result.* We found that among the four studied objective–actuator assignments, only the proposed ctrl *D* is suitable for our application case. However, ctrl *D* without error weighting ($\alpha$-tuning *a*) exhibits very high errors for $\dot{Q}$ and $T_{low\_prio}$ under system configuration *2*. Using the weighted error functions in ctrl *D.b* & *D.c* leads to a significant improvement (see Fig. 8). This underlines the necessity and benefits of using the proposed weighted error approach.

*Analysis method.* To illustrate and analyze the effects of error weighting, we use graphs that show the power error $e_Q$ over the temperature errors $e_T$ of a specific steady-state of one simulation scenario (see Fig. 9). The weighting is represented in these graphs by a straight line that depicts all combinations of $e_Q$ and $e_T$ satisfying the weighted error $\varepsilon$ to be zero. The slope $s$ of the line indicates the relative weighting and depends on the $\alpha$-tuning. Its absolute value is defined by

$$|s| = \frac{|G|}{|K|} = \frac{\dot{Q}^{nor}}{\Delta T^{nor}} \cdot \frac{(1-\alpha)}{\alpha} \tag{25}$$

The slope is positive or negative, depending on the signs in Table 4. The slopes are different for the primary and the secondary side, depending on the respective $\alpha$-values. The shortest distance of a point to the line of $\varepsilon = 0$ represents the weighted error $\varepsilon$ that is aimed to be minimized by the controller. The value of $e_Q$ is always the same on the primary side and the secondary side as the heat transfer power physically couples the two sides — this is exemplarily illustrated for one operation point by the dotted line in Fig. 9. Further, by arrows in Fig. 9 the influence of changes to the control variables $\dot{V}_1$ and $\dot{V}_2$ and to the primary side inlet temperatures are illustrated. These relations directly follow from the heat exchanger physics described in Section 2. The origin of the coordinate system $(e_Q, e_{T,1}, e_{T,2}) = (0,0,0)$ is the ideal operating point that minimizes all errors and thereby achieves all objectives simultaneously. Any optimal operating point lies on the $\varepsilon = 0$ line with slope $s$.

*Analyzed sample.* In order to explain the reasons behind the necessity and benefits of the error weighting, we compare in the following the behavior of ctrl *D.a* to the behavior of ctrl *D.b* & *D.c* under system configuration *2*. Under system configuration *2* the consumer control is decisive due to the unachievable heat transfer setpoints, because of heat losses in the network. Therefore, we investigate in depth the influence of the $\alpha$-tunings on the steady-state when prosumer 1 and 3 are consumers and prosumer 2 is in production mode (hour *1–2*). Table 8 shows the according control signals and volume flows, while Fig. 9 explains the controller behavior determined by the absolute errors w.r.t. the objectives and the weighted error functions.

Looking at Fig. 9 Fig. 10, for controller variant *D* the slope of the line $\varepsilon = 0$ is positive in consumption mode and negative in production mode. Decreasing the volume flows by the same factor while keeping the ratio constant increases $e_Q$ for both substation sides and vice versa (see arrow markers in Fig. 9). A higher $T_{1,s}$ decreases both errors for both substation sides — however this primary side inlet temperature cannot be controlled directly and is a given disturbance for the isolated substation control. Considering only the behavior of a single substation, an in-/decrease of the volume flow ratio influences $e_{T,1}$ and $e_{T,2}$ in opposite directions (see arrow markers in Fig. 9). Due to this opposite effects of changes to the volume flow ratio and the coupling by $\dot{Q}$, there is only a single operating point that simultaneously satisfies $\varepsilon_1 = 0$ and $\varepsilon_2 = 0$. This is the optimal operating point.

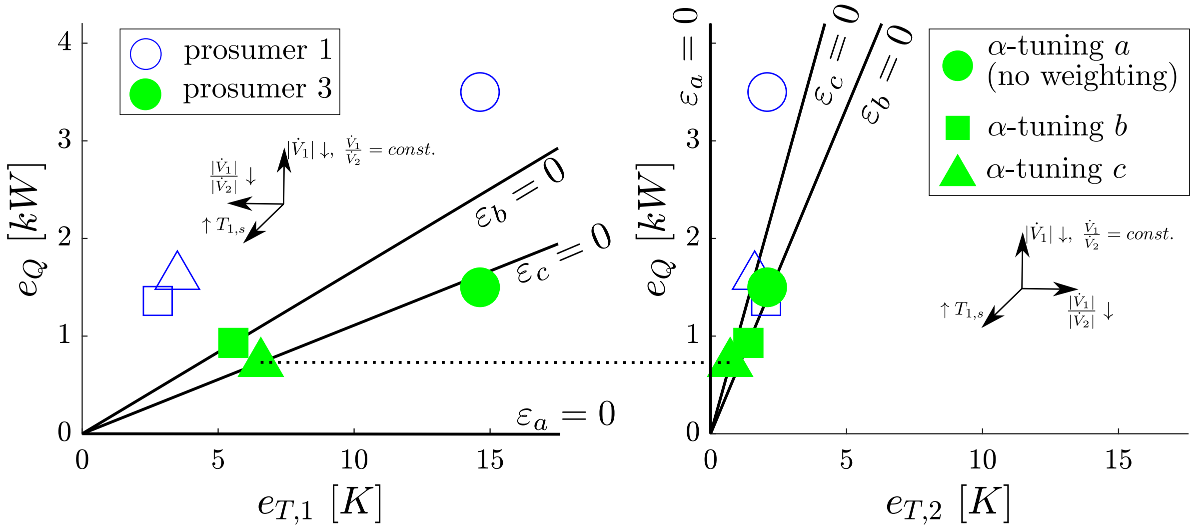


**Fig. 9.** Absolute errors in transferred heat over the relevant absolute temperature errors (left: primary side, right: secondary side). Observed is the simulation case *2.D* in the steady-state of simulation hour *1–2*. The different shapes of the markers represent the different $\alpha$-tunings. Unfilled markers in blue represent operation points of prosumer 1, filled markers in green represent prosumer 3 — these are the two consumers in the observed scenario (see Table 5).

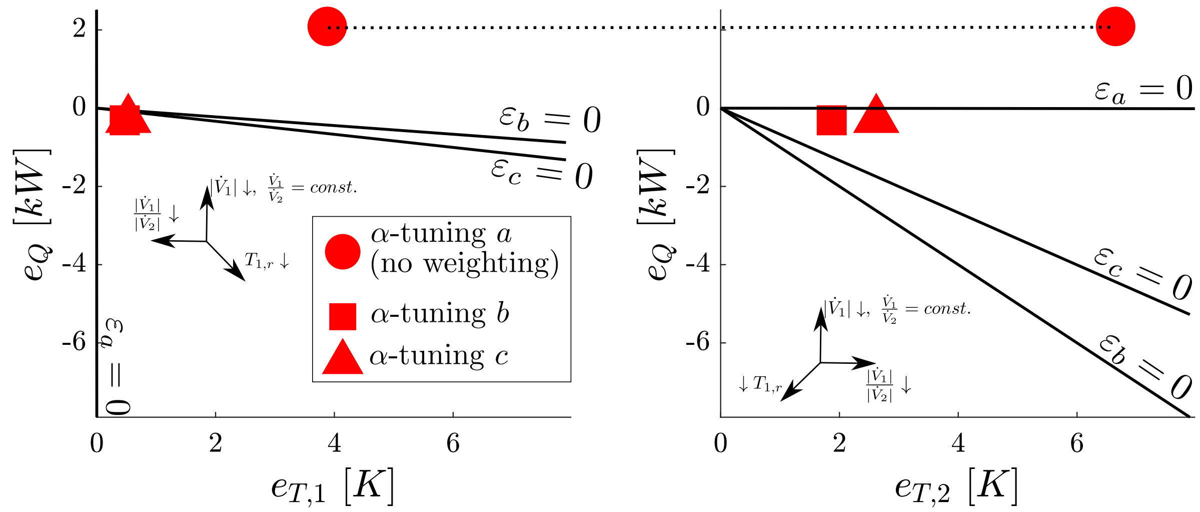


**Fig. 10.** Absolute errors in transferred heat over the relevant absolute temperature errors (left: primary side, right: secondary side). Observed are the simulation cases *2.D* in the steady-state of simulation hour *1–2*. The different shapes of the markers represent the different $\alpha$-tunings. The figure illustrates operation points of prosumer 2, the producer in the observed scenario (see Table 5).

*Abstract impact of error weighting.* Without weighted errors ($\alpha$-tuning $a$), the optimal point is at the same time the ideal operating point — the origin of a coordinate system. However, the origin is not reached, as we see in Fig. 9. To improve $e_Q$, an increase of both volume flows would be necessary, while to improve $e_{T,2}$ the ratio $\dot{V}_1/\dot{V}_2$ would have to be increased. This could only be achieved by increasing $\dot{V}_1$ proportionally more than $\dot{V}_2$. This is not possible, as all primary side control signals $u_1$ are already at 100% (Table 8). The control is stuck, the ideal and optimal operation point cannot be reached. Even with bigger pumps and higher volume flows, $e_Q = 0$ would not be reachable, as the producer feeds in the requested heat, but due to heat losses in the network the same amount of heat will never reach the consumer. Introducing error weighting ($\alpha$-tuning $b$ and $c$) relaxes the control problem as $e_Q \neq 0$ can be accepted and compensated by $e_T \neq 0$ to still achieve an overall weighted error of $\varepsilon = 0$. In the graphs of Figs. 9 and 10, the optimal point that satisfies $\varepsilon_1 = 0$ and $\varepsilon_2 = 0$ simultaneously is shifted away from the ideal operating point in the origin. With weighted errors the controller for consumption also considers $\Delta T_1$, which couples it to the control of the producers and allows to indirectly manipulate the former disturbance $T_{1,s}$.

*Concrete impact of weighting on analyzed sample.* In the simulation results we see that due to the weighted error functions, ctrl *D.b* and ctrl *D.c* reduce $\dot{V}_1/\dot{V}_2$ to increase $\Delta T_1$, which reduces $e_{T,1}$ for the consumers. This is done by closing the CV of the consumer with lower power demand (pros 3) (see Table 8). The CV of the consumer with the highest demand (pros 1) stays opened completely, which is efficient from a pumping point of view as it avoids unnecessary pressure losses in the network. The CP of the consumers are speeded up for higher heat transfer. Together with the increased $\Delta T_1$ this reduces $e_Q$ for the consumers. The increased $\Delta T_1$ at the consumers, decreases the primary side inlet temperature $T_{1,r}$ for the producer and the controller of the producer reduces $\dot{V}_1$ and $\dot{V}_1/\dot{V}_2$ by slowing down the FP for satisfying $T_{1,s}^{ref}$ (see Fig. 10). Due to the increased $\Delta T_1$, the producer can with reduced $\dot{V}_1$ achieve $\dot{Q}^ref$ with lower $e_Q$.

Due to the matching signs for the error weights in producer mode (see Table 4), the slope for $\varepsilon = 0$ is negative, meaning $e_Q$ and $e_T$ must have opposite sings the compensate each other. Like this, producers are motivated to over-perform in the supplied heat (negative $e_Q$) in order to compensate for temperature errors. This controller characteristic is good, as it intrinsically anticipates heat losses in the network.

**Table 8**
Steady-state values of controller outputs $u_1$ and $u_2$, resulting volume flows and primary side inlet temperatures under system configuration *2*, comparing controllers *D.a* (without weighting) to *D.b* & *D.c* (with weighting). Situation with two consumers and one producer, power setpoints are in the first row for each prosumer.

| | | 2.$D.a$ | 2.$D.b$ | 2.$D.c$ |
|---|---|---|---|---|
| Pros 1 (con) | $Q^{ref}$ | −6 kW | −6 kW | −6 kW |
| | $u_1$ | 100% | 100% | 100% |
| | $\dot{V}_1$ [$l/min$] | −6.7 | −3.9 | −3.8 |
| | $u_2$ | 24% | 44% | 40% |
| | $\dot{V}_2$ [$l/min$] | −2 | −3.7 | −3.4 |
| | $\dot{V}_1/\dot{V}_2$ | 3.35 | 1.05 | 1.11 |
| | $T_{1,s}$ [°$C$] | 47.9 | 49.9 | 49.8 |
| Pros 2 (prod) | $Q^{ref}$ | +10 kW | +10 kW | +10 kW |
| | $u_1$ | 100% | 54% | 56% |
| | $\dot{V}_1$ [$l/min$] | 13.4 | 6.9 | 7.3 |
| | $u_2$ | 100% | 95% | 100% |
| | $\dot{V}_2$ [$l/min$] | 8.5 | 8.2 | 8.5 |
| | $\dot{V}_1/\dot{V}_2$ | 1.58 | 0.84 | 0.86 |
| | $T_{1,r}$ [°$C$] | 41.1 | 31.6 | 32.8 |
| Pros 3 (cons) | $Q^{ref}$ | −4 kW | −4 kW | −4 kW |
| | $u_1$ | 100% | 35% | 55% |
| | $\dot{V}_1$ [$l/min$] | −6.7 | −3 | −3.5 |
| | $u_2$ | 24% | 28% | 29% |
| | $\dot{V}_2$ [$l/min$] | −2 | −2.4 | −2.4 |
| | $\dot{V}_1/\dot{V}_2$ | 3.35 | 1.2 | 1.46 |
| | $T_{1,s}$ [°$C$] | 47.9 | 49.1 | 49.6 |

*Further insights.* It is noticeable that not all weighted operating points for both consumers and producers are at $\varepsilon = 0$. Due to insufficient heat supply caused by heat losses in the network that are not taken into account in the setpoints and due to competing influences of volume flow changes on the controlled variables, not all control objectives can be simultaneously achieved. In the case of prosumer 1 (con), the primary side temperature difference shifts the operating points away from $\varepsilon = 0$, while for prosumer 2 (prod) it is the secondary temperature difference. As desired, the weighted control assigns higher priority to the secondary supply temperature $T_{2,s}$ for the consumers, while for the producer, higher priority is given to the primary supply temperature $T_{1,s}$. Additionally, as desired, the relative importance between temperature objectives of one substation can be adjusted through different $\alpha$-tunings. $\alpha$-tuning $c$ is slightly more balanced compared to tuning $b$ since the values are closer to 0.5.

### 5.3. Evaluation

As outcome of the conducted case studies, we find that our proposed ctrl $D$ is the only suitable objective–actuator assignment and must be combined with the presented weighted error functions to be effective for the targeted use case.

The simulation results show that the proposed approach relaxes the control problem to cope with insufficient supply when having balanced setpoints from the management, but heat losses in the network. Further, we see how our approach makes use of the coupling of prosumers across the network and thereby allows to indirectly manipulate the primary side inlet temperatures for consumers, which would otherwise not be accessible and stay a disturbance that cannot be influenced. Also, the weighted control intrinsically motivates producers to supply a bit more heat than requested by the balanced setpoints. Consequently, they intrinsically anticipate heat losses in the network. Like this, improved operation points, closer to the setpoints can be achieved than without weighting.

## 6. Summary and conclusion

Subject of this paper is to develop a suitable control approach for bidirectional prosumer substations, that is able to directly process setpoints for the heat transfer power and to cope with the characteristics of prosumer networks. To do so, we considered prosumer-based heat networks without central generation, balancing or pumping units and assumed a prosumer substation configuration based on common feed-in & extraction principles from the literature and in compliance with 4&5GDH. We defined and relaxed the control problem. We chose proportional–integral–derivative (PID) control and proposed a weighted error function approach that combines heat transfer setpoints with temperature objectives. We investigated different variants of assigning temperature objectives to actuators. Through simulative case studies, we compared the performance of different controllers. Finally, we proposed and evaluated a suitable approach.

The proposed control approach has the following distinguishing properties:

- It aims for all technically relevant temperature objectives of the control problem. Using parameters of the weighted error approach, the relative importance of the temperature objectives to each other can be adjusted.
- It directly processes and tracks heat transfer setpoints for the substation control and is therefore compliant with overarching management systems. By not utilizing pressure difference as a means of indirect control for volume flows and hence transferred power, but rather directly utilizing power values as the control variable, the proposed control approach is less reliant on the associated hydraulic circuit and thus system-agnostic.
- It manages conflicting objectives by utilizing weighted error functions, which allow for deviations from specific objectives in order to minimize overall deviation from the ideal operating point. This enables the controller to handle inherent control errors arising from unattainable setpoints, which contribute to conflicting control objectives. In particular, the controller can handle power setpoints that are unachievable due to insufficient consideration of network losses at the management level.
- It copes with the prosumer interaction within the network, even without direct communication or coordination between substations. We showed that the proposed objective–actuator assignment successfully avoids pump blocking. Further, we showed that the proposed control approach leverages the intrinsic representation of physical network mechanics (see above) to indirectly and favorably influence network boundary conditions that would otherwise not be manipulable. As a result, significantly improved operation is achieved compared to non-weighted control.
- It is pragmatic for direct application on the field-level. It can be implemented using standard PID controllers, one for each actuator. Therefore it is agnostic to the concrete actuator. It is capable of real-time operation and takes into account the dynamic behavior of the components. Only simple measurement processing is needed for calculating the weighted errors, involving basic operations like addition and multiplication. There is no need for an internal system model, complex calculations, or communication between substations.

For future work, the dynamic controller behavior can be analyzed, covering also experimental studies to investigate the interaction with real devices. A sensibility analysis w.r.t the $\alpha$- and PID- tuning can help to identify the optimal controller parameters for different setups. Adding online-learning methods to dynamically adapt the controller parameters can further improve the control performance. Control-theoretical analyses of the control system with and without controller can help to understand the stability boundaries.

The main contributions of this paper are:

- We provide a systematic analysis of the control problem of bidirectional prosumer substations in smart thermal grids, revealing objectives and characteristics of the problem. Based on this, we conduct the first systematic study on the assignment of the different temperature objectives to the multiple actuators in bidirectional substations.
- We identified and validated a suitable controller for bidirectional prosumer substations that considers the mutual influence within the network. The controller can be applied not only in the purely prosumer-based networks but also in networks with less prosumer penetration. Further, the principles can be transferred to other network concepts, such as 5GDHC systems due to the independence from specific actuators and technical systems along with the universality of the feed-in and extraction principles.
- We bridge the gap between management level and field-level control in prosumer networks: The suggested control approach enables direct processing and implementation of heat transfer setpoints in substation control. It allows to control each substation as an independent unit without communication or coordination among them, while still considering the mutual influences.

With our contributions, we advance the understanding and implementation of effective control strategies in the evolving landscape of decentralized district heating systems as a part of future smart energy systems.

## CRediT authorship contribution statement

**Thomas Licklederer:** Writing – original draft, Visualization, Validation, Software, Methodology, Conceptualization. **Daniel Zinsmeister:** Writing – review & editing, Validation, Methodology, Conceptualization. **Lorenz Lukas:** Writing – review & editing, Investigation. **Fabian Speer:** Writing – review & editing, Software. **Thomas Hamacher:** Supervision, Resources, Funding acquisition. **Vedran S. Perić:** Writing – review & editing, Project administration.

## Declaration of competing interest

The authors declare that they have no known competing financial interests or personal relationships that could have appeared to influence the work reported in this paper.

## Data availability

The modelica simulation models that implement the proposed control approach and are used for the case studies in the paper are publicly available in a github repository, https://github.com/thomaslicklederer/ProsNet.

## Declaration of Generative AI and AI-assisted technologies in the writing process

During the preparation of this work the author(s) used *ChatGPT* by OpenAI and *DeepL Translator* by DeepL SE in order to improve language and readability. After using this tool/service, the author(s) reviewed and edited the content as needed and take(s) full responsibility for the content of the publication.

## References


[1] Buffa S, Cozzini M, D'Antoni M, Baratieri M, Fedrizzi R. 5th generation district heating and cooling systems: A review of existing cases in Europe. Renew Sustain Energy Rev 2019;104:504–22.

[2] Nussbaumer T, Thalmann S, Jenni A, Ködel J. Planungshandbuch Fernwärme. 2021, p. 1–230.

[3] Frederiksen S, Werner S. District heating and cooling. Professional Publishing Svc; 2013.

[4] Lund H, Werner S, Wiltshire R, Svendsen S, Thorsen JE, Hvelplund F, et al. 4Th generation district heating (4GDH). Energy 2014;68:1–11.

[5] Angelidis O, Ioannou A, Friedrich D, Thomson A, Falcone G. District heating and cooling networks with decentralised energy substations: Opportunities and barriers for holistic energy system decarbonisation. Energy 2023;269(September 2022):126740.

[6] Mathiesen BV, Lund H, Connolly D, Wenzel H, Ostergaard PA, Möller B, et al. Smart Energy Systems for coherent 100 solutions. Appl Energy 2015;145:139–54.

[7] Paulus C, Papillon P. Substations for decentralized solar district heating: Design, performance and energy cost. Energy Procedia 2014;48:1076–85.

[8] Lamaison N, Bavière R, Cheze D, Paulus C. A multi-criteria analysis of bidirectional solar district heating substation architecture. In: Proceedings of SWC2017/SHC2017. Freiburg, Germany: International Solar Energy Society; 2017, p. 1–11.

[9] Licklederer T, Zinsmeister D, Elizarov I, Perić V, Tzscheutschler P. Characteristics and challenges in prosumer-dominated thermal networks. J Phys Conf Ser 2021;2042(1):012039.

[10] Brand L, Calvén A, Englund J, Landersjö H, Lauenburg P. Smart district heating networks – A simulation study of prosumers' impact on technical parameters in distribution networks. Appl Energy 2014;129:39–48.

[11] Vandermeulen A, van der Heijde B, Helsen L. Controlling district heating and cooling networks to unlock flexibility: A review. Energy 2018;151:103–15.

[12] Geidl M, Andersson G. Optimal power flow of multiple energy carriers. IEEE Trans Power Syst 2007;22(1):145–55.

[13] Bytschkow D, Capone A, Mayer J, Kramer M, Licklederer T. An OPC UA-based energy management platform for multi-energy prosumers in districts. In: 2019 IEEE PES innovative smart grid technologies Europe. IEEE; 2019, p. 1–5.

[14] Frölke L, Sousa T, Pinson P. A network-aware market mechanism for decentralized district heating systems. Appl Energy 2022;306(PA):117956.

[15] Wang N, Liu Z, Heijnen P, Warnier M. A peer-to-peer market mechanism incorporating multi-energy coupling and cooperative behaviors. Appl Energy 2022;311:118572.

[16] Huynh T, Schmidt F, Thiem S, Kautz M, Steinke F, Niessen S. Local energy markets for thermal-electric energy systems considering energy carrier dependency and energy storage systems. Smart Energy 2022;6:100065.

[17] Elizarov I. Analysis, modelling and control strategy development for prosumer-based heat networks (Ph.D. thesis), Technical University of Munich; 2020.

[18] Paulick S, Schroth C, Guddusch S, Rühling K. Resulting effects on decentralized feed-in into district heating networks - a simulation study. In: Energy procedia, Vol. 149. Elsevier Ltd; 2018, p. 49–58.

[19] Pipiciello M, Caldera M, Cozzini M, Ancona MA, Melino F, Di Pietra B. Experimental characterization of a prototype of bidirectional substation for district heating with thermal prosumers. Energy 2021;223:120036.

[20] Sdringola P, Ricci M, Ancona MA, Gianaroli F, Capodaglio C, Melino F. Modelling a Prototype of Bidirectional Substation for District Heating with Thermal Prosumers. Sustainability 2023;15(6):4938.

[21] Rosemann T, Löser J, Rühling K. A new DH control algorithm for a combined supply and feed-in substation and testing through hardware-in-the-loop. Energy Procedia 2017;116:416–25.

[22] Heymann M, Rosemann T, Rühling K, Tietze T, Hafner B. Concept and measurement results of two decentralized solar thermal feed-in substations. Energy Procedia 2018;149:363–72.

[23] Lennermo G, Lauenburg P, Werner S. Control of decentralised solar district heating. Sol Energy 2019;179:307–15.

[24] Zinsmeister D, Licklederer T, Adldinger S, Christange F, Tzscheutschler P, Hamacher T, et al. A prosumer-based sector-coupled district heating and cooling laboratory architecture. Smart Energy 2023;9(February):100095.

[25] Lottis D, Kallert A. Simulative comparison of concepts for simultaneous control of heat flow and outlet temperature of heat exchangers for highly flexible use in the test facility "District LAB". Energy Inf 2022;5:16.

[26] Hassine IB, Eicker U. Control aspects of decentralized solar thermal integration into district heating networks. Energy Procedia 2014;48:1055–64.

[27] Licklederer T, Hamacher T, Kramer M, Perić VS. Thermohydraulic model of Smart Thermal Grids with bidirectional power flow between prosumers. Energy 2021;230:120825.

[28] Roetzel W, Spang B. C1 thermal design of heat exchangers. In: VDI heat atlas. Berlin, Heidelberg: Springer; 2010, p. 31–66.

[29] Ancona M, Branchini L, Di Pietra B, Melino F, Puglisi G, Zanghirella F. Utilities substations in smart district heating networks. Energy Procedia 2015;81:597–605, 69th Conference of the Italian Thermal Engineering Association, ATI 2014.

[30] Beckenbauer D, Ehrenwirth M, Klärner M, Zörner W, Cheng V. Validation of a district heating system model and simulation-based investigation of bidirectional heat transport by decentralised solar thermal plants. In: Proceedings of SWC2017/SHC2017. 2007. Freiburg, Germany: International Solar Energy Society; 2017, p. 1–12.

[31] Abugabbara M, Javed S, Johansson D. A simulation model for the design and analysis of district systems with simultaneous heating and cooling demands. Energy 2022;261:125245.

[32] Gustafsson J, Delsing J, van Deventer J. Improved district heating substation efficiency with a new control strategy. Appl Energy 2010;87(6):1996–2004.

[33] Guelpa E, Marincioni L. Demand side management in district heating systems by innovative control. Energy 2019;188:116037.

[34] Lazarević S, Čongradac V, Anđelković AS, Čapko D, Kanović Ž. A novel approach to real-time modelling of the district heating substation system using LabVIEW. J Clean Prod 2019;217:360–70.

[35] Sun C, Chen J, Cao S, Gao X, Xia G, Qi C, et al. A dynamic control strategy of district heating substations based on online prediction and indoor temperature feedback. Energy 2021;235:121228.

[36] Chaudhry AM, Lezaun NP, Fontes FACC, Bram S. Model predictive control of a substation of a district heating system for enhanced environmental and economic performance. In: International conference on applied energy 2021. Vol. 21. 2021, p. 1–6.

[37] Bünning F, Wetter M, Fuchs M, Müller D. Bidirectional low temperature district energy systems with agent-based control: Performance comparison and operation optimization. Appl Energy 2018;(October):502–15.

[38] Astroem KJ, Haegglund T. PID controllers : Theory, design, and tuning. International Society for Measurement and Control, Research Triangle Park, N.C.; 1995.

[39] Elizarov I, Licklederer T. ProsNet – a Modelica library for prosumer-based heat networks: description and validation. J Phys Conf Ser 2021;2042(1):012031.

[40] Speer F, Licklederer T, Zinsmeister D, Perić VS. Dimensioning radial prosumer-based thermal networks. In: 13. Internationale Energiewirtschaftstagung an der TU Wien. No. 1. 2023, p. 1–15.

[41] Zinsmeister D, Licklederer T, Christange F, Tzscheutschler P, Perić VS. A comparison of prosumer system configurations in district heating networks. Energy Rep 2021;7:430–9, The 17th International Symposium on District Heating and Cooling.

[42] Willmott C, Matsuura K. Advantages of the mean absolute error (MAE) over the root mean square error (RMSE) in assessing average model performance. Clim Res 2005;30:79–82.

## 8.2 Chapter Conclusion

For the narrative of this dissertation, several conclusions from this chapter shall be highlighted:

Based on the insights gained in the preceding chapters, the focus was shifted from control framework A to control framework B for the operation of PBDH networks. Both structures were initially presented in Section 5.1. Control framework B follows a two-layer approach with a district EMS at the top layer and substation field controllers at the bottom layer.
In this context an advanced control method for bidirectional prosumer substations was developed in Pub7. The approach uses weighted error functions paired with PID controllers. A distinct assignment of the control objectives to the different available substation actuators is chosen based on systematic investigations. In combination, this allows the substation controllers to directly process optimal power flow setpoints from an overarching management system, while anticipating the technical interplay of prosumers within the network. Temperature limitations are addressed by setting required temperatured levels for feed-in and extraction, assuming that the participation prosumers are technically capable to guarantee these temperature levels.

The weighted error functions handle multiple objectives for one actuator and relax the control problem. Although the management layer and the field control are interlinked by the communicated power setpoints, they are just losely coupled due to the weighted error approach. This allows the proposed field controller to handle also power setpoints which are unachievable due to insufficient consideration of technical constraints at the management level (like e.g. losses or temperature levels). The substation controllers converge automatically to an operating point which is as close as possible to the given setpoints under the chosen weighting. The exact weighting can be adopted with parameters to the specific need and characteristics of the individual network setup. Additionally, the included PID controllers allow for the anticipation of the dynamic component and system behavior.

Another speciality of the proposed controller is that the systemic technical interactions between the substations over the network is anticipated without a distinct communication link between the substations. Instead the controller makes use of the intrinsic representation of physical network mechanics to indirectly and favorably influence network boundary conditions that are not manipulable without communication using conventional control approaches.

With the features described above, the proposed controller offers a pragmatic solution to bridge the gap between high-level management and real-time field-level operations in innovative district heating networks with prosumers. Bridging this gap allows to effectively operate PBDH networks with the proposed two-layer control framework B, comprising an overarching smart management and the proposed advanced substation field controller.

# Part IV
# Conclusion and Outlook

# Chapter 9

# Conclusion

The integration of distributed generation and the concept of prosumers are essential aspects of smart thermal grids as sustainable and efficient parts of future smart energy systems. This dissertation studies prosumer-based district heating (PBDH) networks as an archetype of smart thermal grids to advance their general technical implementation and operation. Therefore, three investigated research questions (see Section 2.2) were addressed as follows.

**RQ1** asks for a reference network concept that facilitates the technical implementation of the PBDH principle.

Based on preceding literature and comprehensive reasoning, an appropriate reference network concept for PBDH networks was proposed. It comprises specific network paradigms and a bidirectional prosumer substation configuration. Together, this builds the foundation for further technical investigations. The reference network concept was implemented in the CoSES laboratory environment at TUM, allowing for the safe and flexible testing of advanced control strategies in interaction with real hardware under close-to-reality conditions. A dimensioning method for PBDH networks with linear topologies was presented, allowing for the dimensioning of pipes, pumps, valves, and heat exchangers as the most relevant components.

It was found that PBDH networks with small prosumers show high hydraulic resistances at low required volume flows. This imposes particular challenges for designing and efficiently operating decentralized pumps in prosumer substations. Current DH system pumps are inefficient for this purpose. Costly over-sizing of pumps, limiting the network size and energy exchange, or restricting the feed-in to big producers are potential solutions. Further, it is revealed that bidirectional flows and dynamically changing hydraulic circuits make it complex to determine the reference 'worst case' for component dimensioning, especially in networks without linear topologies.

**RQ2** focuses on the technical system behavior of PBDH networks, depending on the operation of the distributed actuators.

As a basis for studying this aspect, a closed-form mathematical model of the thermohydraulics in PBDH networks was derived. Unlike other models, the proposed model incorporates heat transfer to/from the secondary side, the hydraulic behavior of pumps and valves, and the mode-switching of prosumers. This allows to analyze how distributed actuator operation and prosumer boundary conditions affect the technical network operation. The derived model was implemented in Python, resulting in a software tool for steady-state simulation of PBDH networks. Based on this, a Modelica library was developed, facilitating the rapid setup and dynamic simulation of various PBDH network configurations. Utilizing the developed models in case studies, combined with literature synthesis and logical reasoning, provided a thorough overview of technical characteristics of PBDH networks.

It was found that the complexity of network modeling scales exponentially with the number of connections and participants due to a priori unknown flow directions in the network. Further, it was shown how the overall thermohydraulic network state emerges from the interference of the distributed actuator operation. It responds highly sensitively and nonlinearly to changes in their operating points. Associated with that, the interdependence of the operation points of these actuators was predicted and confirmed by simulations. Specific systemic effects, such as 'pump blocking', were predicted and showcased in simulations and experiments. From these compiled characteristics of PBDH networks, several challenges were derived for network design, control, and integration of smart thermal grids. Anticipating systemic interference effects by specialized operation methods is identified as crucial for the overall network functionality.

**RQ3** aims to develop an appropriate control framework for the seamlessly integrated operation of PBDH networks from the management to the field level.
For this, the main control tasks were identified and allocated to two control frameworks that were explored: a two-layer and a three-layer structure. Both incorporate a district-level EMS responsible for network coordination and synergy exploitation. A software prototype was developed and validated for optimizing power flows in districts in interaction with hardware during live operation. Initially, the three-layer control architecture was favored, focusing on converting the mathematical network simulation model into a middle-layer control model to anticipate systemic technical effects occurring from the interaction of distributed actuators. However, replicating all technical aspects in a comprehensive network model proved impractical for control purposes due to high computational complexity and the need for high-resolution temporal communication to anticipate system dynamics. As a result, the idea of a network control model was discarded in favor of the simpler two-layer architecture, which includes only central management and distributed field control. Nonetheless, the technical network behavior must still be anticipated within the control framework, as purely power-based models were proven insufficient for the practical implementation in experimental studies using the district EMS tool. In response, an advanced field-level controller for bidirectional prosumer substations was developed, considering the identified characteristics and challenges of PBDH networks. It uses weighted PID controllers to manage heat transfer power setpoints from the management level, alongside temperature setpoints as technical requirements. The PID controllers enable the handling of dynamic behaviors. Due to the problem relaxation by error weighting and a specific actuator to objective assignment, the control incorporates a model-free representation of physical network mechanics. Thereby, it can anticipate systemic technical interactions between the substations over the network without distinct communication links between the substations.
Overall, the developed control framework features distributed technical control coordinated by abstract power flow optimization without relying on a complex technical network model. This framework is modular, and the power setpoints provide a universal interface, facilitating interchangeability on the different layers and enabling integration with other methods and models.

**Broader context** Upon the investigation of prosumer-based district heating networks, it's evident that they are an idealized niche concept suitable only for particular contexts. The studies on hydraulic system behavior indicate that these networks are particularly suited for smaller systems with a limited number of participants (e.g., 3-15) and smaller network extents. However, as prosumers are the most generic network participants, insights from PBDH networks apply to smart thermal grids in general. With an increasing share of decentralized participation and increasing flexibility, focusing on small scales or limited interaction is crucial for managing hydraulic issues. Appropriate application contexts include small, self-contained areas like campuses, industrial sites, residential complexes, compact villages with diverse sources and sinks, or smaller mixed urban districts. More centralized network concepts are preferable for broader coverage in cities or large districts. A hybrid model with multiple hierarchical layers (see outlook in Chapter 10) could leverage the benefits of smart thermal grids at small scales while allowing for the coverage of an extended area. Another related direction are 5GDHC systems with a high co-occurrence of heating and cooling demands supplied by prosumers over a shared network with very low temperatures.

**Contribution** The concept of smart thermal grids and prosumer-based district heating (PBDH) in particular opens the potential to use distributed (renewable) generation and to utilize synergies between various network participants and across energy sectors, thereby making thermal energy supply more integrated, efficient, and sustainable. However, this introduces increased complexity in network implementation and operation.

> **Contribution**
> This dissertation investigates the design, analysis, and operation of PBDH networks as archetypes of smart thermal grids. Thereby, it provides valuable insights into the complexities of network implementation and operation induced by flexibilization and decentralization. To address the inherent technical complexities, this dissertation introduces a comprehensive control framework, including effective control methods. These methods enhance systemic efficiency by exploiting synergies with overarching optimization and ensure technical viability by implementing the optimized trajectories on the field level in real-time operation.
> Therefore, this dissertation contributes to a deeper understanding of the dynamics within smart thermal grids, especially concerning the intricate interactions among participants on the technical level. This reveals the limits of technical feasibility for decentralized and bidirectional DH networks and permits inferences about technically sensible application areas. These insights guide future research and offer starting points for economic-regulatory assessments funding on the technical system feasibility. Overall, this dissertation advances the technical implementation and operation of smart thermal grids.

With its contributions, this dissertation paves the way for the potential and theoretical benefits of smart thermal grids to be leveraged practically in the field. Ultimately, this promotes a more sustainable thermal energy supply in the future.

# Chapter 10

# Outlook

The investigations and insights of this dissertation build a solid foundation for future research endeavours. Potential starting points in form of aspects that emerged from the conducted investigations will be outlined in the following.

Potential future research directions on the **design and dimensioning** of smart thermal grids:

- Development of an efficient method for dimensioning PBDH networks with various topologies (radial, meshed, mixed). All possible network states and combinations of flow directions have to be considered. Possibly an optimization-based approach is suitable, similar to the ones described in Ref. [63], [64]. An alternative approach can be to simplify complex topologies into combinations of linear networks using the method presented in this dissertation.
- Formulation of a method for selecting appropriate unified temperature levels for feeding into and extracting from a network that connects diverse participants with different temperature requirements or characteristics. Dynamically changing temperature levels over different periods in the year can be considered, as suggested in [119]. Potential objectives could be to maximize energy exchange over the year or to achieve the highest possible coverage of consumer demands in the district through the network.
- Investigation on the series connection of two pumps for decentralized feed-in to enable high pressure differences at low flow rates while operating each pump at an efficient operating point (see also subsection 6.2.3).
- Examination of the technical transformation of existing TDH networks into networks with distributed generation and/or prosumers. Assess to what extend the existing network infrastructure can be re-utilized or how it would need to be modified from a technical point of view.
- Derivation of reference networks that are representative for benchmarking algorithms and operational frameworks, offering a standardized basis for comparison. Accessing detailed information and data from existing systems can be challenging for researchers and developers. The reference networks should therefore include topologies, technical design specifications, and (synthetic) operational data. The fundamental research question is to determine the essential features that reference networks must possess to be effective for benchmarking purposes. An initial step is a comprehensive categorization of existing networks, as done for example in [37], [45].
- Studying hierarchical thermal networks. This is particularly relevant since it was concluded that several hydraulic constraints make PBDH networks more suited for small scale networks. Within an hierarchical approach, multiple small PBDH networks can be part of an interconnecting infrastructure. There are first considerations for two approaches: An analogy to the transmission and distribution level in electrical networks - manageable hydraulic units at the distribution level are

separated by heat exchangers from the transmission level [120]. Cascaded DH networks, where sub-networks are connected to one line of the superordinated network [121]–[125].

Potential future research directions on the **operation and control** of smart thermal grids:

- Experimental validation of the developed weighted PID approach for bidirectional prosumer substations using actual hardware. The CoSES laboratory (see Section 6.2) is well suited for this type of investigation. Develop and establish best practices for tuning the PID and their weighting parameters in this specific context. Additionally, compare the performance of the proposed substation controller with other approaches, e.g. those detailed in Ref. [126].

- Examination of the stability of the proposed weighted PID approach in networks with many participants and conduct a sensitivity analysis. First steps in this direction were made by Ref. [127]. Other related literature is Ref. [128], [129]

- Investigation of the proposed weighted PID in the context of 5GDHC networks and innovative network concepts other than PBDH networks. While the PBDH concept's generality suggests potential transferability of the weighted PID approach, specific characteristics of booster heat pumps in 5GDHC may affect the performance and necessitate unique tuning.

- Analysis of operational aspects of prosumers in 4GDH and 5GDHC systems to derive a common hardware configuration that allows general investigations and statements for these most relevant network types.

- Exploration of methods for automated network state estimation and error analysis in DH networks, leveraging limited field measurements. Techniques such as anomaly detection could be employed to automatically pinpoint errors or sources of inefficiency, like poorly balanced hydraulic conditions in customers. Essential factors include accuracy of estimation from available data, suitability of the model (physical, black box, grey box), types of errors, and reliability in identification, aiming to improve network efficiency and automation.

Potential future research directions on **systemic analysis** of smart thermal grids:

- Inversion of the derived thermohydraulic network model (*ProHeatNet_Sim*) for control purposes as initiated in Pub4, by utilizing relaxation methods (such as in Ref. [130]) or machine learning techniques.

- Incorporation of technical details of the prosumer side into network investigations. Within this dissertation the prosumer side was simplified by idealizing it. A logical progression in this area is the coupling of the Modelica libraries *ProsNet* (Pub5) and *ProHMo* [117], [118].

- Exploration of how central EMS optimization can be abstracted to eliminate the need for detailed information about prosumers' internal technical systems at the management level. Focus on how prosumers can communicate only capacities and flexibilities, and explore methods for their quantification.

- Investigation of the system reliability and resilience: What happens if a producer cannot deliver at the technical level what is assumed at the management level? Identify measures that can ensure reliable energy supply.

- Conduction of comprehensive testing and validation of the entire assembly of integrated network operation levels developed in this dissertation through a combination of experimental and simulation-based case studies, including the necessary interfaces.

Potential future research directions on smart thermal grids in the **broader context**:

- Analysis on the economic performance of PBDH networks and smart thermal grids in general, as this dissertation had a focus on the technical feasibility. Assess whether the gains in efficiency justify the financial investment, considering the increased system complexity. Compare the performance of networks with distributed generation against TDH networks, focusing on the sensitivity to the proportion of decentralized generation and prosumers. Initial investigations in this direction are documented in Ref. [131].
- Systematical investigations where PBDH networks are economically viable and to what extent (for example, across Bavaria or Germany). Determine for which demand and generation settings smart thermal grids with prosumers and distributed generation are advantageous. Evaluate where hierarchical network approaches are suitable and where TDH or decentralized supply should be preferred.

Moreover, in the context of this dissertation several tools were created and established that are available for continued use. The CoSES laboratory environment functions beyond research purposes as a valuable resource for the education of students, researchers, and industry professionals. In addition, the suite of software tools — namely, *MEMAP*, *ProsNet*, *ProHeatNet_Sim*, and *ProHMo* — can be used for detailed case studies and be enhancement within a wider scope of research activities.

Overall, the multifaceted research opportunites outlined above encompass various aspects, including technical, economical, operational, and control aspects. Pursuing these directions can contribute to accelerating the broader practical application of PBDH networks and smart thermal grids in the field, beyond the scope of this dissertation.

# Part V
# Appendix

# Appendix A

# List of Figures

# Appendix B

# List of Acronyms

**HP** heat pump . . . 3
**DH** district heating . . . 3
**DC** district cooling . . . 26
**DHC** district heating and cooling . . . 27
**CHC** combined heating and cooling . . . 27
**TDH** traditional district heating . . . 3
**R&D** research and development . . . 4
**CHP** combined heat and power . . . 4
**CV** control valve . . . 23
**FP** feed-in pump . . . 69
**DER** distributed energy resource . . . 4
**PBDH** prosumer-based district heating . . . 10
**KCL I** first Kirchhoff circuit law . . . 18
**KCL II** second Kirchhoff circuit law . . . 18
**KCL** Kirchhoff circuit law . . . 18
**LMTD** logarithmic mean temperature difference . . . 20
**PID** proportional-integral-derivative . . . 24
**CP** consumption pump . . . 24
**PP** production pump . . . 69
**1GDH** first generation district heating . . . 26
**2GDH** second generation district heating . . . 26
**3GDH** third generation district heating . . . 26
**4GDH** fourth generation district heating . . . 26
**5GDHC** fifth generation district heating and cooling . . . 27
**5GDH** fifth generation district heating . . . 27
**BHP** booster heat pump . . . 27
**LTDH** low temperature district heating . . . 28
**ULTDH** ultra low temperature district heating . . . 28
**AN** ambient networks . . . 28
**RD** research direction . . . 9
**RQ** research questions . . . 9
**Pub** publication . . . 12
**CoSES** Combined Smart Energy Systems . . . 72
**TUM** Technical University of Munich . . . 13

# Appendix C

# Bibliography


[1] European Commission, Joint Research Centre, J. Jiménez-Navarro, F. Filippidou, K. Kavvadias, and J. Carlsson, *Efficient district heating and cooling*. Publications Office of the European Union, 2022. DOI: doi/10.2760/854480.

[2] H. Lund, S. Werner, R. Wiltshire, *et al.*, "4th generation district heating (4gdh): Integrating smart thermal grids into future sustainable energy systems," *Energy*, vol. 68, pp. 1–11, 2014, ISSN: 0360-5442. DOI: https://doi.org/10.1016/j.energy.2014.02.089. [Online]. Available: https://www.sciencedirect.com/science/article/pii/S0360544214002369.

[3] European Commission, Directorate-General for Energy, L. Kranzl, *et al.*, *Renewable space heating under the revised Renewable Energy Directive – ENER/C1/2018-494 – Final report*. Publications Office of the European Union, 2022. DOI: doi/10.2833/525486.

[4] E. Commission, D.-G. for Energy, A. Bacquet, *et al.*, *District heating and cooling in the European Union – Overview of markets and regulatory frameworks under the revised Renewable Energy Directive*. Publications Office of the European Union, 2022. DOI: doi/10.2833/962525.

[5] International Energy Agency (IEA). "Tracking district heating." (2023), [Online]. Available: https://www.iea.org/energy-system/buildings/district-heating (visited on 11/14/2023).

[6] Deutsche Bundesregierung (The German Federal Government), *Gesetz für die Wärmeplanung und zur Dekarbonisierung der Wärmenetze*, 2023. [Online]. Available: https://www.bmwsb.bund.de/SharedDocs/gesetzgebungsverfahren/Webs/BMWSB/DE/kommunale-waermeplanung.html (visited on 11/14/2024).

[7] International Energy Agency, "Net zero by 2050," International Energy Agency, 2021, License: CC BY 4.0. [Online]. Available: https://www.iea.org/reports/net-zero-by-2050.

[8] European Parliament Council, *Directive (eu) 2023/1791 of 13 september 2023 on energy efficiency and amending regulation (eu) 2023/955 (recast) (text with eea relevance)*, 2023. [Online]. Available: http://data.europa.eu/eli/dir/2023/1791 (visited on 11/14/2024).

[9] Deutsche Bundesregierung (The German Federal Government), *Entwurf eines Gesetzes zur Änderung des Gebäudeenergiegesetzes, zur Änderung der Heizkostenverordnung und zur Änderung der Kehr und Überprüfungsordnung*, 2023. [Online]. Available: https://dserver.bundestag.de/btd/20/068/2006875.pdf (visited on 12/13/2024).

[10] M. Sayegh, J. Danielewicz, T. Nannou, *et al.*, "Trends of european research and development in district heating technologies," *Renewable and Sustainable Energy Reviews*, vol. 68, pp. 1183–1192, 2017, ISSN: 1364-0321. DOI: https://doi.org/10.1016/j.rser.2016.02.023. [Online]. Available: https://www.sciencedirect.com/science/article/pii/S1364032116002318.

[11] T. Tereshchenko and N. Nord, "Future trends in district heating development," *Current Sustainable/Renewable Energy Reports*, vol. 5, no. 2, pp. 172–180, Jun. 2018, ISSN: 2196-3010. DOI: 10.1007/s40518-018-0111-y. [Online]. Available: https://doi.org/10.1007/s40518-018-0111-y.

[12] H. Lund, P. A. Østergaard, M. Chang, *et al.*, "The status of 4th generation district heating: Research and results," *Energy*, vol. 164, pp. 147–159, 2018, ISSN: 0360-5442. DOI: https://doi.org/10.1016/j.energy.2018.08.206. [Online]. Available: https://www.sciencedirect.com/science/article/pii/S0360544218317420.

[13] P. Huang, B. Copertaro, X. Zhang, *et al.*, "A review of data centers as prosumers in district energy systems: Renewable energy integration and waste heat reuse for district heating," *Applied Energy*, vol. 258, p. 114 109, 2020, ISSN: 0306-2619. DOI: https://doi.org/10.1016/j.apenergy.2019.114109. [Online]. Available: https://www.sciencedirect.com/science/article/pii/S0306261919317969.

[14] Danfoss. "Smart energy systems impact on supermarkets." (2017), [Online]. Available: https://www.danfoss.com/en/service-and-support/case-stories/dcs/smart-energy-systems-impact-on-supermarkets/ (visited on 09/22/2023).

[15] P. Crossley, *Microgrids and Active Distribution Networks* (Energy Engineering). Institution of Engineering and Technology, 2009. [Online]. Available: https://digital-library.theiet.org/content/books/po/pbrn006e.

[16] M. E. El-hawary, "The smart grid—state-of-the-art and future trends," *Electric Power Components and Systems*, vol. 42, no. 3-4, pp. 239–250, 2014. DOI: 10.1080/15325008.2013.868558. eprint: https://doi.org/10.1080/15325008.2013.868558. [Online]. Available: https://doi.org/10.1080/15325008.2013.868558.

[17] M. Hossain, N. Madlool, N. Rahim, J. Selvaraj, A. Pandey, and A. F. Khan, "Role of smart grid in renewable energy: An overview," *Renewable and Sustainable Energy Reviews*, vol. 60, pp. 1168–1184, 2016, ISSN: 1364-0321. DOI: https://doi.org/10.1016/j.rser.2015.09.098. [Online]. Available: https://www.sciencedirect.com/science/article/pii/S1364032116002148.

[18] H. Lund, P. A. Østergaard, D. Connolly, and B. V. Mathiesen, "Smart energy and smart energy systems," *Energy*, vol. 137, pp. 556–565, 2017, ISSN: 0360-5442. DOI: https://doi.org/10.1016/j.energy.2017.05.123. [Online]. Available: https://www.sciencedirect.com/science/article/pii/S0360544217308812.

[19] B. Mathiesen, H. Lund, D. Connolly, *et al.*, "Smart energy systems for coherent 100% renewable energy and transport solutions," *Applied Energy*, vol. 145, pp. 139–154, 2015, ISSN: 0306-2619. DOI: https://doi.org/10.1016/j.apenergy.2015.01.075. [Online]. Available: https://www.sciencedirect.com/science/article/pii/S0306261915001117.

[20] European Commission, Joint Research Centre, J. Volt, *et al.*, *Clean Energy Technology Observatory, District heat and cold management in the European Union – Status report on technology development, trends, value chains and markets – 2022.* Publications Office of the European Union, 2022. DOI: doi/10.2760/168004.

[21] T. Schluck, P. Kräuchi, and M. Sulzer, "Non-linear thermal networks - how can a meshed network improve energy efficiency?," Sep. 2015.

[22] G. K. Batchelor, *An Introduction to Fluid Dynamics* (Cambridge Mathematical Library). Cambridge University Press, 2000. DOI: 10.1017/CBO9780511800955.

[23] W. Heidemann, *Technische Thermodynamik: Kompaktkurs für das Bachelorstudium.* Wiley, 2015, ISBN: 9783527692835. [Online]. Available: https://books.google.de/books?id=akBcCwAAQBAJ.

[24] VDI e. V., Ed., *VDI Heat Atlas.* Springer Berlin, Heidelberg, 2010. DOI: https://doi.org/10.1007/978-3-540-77877-6.

[25] T. Licklederer, D. Zinsmeister, L. Lukas, F. Speer, T. Hamacher, and V. S. Perić, "Control of bidirectional prosumer substations in smart thermal grids: A weighted proportional-integral control approach," *Applied Energy*, vol. 354, p. 122 239, 2024, ISSN: 0306-2619. DOI: 10.1016/j.apenergy.2023.122239. [Online]. Available: https://www.sciencedirect.com/science/article/pii/S0306261923016033.

[26] SWEP International AB. "Co-versus counter-current flow." (2022), [Online]. Available: https://www.swep.de/refrigerant-handbook/1.-basic-heat-transfer/as2/ (visited on 09/25/2023).

[27] T. Nussbaumer, S. Thalmann, A. Jenni, and J. Ködel, *Handbook on Planning of District Heating Networks*. Swiss Federal Office of Energy SFOE, 3003 Bern (Switzerland): swissenergy, 2020.

[28] S. Frederiksen and S. Werner, *District Heating and Cooling*. Professional Publishing Svc., 2013, ISBN: 9789144085302. [Online]. Available: https://books.google.de/books?id=vH5zngEACAAJ.

[29] J. E. Thorsen and O. Gudmundsson, "District heating handbook," Danfoss A/S – District Energy, technical report, 2012. [Online]. Available: https://files.danfoss.com/download/Heating/Handbooks/Application-Handbook_sep14.pdf.

[30] S. München, "Tab heizwasser," SWM Versorgungs GmbH, technical report, 2022. [Online]. Available: https://www.swm.de/installateure/fernwaerme#tab-heizwassernetz.

[31] S. Buffa, M. H. Fouladfar, G. Franchini, I. Lozano Gabarre, and M. Andrés Chicote, "Advanced control and fault detection strategies for district heating and cooling systems—a review," *Applied Sciences*, vol. 11, no. 1, 2021, ISSN: 2076-3417. DOI: 10.3390/app11010455. [Online]. Available: https://www.mdpi.com/2076-3417/11/1/455.

[32] A. Vandermeulen, B. van der Heijde, and L. Helsen, "Controlling district heating and cooling networks to unlock flexibility: A review," *Energy*, vol. 151, pp. 103–115, 2018, ISSN: 0360-5442. DOI: https://doi.org/10.1016/j.energy.2018.03.034. [Online]. Available: https://www.sciencedirect.com/science/article/pii/S0360544218304328.

[33] K. Åström and T. Hägglund, *PID Controllers: Theory, Design, and Tuning*, English. ISA - The Instrumentation, Systems and Automation Society, 1995, ISBN: 1-55617-516-7.

[34] German Government, *Honorarordnung für architekten und ingenieure*, vom 10. Juli 2013 (BGBl. I S. 2276), ), zuletzt durch Artikel 3 des Gesetzes vom 22. März 2023 (BGBl. 2023 I Nr. 88) geändert worden ist. [Online]. Available: https://www.gesetze-im-internet.de/hoai_2013/ (visited on 10/31/2023).

[35] O. Gudmundsson and J. E. Thorsen. "District heating generations explained." (2023), [Online]. Available: https://www.danfoss.com/en/about-danfoss/articles/dhs/district-energy-generations-explained/#:~:text=Currently%2C%20most%20district%20heating%20(DH,and%20renewable%2Dbased%20energy%20system (visited on 09/12/2023).

[36] S. Werner, "Network configurations for implemented low-temperature district heating," *Energy*, vol. 254, p. 124 091, 2022, ISSN: 0360-5442. DOI: https://doi.org/10.1016/j.energy.2022.124091. [Online]. Available: https://www.sciencedirect.com/science/article/pii/S036054422200994X.

[37] M. S. Triebs, E. Papadis, H. Cramer, and G. Tsatsaronis, "Landscape of district heating systems in germany – status quo and categorization," *Energy Conversion and Management: X*, vol. 9, p. 100 068, 2021, ISSN: 2590-1745. DOI: https://doi.org/10.1016/j.ecmx.2020.100068. [Online]. Available: https://www.sciencedirect.com/science/article/pii/S2590174520300404.

[38] P. A. Østergaard, S. Werner, A. Dyrelund, *et al.*, "The four generations of district cooling - a categorization of the development in district cooling from origin to future prospect," *Energy*, vol. 253, p. 124 098, 2022, ISSN: 0360-5442. DOI: https://doi.org/10.1016/j.energy.2022.124098. [Online]. Available: https://www.sciencedirect.com/science/article/pii/S0360544222010015.

[39] M. Jakubcionis and J. Carlsson, "Estimation of european union residential sector space cooling potential," *Energy Policy*, vol. 101, pp. 225–235, 2017, ISSN: 0301-4215. DOI: https://doi.org/10.1016/j.enpol.2016.11.047. [Online]. Available: https://www.sciencedirect.com/science/article/pii/S030142151630653X.

[40] European Commission and Directorate-General for Energy, S. Pezzutto, A. Novelli, *et al.*, *Cooling technologies overview and market shares. Part 1 of the study "Renewable cooling under the revised Renewable Energy Directive ENER/C1/2018-493"*. Publications Office of the European Union, 2022. DOI: doi/10.2833/799633.

[41] S. Buffa, M. Cozzini, M. D'Antoni, M. Baratieri, and R. Fedrizzi, "5th generation district heating and cooling systems: A review of existing cases in europe," *Renewable and Sustainable Energy Reviews*, vol. 104, pp. 504–522, 2019, ISSN: 1364-0321. DOI: https://doi.org/10.1016/j.rser.2018.12.059. [Online]. Available: https://www.sciencedirect.com/science/article/pii/S1364032118308608.

[42] M. Wirtz, L. Kivilip, P. Remmen, and D. Müller, "5th generation district heating: A novel design approach based on mathematical optimization," *Applied Energy*, vol. 260, p. 114 158, 2020, ISSN: 0306-2619. DOI: https://doi.org/10.1016/j.apenergy.2019.114158. [Online]. Available: https://www.sciencedirect.com/science/article/pii/S0306261919318458.

[43] J. Barco-Burgos, J. Bruno, U. Eicker, A. Saldaña-Robles, and V. Alcántar-Camarena, "Review on the integration of high-temperature heat pumps in district heating and cooling networks," *Energy*, vol. 239, p. 122 378, 2022, ISSN: 0360-5442. DOI: https://doi.org/10.1016/j.energy.2021.122378. [Online]. Available: https://www.sciencedirect.com/science/article/pii/S036054422102627X.

[44] S. Schmitt, R. Zeh, and V. Stockinger, "Quantification of heat losses and gains of 5th generation district heating and cooling networks compared to conventional heating networks," *Bauphysik*, vol. 44, no. 6, pp. 337–343, 2022. DOI: https://doi.org/10.1002/bapi.202200036. eprint: https://onlinelibrary.wiley.com/doi/pdf/10.1002/bapi.202200036. [Online]. Available: https://onlinelibrary.wiley.com/doi/abs/10.1002/bapi.202200036.

[45] M. Wirtz, T. Schreiber, and D. Müller, "Survey of 53 fifth-generation district heating and cooling (5gdhc) networks in germany," *Energy Technology*, vol. 10, no. 11, p. 2 200 749, 2022. DOI: https://doi.org/10.1002/ente.202200749. eprint: https://onlinelibrary.wiley.com/doi/pdf/10.1002/ente.202200749. [Online]. Available: https://onlinelibrary.wiley.com/doi/abs/10.1002/ente.202200749.

[46] M. Abugabbara, S. Gehlin, J. Lindhe, *et al.*, "How to develop fifth-generation district heating and cooling in sweden? application review and best practices proposed by middle agents," *Energy Reports*, vol. 9, pp. 4971–4983, 2023, ISSN: 2352-4847. DOI: https://doi.org/10.1016/j.egyr.2023.04.048. [Online]. Available: https://www.sciencedirect.com/science/article/pii/S2352484723004092.

[47] O. Angelidis, A. Ioannou, D. Friedrich, A. Thomson, and G. Falcone, "District heating and cooling networks with decentralised energy substations: Opportunities and barriers for holistic energy system decarbonisation," *Energy*, vol. 269, p. 126 740, 2023, ISSN: 0360-5442. DOI: https://doi.org/10.1016/j.energy.2023.126740. [Online]. Available: https://www.sciencedirect.com/science/article/pii/S0360544223001342.

[48] F. Calise, F. L. Cappiello, L. Cimmino, M. Dentice d'Accadia, and M. Vicidomini, "A comparative thermoeconomic analysis of fourth generation and fifth generation district heating and cooling networks," *Energy*, vol. 284, p. 128 561, 2023, ISSN: 0360-5442. DOI: https://doi.org/10.1016/j.energy.2023.128561. [Online]. Available: https://www.sciencedirect.com/science/article/pii/S0360544223019552.

[49] K. Gjoka, B. Rismanchi, and R. H. Crawford, “Fifth-generation district heating and cooling systems: A review of recent advancements and implementation barriers,” *Renewable and Sustainable Energy Reviews*, vol. 171, p. 112 997, 2023, ISSN: 1364-0321. DOI: https://doi.org/10.1016/j.rser.2022.112997. [Online]. Available: https://www.sciencedirect.com/science/article/pii/S1364032122008784.

[50] Y. Zhang, P. Johansson, and A. S. Kalagasidis, “Quantification of overlapping heating and cooling demand for the feasibility assessment of bi-directional systems over europe,” *Energy and Buildings*, vol. 294, p. 113 244, 2023, ISSN: 0378-7788. DOI: https://doi.org/10.1016/j.enbuild.2023.113244. [Online]. Available: https://www.sciencedirect.com/science/article/pii/S0378778823004747.

[51] H. Lund, P. A. Østergaard, T. B. Nielsen, *et al.*, “Perspectives on fourth and fifth generation district heating,” *Energy*, vol. 227, p. 120 520, 2021, ISSN: 0360-5442. DOI: https://doi.org/10.1016/j.energy.2021.120520. [Online]. Available: https://www.sciencedirect.com/science/article/pii/S0360544221007696.

[52] M. Sulzer, S. Werner, S. Mennel, and M. Wetter, “Vocabulary for the fourth generation of district heating and cooling,” *Smart Energy*, vol. 1, p. 100 003, 2021, ISSN: 2666-9552. DOI: https://doi.org/10.1016/j.segy.2021.100003. [Online]. Available: https://www.sciencedirect.com/science/article/pii/S2666955221000034.

[53] S. Frank and S. Rebennack, “An introduction to optimal power flow: Theory, formulation, and examples,” *IIE Transactions*, vol. 48, no. 12, pp. 1172–1197, 2016. DOI: 10.1080/0740817X.2016.1189626. eprint: https://doi.org/10.1080/0740817X.2016.1189626. [Online]. Available: https://doi.org/10.1080/0740817X.2016.1189626.

[54] N. P. R. E. Vespermann, “Market design for energy communities,” en, Ph.D. dissertation, Technische Universität München, 2022, p. 127.

[55] L. Frölke, “Market design for future district heating systems,” English, Ph.D. dissertation, 2023. DOI: 10.11581/dtu.00000253.

[56] European Comission - Directorate-General for Energy. “Energy communities.” (2023), [Online]. Available: https://energy.ec.europa.eu/topics/markets-and-consumers/energy-communities_en (visited on 09/08/2023).

[57] Y. Amanbek, A. Kalakova, S. Zhakiyeva, K. Kayisli, N. Zhakiyev, and D. Friedrich, “Distribution locational marginal price based transactive energy management in distribution systems with smart prosumer; a multi-agent approach,” *Energies*, vol. 15, no. 7, 2022, ISSN: 1996-1073. DOI: 10.3390/en15072404. [Online]. Available: https://www.mdpi.com/1996-1073/15/7/2404.

[58] J. B. Rawlings, D. Q. Mayne, and M. M. Diehl, *Model predictive control: theory, computation, and design*. Nob Hill Publishing, 2017.

[59] R. Zarin Pass, M. Wetter, and M. Piette, “A thermodynamic analysis of a novel bidirectional district heating and cooling network,” *Energy*, vol. 144, pp. 20–30, 2018, ISSN: 0360-5442. DOI: https://doi.org/10.1016/j.energy.2017.11.122. [Online]. Available: https://www.sciencedirect.com/science/article/pii/S0360544217319801.

[60] T. Blacha, M. Mans, P. Remmen, and D. Müller, “Dynamic simulation of bidirectional low-temperature networks - a case study to facilitate the integration of renewable energies,” 2019, pp. 3491–3498. DOI: 10.26868/25222708.2019.210670.

[61] M. Wirtz, L. Kivilip, P. Remmen, and D. Müller, “Quantifying demand balancing in bidirectional low temperature networks,” *Energy and Buildings*, vol. 224, p. 110 245, 2020, ISSN: 0378-7788. DOI: https://doi.org/10.1016/j.enbuild.2020.110245. [Online]. Available: https://www.sciencedirect.com/science/article/pii/S0378778820309889.

[62] M. Wirtz, M. Hahn, T. Schreiber, and D. Müller, "Design optimization of multi-energy systems using mixed-integer linear programming: Which model complexity and level of detail is sufficient?" *Energy Conversion and Management*, vol. 240, p. 114 249, 2021, ISSN: 0196-8904. DOI: https://doi.org/10.1016/j.enconman.2021.114249. [Online]. Available: https://www.sciencedirect.com/science/article/pii/S0196890421004258.

[63] M. Blommaert, Y. Wack, and M. Baelmans, "An adjoint optimization approach for the topological design of large-scale district heating networks based on nonlinear models," *Applied Energy*, vol. 280, p. 116 025, 2020, ISSN: 0306-2619. DOI: https://doi.org/10.1016/j.apenergy.2020.116025. [Online]. Available: https://www.sciencedirect.com/science/article/pii/S0306261920314653.

[64] Y. Wack, M. Baelmans, R. Salenbien, and M. Blommaert, "Economic topology optimization of district heating networks using a pipe penalization approach," *Energy*, vol. 264, p. 126 161, 2023, ISSN: 0360-5442. DOI: https://doi.org/10.1016/j.energy.2022.126161. [Online]. Available: https://www.sciencedirect.com/science/article/pii/S036054422203047X.

[65] G. Sandou, S. Font, S. Tebbani, A. Hiret, and C. Mondon, "Predictive control of a complex district heating network," in *Proceedings of the 44th IEEE Conference on Decision and Control*, 2005, pp. 7372–7377. DOI: 10.1109/CDC.2005.1583351.

[66] C. Saletti, A. Gambarotta, and M. Morini, "Development, analysis and application of a predictive controller to a small-scale district heating system," *Applied Thermal Engineering*, vol. 165, p. 114 558, 2020, ISSN: 1359-4311. DOI: https://doi.org/10.1016/j.applthermaleng.2019.114558. [Online]. Available: https://www.sciencedirect.com/science/article/pii/S135943111935392X.

[67] M. Taylor, S. Long, O. Marjanovic, and A. Parisio, "Model predictive control of smart districts with fifth generation heating and cooling networks," *IEEE Transactions on Energy Conversion*, vol. 36, no. 4, pp. 2659–2669, 2021. DOI: 10.1109/TEC.2021.3082405.

[68] J. Jansen, F. Jorissen, and L. Helsen, "Optimal control of a fourth generation district heating network using an integrated non-linear model predictive controller," *Applied Thermal Engineering*, vol. 223, p. 120 030, 2023, ISSN: 1359-4311. DOI: https://doi.org/10.1016/j.applthermaleng.2023.120030. [Online]. Available: https://www.sciencedirect.com/science/article/pii/S1359431123000595.

[69] C. Paulus and P. Papillon, "Substations for decentralized solar district heating: Design, performance and energy cost," *Energy Procedia*, vol. 48, pp. 1076–1085, 2014, Proceedings of the 2nd International Conference on Solar Heating and Cooling for Buildings and Industry (SHC 2013), ISSN: 1876-6102. DOI: https://doi.org/10.1016/j.egypro.2014.02.122. [Online]. Available: https://www.sciencedirect.com/science/article/pii/S1876610214003841.

[70] G. Lennermo, P. Lauenburg, and L. Brand, "Decentralized heat supply in district heating systems - implications of varying differential pressure," *14th International Symposium on DH and Cooling*, p. 6, 2014, lack of investigations on hydraulic infrastructure and operation. [Online]. Available: http://www.svenskfjarrvarme.se/Global/Konferenser/DHC14/Proceedings/_5.2%20Gunnar%20Lennermo%20DECENTRALISED%20HEAT%20SUPPLY%20IN%20DISTRICT%20HEATING%20SYSTEMS%20IMPLICATIONS%20OF%20VARYING%20DIFFERENTIAL%20PRESSURE.pdf.

[71] I. B. Hassine and U. Eicker, "Control aspects of decentralized solar thermal integration into district heating networks," *Energy Procedia*, vol. 48, pp. 1055–1064, 2014, Proceedings of the 2nd International Conference on Solar Heating and Cooling for Buildings and Industry (SHC 2013), ISSN: 1876-6102. DOI: https://doi.org/10.1016/j.egypro.2014.02.120. [Online]. Available: https://www.sciencedirect.com/science/article/pii/S1876610214003828.

[72] M. Ancona, L. Branchini, B. Di Pietra, F. Melino, G. Puglisi, and F. Zanghirella, "Utilities substations in smart district heating networks," *Energy Procedia*, vol. 81, pp. 597–605, 2015, 69th Conference of the Italian Thermal Engineering Association, ATI 2014, ISSN: 1876-6102. DOI: https://doi.org/10.1016/j.egypro.2015.12.044. [Online]. Available: https://www.sciencedirect.com/science/article/pii/S1876610215026934.

[73] M. Ancona, L. Branchini, A. De Pascale, and F. Melino, "Smart district heating: Distributed generation systems' effects on the network," *Energy Procedia*, vol. 75, pp. 1208–1213, 2015, Clean, Efficient and Affordable Energy for a Sustainable Future: The 7th International Conference on Applied Energy (ICAE2015), ISSN: 1876-6102. DOI: https://doi.org/10.1016/j.egypro.2015.07.157. [Online]. Available: https://www.sciencedirect.com/science/article/pii/S187661021500925X.

[74] D. Beckenbauer, M. Ehrenwirth, M. Klärner, W. Zörner, and V. Cheng, "Validation of a district heating system model and simulation-based investigation of bidirectional heat transport by decentralised solar thermal plants," International Solar Energy Society, 2017, pp. 1–12, ISBN: 978-3-9814659-7-6. DOI: 10.18086/swc.2017.06.01. [Online]. Available: http://proceedings.ises.org/citation?doi=swc.2017.06.01.

[75] N. Lamaison, R. Bavière, D. Cheze, and C. Paulus, "A multi-criteria analysis of bidirectional solar district heating substation architecture," International Solar Energy Society, 2017, pp. 1–11, ISBN: 978-3-9814659-7-6. DOI: 10.18086/swc.2017.10.02. [Online]. Available: http://proceedings.ises.org/citation?doi=swc.2017.10.02.

[76] M. Heymann, K. Rühling, and C. Felsmann, "Integration of solar thermal systems into district heating – dh system simulation," *Energy Procedia*, vol. 116, pp. 394–402, 2017, 15th International Symposium on District Heating and Cooling, DHC15-2016, 4-7 September 2016, Seoul, South Korea, ISSN: 1876-6102. DOI: https://doi.org/10.1016/j.egypro.2017.05.086. [Online]. Available: https://www.sciencedirect.com/science/article/pii/S1876610217322932.

[77] M. Heymann, T. Rosemann, K. Rühling, T. Tietze, and B. Hafner, "Concept and measurement results of two decentralized solar thermal feed-in substations," *Energy Procedia*, vol. 149, pp. 363–372, 2018, 16th International Symposium on District Heating and Cooling, DHC2018, 9–12 September 2018, Hamburg, Germany, ISSN: 1876-6102. DOI: https://doi.org/10.1016/j.egypro.2018.08.200. [Online]. Available: https://www.sciencedirect.com/science/article/pii/S187661021830496X.

[78] M. A. Ancona, L. Branchini, A. De Pascale, and F. Melino, "Smart district heating: Cogeneration and solar systems integration to convert an existing utility substation," *AIP Conference Proceedings*, vol. 2191, no. 1, p. 020 008, Dec. 2019, ISSN: 0094-243X. DOI: 10.1063/1.5138741. eprint: https://pubs.aip.org/aip/acp/article-pdf/doi/10.1063/1.5138741/13147721/020008_1_online.pdf. [Online]. Available: https://doi.org/10.1063/1.5138741.

[79] G. Lennermo, P. Lauenburg, and S. Werner, "Control of decentralised solar district heating," *Solar Energy*, vol. 179, pp. 307–315, 2019, ISSN: 0038-092X. DOI: https://doi.org/10.1016/j.solener.2018.12.080. [Online]. Available: https://www.sciencedirect.com/science/article/pii/S0038092X18312775.

[80] M. A. Ancona, M. Bianchi, L. Branchini, *et al.*, "Influence of the prosumer allocation and heat production on a district heating network," *Frontiers in Mechanical Engineering*, vol. 7, 2021, ISSN: 2297-3079. DOI: 10.3389/fmech.2021.623932. [Online]. Available: https://www.frontiersin.org/articles/10.3389/fmech.2021.623932.

[81] L. Brand, A. Calvén, J. Englund, H. Landersjö, and P. Lauenburg, "Smart district heating networks – a simulation study of prosumers' impact on technical parameters in distribution networks," *Applied Energy*, vol. 129, pp. 39–48, 2014, ISSN: 0306-2619. DOI: https://doi.org/10.1016/j.apenergy.2014.04.079. [Online]. Available: https://www.sciencedirect.com/science/article/pii/S0306261914004425.

[82] S. Paulick, C. Schroth, S. Guddusch, and K. Rühling, "Resulting effects on decentralized feed-in into district heating networks – a simulation study," *Energy Procedia*, vol. 149, pp. 49–58, 2018, 16th International Symposium on District Heating and Cooling, DHC2018, 9–12 September 2018, Hamburg, Germany, ISSN: 1876-6102. DOI: https://doi.org/10.1016/j.egypro.2018.08.168. [Online]. Available: https://www.sciencedirect.com/science/article/pii/S1876610218304648.

[83] I. Elizarov, "Analysis, modelling, and control strategy development for prosumer-based heat networks," Technical University of Munich, 2020.

[84] T. Sommer, M. Sulzer, M. Wetter, A. Sotnikov, S. Mennel, and C. Stettler, "The reservoir network: A new network topology for district heating and cooling," *Energy*, vol. 199, p. 117 418, 2020, ISSN: 0360-5442. DOI: https://doi.org/10.1016/j.energy.2020.117418. [Online]. Available: https://www.sciencedirect.com/science/article/pii/S0360544220305259.

[85] M. Wetter and J. Hu, "Quayside energy systems analysis," Berkeley Lab, Tech. Rep., 2019. [Online]. Available: https://buildings.lbl.gov/publications/quayside-energy-systems-analysis (visited on 12/13/2023).

[86] T. Meudt, M. Pohl, and J. Metternich, "Die automatisierungspyramide - ein literaturüberblick," de, Darmstadt, Tech. Rep., Jun. 2017. [Online]. Available: http://tuprints.ulb.tu-darmstadt.de/6298/.

[87] A. Fernbach, W. Granzer, and W. Kastner, "Interoperability at the management level of building automation systems: A case study for bacnet and opc ua," in *ETFA2011*, 2011, pp. 1–8. DOI: 10.1109/ETFA.2011.6059106.

[88] T. Licklederer, J. Mayer, D. Bytschkow, *et al.*, "Abschlussbericht „Multi-Energie Management und Aggregationsplattform (MEMAP)“ der TU München," Technische Universität München, Tech. Rep., 2022, p. 196. DOI: 10.2314/KXP:1839282886. [Online]. Available: https://doi.org/10.2314/KXP:1839282886.

[89] R. E. Carrillo, A. Peppas, Y. Stauffer, C. Politi, T. Gorecki, and P.-J. Alet, "A multilevel control approach to exploit local flexibility in districts evaluated under real conditions," *Energies*, vol. 15, no. 16, 2022, ISSN: 1996-1073. DOI: 10.3390/en15165887. [Online]. Available: https://www.mdpi.com/1996-1073/15/16/5887.

[90] D. Bytschkow, A. Capone, J. Mayer, M. Kramer, and T. Licklederer, "An opc ua-based energy management platform for multi-energy prosumers in districts," IEEE, Sep. 2019, pp. 1–5, ISBN: 978-1-5386-8218-0. DOI: 10.1109/ISGTEurope.2019.8905725. [Online]. Available: https://ieeexplore.ieee.org/document/8905725/.

[91] L. Heidemann, D. Bytschkow, A. Capone, T. Licklederer, and M. Kramer, "Sector coupling with optimization: A comparison between single buildings and combined quarters.," in *Abstracts from the 8th DACH+ Conference on Energy Informatics*, vol. 2, Sep. 2019, p. 31. DOI: 10.1186/s42162-019-0098-7. [Online]. Available: https://energyinformatics.springeropen.com/articles/10.1186/s42162-019-0098-7.

[92] MEMAP Research Group, "Quartiere nachhaltig betreiben," *IKZ Fachplaner*, vol. 07, 2021. [Online]. Available: https://www.ikz.de/medien/ikz-fachplaner/heftarchiv/jahrgang-2021/ausgabe-07/news/detail/quartiere-nachhaltig-betreiben/ (visited on 10/08/2023).

[93] L. Allen, A. O'Connell, and V. Kiermer, "How can we ensure visibility and diversity in research contributions? how the contributor role taxonomy (credit) is helping the shift from authorship to contributorship," *Learned Publishing*, vol. 32, pp. 71–74, 1 Jan. 2019, ISSN: 09531513. DOI: 10.1002/leap.1210. [Online]. Available: https://onlinelibrary.wiley.com/doi/10.1002/leap.1210.

[94] M. Abugabbara, S. Javed, and D. Johansson, "A simulation model for the design and analysis of district systems with simultaneous heating and cooling demands," *Energy*, vol. 261, p. 125 245, 2022, ISSN: 0360-5442. DOI: https://doi.org/10.1016/j.energy.2022.125245. [Online]. Available: https://www.sciencedirect.com/science/article/pii/S0360544222021314.

[95] M. Pipiciello, M. Caldera, M. Cozzini, M. A. Ancona, F. Melino, and B. Di Pietra, "Experimental characterization of a prototype of bidirectional substation for district heating with thermal prosumers," *Energy*, vol. 223, p. 120 036, 2021, ISSN: 0360-5442. DOI: https://doi.org/10.1016/j.energy.2021.120036. [Online]. Available: https://www.sciencedirect.com/science/article/pii/S0360544221002851.

[96] G. E. Dino, P. Catrini, A. Buscemi, A. Piacentino, V. Palomba, and A. Frazzica, "Modeling of a bidirectional substation in a district heating network: Validation, dynamic analysis, and application to a solar prosumer," *Energy*, vol. 284, p. 128 621, 2023, ISSN: 0360-5442. DOI: https://doi.org/10.1016/j.energy.2023.128621. [Online]. Available: https://www.sciencedirect.com/science/article/pii/S0360544223020157.

[97] T. Rosemann, J. Löser, and K. Rühling, "A new dh control algorithm for a combined supply and feed-in substation and testing through hardware-in-the-loop," *Energy Procedia*, vol. 116, pp. 416–425, 2017, 15th International Symposium on District Heating and Cooling, DHC15-2016, 4-7 September 2016, Seoul, South Korea, ISSN: 1876-6102. DOI: https://doi.org/10.1016/j.egypro.2017.05.089. [Online]. Available: https://www.sciencedirect.com/science/article/pii/S1876610217322968.

[98] D. Zinsmeister, T. Licklederer, F. Christange, P. Tzscheutschler, and V. S. Perić, "A comparison of prosumer system configurations in district heating networks," *Energy Reports*, vol. 7, pp. 430–439, Oct. 2021, ISSN: 23524847. DOI: 10.1016/j.egyr.2021.08.085. [Online]. Available: https://linkinghub.elsevier.com/retrieve/pii/S2352484721006879.

[99] D. Zinsmeister, *Possible prosumer side configurations*, Jun. 2021. DOI: 10.13140/RG.2.2.25761.12642.

[100] T. Licklederer, J. Mayer, D. Bytschkow, *et al.*, "A digital platform for real-time multi-energy management in districts using opc ua: Conceptualization, modeling, software implementation, and laboratory validation," *manuscript submitted to 'Energy and Buildings'*, 2024, (revision process ongoing at submission date of this dissertation, preprint is accessible online). DOI: 10.2139/ssrn.4861866. [Online]. Available: https://papers.ssrn.com/sol3/papers.cfm?abstract_id=4861866.

[101] O. Angelidis, D. Zinsmeister, A. Ioannou, *et al.*, "Advancing operational and control philosophies for 5th generation district heating and cooling networks: Development and experimental validation," 2024, work in progress, manuscript to be submitted to 'Energy'.

[102] D. Zinsmeister and T. Licklederer, "Characterization of a combined heat and power unit at the coses laboratory," Technical University of Munich - Center for Combined Smart Energy Systems (CoSES), Tech. Rep., 2021. DOI: 10.13140/RG.2.2.31035.34089/1. [Online]. Available: https://www.researchgate.net/publication/357049101_Characterization_of_a_Combined_Heat_and_Power_Unit_at_the_CoSES_laboratory.

[103] D. Zinsmeister and T. Licklederer, "Characterization of a combined heat and power unit at the coses laboratory - data," Technical University of Munich - Center for Combined Smart Energy Systems (CoSES), Tech. Rep., 2021. DOI: 10.13140/RG.2.2.17613.56809. [Online]. Available: https://www.researchgate.net/publication/357049522_Characterization_of_a_Combined_Heat_and_Power_Unit_at_the_CoSES_laboratory_-_Data.

[104] D. Zinsmeister and T. Licklederer, “Characterization of a thermal storage at the coses laboratory,” Technical University of Munich - Center for Combined Smart Energy Systems (CoSES), Tech. Rep., 2022. DOI: 10.13140/RG.2.2.13461.19687. [Online]. Available: https://www.researchgate.net/publication/359442024_Characterization_of_a_Thermal_Storage_at_the_CoSES_laboratory.

[105] D. Zinsmeister and T. Licklederer, “Characterization of a thermal storage at the coses laboratory - data,” Technical University of Munich - Center for Combined Smart Energy Systems (CoSES), Tech. Rep., 2022. DOI: 10.13140/RG.2.2.20172.08321. [Online]. Available: https://www.researchgate.net/publication/359441886_Characterization_of_a_Thermal_Storage_at_the_CoSES_laboratory_-_Data.

[106] I. D. la Cruz-Loredo, D. Zinsmeister, T. Licklederer, *et al.*, “Experimental validation of a hybrid 1-d multi-node model of a hot water thermal energy storage tank,” *Applied Energy*, vol. 332, p. 120 556, November 2022 Feb. 2023, ISSN: 03062619. DOI: 10.1016/j.apenergy.2022.120556. [Online]. Available: https://linkinghub.elsevier.com/retrieve/pii/S030626192201813X.

[107] D. Zinsmeister, P. Tzscheutschler, V. S. Perić, and C. Goebel, “Stratified thermal energy storage model with constant layer volume for predictive control — formulation, comparison, and empirical validation,” *Renewable Energy*, vol. 219, p. 119 511, 2023, ISSN: 0960-1481. DOI: https://doi.org/10.1016/j.renene.2023.119511. [Online]. Available: https://www.sciencedirect.com/science/article/pii/S096014812301426X.

[108] V. S. Perić, T. Hamacher, A. Mohapatra, *et al.*, “Coses laboratory for combined energy systems at tu munich,” in *2020 IEEE Power & Energy Society General Meeting (PESGM)*, 2020, pp. 1–5. DOI: 10.1109/PESGM41954.2020.9281442.

[109] A. Mohapatra, T. Hamacher, and V. S. Perić, “Phil infrastructure in coses microgrid laboratory,” in *2022 IEEE PES Innovative Smart Grid Technologies Conference Europe (ISGT-Europe)*, 2022, pp. 1–6. DOI: 10.1109/ISGT-Europe54678.2022.9960295.

[110] M. Mayer, A. Mohapatra, and V. S. Perić, “Iot integration for combined energy systems at the coses laboratory,” in *2021 IEEE 7th World Forum on Internet of Things (WF-IoT)*, 2021, pp. 195–200. DOI: 10.1109/WF-IoT51360.2021.9596000.

[111] A. Mohapatra, T. Hamacher, and V. S. Perić, “Phil infrastructure in coses microgrid laboratory,” in *2022 IEEE PES Innovative Smart Grid Technologies Conference Europe (ISGT-Europe)*, 2022, pp. 1–6. DOI: 10.1109/ISGT-Europe54678.2022.9960295.

[112] C. Aigner, “Konzepte zur statischen spannungshaltung in verteilnetzen mit hoher dezentraler eispeisung,” de, Ph.D. dissertation, Technische Universität München, 2021.

[113] L. Lukas, “Inbetriebnahme und Charakterisierung einer prototypischen bidirektionalen Wärmeübergabestation,” Bachelor Thesis, Technical University of Munich, 2023.

[114] F. Christange, “The combined smart energy systems laboratory,” en, Ph.D. dissertation, Technische Universität München, 2021, p. 168.

[115] G. M. A/S, “Pump handbook,” GRUNDFOS Management A/S, 2016. [Online]. Available: https://www.grundfos.com/solutions/learn/research-and-insights/get-the-pump-handbook.

[116] T. Licklederer, T. Hamacher, M. Kramer, and V. S. Perić, “Thermohydraulic model of smart thermal grids with bidirectional power flow between prosumers,” *Energy*, vol. 230, p. 120 825, Sep. 2021, ISSN: 03605442. DOI: 10.1016/j.energy.2021.120825. [Online]. Available: https://linkinghub.elsevier.com/retrieve/pii/S0360544221010732.

[117] D. Zinsmeister and V. Peric, “Implementation of a digital twin of the coses district heating prosumer laboratory,” in *Energy Proceedings*, 26 vols., 2022. DOI: 10.46855/energy-proceedings-10153.

[118] D. Zinsmeister, U. Ludolfinger, V. S. Peric, and C. Goebel, "Experimentally validated building energy models for benchmarking energy management systems," 2024, manuscript submitted to 'Energy', under review.

[119] S. Adldinger, L. Behringer, T. Licklederer, D. Zinsmeister, and T. Hamacher, "Temperature flexible operation of district heating with booster heat pumps – improving efficiency of existing networks," *Journal of Physics: Conference Series*, vol. 2600, no. 8, p. 082 028, Nov. 2023. DOI: 10.1088/1742-6596/2600/8/082028. [Online]. Available: https://dx.doi.org/10.1088/1742-6596/2600/8/082028.

[120] S. Moser and S. Puschnigg, "Supra-regional district heating networks: A missing infrastructure for a sustainable energy system," *Energies*, vol. 14, no. 12, 2021, ISSN: 1996-1073. DOI: 10.3390/en14123380. [Online]. Available: https://www.mdpi.com/1996-1073/14/12/3380.

[121] J. C. Flores, B. Lacarrière, J. Chiu, and V. Martin, "Assessing the techno-economic impact of low-temperature subnets in conventional district heating networks," *Energy Procedia*, vol. 116, pp. 260–272, 2017, ISSN: 18766102. DOI: 10.1016/j.egypro.2017.05.073.

[122] M. Imran, M. Usman, Y. H. Im, and B. S. Park, "The feasibility analysis for the concept of low temperature district heating network with cascade utilization of heat between networks," *Energy Procedia*, vol. 116, pp. 4–12, 2017, ISSN: 18766102. DOI: 10.1016/j.egypro.2017.05.050.

[123] M. Köfinger, D. Basciotti, and R.-R. Schmidt, "Reduction of return temperatures in urban district heating systems by the implementation of energy-cascades," *Energy Procedia*, vol. 116, pp. 438–451, 2017, ISSN: 18766102. DOI: 10.1016/j.egypro.2017.05.091.

[124] A. Volkova, I. Krupenski, A. Ledvanov, *et al.*, "Energy cascade connection of a low-temperature district heating network to the return line of a high-temperature district heating network," *Energy*, vol. 198, p. 117 304, 2020, ISSN: 03605442. DOI: 10.1016/j.energy.2020.117304.

[125] A. Volkova, S. Reuter, S. Puschnigg, *et al.*, "Cascade sub-low temperature district heating networks in existing district heating systems," *Smart Energy*, vol. 5, p. 100 064, 2022, ISSN: 26669552. DOI: 10.1016/j.segy.2022.100064.

[126] D. Lottis and A. Kallert, "Simulative comparison of concepts for simultaneous control of heat flow and outlet temperature of heat exchangers for highly flexible use in the test facility "district lab"," *Energy Informatics*, vol. 5, p. 16, S1 Sep. 2022, ISSN: 2520-8942. DOI: 10.1186/s42162-022-00202-x. [Online]. Available: https://energyinformatics.springeropen.com/articles/10.1186/s42162-022-00202-x.

[127] S. Schmidt, "Formal stability analysis of a pid-based control system for bidirectional heat transfer stations," Research Internship Report, Technical University of Munich, 2023.

[128] F. Strehle, J. Vieth, M. Pfeifer, and S. Hohmann, "Passivity-based stability analysis of hydraulic equilibria in 4th generation district heating networks," *IFAC-PapersOnLine*, vol. 54, no. 19, pp. 261–266, 2021, 7th IFAC Workshop on Lagrangian and Hamiltonian Methods for Nonlinear Control LHMNC 2021, ISSN: 2405-8963. DOI: https://doi.org/10.1016/j.ifacol.2021.11.088. [Online]. Available: https://www.sciencedirect.com/science/article/pii/S2405896321021121.

[129] S. Ahmed, J. E. Machado, M. Cucuzzella, and J. M. Scherpen, "Control-oriented modeling and passivity analysis of thermal dynamics in a multi-producer district heating system," *IFAC-PapersOnLine*, vol. 56, no. 1, pp. 175–180, 2023, 12th IFAC Symposium on Nonlinear Control Systems NOLCOS 2022, ISSN: 2405-8963. DOI: https://doi.org/10.1016/j.ifacol.2023.02.030. [Online]. Available: https://www.sciencedirect.com/science/article/pii/S2405896323002185.

[130] L. Moretti, G. Manzolini, and E. Martelli, "Milp and minlp models for the optimal scheduling of multi-energy systems accounting for delivery temperature of units, topology and non-isothermal mixing," *Applied Thermal Engineering*, vol. 184, p. 116 161, 2021, ISSN: 1359-4311. DOI: https://doi.org/10.1016/j.applthermaleng.2020.116161. [Online]. Available: https://www.sciencedirect.com/science/article/pii/S1359431120336413.

[131] F. Speer, "Planning, dimensioning, and economic assessment of bidirectional thermal networks with prosumers," Technical University of Munich, 2023.

**Declaration of generative AI and AI-assisted technologies in the writing process**
During the preparation of this work the author used *ChatGPT* by OpenAI, *DeepL Translator* by DeepL SE and *grammarly* by Grammarly Inc. in order to improve language and readability. After using these tools/services, the author reviewed and edited the content as needed and takes full responsibility for the content of the publication.

# Appendix D

# Doctoral Journey

## D.1 Publications

### First Author Publications

[1] T. Licklederer, T. Hamacher, M. Kramer, and V. S. Perić, “Thermohydraulic model of smart thermal grids with bidirectional power flow between prosumers,” *Energy*, vol. 230, p. 120 825, Sep. 2021, ISSN: 03605442. DOI: 10.1016/j.energy.2021.120825. [Online]. Available: https://linkinghub.elsevier.com/retrieve/pii/S0360544221010732.

[2] T. Licklederer, D. Zinsmeister, I. Elizarov, V. S. Perić, and P. Tzscheutschler, “Characteristics and challenges in prosumer-dominated thermal networks,” *Journal of Physics: Conference Series*, vol. 2042, p. 012 039, 1 Nov. 2021, ISSN: 1742-6588. DOI: 10.1088/1742-6596/2042/1/012039. [Online]. Available: https://iopscience.iop.org/article/10.1088/1742-6596/2042/1/012039.

[3] T. Licklederer, J. Mayer, D. Bytschkow, *et al.*, “Abschlussbericht „Multi-Energie Management und Aggregationsplattform (MEMAP)“ der TU München,” Technische Universität München, Tech. Rep., 2022, p. 196. DOI: 10.2314/KXP:1839282886. [Online]. Available: https://doi.org/10.2314/KXP:1839282886.

[4] T. Licklederer, D. Zinsmeister, L. Lukas, F. Speer, T. Hamacher, and V. S. Perić, “Control of bidirectional prosumer substations in smart thermal grids: A weighted proportional-integral control approach,” *Applied Energy*, vol. 354, p. 122 239, 2024, ISSN: 0306-2619. DOI: 10.1016/j.apenergy.2023.122239. [Online]. Available: https://www.sciencedirect.com/science/article/pii/S0306261923016033.

[5] T. Licklederer, J. Mayer, D. Bytschkow, *et al.*, “A digital platform for real-time multi-energy management in districts using opc ua: Conceptualization, modeling, software implementation, and laboratory validation,” *manuscript submitted to ’Energy and Buildings’*, 2024, (revision process ongoing at submission date of this dissertation, preprint is accessible online). DOI: 10.2139/ssrn.4861866. [Online]. Available: https://papers.ssrn.com/sol3/papers.cfm?abstract_id=4861866.

### Co-authored publications

[1] D. Bytschkow, A. Capone, J. Mayer, M. Kramer, and T. Licklederer, “An opc ua-based energy management platform for multi-energy prosumers in districts,” IEEE, Sep. 2019, pp. 1–5, ISBN: 978-1-5386-8218-0. DOI: 10.1109/ISGTEurope.2019.8905725. [Online]. Available: https://ieeexplore.ieee.org/document/8905725/.

[2] L. Heidemann, D. Bytschkow, A. Capone, T. Licklederer, and M. Kramer, "Sector coupling with optimization: A comparison between single buildings and combined quarters.," in *Abstracts from the 8th DACH+ Conference on Energy Informatics*, vol. 2, Sep. 2019, p. 31. DOI: 10.1186/s42162-019-0098-7. [Online]. Available: https://energyinformatics.springeropen.com/articles/10.1186/s42162-019-0098-7.

[3] D. Zinsmeister, T. Licklederer, F. Christange, P. Tzscheutschler, and V. S. Perić, "A comparison of prosumer system configurations in district heating networks," *Energy Reports*, vol. 7, pp. 430–439, Oct. 2021, ISSN: 23524847. DOI: 10.1016/j.egyr.2021.08.085. [Online]. Available: https://linkinghub.elsevier.com/retrieve/pii/S2352484721006879.

[4] I. Elizarov and T. Licklederer, "Prosnet – a modelica library for prosumer-based heat networks: Description and validation," *Journal of Physics: Conference Series*, vol. 2042, p. 012 031, 1 Nov. 2021, ISSN: 1742-6588. DOI: 10.1088/1742-6596/2042/1/012031. [Online]. Available: https://iopscience.iop.org/article/10.1088/1742-6596/2042/1/012031.

[5] I. D. la Cruz-Loredo, D. Zinsmeister, T. Licklederer, *et al.*, "Experimental validation of a hybrid 1-d multi-node model of a hot water thermal energy storage tank," *Applied Energy*, vol. 332, p. 120 556, November 2022 Feb. 2023, ISSN: 03062619. DOI: 10.1016/j.apenergy.2022.120556. [Online]. Available: https://linkinghub.elsevier.com/retrieve/pii/S030626192201813X.

[6] D. Zinsmeister, T. Licklederer, S. Adldinger, *et al.*, "A prosumer-based sector-coupled district heating and cooling laboratory architecture," *Smart Energy*, vol. 9, p. 100 095, February Feb. 2023, ISSN: 26669552. DOI: 10.1016/j.segy.2023.100095. [Online]. Available: https://linkinghub.elsevier.com/retrieve/pii/S2666955223000023.

[7] F. Speer, T. Licklederer, D. Zinsmeister, and V. S. Perić, "Dimensioning radial prosumer-based thermal networks," 2023, pp. 1–15. [Online]. Available: https://www.researchgate.net/publication/369480633_Dimensioning_radial_prosumer-based_thermal_networks.

[8] S. Adldinger, L. Behringer, T. Licklederer, D. Zinsmeister, and T. Hamacher, "Temperature flexible operation of district heating with booster heat pumps – improving efficiency of existing networks," *Journal of Physics: Conference Series*, vol. 2600, no. 8, p. 082 028, Nov. 2023. DOI: 10.1088/1742-6596/2600/8/082028. [Online]. Available: https://dx.doi.org/10.1088/1742-6596/2600/8/082028.

## Magazines

[1] MEMAP Research Group, "Werkzeuge für die Realisierung von nachhaltigen Quartieren," *BWK ENERGIE.*, pp. 10–13, 04-05 2020. DOI: 10.37544/1618-193X-2020-04-05. [Online]. Available: https://memap-projekt.de/wp-content/uploads/2021/05/MEMAP-Entwicklung-einer-Softwareumgebung-Vernetzte-Quartiere.pdf (visited on 10/08/2023).

[2] MEMAP Research Group, "Quartiere nachhaltig betreiben," *IKZ Fachplaner*, vol. 07, 2021. [Online]. Available: https://www.ikz.de/medien/ikz-fachplaner/heftarchiv/jahrgang-2021/ausgabe-07/news/detail/quartiere-nachhaltig-betreiben/ (visited on 10/08/2023).

## Experimental results

[1] D. Zinsmeister and T. Licklederer, "Characterization of a combined heat and power unit at the coses laboratory," Technical University of Munich - Center for Combined Smart Energy Systems (CoSES), Tech. Rep., 2021. DOI: 10.13140/RG.2.2.31035.34089/1. [Online]. Available: https://www.researchgate.net/publication/357049101_Characterization_of_a_Combined_Heat_and_Power_Unit_at_the_CoSES_laboratory.

[2] D. Zinsmeister and T. Licklederer, "Characterization of a combined heat and power unit at the coses laboratory - data," Technical University of Munich - Center for Combined Smart Energy Systems (CoSES), Tech. Rep., 2021. DOI: 10.13140/RG.2.2.17613.56809. [Online]. Available: https://www.researchgate.net/publication/357049522_Characterization_of_a_Combined_Heat_and_Power_Unit_at_the_CoSES_laboratory_-_Data.

[3] D. Zinsmeister and T. Licklederer, "Characterization of a thermal storage at the coses laboratory," Technical University of Munich - Center for Combined Smart Energy Systems (CoSES), Tech. Rep., 2022. DOI: 10.13140/RG.2.2.13461.19687. [Online]. Available: https://www.researchgate.net/publication/359442024_Characterization_of_a_Thermal_Storage_at_the_CoSES_laboratory.

[4] D. Zinsmeister and T. Licklederer, "Characterization of a thermal storage at the coses laboratory - data," Technical University of Munich - Center for Combined Smart Energy Systems (CoSES), Tech. Rep., 2022. DOI: 10.13140/RG.2.2.20172.08321. [Online]. Available: https://www.researchgate.net/publication/359441886_Characterization_of_a_Thermal_Storage_at_the_CoSES_laboratory_-_Data.

### Open-source repositories

1. **MEMAP** - Source code of the Multi-Energy Management and Aggregation Platform: https://git.fortiss.org/ASCI-public/memap/-/tree/main

2. **ProHeatNet_Sim** - A python based simulation framework for the thermohydraulic simulation of prosumer-dominated heat networks: https://github.com/thomaslicklederer/ProHeatNet_Sim

3. **ProsNet** - A modelica library for the simulation of prosumer-domintaed heat networks: https://github.com/thomaslicklederer/ProsNet

## D.2 Research Projects

**MEMAP** Aggregationsplattform zur gebäudeübergreifenden Optimierung der Energieeffizienz; Teilvorhaben Modellierung, Optimierung und Simulation Energiesysteme

| | |
|---|---|
| **Funding program** | Energieforschungsprogramm der Bundesregierung |
| **Funding agency** | Bundesministerium für Wirtschaft und Klimaschutz (BMWK.IIC6) |
| **Project Agency** | Forschungszentrum Jülich GmbH (PT-J.ESN3) |
| **Project identifier** | 03ET1413B |
| **Project duration** | 2017/06/01 bis 2021/09/30 |
| **URL** | https://memap-projekt.de/ |
| **Final report** | https://doi.org/10.2314/KXP:1843065479 |
| **Repositories** | https://git.fortiss.org/ASCI-public/memap |

| | |
|---|---|
| **Involved as** | Research Associate at academic project partner TUM - MSE |
| **Duration of involvement** | 2018/10/01 - 2021/09/30 |
| **Main tasks** | literature review, research gap identification, modeling, programming, simulation, experiment preparation and conduction, data analysis, documentation, exchange with research community, dissemination of results, continued learning, coordination with project partners, event organization and participation, project planning, budgeting and finance management, reporting to funding agency and professor |

**OSkit** Optimierte Sektorkopplung in Quartieren durch intelligente thermische Prosumernetze; Teilvorhaben: Modellierung, Laborevaluation und Rückwirkungen auf das Stromsystem

| | |
|---|---|
| **Funding program** | Energieforschungsprogramm der Bundesregierung |
| **Funding agency** | Bundesministerium für Wirtschaft und Klimaschutz (BMWK.IIC6) |
| **Project Agency** | Forschungszentrum Jülich GmbH (PT-J.ESN3) |
| **Project identifier** | 03EN3032A |
| **Project duration** | 2020/12/01 - 2024/05/31 |

| | |
|---|---|
| **Involved as** | Research Associate at academic project partner TUM - MSE |
| **Duration of involvement** | 2021/10/01 - 2023/12/31 |
| **Main tasks** | literature review, research gap identification, modeling, programming, simulation, experiment preparation and conduction, data analysis, documentation, exchange with research community, dissemination of results, continued learning, coordination with project partners, event organization and participation, project planning, budgeting and finance management, reporting to funding agency and professor, team formation and hiring. |

## D.3 Supervision and Teaching

**Master Thesis** of Sherif Hashem on *Convex thermal modelling of hydronic radiators for model predictive control of HVAC systems to enable demand side flexibility.* Garching, December 2019. Co-supervision together with M.Sc. Sebastian Troitzsch. Examiner: Prof. Thomas Hamacher.

**Master Thesis** of Ilya Elizarov on *Analysis, Modelling, and Control Strategy Development for Prosumer-based Heat Networks.* Garching, July 2020. Examiner: Prof. Thomas Hamacher. Access: https://mediatum.ub.tum.de/1719246 .

**Master Thesis** of Fabian Speer on *Planning, Dimensioning, and Economic Assessment of Bidirectional Thermal Networks with Prosumers.* Garching, March 2023. Examiner: Prof. Thomas Hamacher. Access: https://mediatum.ub.tum.de/1719254 .

**Bachelor Thesis** of Lorenz Lukas on *Commissioning and Characterization of a Prototypical Bidirectional Heat Transfer Station..* Garching, November 2022. Examiner: Prof. Thomas Hamacher. Access: https://mediatum.ub.tum.de/1719248 .

**Research Internship** of Nishard Ghouse on *Multi-Energy Management and Aggregation Platform.* Garching, October 2020. Co-supervision together with M.Sc. Sebastian Troitzsch. Examiner: Prof. Thomas Hamacher.

**Research Internship** of Hugo Schütz on *Energetic analysis of ZEI Building.* Garching, August 2022. Examiner: Prof. Thomas Hamacher.

**Research Internship** of Sarah Schmidt on *Formal stability analysis of a PID-based control system for bidirectional heat transfer station.* Garching, March 2023. Examiner: Prof. Thomas Hamacher. Access: https://mediatum.ub.tum.de/1719249 .

**Student seminar thesis** of Julian Scheer on *Literature review on bidirectional heat networks: Design and operating concepts in science and practise.* Garching, July 2020. Examiner: Prof. Thomas Hamacher.

**Student seminar thesis** of Monika Syed on *Literature review on local thermal energy markets: existing concepts in science and practice.* Garching, January 2022. Examiner: Prof. Thomas Hamacher.

**Student Research Assistant (Hiwi) Supervision** Supervision of student research assistants incl. hiring, administration, trainig, work task planing and assignment, monitoring, evaluation and mentorship.

- Ilya Elizarov: 2020/09/01 - 2021/12/31
- Johannes Burger: 2020/11/01 - 2021/05/31
- Luis Theel: 2022/10/01 - 2023/11/30
- Lorenz Lukas: 2022/12/01 - 2023/12/31

**Laboratory Internship** Supervision of student laboratory experiments on combined heat and power (CHP) systems and condensing boilers in the context of the lecture *Praktikum Energieerzeugungstechnik.* Including initial assessment, practical experiment, and report evaluation.

**Lecture** on "Energie- und Gebäudetechnik an der MSE" as part of the MINT orientation semester at TUM, followed by guided tour through the CoSES laboratory.

## D.4 Involvement at the Institute and University

**Center for Combined Smart Energy Systems (CoSES)** Member of the CoSES research group and proactive support of the group formation process, as well as the setup and operation of the associated laboratory infrastructure.

- Research Group
  - development of research direction and strategy
  - scientific discourse
  - team building
  - establishment of internal processes
  - public relations and dissemination of research results
  - guided tours through the laboratory
  - networking and establishing research collaborations
  - progression to taking over the shared group leadership
- Laboratory
  - system design
  - setup of hardware and software infrastructure
  - operation and maintenance
  - safety aspects
  - experiment design and conduction

**Munich School of Engineering (MSE),** later **Munich Institute of Integrated Materials, Energy and Process Engineering (MEP)** Engagement at the MSE / MEP, an integrated research center of the TUM.

- Adjunct member of the Professors' Council as governing body of the MSE
- Active Participation in the MSE Colloquia 2019, 2020, 2021 & the MEP Colloquium 2022
- Monitoring of the energy infrastructure in the ZEI buildung
- Supporting the preparation and writing of research proposals
- Close exchange with partner chairs at TUM: i.e. Lehrstuhl für Erneuerbare und Nachhaltige Energiesysteme (ENS) & Lehrstuhl für Energiewirtschaft und Anwendungstechnik (EWK)
- Progression to taking over the role of Focus Area Leader "Energy" at MEP

**Others**

- Elected **Doctoral Candidate Representative** for approx. 2000 doctoral candidates at the TUM School of Engineering and Design in the period of 10/2021 - 09/2022.

## D.5 Selected Events

| Date | Location | Name | Type of participation |
|---|---|---|---|
| 2018, October | Munich | *LabVIEW Course*: Certified LabVIEW Associate Developer (Certificate-ID: 100-318-14091) | participant |
| 2018, December | Detmold | 5. Projektleitertreffen der wiss. Begleitforschung "EnergieWendeBauen" on *Cooling and Refrigeration - Active and Passive Concepts* | participant |
| 2019, April | Munich | Course on *Competently supervising student theses* by TUM ProLehre Medien und Didaktik | participant |
| 2019, April | Garching | Workshop on *Programming with Python* by the TUM Graduate School | participant |
| 2019, May | Garching | *VeriStand Fundamentals Course* by National Instruments | participant |
| 2019, June | Copenhagen | Summer School on *Data-Driven Analytics and Optimization for Energy Systems* at the Technical University of Denmark (DTU) | participant |
| 2019, July | Garching | Official opening event of the *Laboratory for Combined Smart Energy System* (CoSES) at TUM | host, participant |
| 2019, July | Raitenhaslach | *Kick-off seminar* for the doctorate by TUM Graduate School; Skill course: "Evidence-based problem-solving strategies" | participant |
| 2019, July | Garching | *Customized VeriStand Integrator Training* by National Instruments | participant |
| 2019, August | Garching | *9th Energy Colloquium of the Munich School of Engineering* | participant |
| 2019, September | Garching | *Modelica Workshop* by the TUM Graduate School and the Modelica Association | participant |
| 2019, November | Garching | 7. Projektleitertreffen der wiss. Begleitforschung "EnergieWendeBauen" on *Tools for the Energy Transition* | host, organizer, participant |
| 2019, November | Munich | Course on *Fundamentals in Third-Party Funding* by TUM horizons | participant |
| 2020, February | Garching | Course on *Scientific Paper Writing* by TUM Graduate School | participant |

| | | | |
|---|---|---|---|
| 2020, April | online | Network Meeting of the *SmartQ Research Network for Smart Districts*: Presentation of the MEMAP Research Project | presenter |
| 2020, June | online | Speaker at the *Tech Days Munich 2020* on "Five buildings in a lab: Testbed for energy-optimized neighborhoods" | speaker |
| 2020, June | online | Workshop on *Digital District Energy Management* by the Begleitforschung "EnergieWendeBauen" | participant |
| 2020, Juli | Garching | *10th Energy Colloquium of the Munich School of Engineering* | presenter, participant |
| 2020, October | online | *6th International Conference on Smart Energy Systems (SES)*; Presentation on "A Thermohydraulic Model of Bidirectional Heat Networks with Prosumers" | presenter, participant |
| 2021, April | Garching | *11th Energy Colloquium of the Munich School of Engineering* | presenter, participant |
| 2021, September | online | *CISBAT 2021, Carbon Neutral Cities - Energy Efficiency & Renewables in the Digital Era*; Presentation on "Characteristics and Challenges in Prosumer-Dominated Thermal Networks" | presenter, participant |
| 2021, September | online | *Project closing event* of the MEMAP project | organizer, presenter |
| 2022, January | online | Seminar on *Good scientific pratice* by TUM Graduate School | participant |
| 2022, January | online | *Workshop on smart thermal prosumer networks*: Knowledge exchange and networking in the context of the OSkit Research Project | host, organizer, participant |
| 2022, May | online | Webinar on *Core Aspects of Neighborhood Concepts* by the Open District Hub e.V. and the C.A.R.M.E.N. e.V. | presenter |
| 2022, May | Garching | Workshop on *Agile Project Management with SCRUM in an Engineering Context* by the TUM Graduate School | participant |
| 2022, May | Mitteralm | Alpine Seminar on *Leadership and Self-Leadership* | participant |
| 2022, July | Garching | *12th Energy Colloquium of the Munich Institute of Integrated Materials, Energy and Process Engineering*; Awarded for the 2nd best oral presentation. | participant |

| | | | |
|---|---|---|---|
| 2022, August | Oxford | *Oxford Machine Learning Summer School 'OxML 2022'* by AI for Global Goals in partnership with CIFAR and the University of Oxford's Deep Medicine Program | participant |
| 2022, September | Aalborg | *8th International Conference on Smart Energy Systems (SES)*; Presentation on "A field-level control approach for bidirectional heat transfer stations in prosumer-based thermal networks" | presenter, participant |
| 2023, April | Berchtesgaden | *Retreat* for the TUM research group for Combined Smart Energy Systems (CoSES) | organizer, presenter, participant |